CHEMICAL SEDIMENTATION ASSOCIATED WITH MID-PALEOZOIC VOLCANISM IN CENTRAL NEWFOUNDLAND

HAROLD SCOTT SWINDEN

NOTICE

The quality of this microfiche is heavily dependent upon the quality of the original thesis submitted for microfilming. Every effort has been made to ensure the highest quality of reproduction possible.

If pages are missing, contact the university which granted the degree.

Some pages may have indistinct print especially if the original pages were typed with a poor typewriter ribbon or if the university sent us a poor photocopy.

Previously copyrighted materials (journal articles, published tests, etc.) are not filmed.

Reproduction in full or in part of this film is governed by the Canadian Copyright Act, R.S.C. 1970, c. C-30. Please read the authorization forms which accompany this thesis.

THIS DISSERTATION
HAS BEEN MICROFILMED
EXACTLY AS RECEIVED

AVIS

La qualité de cette microfiche dépend grandement de la qualité de la thèse soumise au microfilmage. Nous avons tout fait pour assurer une qualité supérieure de reproduction.

S'il manque des pages, veuillez communiquer avec l'université qui a conféré le grade.

La qualité d'impression de certaines pages peut laisser à désirer, surtout si les pages originales ont été dactylographiées à l'aide d'un ruban usé ou si l'université nous a fait parvenir une photocopie de mauvaise qualité.

Les documents qui font déjà l'objet d'un droit d'auteur (articles de revue, examens publiés, etc.) ne sont pas microfilmés.

La reproduction, même partielle, de ce microfilm est soumise à la Loi canadienne sur le droit d'auteur, SRC 1970, c. C-30. Veuillez prendre connaissance des formules d'autorisation qui accompagnent cette thèse.

LA THÈSE A ÉTÉ
MICROFILMÉE TELLE QUE
NOUS L'AVONS REÇUE

CHEMICAL SEDIMENTATION ASSOCIATED WITH MID-PALEOZOIC VOLCANISM IN CENTRAL NEWFOUNDLAND

by

H. Scott Swinden

A thesis
submitted in partial fulfillment of the
requirements for the degree of
MASTER OF SCIENCE

Memorial University of Newfoundland
July, 1976

ABSTRACT

Chert, ferruginous chert and associated chemical sedimentary rocks are a ubiquitous although volumetrically minor component of the Upper Ordovician-Silurian volcanic succession in Central Newfoundland. They are intimately associated with volcanic lithologies ranging from mafic pillow lava and pillow breccia to silicic flows and pyroclastic rocks, and occur both as thin, discontinuous bedded lenses conformable with the volcanic stratigraphy and as massive pods interstitial to mafic pillows. Although most units appear to be unrelated to base metal mineralization, a laterally continuous horizon at Gull Pond, the Gullbridge ferruginous chert, overlies and is spatially related to two volcanogenic copper deposits.

Two hundred and forty-seven rock samples were analyzed for 10 major and 10 trace elements in order to examine inter-element relationships providing information on the genesis of these sediments and to determine whether chemical concentrations in the Gullbridge ferruginous chert could be developed as a useful exploration tool.

Chemical data suggest that three processes contributed to the formation of these chemical sediments, viz; biogenic processes are inferred to have been responsible for most of the silica which is dominantly present as non-detrital quartz; hydrothermal processes are inferred to have contributed most of the Fe_2O_3, MnO, Ba, and Au; volcaniclastic sedimentation is the probable source of the remaining major and trace elements. Chemical trends in the rocks are strongly influenced by their mineralogy and can usually be related to the presence of specific minerals or groups of minerals.

Bedded chemical sediments were deposited in local topographic depressions on the sea floor during periods of relative volcanic quiescence and underwent diagenesis under oxidizing to mildly reducing conditions. Interpillow chert was deposited in interstitial voids in the pillow lava, probably due to the mixing of hydrothermal fluids with sea water already present in the voids.

No chemical trends are developed in these rocks as a function of their stratigraphic level and it appears that neither the progressive chemical development of the related volcanism nor the changing bulk chemistry of the associated volcanic rocks substantially influences their composition.

The Gullbridge ferruginous chert can be distinguished empirically and statistically from similar lithologies unrelated to mineralization on the basis of its higher Fe_2O_3, MnO, Ba and Au concentrations. These components are inferred to have been contributed hydrothermally which suggests that this feature may be genetically related to the mineralizing process and thus have the potential of being a useful regional exploration tool. Sporadic high Ba values occur near the Southwest Shaft copper deposit at Gull Pond but the narrow strike length and sporadic nature of this feature probably limits its general usefulness in mineral exploration.

TABLE OF CONTENTS

PAGE

CHAPTER 3

GENERAL GEOLOGY

CHAPTER 4

MINERALOGY AND PETROLOGY

LIST OF FIGURES

LIST OF TABLES

LIST OF PLATES

ACKNOWLEDGEMENTS

The author is indebted to the following people who provided much appreciated assistance in the carrying out of this project:

Dr. D.F. Strong supervised the work and provided computer time and much help at all stages of the project. His stimulating discussion on various topics of both immediate and peripheral relevance to the work has been a constant source of inspiration.

Numerous faculty and students at Memorial University provided much appreciated help and discussion on both practical and theoretical aspects of the study.

Mrs. G. Andrews carried out the large majority of the major element analyses and provided much help in the analytical laboratory.

D. Press provided extensive assistance with various aspects of the computer work and with J. Vahtra was of considerable assistance in the trace element and X-ray diffraction determinations.

Grateful thanks is extended to Bernice St. Croix who typed the manuscript.

Cominco Ltd. were responsible for having the gold analyses carried out and their help is gratefully acknowledged.

Particular thanks are due to Atlantic Coast Copper Co. Ltd. who provided logistical support and encouragement during much of the field work in 1974 as well as the opportunity for the author to return to Gull Pond in 1975 and take a detailed look at the geology of this area.

Financial support was provided by a Memorial University fellowship and by National Research Council Operating Grant A7975 and Geological Survey of Canada Research Agreement 1135-D13-4-18/72, both to D.F. Strong.

CHAPTER 1

INTRODUCTION

1.1 General Statement

The intimate association of ferruginous chert and iron-rich sedimentary rocks with volcanic sequences has been recognized from a variety of geologic regimes virtually throughout geologic time (e.g. Goodwin, 1962; Gross, 1965; Grunau, 1965; Bostrom and Peterson, 1966; Berger and von Rad, 1972; Garrison, 1974), although for Phanerozoic times, this association has been more commonly reported from ophiolitic and related sequences (Grunau, 1965; Robertson and Hudson, 1973, 1974; Thurston, 1973; Garrison, 1974; Bonatti et al., 1976) than from sequences related to island arc volcanism. Furthermore, the close spatial relation of this type of sedimentary rocks to base metal mineralization has been remarked from a number of areas (e.g. Horikoshi, 1969; McAllister, 1960; Robertson and Hudson, 1974; Ridler, 1970; Hutchinson et al., 1971; Hutchinson, 1973).

In central Newfoundland, chert and ferruginous sediments have long been known from the Lower Paleozoic volcano-sedimentary sequence (Sampson, 1923; Espenshade, 1937; Heyl, 1936; Helwig, 1967; Dean, 1973) including the Upper Ordovician-Silurian marine succession (Dean and Strong, 1975) which is dominantly composed of volcanic rocks of calc-alkaline affinity (Strong, 1973, 1975). Furthermore, the Gullbridge copper deposit, which occurs within the latter sequence, has a prominent, laterally continuous ferruginous chert horizon associated with it (Upadhyay, 1970; Swinden, 1975).

1.2 Purpose and Scope

The present study is based on an examination of the field relations, petrography and major and trace element geochemistry of chert, ferruginous chert and associated sedimentary rocks throughout the Upper Ordovician-Silurian volcanic sequence in central Newfoundland, with emphasis on the Gullbridge ferruginous chert which overlies the mineralized horizon at Gull Pond. The complete volcanic section was examined in three widely separated areas and samples were taken as much as possible from all stratigraphic levels of the sequence. In addition, the Gullbridge ferruginous chert horizon was extensively sampled all along its exposed strike length. A total of 247 samples were analyzed for 10 major and 10 trace elements and examination of this data coupled with petrologic and field observations and mineralogic data was directed towardsthe following problems:

1) The chemical composition of the sediments and the mineralogic disposition of the elements.

2) The genesis of these sediments, their depositional environment and the source(s) of their various components.

3) The distinguishing features between the Gullbridge ferruginous chert and other similar lithologic units unrelated to mineralization, lateral variations in the chemical composition of this horizon possibly related to the underlying mineralization and the application of these features to mineral exploration.

1.3 General Geology of Southern Notre Dame Bay

Southern Notre Dame Bay is underlain by a thick succession of Early Paleozoic volcanic rocks and volcanogenic sediments (Fig. 1.1). The oldest recognized rocks in this succession are mafic pillow lavas and associated minor sedimentary rocks of the Lushs Bight Group (Espenshade, 1937; MacLean, 1947; Horne and Helwig, 1969; Dean and Strong, 1975) which are of oceanic tholeiite affinity and have been interpreted by Church and Stevens (1971), Smitheringale (1972), and Strong (1973), to comprise Cambrian to Lower Ordovician oceanic crust.

The oldest rocks of island arc affinity in Notre Dame Bay are the mafic pillow lavas with lesser pyroclastic rocks, silicic volcanic domes and greywacke assigned to the Cutwell, Wild Bight, Moretons Harbour, Western Arm and Summerford Groups of dominantly Lower to Middle Ordovician age (Dean and Strong, 1975). Detailed study of the Cutwell Group at Long Island (Kean, 1973; Kean and Strong, 1975) has shown that a progressive change from volcanic rocks of oceanic tholeiite affinity to those of island arc affinity characterizes the base of this succession. These volcanic rocks are interbedded with and conformably overlain by a thick sequence of black shale, chert, greywacke, and minor mafic flows assigned to the Exploits Group of dominantly Middle Ordovician to Lower Silurian age (Williams, 1964; Helwig, 1967; Horne and Helwig, 1969; Dean and Strong, 1975). The top of the Exploits Group is gradational and conformable with the overlying marine, dominantly volcanic sequence of Upper Ordovician and Silurian age, variously assigned to the Roberts Arm Group (Williams, 1964), Chanceport Group (Strong and Payne, 1973) and Cottrell's Cove Group (Dean, 1973; Dean and Strong, 1975). The base of this succession comprises mafic

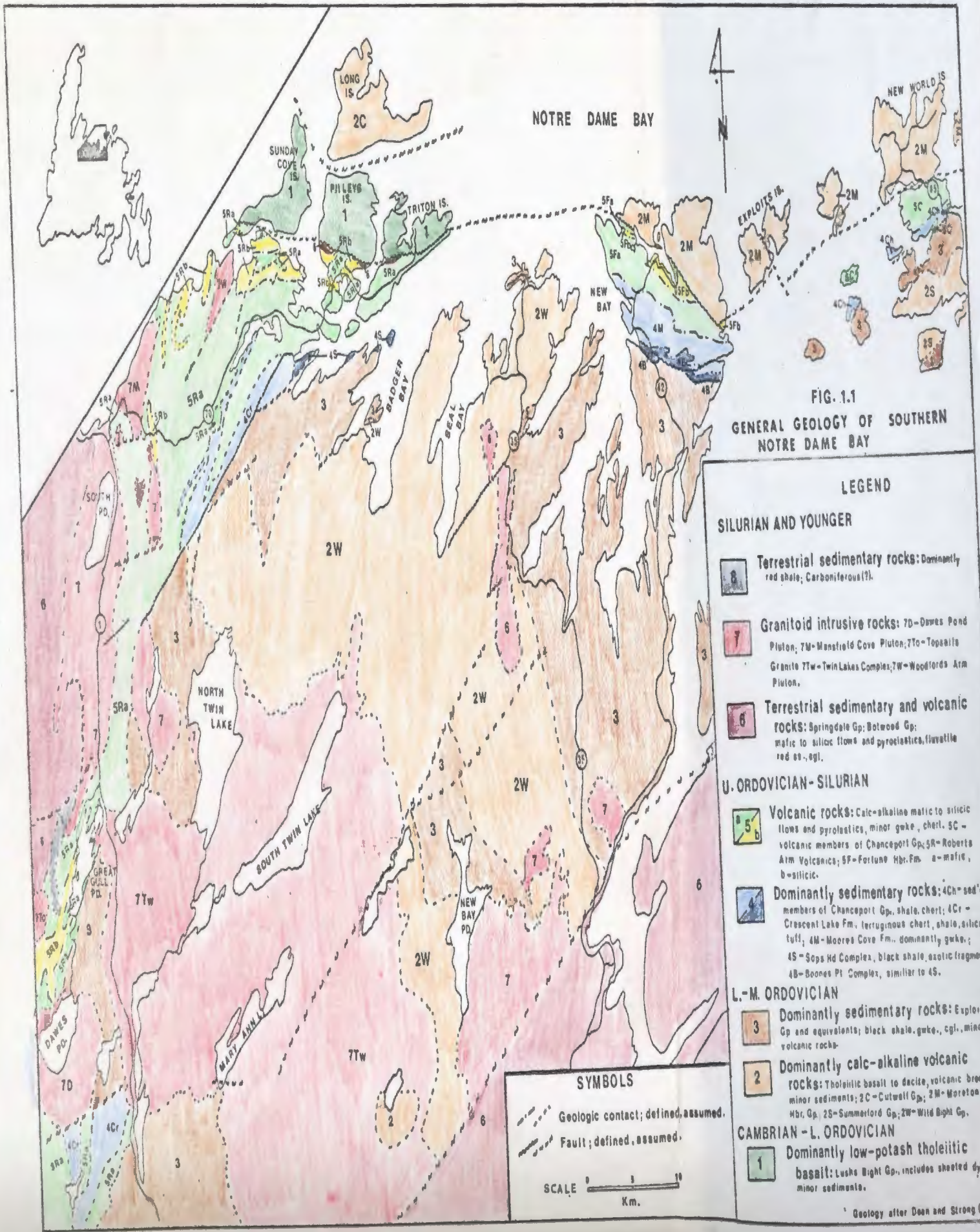

FIG. 1.1
GENERAL GEOLOGY OF SOUTHERN NOTRE DAME BAY

LEGEND

SILURIAN AND YOUNGER

8 Terrestrial sedimentary rocks: Dominantly red shale; Carboniferous(?).

7 Granitoid intrusive rocks: 7D–Dawes Pond Pluton; 7M–Mansfield Cove Pluton; 7To–Topsails Granite 7Tw–Twin Lakes Complex; 7W–Woodfords Arm Pluton.

6 Terrestrial sedimentary and volcanic rocks: Springdale Gp: Botwood Gp: mafic to silicic flows and pyroclastics, fluvatile red ss-, cgl.

U. ORDOVICIAN-SILURIAN

5a/5b Volcanic rocks: Calc-alkaline mafic to silicic flows and pyroclastics, minor gwke., chert. 5C – volcanic members of Chanceport Gp; 5R–Roberts Arm Volcanics; 5F–Fortune Hbr. Fm. a–mafic, b–silicic.

4 Dominantly sedimentary rocks: 4Ch–sed'y members of Chanceport Gp., shale, chert; 4Cr – Crescent Lake Fm., ferruginous chert, shale, silicic tuff; 4M–Moores Cove Fm., dominantly gwke.; 4S–Sops Hd Complex, black shale, exotic fragments; 4B–Boones Pt Complex, similar to 4S.

L.-M. ORDOVICIAN

3 Dominantly sedimentary rocks: Exploits Gp and equivalents; black shale, gwke., cgl., minor volcanic rocks.

2 Dominantly calc-alkaline volcanic rocks: Tholeiitic basalt to dacite, volcanic breccia, minor sediments; 2C–Cutwell Gp; 2M–Moretons Hbr. Gp; 2S–Summerford Gp; 2W–Wild Bight Gp.

CAMBRIAN – L. ORDOVICIAN

1 Dominantly low-potash tholeiitic basalt: Lushs Bight Gp., includes sheeted dykes, minor sediments.

SYMBOLS

Geologic contact; defined, assumed.

Fault; defined, assumed.

SCALE 0 5 10 Km.

Geology after Dean and Strong (1976)

volcanic rocks interbedded with greywacke and shale and overlain by tuffaceous greywacke and siltstone, silicic tuff and ferruginous chert (Dean and Strong, 1975) which give way to a thick sequence of dominantly mafic flows of calc-alkaline affinity (Strong, 1973, 1975). The top of the succession is generally characterized by abundant silicic flows and coarse pyroclastic rocks and tuff (Noranda Mines Staff, 1971; Dean, 1973). The Upper Ordovician-Silurian calc-alkaline sequence attains its maximum thickness in the Roberts Arm area and thins rapidly to the south (Neale and Nash, 1963) and to the east where considerable amounts of greywacke, shale and chert in the succession on the Moretons Harbour Peninsula (Strong and Payne, 1973) may mark the distal end of active volcanism at this time (Dean and Strong, 1975).

In the eastern part of Notre Dame Bay, the top of the calc-alkaline volcanic sequence is truncated by the Chanceport Fault (Dean, 1973; Strong and Payne, 1973) while to the west it is disconformably overlain by fluvatile red sedimentary rocks assigned to the Botwood (Williams, 1964) and/or Springdale (Neale and Nash, 1963; Strong, 1973) Groups of probable Silurian age (Neale and Nash, 1963; Dean and Strong, 1975).

1.4 Choice and Location of Study Areas

Three areas within the Upper Ordovician-Silurian volcanic sequence were chosen for the present study (Fig. 1.2). Their location, access and the reasons for their choice are summarized below:

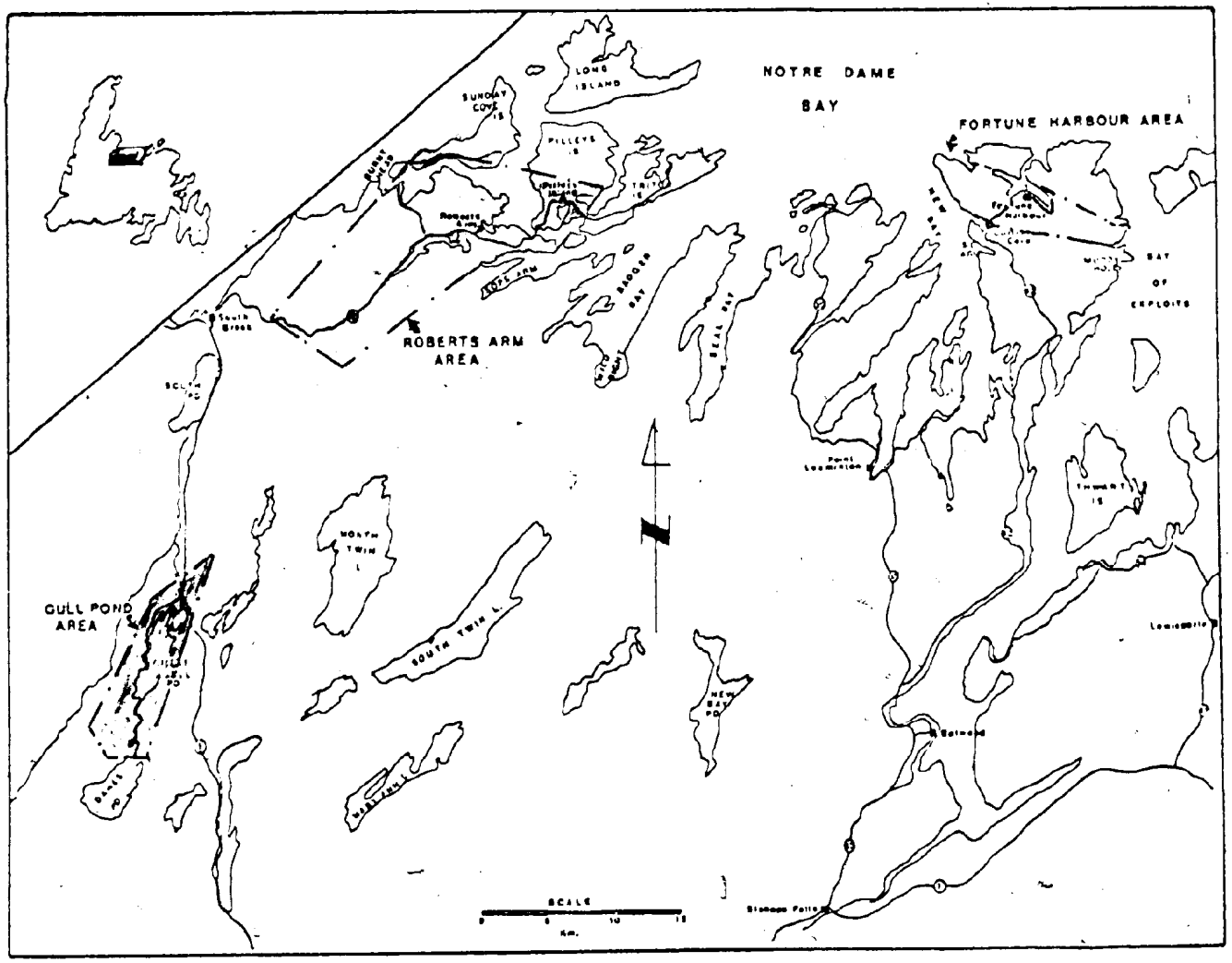

FIG. 1.2 Location of study areas

1) Roberts Arm Area:

This area includes the thickest part of the Upper Ordovician-Silurian volcanic sequence (Fig. 1.1) and is centered on approximate coordinates Lat. 49^{o} 29'N, Long. 55^{o} 53'W. Access is provided mainly by roads connecting the Trans-Canada Highway with Triton and Sunday Cove Islands. A major consideration in the choice of this area was the existence of detailed, relatively large-scale geologic maps (Espenshade, 1937; Hayes, 1951; Noranda Mines Staff, 1971) which provided a maximum of stratigraphic control for sample locations. Another major consideration was the abundance of coastal exposure throughout the section, this being important because the sediments sampled comprise a volumetrically minor part of the volcanic succession and in the absence of almost continuous exposure are difficult to find.

2) Fortune Harbour Area:

This area, in the northern part of the Fortune Harbour Peninsula, is centered at approximately Lat. 49^{o} 39' N, Long. 55^{o} 14' W and is reached via a road connecting the Trans-Canada Highway with the village of Fortune Harbour.

This area was chosen as the representative section in the eastern part of the volcanic sequence for reasons similar to those for the Roberts Arm Area. Detailed geologic maps were available as a result of the work of Helwig (1967) and Dean (1973) and good exposure of the complete section was afforded by coastline in Fortune Harbour and along the west side of the peninsula, as well as by extensive road cuts.

3) Gull Pond Area:

This area encompasses a north-south section of volcanic and sedimentary rocks centered at approximate coordinates Lat. 49° 12' N, Long. 56° 09' W, and good access is provided by the Trans-Canada Highway which cuts the northern part of the area, an all weather road connecting the highway with the Gullbridge townsite, and numerous woods roads and trails.

Of principal interest in this area was the ferruginous chert horizon associated with the Gullbridge ore deposit, along with a number of similar horizons apparently unrelated to mineralization which were also investigated and extensively sampled.

CHAPTER 2

THE OCCURRENCE AND ORIGIN OF CHERT AND FERRUGINOUS SEDIMENTARY ROCKS IN VOLCANIC ENVIRONMENTS

2.1 Introduction

Chert and ferruginous sediments are volumetrically minor but ubiquitous components of volcanic sequences around the world (Grunau, 1965; Garrison, 1974). Until recently, discussion of the origin of these sediments was necessarily based on evidence in ancient deposits where primary features are often partially or completely obliterated by diagenetic and metamorphic processes. However, the discovery of recent siliceous sediments on the ocean floor during the Deep Sea Drilling Project (DSDP), and the concentrated study of ferruginous sediments presently forming in a variety of submarine volcanic environments, has afforded the opportunity to view the modern analogues of ancient chert and ferruginous sediments and to gain a better understanding of their genesis.

This chapter presents a review of current knowledge of the occurrence and origin of modern and ancient siliceous and ferruginous sediments which are chemically and/or environmentally analogous to those studied during the present project.

2.2 The Occurrence and Origin of Bedded Chert

The "chert problem" has been a source of debate among geologists for a considerable time and the resulting volume of literature prohibits a comprehensive review of all relevant publications. Accordingly, this

section is restricted to summarizing contributions leading to the present interpretations of the origin of bedded chert, especially as they bear on the origin of the siliceous sedimentary rocks of the present study. Extensive references beyond the scope of this summary are listed by Cressman (1962), Grunau (1965), and Garrison (1974), and numerous descriptions of modern siliceous sediments can be found in the Initial Reports of the Deep Sea Drilling Project.

The close association of some bedded chert with volcanic rocks led early workers to suggest a genetic tie between them. Davis (1918) concluded as a result of his study of radiolarian chert in the Franciscan Group that the silica was introduced to the sea floor, by volcanic thermal springs, in amounts exceeding the solubility of amorphous silica and was precipitated inorganically by the cooling of the heated water. This notion was later reiterated by Sampson (1923) in his study of chert in Notre Dame Bay and variations of it have appeared intermittently in the literature up to the present (e.g. Iwao, 1970).

The earliest convincing evidence of a biogenic origin for chert was supplied by Bramlette (1946) who suggested that the bedded chert of the Monterey Formation, California, resulted from the conversion of biogenous opal in diatomite to an opaline claystone and thence to quartz chert. Ernst & Calvert (1969) later identified this claystone as disordered cristobalite and experimentally confirmed the nature of the reaction. The general applicability of Bramlette's theory was supported by experimental work on the low temperature solubility of amorphous silica and quartz (Krauskopf, 1959; Siever, 1962) which indicated that inorganic

precipitation of silica cannot take place in normal sea water because of its marked undersaturation in dissolved silica with respect to amorphous silica. However Siever (1962) noted that extensive dissolution of biogenous opal on the sea floor due to the metastability of amorphous silica in the marine environment should lead in some cases to interstitial solutions supersaturated with respect to quartz and capable of precipitating that mineral.

The opportunity to observe the above theoretical considerations in the recent geologic record was provided by the recovery of chert and siliceous sediments from widespread DSDP cores ranging from the North Atlantic to the Pacific (Davies and Supko, 1973). Detailed study of these cores revealed that a wide variety of siliceous rocks was present from siliceous ooze through porcellanites in various stages of induration to quartz chert. Heath and Moberly (1971), noting that this lithologic sequence was characterized by increasing age of the deposits, were led to suggest a "maturation theory" of chert genesis in which three steps proceeded naturally with increasing age as follows:

1) Dissolution of opaline debris and/or alteration of montmorillonite and reprecipitation of disordered cristobalite to form a cristobalite - montmorillonite claystone.

2) Creation of a well indurated porcellanite through the crystallization of additional cristobalite.

3) Solid state inversion of cristobalite to quartz with attendant loss of all remaining porosity and obliteration of virtually all siliceous skeletons preserved in the cristobalite-porcellanite.

Berger and von Rad (1972) supplied detailed descriptions of chert and siliceous sediments cored in the Atlantic Ocean and further refined the maturation theory by taking into account an increased variety of deposits. They defined four basic types of chert based on texture, sedimentary fabric, and silica mineralogy ranging from immature opal-lussatite ooze or mud to indurated, homogeneous quartz chert. Their interpretation of the diagenetic changes leading to the various types is summarized in Fig. 2-1.

An opposing theory of chert genesis arising from study of DSDP cores was proposed by Lancelot (1972) who contended that the clay content and permeability of the host rock and the presence of foreign cations determined whether disordered cristobalite or quartz would precipitate at any given time. He suggested that in a clay-free carbonate environment, quartz may form by direct precipitation while in clay-rich sediments, disordered cristobalite will form. The discovery of disordered cristobalite in clay-free chert on the Kerguelen Plateau (Wise et al., 1972) and of quartz cherts in clayey and marley beds in the central Atlantic (von Rad and Rosch, 1974) as well as topological considerations discussed by Calbert (1974) tend to limit the general applicability of this hypothesis.

The role of volcanism in the formation of chert is still a subject of considerable debate in the literature (e.g. see discussion by Calvert, 1974) and while it has been shown that volcanism is not a necessary prerequisite for chert formation (e.g. Wise et al., 1972), there is a considerable body of evidence to suggest that it can be a

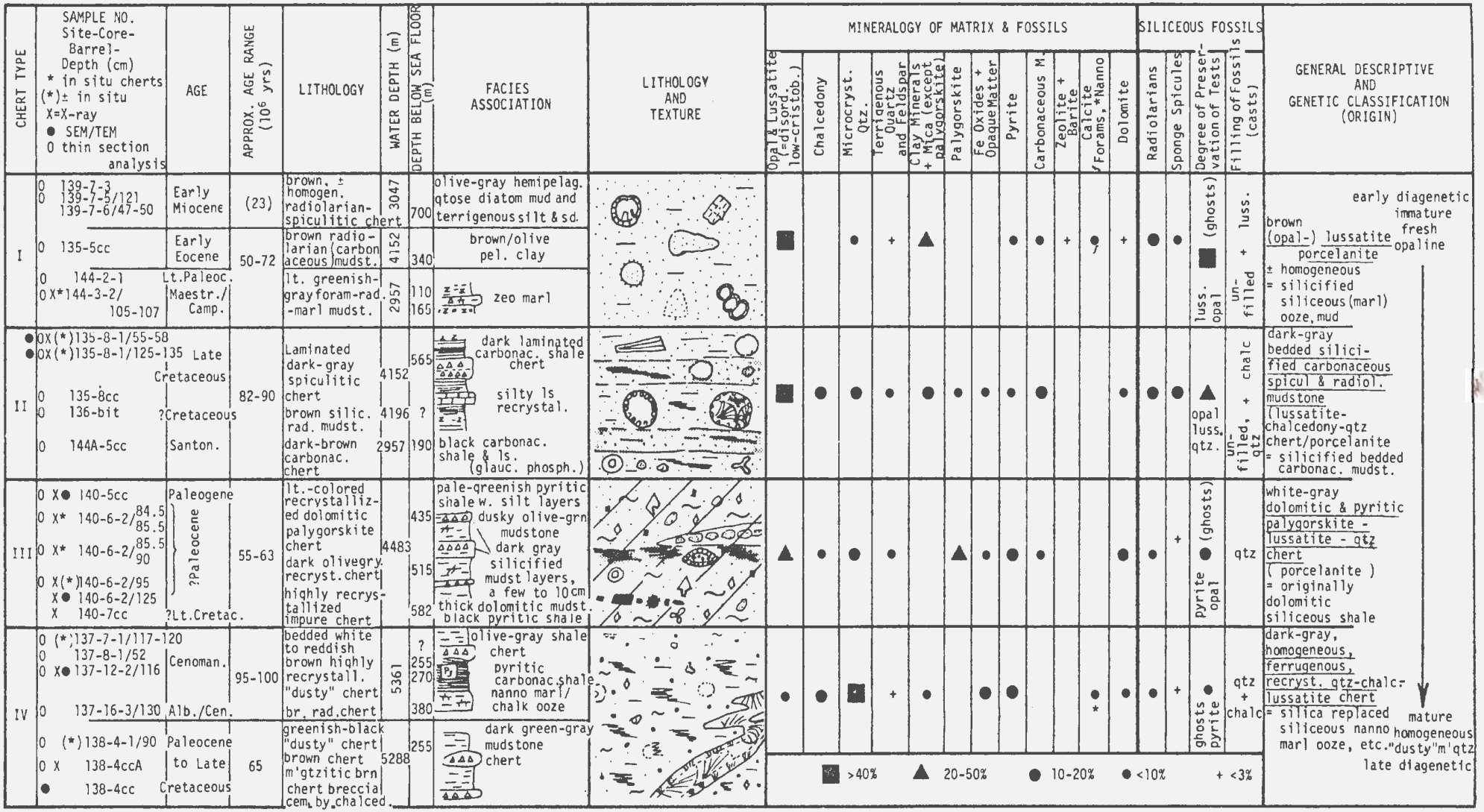

Composition and genesis of chert types I to IV. The sketches in column "Lithology and Texture" are meant to represent the following features (I to IV): (I) light stipples, *opal-lussatite ("cristobalite");* dashes, *montmorillonite, kaolinite, etc.;* particles, *open and filled radiolarians and forams, "ghosts" etc.; (II)* shaded areas, *laminae enriched in carbonaceous matter (stipples), and ferruginous zones (lines),* particles, *spicules, "ghosts", in part filled with chalcedony and quartz; (III)* hachure, *mass polarization, birefringent matrix oriented parallel to bedding; (~,* palygorskite*);* particles, *black: pyritized radiolarians, pyrite crystals; other; as before, also (in part) corroded dolomite crystals; stippled grains: silt size terrigenous quartz; (IV* bold stipples, *microcrystalline quartz and chalcedony; note homogenization, healed fracture (chalcedony).*

Fig. 2.1 (from Berger and von Rad 1972)

positive influence in the process. Some recent workers have speculated that subaqueous volcanic activity may create an environment where siliceous organisms will flourish and/or where their preservation after sedimentation will be enhanced (e.g. Grunau, 1965; Thurston, 1972; Kanmera, 1974; Roberston and Hudson, 1974) while others have noted that the alteration of volcanic detritus in the submarine environment may contribute substantial amounts of silica to interstitial solutions during diagenesis, thus promoting the crystallization of cristobalite (Gibson and Towe, 1971; Heath and Moberly, 1971; Berger and von Rad, 1972; Calvert, 1974; von Rad and Rosch, 1974).

Ramsey (1973) stressed that divergence of surface water masses due to atmospheric and hydrospheric circulation leads to upwelling of nutrient-rich deeper water in modern oceans, and the resulting enhanced productivity of siliceous plankton is reflected in an abundance of siliceous sediments in these areas. He suggested that world-wide distribution of siliceous sediments in Ordovician-Silurian times appears to have been most prominent in a broad zone which, according to continental reconstruction, falls in the Lower Paleozoic equivalent of the modern equatorial "silica zone".

Although there is still much debate concerning chert genesis, a consensus of opinion seems to be developing in the literature on some aspects of the problem and the present interpretation of this process by most present workers can be summarized as follows (modified after Wise and Weaver, 1974):

1) Chert formation begins with the diagenetic precipitation of disordered cristobalite from interstitial solutions supersaturated in silica with respect to quartz. The immediate source of silica is thought to be dominantly the solution of biogenous opal, although contributions from the alteration of clay and volcanic glass cannot be ruled out.

2) The maturation theory of chert formation (Heath and Moberly, 1971; Berger and von Rad, 1972) closely approximates the actual process. Most siliceous tests are destroyed during diagenesis and the presence of just a few fossil traces in an indurated chert may thus reflect the original presence of many more, obviating the necessity of postulating an exotic source for silica.

3) No amorphous silica gel phase has been detected in modern incipient chert and no such phase is considered to exist during the formation of this lithology.

4) Oceanic chert may form wherever biogenous opal is abundant, independent of water depth, notwithstanding other factors such as dilution by clastic sedimentation and volcanism, dispersal by turbidity currents, etc.

2.3 Occurrence and Origin of Iron-Rich Rocks in Volcanic Environments

Although sediments examined during the present study are as a whole not particularly iron-rich, a significant number of samples contain very high concentrations of total iron and an inquiry into the occurrence and origin of iron-rich sediments in ancient and modern volcanic regimes is thus appropriate.

The nomenclature of the iron-rich sedimentary rocks has never been universally standardized and the useage of the terms "iron formation", "ironstone", "iron-rich sedimentary rock", and "ferruginous sediment" as well as the numerous local terms varies considerably from place to place. Following Gross (1965) "iron-rich sedimentary rocks" are herein defined as stratigraphically concordant, bedded sediments containing greater than 15% total iron, while "ferruginous sediments" are defined after Beukes (1973) as those containing less than 15% total iron but still having an amount significantly above crustal abundance.

2.3.1 Evidence from Ancient Deposits

Iron-rich sedimentary rocks from around the world were classified by Gross (1965) into six major types according to lithologic features, geologic setting and associated sedimentary rocks (Table 2.1). In this classification, iron-rich lithologies in the present study fit most readily into the "Algoma type", an association that will be further explored in Section 2.4.

A second way of subdividing the iron-rich sedimentary rocks is based on facies changes that result from varying environmental factors during deposition and diagenesis. Following the work of Krumbein and Garrels (1952), who showed that the type and amount of chemical precipitation are controlled principally by the pH and Eh of the aqueous medium, James (1954) defined the oxide, carbonate, silicate and sulphide facies (Table 2.2).

Numerous workers have considered the problem of the source of iron in sedimentary iron deposits and three principal mechanisms listed below have been proposed (after James, 1966):

TABLE 2.1

CHARACTERISTIC FEATURES OF THE DIFFERENT TYPES OF IRON-FORMATION

(after Gross, 1965)

1. Algoma type: Thin-banded chert or quartz and iron oxides, silicates, carbonates and sulphides, associated with volcanic rocks, and greywacke; usually in thin lenses with streaky banding; oolitic textures absent or inconspicuous; relatively rare but in rock of all ages, especially early Precambrian; eugeosynclinal; e.g., Moose Mountain and Michipicoten area, Algoma district, Ontario.

2. Superior type: Interbanded chert or quartz and iron minerals with prominent granular or oolitic textures; associated with dolomite, quartzite, black carbon-bearing shales and slate, chert breccias and volcanic rocks; usually well-defined formations of broad regional extent; form in continental shelf and miogeosynclinal environments. Extensively developed in late Precambrian rock groups, e.g., Lake Superior and Labrador iron ranges.

3. Clinton type: Hematite-chamosite-siderite formations; interbedded with carbonaceous shale, carbonate rocks and sandstones; high in phosphorus compared to cherty formations; oolitic to granular texture; miogeosynclinal and shallow-basin environments; lenticular beds restricted to thin formations of broad regional extent as in the Appalachian belt. Most common in rock groups of Cambrian to Devonian age, e.g., Wabana, Newfoundland; Birmingham, Alabama.

4. Minette type: Siderite-chamosite-iron silicate, and goethite beds; usually high in phosphorus; oolitic textures; lenticular beds containing clastic material, sideritic mudstones, and concretionary siderite layers; associated with sandstones, carbonaceous shales, siltstone and limestone; cyclic sedimentation of sandy beds, shale and ironstones, and black shale, common; formed in transition zones between marine- and brackish-water environments. Most common in Mesozoic and younger rocks, e.g., Peace River area of Alberta, Canada; Jurassic beds in England; Minette ores of Lorraine, France, and in Luxembourg and Belgium.

5. Non-oolitic: A heterogeneous group of non-oolitic, lensy, ferruginous beds; vary in composition and type from the blackband sideritic carbonaceous claystones associated with coal; to the Lahn and Dill hematite and goethite beds locally rich in manganese and/or silica; to siderite-iron silicate-goethite lenses in shale. Associated with fine-grained clastic or volcanic rocks; occurring mainly in late Palaeozoic and younger rocks, e.g., Lahn and Dill River area in Hesse, Germany; Vares, Yugoslavia; Gross Ilsede and Peine in Lower Saxony.

6. Clastic: Placer deposits of black sands; mainly magnetite with siderite or hematite in sandstones, usually contain titanium and rare earth elements; thin beds of lensy distribution, varied grade, and quality; deposited along beaches or near shore marine environments, e.g., iron-formation near Burmis, Alberta, in the Belly River sandstone.

TABLE 2.2

CHARACTERISTICS OF VARIOUS FACIES OF IRON FORMATION (data after Gross, 1965)

Facies	Iron Mineralogy	Chemical Conditions for Formation	Physical Features	Depositional Environment
Oxide	Hematite	Hematite-pos. to low neg. Eh, pH weakly acid to alkaline.	Late Precambrian to present-commonly show granular and oolitic textures. Early Precambrian-above textures not common.	At basin margins in relatively shallow water where water agitation leads to oolitic and granular textures and oxygenation.
	Magnetite	Magnetite-Eh intermed. to mildly reducing. pH weakly acid to alkaline.		
Carbonate	Siderite	Strongly reducing; CO_2 partial pressure atmosphere.	Granular and oolitic texture commonly absent. Where above are present, they often occur in the oxide-carbonate transition zone.	Deep, quiet waters, little agitation. Further from shore and cooler water than oxide facies; environment changed with CO_2, possibly from organic decay.
Silicate	Grunerite Minnesotaite Stilpnomelane Chamosite Iron chlorites	Probably reducing; low CO_2 partial pressure. Commonly associated with siderite and magnetite.	Granular textures common.	Environment common to parts of oxide and carbonate facies. Low CO_2.
Sulfide	Pyrite Pyrrhotite Marcasite	Strongly reducing with abundant H_2S and high ferrous iron concentration. pH not critical.	Common types of deposits: -dissem. pyr. in black carbonaceous shale -py. and po. mixed with siderite and carbonate in banded chert. -py. and po. beds with minor siderite. -oolitic pyrite in black shale.	Deeper parts of basins, no water agitation, organic carbon preserved, H_2S formed by bacteria, little clastic sedimentation.

1) Work by Gruner (1922) and later supported by Gill (1927) and James (1954) among others suggested that iron was mainly derived from weathering of continental land masses under humid, tropical and subtropical conditions, a suggestion that is still current in the literature (e.g. Beukes, 1973).

2) The release of iron through sea bottom reaction on clastic materials and its concentration by selective sea bottom precipitation or diagenetic reactions was proposed by Strakhov (1959) and Borchert (1960) among others.

3) The derivation of iron from contemporary volcanism was first propounded by van Hise and Lieth (1911) and later expanded by, among others, Goodwin (1956, 1962) and Oftedahl (1958) who speculated that iron (as well as other metals) enriched in gasses expelled from a crystallizing magma would precipitate on the sea floor upon their discharge into the submarine environment. Oftedahl (1958) termed the deposit thus formed "sedimentary exhalative" and variations of this concept were later invoked to account for the origin of Archean Algoma-type iron formation (e.g. Goodwin, 1962; Ridler, 1970; Hutchinson et al., 1971), ferruginous mudstones associated with ophiolite successions (Elderfield et al., 1972; Robertson and Hudson, 1973, 1974; Bonatti et al., 1976) and ferruginous chert in an island arc environment (Iwao, 1970).

2.3.2 Recent Deposits Related to Volcanism at Spreading Axes

Metalliferous sediments on the East Pacific Rise have been the object of detailed studies as examples of chemical precipitates on an active spreading axis (Bostrom and Peterson, 1966, 1969; Bostrom et al., 1969;

Bostrom, 1970). These sediments are characterized by a high accumulation rate (Bostrom, 1970) and consist dominantly of goethite, iron-rich montmorillonite and manganese hydroxides (Bostrom and Peterson, 1969). They differ significantly from normal pelagic sediments, being relatively enriched in Fe, Mn, V, As, U, Cd, Zn, B and Hg (Bostrom et al., 1972) and depleted in Al and Ti (Bostrom and Peterson, 1966). Similar patterns are also reported from sediments in the median valley of the Mid-Atlantic Ridge where Cronan (1972) reported significant enrichment of Fe, As and sometimes Hg and a depletion of Al relative to normal pelagic sediments.

Bostrom and Peterson (1966, 1969) considered these sediments to be hydrothermal in origin, resulting from the precipitation of metals from mineralizing solutions which originated in the mantle and rose directly to the sea floor at the spreading axis (Fig. 2.2). Other workers have stressed the role of hydrothermal leaching of volcanic rocks as a source of metals in the solutions (Bonatti and Joensuu, 1966; Corliss, 1971; Hart, 1973). Bonatti et al. (1972) suggested that hydrothermal deposits could be distinguished from more slowly accumulating hydrogenous deposits by virtue of their lower Cu+Ni+Co values and high Fe/Mn ratio and by their depletion in thorium relative to uranium (Fig. 2.3) and concluded that hydrothermal deposits predominate in areas of active volcanism.

Basal metalliferous sediments in DSDP cores from the Pacific Ocean were described by von der Borch and Rex (1970) and von der Borch et al. (1971) who noted their similarity with the East Pacific Rise deposits and proposed that these were formerly deposited on the rise and subsequently

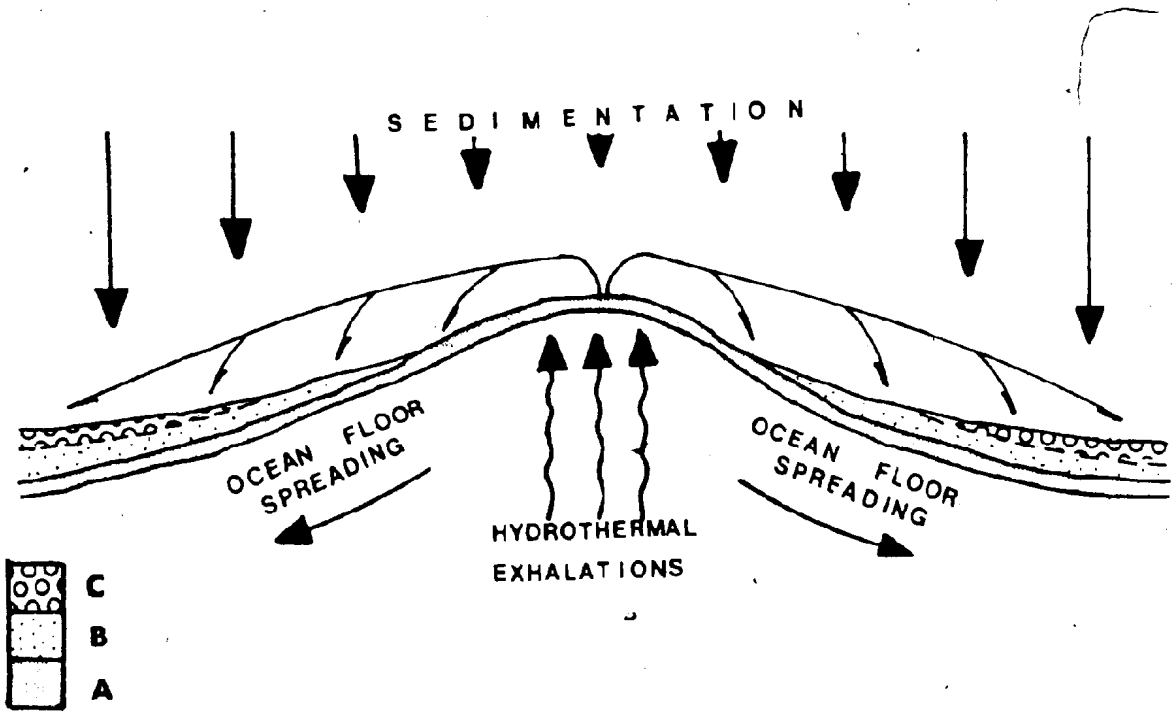

FIG. 2.2 Schematic representation of sedimentation processes on the East Pacific Rise; A - Detrital (+ pelagic) facies; B - mixed amorphous iron oxide-detrital facies; C - basal amorphous iron-manganese oxides. (after Bostrom and Peterson 1969, and von der Borch and Rex, 1970).

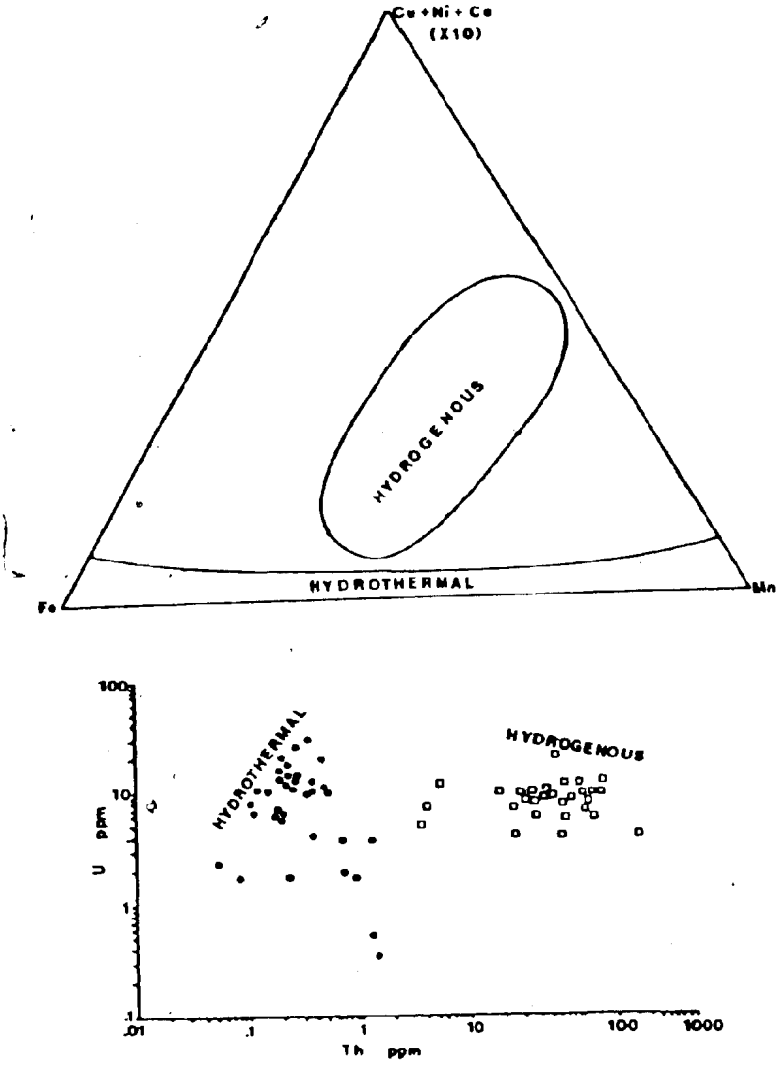

FIG. 2.3 Chemical distinction between recent hydrothermal and hydrogenous ferromanganese deposits on the basis of Fe/Mn/(Cu+Ni+Co) and U/Th ratios (after Bonatti et al., 1972)

transported out of the active spreading zone as a result of sea floor spreading. Dymond et al. (1973) reviewed the chemistry of metalliferous sediments from the East Pacific Rise, Bauer Deep and basal cores at a number of DSDP sites and concluded that similarities in their distinctive chemical, mineralogical and isotopic compositions pointed to a common origin. These characteristics included a high transition metal versus low Al content and predominance of goethite, iron-montmorillonite and manganese hydroxides. They noted that in all cases, while sulfur, uranium and oxygen isotope compositions are consistent with formation from sea water at low temperatures and Sr isotope composition and REE patterns are similar to sea water, lead isotope compositions resemble that of mid-ocean ridge tholeiitic basalts. They affirmed that the chemistry of the deposits is best explained by their precipitation from volcanic hydrothermal exhalations but noted that the mechanism for enrichment of these fluids in the first instance is still uncertain. The REE, Sr, U and sulfur are thought to originate in sea water and Fe, Mn, Si, and Pb are probably of magmatic origin but the original source of other enriched elements is still uncertain (Dymond et al., 1973).

Metalliferous sediments associated with thermal brines in the Red Sea have been described by Miller et al. (1966), Bischoff (1969) and Bignell et al. (1976) among others. These sediments are highly enriched in Fe, Mn, Zn, Cu, Cd, Pb and Hg (Miller et al., 1966) and show considerable vertical and lateral variability (Bischoff, 1969; Bignell et al., 1976). Bischoff (1969) described sediments from the Atlantis II, Discovery and Chain deeps and suggested that hot metal-rich brines were being discharged

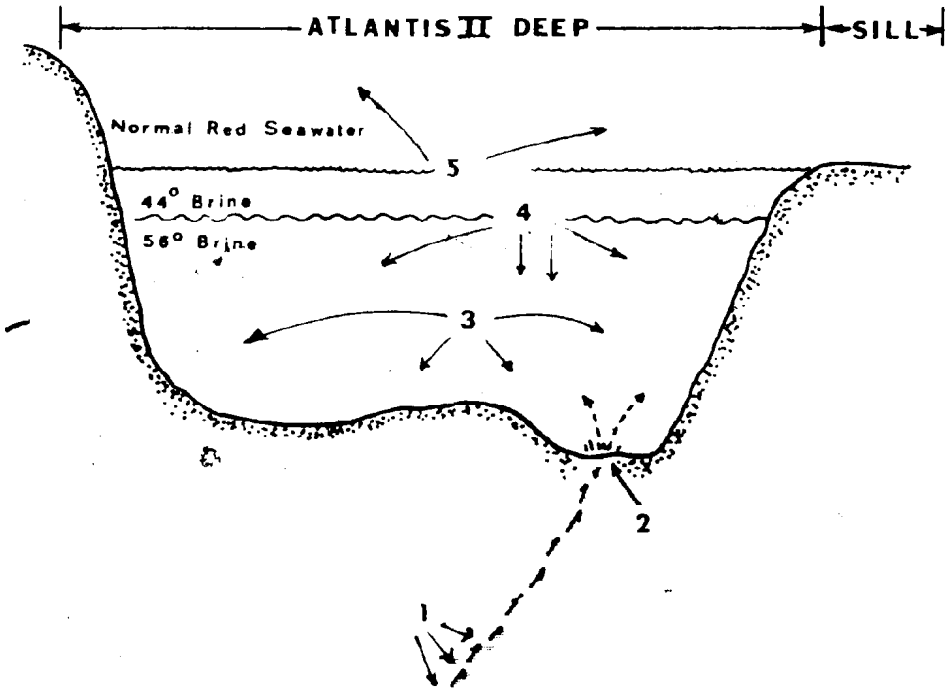

FIG. 2.4 Schematic representation of some mineral precipitation processes in the Atlantis II Deep, Red Sea; 1 - ZnS and PbS precipitate along cracks and fissures from cooling and release of metals from complexes; 2 - point of brine discharge; 3 - ZnS precipitates due to cooling and release of metals from complexes; 4 - $CaSO_4$ precipitates due to mixing; Fe^{2+}, $Fe^{3+}Si_8O_{20}(OH)_4.nH_2O$ precipitates due to partial oxidation and cooling; 5 - $Fe(OH)_3$ precipitates due to oxidation (after Bischoff, 1969).

into the Atlantis II Deep where precipitation of the sediments due to cooling and mixing of the brines with Red Sea water occurred (Fig. 2.4). Craig (1969) suggested that the brines were composed of recirculated Red Sea water which had been heated and enriched in soluble components during passage through the subsurface. Bignell et al. (1976) described sediments from brine pools discovered subsequent to Bischoff's work and, noting the similarity of these sediments to the previously discussed deposits in the Pacific Ocean, suggested a similar origin for the Red Sea and Pacific Deposits.

2.3.3 Recent Deposits Related to Volcanism at Consuming Plate Margins

Highly ferruginous and/or manganiferous sediments enriched in a number of metals and associated with post-volcanic fumarolic activity at or near consuming plate margins have been documented from a number of areas including Indonesia (Zelenov, 1964), the Mediterranean (Pushkina, 1967; Butuzova, 1966; Bonatti et al., 1972; Puchelt, 1973), and New Britain, T.P.N.G. (Ferguson and Lambert, 1972; Ferguson et al., 1973). The nature of these deposits is briefly described below.

The composition of thermal waters and associated chemical precipitates at the submarine Banu Wuhu volcano, Indonesia, an andesite-dacite dome with a history of recent eruptions, was examined by Zelenov (1964). He observed that around the margins of the volcano, jets of hot water were being discharged into sea water and that iron and manganese hydroxides could be seen precipitating in the water column adjacent to these springs. In addition the thermal waters were found to be enriched in silica relative to sea water. Encrustations on boulders proximal to the

springs were found to carry up to 40% Fe and 7% Mn and to be enriched in V, Sr, Mo, Cu, Zn, Ba, Ni, Co, Zr, Pb, Sn, Ge, Ga, Y and Yb in amounts comparable to pelagic manganese nodules. Zelenov (1964) estimated that between 900 and 9000 tons of suspended Fe and Mn was introduced into the ocean each year by fumarolic activity at this volcano.

Detailed studies of thermal waters and their deposits resulting from post-volcanic fumarolic activity on the island of New Britain have been reported by Ferguson and Lambert (1972) and Ferguson et al. (1973). Analysis of thermal waters at Matupi Harbour by Ferguson and Lambert (1972) showed them to be hot, acid and slightly to highly oxidizing and to be significantly enriched in Fe,Mn, Zn, Cu, Pb and As and depleted in most salts relative to sea water. Precipitates around these springs commonly consist of dominantly amorphous iron oxide with sporadic crystalline goethite carrying Mn, Zn, Cu and Pb. They appear to result from the cooling of the hot solutions coupled with increasing pH and Eh due to mixing of the brines with sea water. Mn tends to increase in concentration relative to Fe away from the springs. Ferguson and Lambert (1972) noted that SO_4/Cl, Br/Cl, and B/Cl ratios in the thermal waters differed little from those of average sea water and suggested that the thermal water originated as sea water and became enriched in metals through subsurface leaching of volcanic rocks. The role of the environment in determining the nature of sediments resulting from fumarolic activity is illustrated by the deposits at Talasea, New Britain where exhalations similar to those at Matupi Harbour are being discharged into a reducing environment producing sediments dominated by iron sulfides (Ferguson et al., 1973).

Fumarolic activity and chemical sedimentation associated with recent volcanism in the Mediterranean area has been reported from Stromboli, Italy (Bonatti et al., 1973) and from the Santorini Islands, Greece (Pushkina, 1967; Butuzova, 1966; Bonatti et al., 1972; Puchelt, 1973; Cronin et al., 1976). In the former area, sediments enriched in Fe, Mn, and Si (opal) and depleted in Al and Ti were recovered from the flanks of the Stromboli volcano although no presently active fumaroles were seen (Bonatti et al., 1973). In the latter area, Pushkina (1967) analyzed the waters proximal to thermal springs on the island of Nea Kameni, and found that while they were significantly enriched in Fe, Mn, Si and P, the principal cation and anion composition of the water was not noticeably affected. She further noted that the waters tended to be slightly acidic near the springs but that the pH as well as the element concentrations tended to normalize away from the spring towards the mouth of the bay. Sediments being formed from these solutions are rich in Fe (mainly ferric hydroxide gel), Mn and Si, and a gradual decrease in the Fe/Mn ratio towards the periphery of the basin was noted by Butuzova (1966) who ascribed this feature to the decreasing relative solubility of Mn with increasing pH. Silica in the sediments is dominantly opalline and is ascribed by Butuzova (1966) to biogenic precipitation.

2.3.4 Summary

The features of the origin and occurrence of iron-rich and ferruginous sedimentary rocks relevant to the present study as revealed from ancient and modern deposits can be summarized as follows;

1) Highly ferruginous, rapidly accumulating deposits in active volcanic terrains result from the fumarolic discharge of iron-rich thermal waters and subsequent precipitation of the iron in the submarine environment. Significant contributions may also be made by the weathering of land masses in a humid, tropical to subtropical environment.

2) The thermal waters are dominantly composed of recirculated sea water which has been heated and enriched in metals via leaching in the subsurface.

3) The initial precipitation of ferric hydroxides may take place in the water column. The final form and mineralogy of the ferruginous deposit is dependent on Eh and pH conditions during diagenesis.

4) These processes are operative in any area characterized by high heat flow, i.e. at both spreading and consuming plate margins.

2.4 Chemical Sedimentation in Ancient Island Arc Regimes

Algoma-type iron formation and associated sedimentary rocks are found in Archean greenstone belts around the world (see review papers by Goodwin, Bayley, James, Beukes, Von Dorr, Trendall and Alexandrov in James and Sims, 1973) and apparently reached their greatest abundance at this time (Gross, 1965). It has been suggested that the closest modern analogues to Archean greenstone belts, on the basis of volcanic lithologies, associated sedimentary rocks, and general tectonic environment, are the island arc regimes (Goodwin and Ridler, 1970; Goodwin, 1973a), but as yet there is no agreement as to whether similar tectonic processes were operative during their formation (e.g. Sutton and Bridgewater, 1974). The chemical

sedimentary association of the greenstone belts is more abundant than is its counterpart in the Phanerozoic island arcs but the two are very similar in many respects. The essential features of the Archean deposits as compared to the sedimentary association studied during the present project (see also Chap. 3) can be summarized as follows:

1) Single deposits in the Archean range from centimeters to many tens of meters in thickness and are typically lenticular and discontinuous. The present deposits are of similar physical form while commonly not attaining as great a maximum thickness.

2) The Archean stratigraphic assemblages are heterogeneous, typically containing interbanded ferruginous chert and hematite or magnetite associated with various volcanic rocks, greywacke, ferruginous and/or siliceous shale and tuff (Gross, 1965) as shown by Fig. 2.5 (after Beukes, 1973). A similar association is present in the Upper Ordovician-Silurian volcanic succession of Central Newfoundland.

3) The oxide facies of iron formation, characterized by magnetite and lesser hematite, is typically predominant in the Archean although minor amounts of the carbonate and sulfide facies' are usually present (Goodwin, 1962, 1973). In the Central Newfoundland succession, only the oxide facies is developed and this is characterized by hematite rather than magnetite suggesting that these sediments were deposited in a more oxidizing environment than their Archean counterparts.

4) Archean iron formation is commonly associated with andesite/dacite pyroclastic domes interpreted to reflect volcanic centers (Goodwin, 1962; Ridler, 1970; Hutchinson et al., 1971; Fig. 2.6). A similar situation prevails, although on a smaller scale, in the depositional basin of the

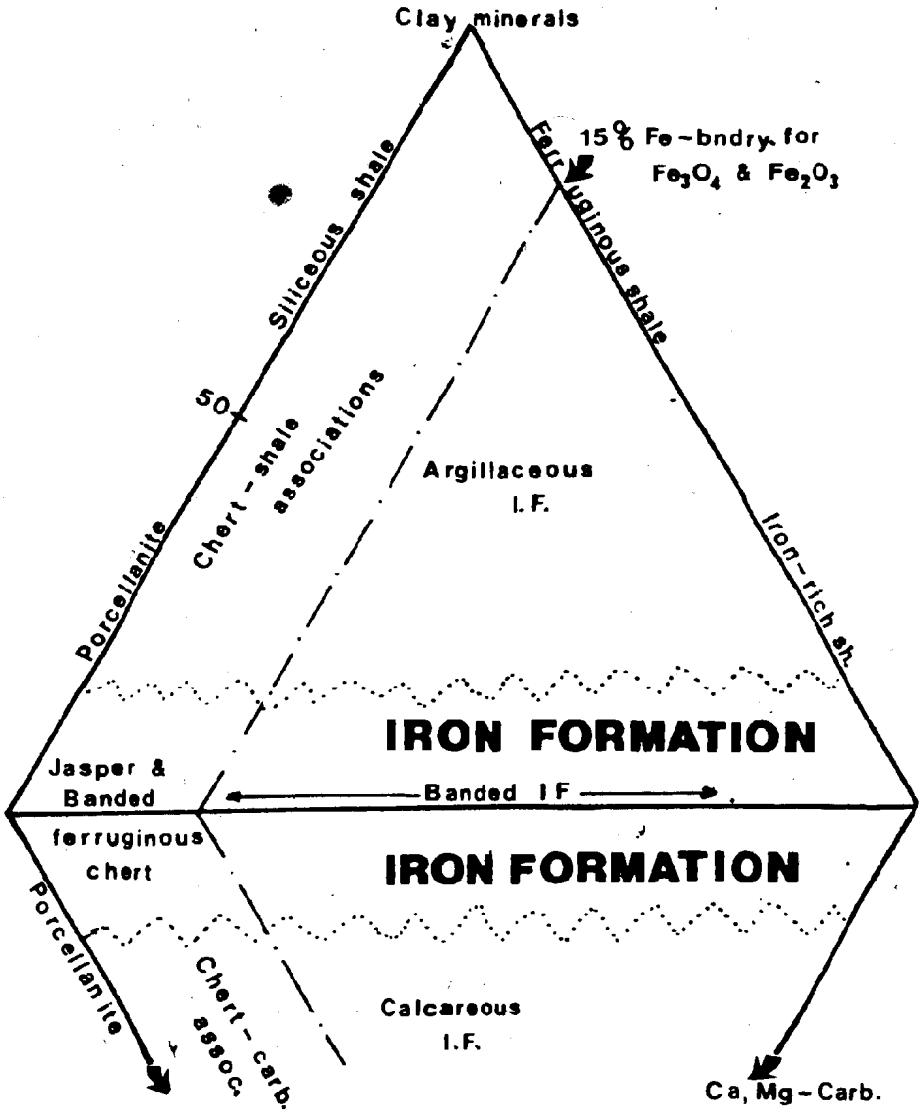

FIG. 2.5 Classification of iron-formation and related rocks (after Beukes, 1973)

Gullbridge ferruginous chert and the abundance of silicic pyroclastic rocks in the Fortune Harbour area is suggestive of a similar geologic setting. This association is not commonly present in the Roberts Arm area.

The close association of Algoma-type iron formation and its related sediments with volcanism has led most recent workers to suggest that at least the iron and the silica in these sediments, as well as the metals in their sulfide-rich equivalents, are of volcanic-exhalative origin (e.g. Goodwin, 1962; Gross, 1965; Ridler, 1970; Hutchinson et al., 1971). The exhalative components are generally considered to have precipitated inorganically on the sea floor in response to changing Eh and pH conditions (Gross, 1965; Goodwin, 1973) which in turn reflect the sedimentary basin configuration during deposition (represented schematically by the lateral extent of the various iron minerals in Fig. 2.6). There is some recent evidence to suggest that biogenic precipitation of silica may have occurred as well (LaBarge, 1973).

In the Phanerozoic, chert and ferruginous sediments are generally considered to be typical of ophiolite rather than island arc regimes (e.g. Grunau, 1965; Garrison, 1974), a fact that is generally explained by the assumption that extensive clastic sedimentation and volcanism around an active arc (Dickenson, 1974) would tend to dilute the more slowly deposited chemical sediments beyond recognition (Garrison, 1974). Kanmera (1974) noted that in the Paleozoic volcanic sequences of Japan, chert is rare in the Silurian-Devonian active arc sequence but becomes extensive in the alkalic and tholeiitic Carboniferous to Permian sequence which is interpreted by him to represent a marginal basin (spreading) environment.

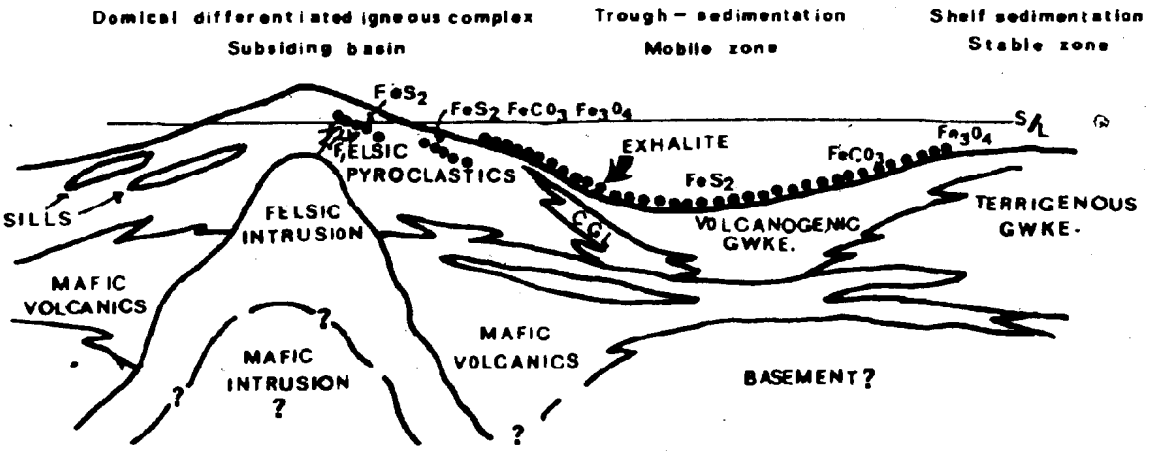

FIG. 2.6 Archean tectonostratigraphic relations in the Abitibi belt. Exhalite facies are indicated by the various iron minerals. Full width of section - approx. 80 km, maximum vertical thickness 16 km (after Hutchinson et al., 1971).

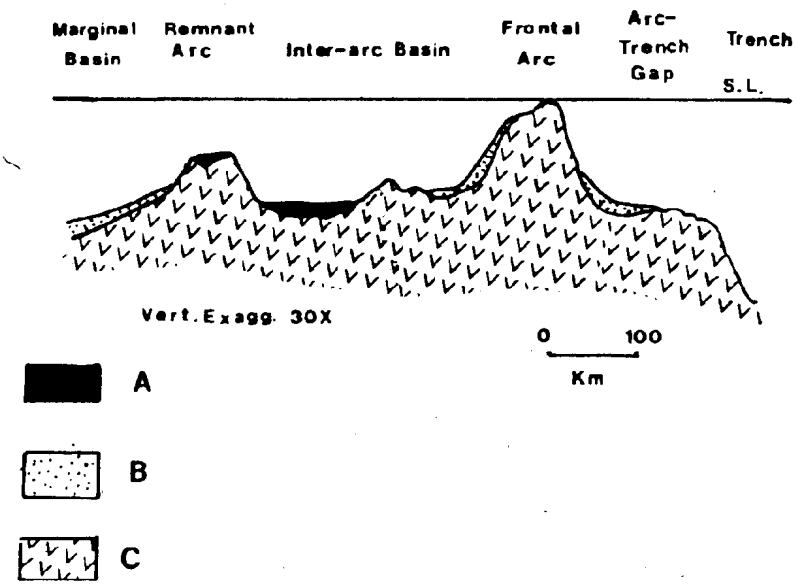

FIG. 2.7 Hypothetical areas of pelagic sedimentation in an island arc regime. A - pelagic sediment, B - volcaniclastic aprons, C - effusive volcanic rocks (after Garrison, 1974).

Mention of chert and ferruginous sedimentary rocks in the Phanerozoic island arc sequences is commonly restricted to those horizons spatially related to sulfide deposition. Perhaps one of the most intensely studied of these is the Lower Ordovician iron formation which overlies the massive sulfide deposits in the Bathurst, New Brunswick area (McAllister, 1960; Davies, 1972; Whitehead, 1973). These units commonly include a hematite-chert oxide facies apparently similar to that developed in the present study area but which, in contrast to the Central Newfoundland deposits, can often be traced for considerable distances along strike. The New Brunswick ferruginous deposits are commonly magnetite-bearing in the oxide facies, and are locally developed in the silicate, carbonate and sulfide facies (Davies, 1972). Most recent workers link the iron formation to fumarolic activity which is seen as having been responsible for deposition of both the iron formation and the underlying sulfide deposits in topographic depressions on the sea floor (McAllister, 1960; Whitehead, 1973; Davies, 1972).

The author is not aware of any comprehensive survey of chemical sedimentation in a complete island arc sequence. Garrison (1974) has summarized the types of pelagic sediments expected around an island arc noting that these would be typically small, lenticular, scattered and interbedded with thick volcanic sequences and would be most abundant in the more detritus-free settings such as inter arc basins or the tops of remanent arc ridges (Fig. 2.7).

CHAPTER 3

GENERAL GEOLOGY

3.1 Introduction

This chapter describes the local geology in each of the three areas studied and places them in their regional geological and tectonic framework. Because of the considerable amount of relatively local geologic work conducted in Central Newfoundland in the past, a serious problem of nomenclature has arisen which has hampered attempts to correlate units over any distance. Thus, this chapter will proceed from the specific to the general, first describing the local geology and history of the Roberts Arm, Fortune Harbour and Gull Pond areas separately and noting attempts at correlation of the units involved in the present study (Fig. 3.2), followed by a description of their presently interpreted tectonic setting.

3.2 Roberts Arm Area

3.2.1 Previous Work

The earliest geological studies in the Roberts Arm area were carried out by Alexander Murray and James Howley (1881, 1918) as part of their comprehensive study of insular Newfoundland. Murray, influenced by the work of Sir William Logan, assigned the volcanic and sedimentary rocks in this area to the "Quebec Group". Detailed maps were prepared but later destroyed by fire in the Crown Lands office, St. John's.

Regional mapping was undertaken in Notre Dame Bay by the Princeton University Geological Expeditions to Newfoundland of 1915, 1916

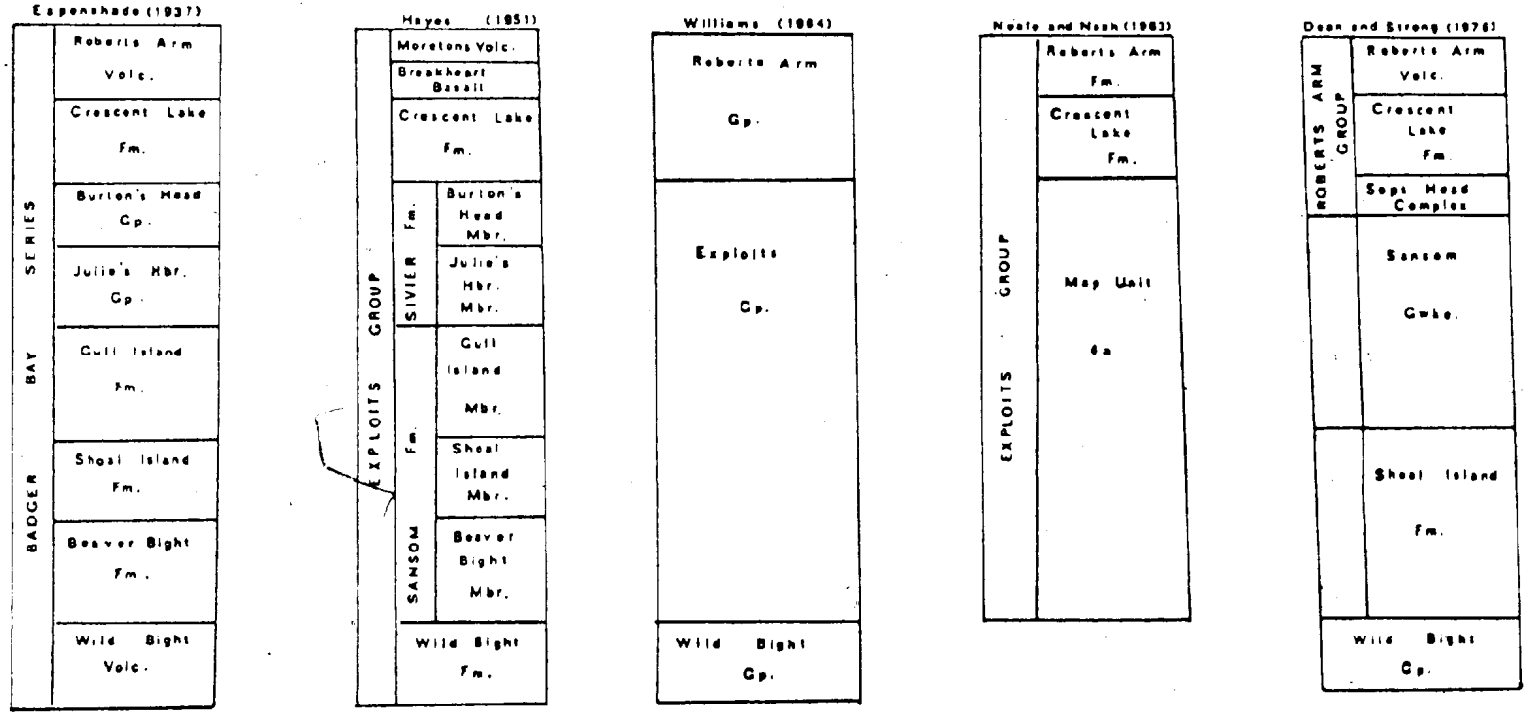

FIG. 3.1 Comparative stratigraphic nomenclature of previous workers in the Roberts Arm area.

and 1919. Results of particular relevance to this study were reported by Sampson (1923) from his study of the ferruginous cherts of Notre Dame Bay who noted the similarity between the geology of central Newfoundland and parts of Great Britain and assigned Cambrian (?) and Ordovician ages to the volcanic and sedimentary rocks he found.

Probably the most significant early contribution to the understanding of Western Notre Dame Bay stratigraphy was made by Espenshade (1937) as a result of his mapping of the coastline and adjacent islands between Burnt Heat on the west and Wild Bight on the east (see Fig. 1.2). He was the first to recognize the fundamental structural break marked by the Lobster Cove fault and named the two distinct sequences separated by it the "Pilley's Series" and the "Badger Bay Series" to the north and south respectively. Espenshade assigned a probable Ordovician age to both series but noted that their relative ages were uncertain. He coined the name "Roberts Arm Volcanics" for the uppermost unit of the Badger Bay Series and divided the underlying sediments into several formations (Fig. 3.1).

The first geological map to include the complete Roberts Arm study area was produced by Hayes (1951) who extended Espenshade's work inland to the south. He demonstrated the southward continuity of Espenshade's coastal stratigraphy but was much impressed by the lithologic similarity of the "Badger Bay Series" with strata mapped by Heyl (1936) in the Bay of Exploits. Reasoning that Heyl's nomenclature should stand because of precedence, he renamed much of the stratigraphy according to the latter's work.

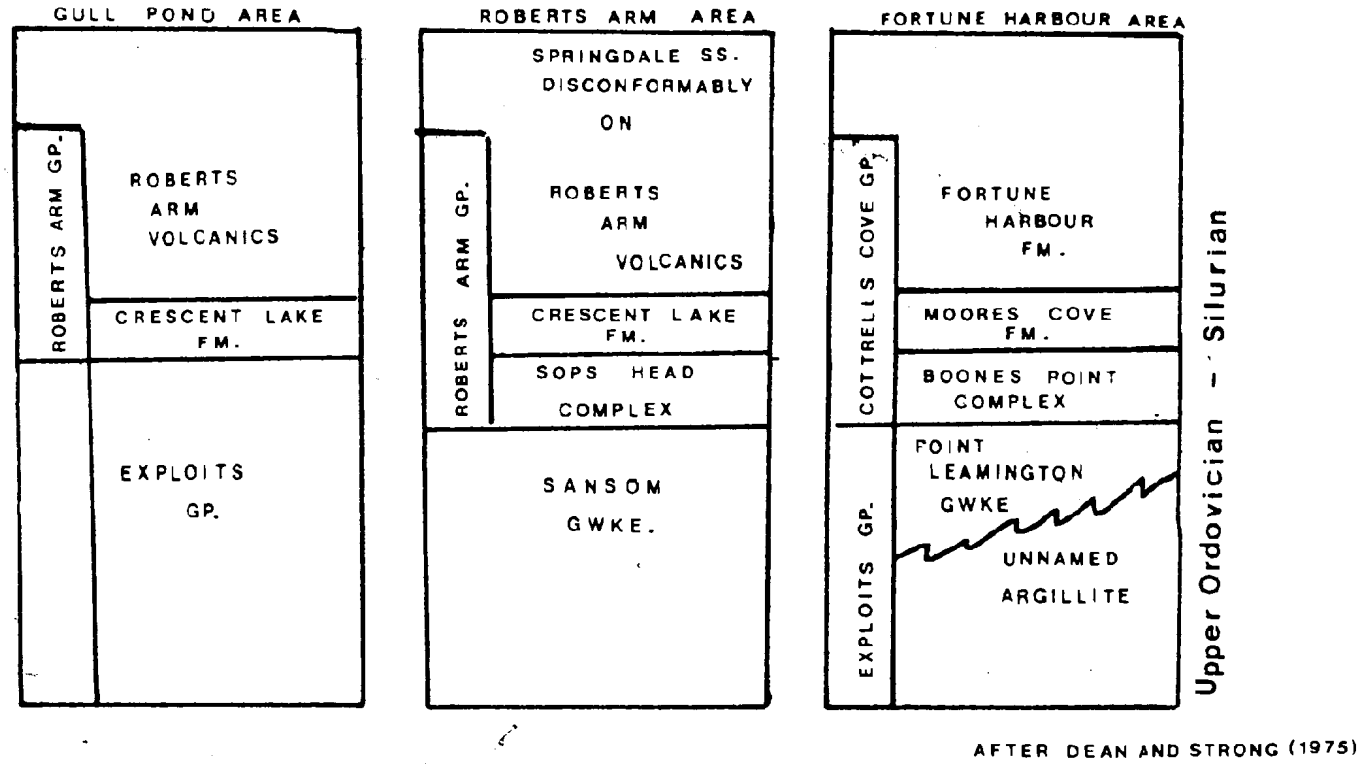

FIG. 3.2 Stratigraphic correlation between the three study areas (after Dean and Strong, 1975).

Williams' (1962,1964) geologic compilation of the Botwood map sheet at a scale of 1" = 4 mi. was the first attempt to put the Roberts Arm area into a regional perspective. In the 1962 work, Williams considered the whole of Espenshade's Badger Bay Series to be correlative with Heyl's (1936) Exploits Group but in the later edition (1964), he redefined the Exploits Group to include only the dominantly sedimentary sequence overlying the Wild Bight Group and underlying Espenshade's Crescent Lake Formation. The Crescent Lake Formation and the Roberts Arm Volcanics were combined to form the Roberts Arm Group.

Detailed (unpublished) mapping at 1" = 1/4 mi. by Noranda Mines staff (1971) further clarified the distribution of lithologies within the Roberts Arm Group and clearly indicated the relative concentration of felsic volcanics and economic mineralization at the top of the sequence.

Recent mapping by Bostock (1975, 1976) has further refined the detailed distribution of lithologies in the Roberts Arm area while confirming the general stratigraphy presented by previous workers.

Detailed mapping and geochemical studies within the Roberts Arm Group by Strong (1973, 1975) has outlined the geochemical nature of the Roberts Arm Volcanics and this will be further described in a subsequent section.

Dean and Strong (1975, 1976), on the basis of regional correlations across Notre Dame Bay, redefined the Roberts Arm Group to include the basal Sops Head Complex comprising intercalated mafic volcanic rocks, greywacke and shale previously assigned to the upper Burton's Head Formation of the Exploits Group (Fig. 3.2).

3.2.2 General Geology

The Roberts Arm Group is divisible into three units, the basal Sops Head Complex, the Crescent Lake Formation and the uppermost Roberts Arm Volcanics (Dean and Strong, 1976). It is underlain, in part conformably, by the Exploits Group, a thick succession of turbidites, marine shale, chert and minor mafic flows.

The Sops Head Complex consists of mafic flow rocks intercalated with greywacke and shale. Volcanic rocks are relatively rare at the base of the sequence but tend to increase in abundance with increasing stratigraphic level (Dean and Strong, 1976).

The Crescent Lake Formation comprises a relatively deformed sequence of interbedded red and green chert, red siltstone and shale and acid tuff possibly up to 170 meters thick (Hayes, 1951). The overlying Roberts Arm Volcanics consist of a suite of basaltic and dacitic flows and pyroclastics which are chemically bimodal but of calc-alkaline affinity (Strong, 1973) and include vesicular lavas, massive and pillowed flows, volcanic breccia, massive silicic flows and fine to coarse grained pyroclastic rocks. The lower portions of the volcanic pile are dominantly pillowed and massive flows with intercalated red siltstone and chert similar to the Crescent Lake Formation lithologies. The upper portion of the sequence contains a higher proportion of silicic flows and pyroclastic rocks, the distribution of which suggests that at least two centers of explosive silicic volcanism, located in Sunday Cove west of Pilley's Island and in Halls Bay west of Burnt Head, were active during late Roberts Arm time (Bostock, 1975). Locally, the volcanic pile is

unconformably overlain by the Springdale Group consisting in this area mainly of fluvatile red sandstones and conglomerate of probable Silurian age (Neale & Nash, 1963).

The northern boundary of the Roberts Arm Group is marked by the Lobster Cove fault, interpreted to be a major thrust of probable upper Silurian age (Dean and Strong, 1975). Rocks immediately north of this fault, assigned to the Lushs Bight Group (Espenshade's "Pilleys Series"), are mainly massive and pillowed basalts and diabase dykes of oceanic tholeiite affinity thought to represent Lower Ordovician ocean crust (Smitheringale, 1972; Strong, 1973).

The Roberts Arm Group is intruded southeast of Woodford's Arm by the Woodford's Arm granite pluton which may be consanguinous with the silicic volcanic rocks in the upper part of the volcanic pile (Espenshade, 1937; Bostock, 1975). Further west, the Mansfield Cove granodiorite is in fault contact with the volcanic rocks and its relative age is uncertain (Bostock, 1975).

The structure within the Roberts Arm Group is relatively uncomplicated. The beds are typically steep to vertically dipping and, at least in the upper two-thirds of the sequence, north-facing. Minor exceptions are present on Haywards Head where south-facing pillows may be due to local faulting (Bostock, 1975). South of Crescent Lake, the less competent Crescent Lake Formation has been folded into a series of northeast to north-trending folds (Hayes, 1951) which appear to repeat the stratigraphy and allow the Crescent Lake Formation to be exposed in the cores of anticlines.

A fault system which may be of some stratigraphic importance, cuts the approximate center of the volcanic section. This fault trends at a small angle to the stratigraphy northeast into Woodford's Arm where it forms part of the southern boundary of the Woodford's Arm pluton. From Woodford's Arm, it swings (or branches) eastward emerging on the coast in Stag Cove. It has not proved possible to correlate stratigraphy across this fault and the extent to which it may interrupt (or repeat) the succession is not known.

3.3.3 Occurrence of Chert and Ferruginous Sediments in The Roberts Arm Area

Chert, ferruginous chert and iron-rich sedimentary rocks commonly associated with siliceous and ferruginous siltstone, shale, greywacke, tuff and mafic flow rocks are present in minor amounts throughout the Roberts Arm Group. They are commonly various shades of red and green with sporadic black, white and light brown varieties being found. They are usually colour-laminated with individual laminae ranging from less than 1 millimeter to several centimeters.

Ferruginous chert is widespread within the Crescent Lake Formation and is commonly well-bedded and intercalated with red siltstone and silicic tuff (Plate 3.1). This chert is typically red although rare green varieties are sometimes seen. There appears to be a complete gradation between relatively pure red chert and red siltstone with an abundance of intermediate varieties consisting of ferruginous chert diluted by clastic and/or tuffaceous material.

PLATE 3.1 Red ferruginous chert interbedded with silicic tuff and tuffaceous greywacke in the Crescent Lake Formation.

PLATE 3.2 Red chert surrounding mafic pillows in the Roberts Arm Volcanics.

In the lower regions of the Roberts Arm Volcanics, chert and ferruginous sediments are typically bedded, occurring in thin, laterally discontinuous lenses. They are often intercalated with red siltstone, greywacke and tuff, especially near the base of the volcanic sequence, and in some stratigraphically higher regions occasionally lie directly on top of pillow lavas. Rare, narrow (up to 30 cm) beds of massive hematite are present and occasional sole markings and minor slump features are the only sedimentary structures visible in outcrop.

Higher in the volcanic sequence, particularly north of the Woodford's Arm-Stag Cove fault system, chert and ferruginous sediments less commonly form coherent beds. Abundant chert occurs marginal to pillows where it may completely surround individual pillows or more typically occur in pods filling openings at pillow junctions (Plate 3.2). Rarely, convolute, thin lenses and pods of red chert are found within the pillows themselves and around the pillow margins, chaotic fine laminations and irregular wispy fragments suggesting soft-sediment brecciation are often present.

Veining by calcite, epidote and quartz is present sporadically in the sediments throughout the volcanic sequence and rare grains of pyrite and chalcopyrite are seen.

3.3 Fortune Harbour Area

3.3.1 Previous Work

The earliest work in the Fortune Harbour area, as in the Roberts Arm area, was carried out by Murray and Howley (1881, 1918) and by the Princeton University Geological Expeditions to Newfoundland.

Geologists from Princeton University returned to Notre Dame Bay in the 1930's and Heyl (1936) mapped the eastern part of the Fortune Harbour peninsula during his study of the geology of the Bay of Exploits. He presented an interpretation of the Ordovician-Silurian stratigraphy in this area and coined the term Exploits Series to define a thick sequence of volcanic and sedimentary rocks which included those of the present study.

The area was included in Williams' (1962, 1964) compilations of the Botwood map sheet at 1" = 1/4 mi. In the final (1964) version, he postulated a major break, the Lukes Arm fault, running ESE from Southeast Arm to Muddy Hole and, by inference, correlated all volcanic and sedimentary rocks north of this fault with Espenshade's (1937) "Pilleys Series" to the west. Because of the inclusion of units directly south of the fault in the Exploits Group, this precluded the presence of Roberts Arm Group equivalents in this area.

The first detailed map of the Fortune Harbour peninsula was produced by Helwig (1967) who supported Williams' (1964) implied correlation of the Lukes Arm and Lobster Cove faults and assigned all rocks north of this fault at Fortune Harbour to the Lushs Bight Group.

Remapping of the northern part of the peninsula was carried out by Dean (1973), who recognized that the major break separating the Lushs Bight Group from younger volcanic rocks was, contrary to previous thought, considerably north of the Lukes Arm fault. He correlated this break with the Chanceport fault previously identified on New World Island to the east (Strong and Payne, 1973) and with Espenshade's (1937) Lobster

Cove fault to the west. He named the volcanic sequence north of this fault the "Moreton's Harbour Group" (after Strong and Payne, 1973) and the volcano-sedimentary sequence south of it, the Cottrell's Cove Group, which he suggested was a lithologic and probably a time equivalent of the Roberts Arm Group to the west and Strong and Payne's (1973) Chanceport Group to the east. This interpretation of the stratigraphy and correlations in this part of Notre Dame Bay provided the incentive to include the Fortune Harbour area in the present study.

3.3.2 General Geology

Previous workers in the area have proposed a varied nomenclature based on their interpretation of the geologic relations. The present study accepts the interpretation of Dean (1973) and further refined by Dean and Strong (1976) and the nomenclature used herein is based on the latter work (Fig. 3.1).

The Cottrell's Cove Group encompasses the Upper Ordovician-Silurian volcano-sedimentary sequence on the Fortune Harbour Peninsula comprising in ascending stratigraphic order the Boones Point Complex, the Moores Cove Formation and the Fortune Harbour Formation.

The present study was carried out within the Fortune Harbour Formation which is similar in stratigraphy to the Roberts Arm Volcanics and conformably overlies the Moore's Cove Formation, a sequence of tuffaceous greywackes correlative with similar strata at the base of the Roberts Arm Group. At the base of the volcanic sequence, a relatively thin (approximately 20 m) unit of intercalated red and green chert, red siltstone and silicic tuff is exposed in North Harbour and in Rowsells

Cove. The lower part of the volcanic succession comprises up to 2000 meters of mainly mafic pillow lava and volcanic breccia, locally containing minor interbeds of chert and siltstone. Within the upper Fortune Harbour Formation, there is a distinct member of coarse to fine silicic pyroclastics and porphyritic flows interbedded with red and green chert which reaches a maximum thickness of 1000 meters in the Fortune Harbour area. This unit and its equivalents in the Bay of Exploits were previously designated the "Fortune tuffs and cherts" by Heyl (1936). The silicic tuff and chert member is overlain by a thin mafic pillow lava unit near Fleury Bight but to the southeast the Chanceport Fault cuts it and the overlying units are not seen. Chemical analysis of volcanic rocks in the Fortune Harbour Formation show them to be of calc-alkaline affinity and comparable to those of the Roberts Arm Group (Strong, 1975).

The Fortune Harbour Formation is intruded by minor concordant gabbroic and diabasic sills, mainly within the silicic member, and later lamprophyre dykes of probable late Cretaceous age (Wanless et al., 1965).

The Cottrell's Cove Group is consistently steeply dipping and north- to northeast-facing, and there appears to be a continuous stratigraphic section present between Muddy Hole and the Chanceport fault. Minor folds are occasionally seen on outcrop scale, but they do not appear to significantly repeat the stratigraphy.

3.3.3 Occurrence of Chert and Ferruginous Sediments in the Fortune Harbour Formation

Chert is present throughout the Fortune Harbour Formation, but not as widespread as within the Roberts Arm Group. Red chert is occasionally found in the interstices between pillows in the mafic flows but is more commonly seen as thin, conformable lenses between flows and as fragments in volcanic breccia. Occasional relatively thick (greater than 10 meters) sections of red, green and white chert interbedded with red siltstone, shale and silicic tuff are found, the most prominent of which occurs in Rowsell's Cove very near the base of the Fortune Harbour Formation where more than 20 meters of red and green chert intercalated with silicic tuff is exposed in a series of tight isoclines.

Chert is considerably more common in the silicic volcanic member where beds of red, green and white chert are typically interbedded with fine to coarse pyroclastic rocks, and chert fragments are common in the volcanic breccia.

Near the south end of Fortune Harbour and adjacent to the Chanceport fault, red chert occurs intimately associated with bedded manganese oxides. The deposit was mined in the early twentieth century and is now rather poorly exposed in a series of old pits. It appears to be in excess of 7 meters thick and can be traced along strike for more than 85 meters.

3.4 Gull Pond Area

3.4.1 Previous Work

Copper mineralization has been known in the Gull Pond area since the early 1900's, and much of the early geological work in this area was connected with exploration. The first geological map of the area was prepared at a scale of 1" = 400 ft. by A.C. Bray of the Great Gull Copper Company in 1929. Exploration was carried out intermittently through the early part of the century and a summary of known geology was presented by Douglas et al. (1940) as part of a survey of Newfoundland copper deposits.

Kalliokoski (1951) produced a preliminary map of the Gull Pond area at a scale of 1" = 1 mi. and a more refined version of this map with marginal notes was published three years later (Kalliokoski, 1955). He adopted the terms "Roberts Arm Formation" and "Crescent Lake Formation" for the volcanic and underlying tuffaceous sediments respectively and "Badger Bay Series" for the Ordovician sequence as a whole, suggesting their correlations with those mapped by Espenshade (1937) further north.

The area was included in the Geological Survey of Canada 1" = 4 mi. compilation map of the Sandy Lake sheet prepared by Neale and Nash (1963) who renamed Kalliokoski's "Badger Bay Series" the "Exploits Group" after the useage of Heyl (1936) and Williams (1962).

The subdivision of the Exploits Group by Williams (1964) has never formally been extended to this area but has been used by Upadhyay and Smitheringale (1972), Noranda Mines Staff (1971) and Dean (1974) and is thus retained in the present work.

Considerable knowledge of the geology of the immediate mine area has been acquired as a result of extensive diamond drilling and underground mapping shortly before and during production from 1967 to 1971. Much of this information was compiled by the Gullbridge Mines Staff (K. Newman, chief geologist) and is available on mine plans and sections. A study of the underground geology of the Gullbridge deposit was done by Upadhyay (1970) and certain aspects of this work were later published by Upadhyay and Smitheringale (1972).

During the summer of 1975, the entire Gullbridge Mines Ltd. property was remapped at a scale of 1" = 400 ft. by the author (Swinden, 1975).

3.4.2 General Geology

The Roberts Arm Volcanics in this area attain a maximum thickness of approximately 4500 meters north of Dawes Pond but average less than 3000 meters. They conformably and gradationally overlie the Crescent Lake Formation which, unlike its type section at Crescent Lake, consists mainly of siliceous, fine to medium grained tuffaceous clastic sediments and contains little if any red ferruginous siltstone or chert. Lenses of this lithology persist intermittently for up to 1000 meters into the overlying volcanic sequence (Swinden, 1975).

The basal Roberts Arm Formation consists of from 600 to 900 meters of dominantly mafic flows in which pillows are well preserved and top directions are to the west. West and south of Gull Pond, a thick pile of fine grained silicic tuff, massive rhyolite, ferruginous chert and volcanic breccia attains a maximum thickness greater than 1500 meters.

The major component of this unit is fine grained silicic tuff and sericite schist with massive rhyolitic flows being present in greatest abundance immediately west of the Gullbridge Mine and decreasing to the north and south. Coarse pyroclastic rocks are present locally but seldom are widespread enough to form mappable units. Towards the north end of Gull Pond, the rhyolite sequence is greatly attenuated into several narrow bands of dominantly fine to medium grained siliceous clastic sediments similar to Crescent Lake Formation lithologies.

The silicic member is everywhere overlain by a second mafic volcanic member comprising fine grained basaltic flows with minor interbedded tuff.

Large intrusive bodies virtually surround the Gull Pond study area: The Twin Lakes Complex, a composite intrusion with phases ranging from granodiorite to gabbro intrudes the volcanic sequence from the west; The Topsails Granite, comprising mainly granite with minor granodiorite and quartz-diorite phases, is present to the west and a large circular granitic body, herein termed the Dawes Pond pluton, intrudes the sequence to the south. Minor dykes and sills of feldspar and quartz-feldspar porphyry are locally common as are small diabase to gabbro intrusions.

The rocks in the Gull Pond area are considerably more deformed than those in the other two areas studied. All tuffaceous rocks are highly schistose, with the foliation being axial planar to tight, upright isoclinal folds and trending N40^{o}E with steep dips

variously to the east or west. A well developed crenulation cleavage is commonly present trending slightly south of east, and kink bands are often encountered. Top directions in the volcanic sequence are scarce but those recorded are uniformly to the west and there is presently no evidence to suggest major repetition of strata by folding in the area.

A northeast-trending fault set truncates the stratigraphy in the immediate mine area, resulting in minor omission of units (Upadhyay, 1970). A second fault set trends east to southeast and can be shown to have offset the stratigraphy up to several tens of meters.

3.4.3 The Gullbridge and Southwest Shaft Copper Deposits

The Gullbridge copper deposit consists of disseminated and stringer pyrite and chalcopyrite mineralization occurring in a cordierite-anthophyllite-chlorite alteration zone which spans the uppermost 20 meters of the basal mafic pillow lava unit and the lower 50-70 meters of the overlying silicic tuff. The deposit has been described in detail by Upadhyay (1970). Approximately 3 million tons of ore averaging less than 1% copper were mined from 1967 to 1971.

The ore-bearing alteration zone, which can be traced south of the orebody for at least 5000 meters along strike, is roughly conformable with local stratigraphy and is typified away from the mine by a pyrite-chlorite-sericite-(cordierite) assemblage. Units within the alteration zone are commonly bedded, highly deformed and commonly contain discrete beds of gossan after pyrite. Pyrrhotite, magnetite and minor chalcopyrite are common constituents near the mine.

A second deposit known as the Southwest Shaft deposit, occurs at approximately the same stratigraphic level 1400 meters southwest of the main ore zone. A prominent, dominantly pyritic gossan crops out here and a shaft was sunk on it in the late 1920's to a depth of about 27 meters. The host rock is probably a metabasalt, highly altered to cordierite and anthophyllite and containing abundant disseminated and stringer chalcopyrite and pyrite. Locally intense alteration and deformation considerably complicates the detailed stratigraphy here (D. Gemmell, pers. comm., 1974) but this zone has been shown geophysically to be laterally equivalent the main ore zone (Gullbridge Mines Staff, unpub. data) and is unquestionably stratigraphically equivalent to the main ore deposit.

Upadhyay and Smitheringale (1972) considered the Gullbridge deposit to be of volcanogenic origin, suggesting that fumarolic fluids were initially responsible for the magnesium alteration and sulfide deposition in a zone which was later metamorphosed to its present form. They noted the stratigraphic relationship between the main ore zone and the Southwest Shaft deposit, implying that the latter zone also represents a zone of intense fumarolic activity.

3.4.4 Occurrence of Ferruginous Chert and Iron Rich Sediments in the Gull Pond Area

Chert and ferruginous sediments occur in a remarkably continuous horizon overlying and extending considerably beyond the Gullbridge orebody and the Southwest Shaft deposit (the "Gullbridge ferruginous chert"). This unit commonly comprises several beds of

PLATE 3.3 Thin beds of the Gullbridge ferruginous chert interbedded with silicic tuff approximately 300 m south of the Gullbridge ore body.

ferruginous (and sometimes tuffaceous) chert separated from each other by up to three meters of fine to medium grained silicic tuff. It is present stratigraphically above both the Gullbridge orebody and the Southwest Shaft deposit, generally 10 to 50 meters above the ore horizon, and appears to be laterally continuous paralleling the alteration zone between these deposits. The individual cherty beds tend to be relatively thin (less than 20 cm) and widely separated by tuffaceous material immediately above the mineralization (Plate 3.3), although about 120 meters north of the Southwest shaft, the individual beds are up to 15 meters wide and contain very little interbedded tuff. In this latter area, the chert is commonly capped by 1 to 2 cm of interbanded hematite and magnetite.

North of the Gullbridge mine, the chert horizon disappears under the lake and upon its reappearance at the north end of Gull Pond, it is considerably more discontinuous, cropping out only sporadically. Individual beds seldom exceed 30 cm and the total thickness is generally less than 10 meters. Tuff interbedded with the chert here tends to be coarser grained than that to the south, sometimes contains rounded quartz and rhyolite grains, and displays graded bedding and slump features. Narrow beds of ferruginous chert are occasionally broken up and the pieces rotated and slumped into the underlying tuff (Plate 3.4). Explosive volcanism following lithification of the chert has produced coarse volcanic breccia with included fragments of this unit (Plate 3.5).

A second major continuous horizon of ferruginous chert is present south of Gull Pond at a basalt/rhyolite contact approximately

PLATE 3.4 Broken beds of ferruginous chert (dark grey) slumped and rotated in a silicic tuff matrix.

PLATE 3.5 Ferruginous chert fragments in a coarse volcanic breccia. White matrix surrounding the fragments is poorly-sorted silicic tuff.

500 meters structurally below the mineralized zone. Its northern extremity is exposed immediately south of the southeast corner of Gull Pond from where it can be traced for over 5300 meters south along strike. It is commonly 20 to 50 meters thick consisting of massive, red to deep purple, finely laminated ferruginous chert with relatively little interbedded tuffaceous material. The physical characteristics of this unit change remarkably little along strike, although towards the south, tuffaceous components become more common, occasionally comprising up to 40% of the total thickness. There are no sulphides spatially associated with this horizon, nor is there any evidence of alteration similar to that near the ore horizon.

A number of smaller, discontinuous lenses of ferruginous chert are present throughout the volcanic sequence at Gull Pond commonly comprising one or more narrow beds intercalated with silicic and lesser mafic tuff. The basal contact is locally gradational with the first hints of reddish colour occurring in the tuff up to 50 cm below the first chert bed. The beds are locally broken and slumped into underlying material and fragments sometimes occur in local volcanic breccia.

3.5 Tectonic Setting of Notre Dame Bay

The island of Newfoundland comprises the northeastern limit of the Appalachian orogen in North America. Early interpretation of this orogen in terms of geosynclinal theory viewed it as a one sided system bounded to the east by an older craton and to the west by an

ocean basin (Dietz, 1963). Williams (1964a) was the first to recognize that the Appalachians in Newfoundland are actually a two-sided symmetrical system and on this basis divided the island into three geological provinces represented by late Precambrian to early Paleozoic cratonic areas to the east and west respectively, separated by a Lower to Middle Paleozoic mobile belt.

Wilson's (1966) hypothesis that the Atlantic Ocean opened and then closed again in Paleozoic times and the advent of plate tectonic theory enabled later workers to view Williams' (1964a) two-sided symmetrical system in a new light. Bird and Dewey (1970) and Dewey and Bird (1971) presented plate tectonic models for Central Newfoundland in which early Paleozoic opening of the Proto-Atlantic Ocean was succeeded by closure in the Ordovician. The Western Platform was, in their view, the North American continental edge in pre-Ordovician times and the eugeosynclinal sequences of the Central Mobile Belt were built on oceanic crust in a series of marginal basins and island arcs above a Lower-Middle Ordovician subduction zone. Stevens (1970) and Church and Stevens (1971) were the first to recognize that allochthonous layered ultramafic complexes on the Western Platform were in fact remnants of Lower Ordovician and earlier ocean floor which had been thrust over the platform during the closing of the Proto-Atlantic Ocean and they further suggested that pillow lavas of the Lushs Bight Terrain might also be ocean floor structurally emplaced along the Lobster Cove Fault. Further evidence to support the first part of this view was presented by Smitheringale (1972) and Strong (1972, 1973) who showed the volcanic rocks of the Lushs Bight Terrain to be of oceanic tholeiite affinity.

Kean (1973) was the first to describe an island arc assemblage in Notre Dame Bay in his study of the Cutwell Group on Long Island. Strong and Payne (1973) interpreted the Moretons Harbour Group on the Moretons Harbour Peninsula to be of island arc origin and suggested that the structurally juxtaposed Chanceport Group was younger, possibly Upper Ordovician to Silurian in age, implying its correlation with the Roberts Arm Group to the west. This interpretation was reinforced by Dean (1973), who extended the correlation to include the Cottrell's Cove Group on the Fortune Harbour Peninsula. Strong (1973) showed that the volcanic rocks of the Roberts Arm Group are chemically of calc-alkaline affinity and later demonstrated their chemical similarity with volcanic rocks of the Cottrell's Cove and Chanceport Groups (Strong, 1975).

Dean and Strong (1975) proposed correlations of units across Notre Dame Bay (Fig. 3.1) and outlined the present interpretation of the tectonic history of Notre Dame Bay which can be summarized as follows:

1) Lower Paleozoic opening of the Proto-Atlantic Ocean resulted in the generation of oceanic crust until the Lower Ordovician. These rocks are presently preserved as the Lushs Bight Group and in the ophiolite allochthons of Western Newfoundland.

2) Initiation of eastward subduction in the Lower Ordovician was accompanied by the commencement of westward ophiolite emplacement and of island arc volcanism whereby a thick sequence of tholeiitic to calc-alkaline volcanic rocks and associated sediments was laid down on

ocean crust (Cutwell, Western Arm, Moretons Harbour, Wild Bight and Summerford Groups).

3) Final ophiolite emplacement in western Newfoundland was accompanied by cessation of volcanic activity in the Middle Ordovician. Erosion of the island arc volcanic sequence resulted in extensive clastic sedimentation producing the Exploits Group shale-turbidite sequence.

4) Resumption of calc-alkaline volcanism in the Upper Ordovician-Silurian produced a basal sequence of interbedded volcanic and sedimentary rocks, followed by the thick succession of mafic to acidic volcanic rocks and associated sediments of the Roberts Arm, Cottrell's Cove and Chanceport Groups. Eastward thinning of this sequence and the presence of substantial volumes of greywacke and shale in the Chanceport Group may indicate that this area approaches the distal end of the volcanism.

5) Major uplift of the volcanic sequence above sea level, probably in the Silurian, was accompanied by deposition of terrestrial volcanic rocks and red beds of the Springdale and Botwood Groups unconformably to disconformably up on the marine succession.

6) Thrusting from the northwest subsequent to deposition of the Springdale Group juxtaposed the oceanic crust - early calc-alkaline volcanic rocks and the upper Ordovician-Silurian succession along the Lobster Cove-Chanceport fault system.

CHAPTER 4

MINERALOGY AND PETROGRAPHY

4.1 Methods

Thin sections were cut from 47 selected hand specimens of chert and ferruginous sedimentary rocks in order to examine their mineralogy and the nature of their sedimentary structures. In addition, the principal minerals present in 20 selected samples, of which 8 were from the Roberts Arm area, 6 from the Fortune Harbour area and 6 from the Gull Pond area, were identified by X-ray diffraction. Analysis was performed on randomly mounted, unseived whole rock powders, the preparation of which is described in Appendix B.

This chapter deals principally with the mineralogy of the analyzed samples as determined by the above methods, especially as it pertains to the chemical composition of the rocks. In addition, the nature of various sedimentary structures and their relation to the genesis of the sediments is discussed.

4.2 Mineralogy of Chert and Ferruginous Sediments

The principal minerals identified in thin section and by X-ray diffraction in the chert and ferruginous sedimentary rocks comprising the present study suite are described in this section in generally decreasing order of abundance.

4.2.1 Quartz

Quartz is by far the most common mineral observed in most thin sections and it commonly dominates the X-ray diffractograms. It

generally occurs as cryptocrystalline to microcrystalline aggregates, the individual crystals of which are often irresolvable under the petrographic microscope. These aggregates comprise the groundmass of most samples and in the Roberts Arm and Fortune Harbour suites may be accompanied by minor amounts of isotropic silica. In the Gull Pond suite, the groundmass is commonly composed of micrographic quartz which is considerably coarser-grained than that in the Roberts Arm or Fortune Harbour suites. This suggests that, in general, substantially more recrystallization has taken place in the chert in this area, possibly due to their relatively intense tectonism (Sec. 3.4.2) and/or to their relative proximity to several large intrusive bodies (Fig. 1.1).

Quartz is also found in minor but varying amounts as angular to subangular detrital grains, as relatively coarse-grained micrographic cavity fillings (Sec. 4.5) and as a major constituent of late veinlets often accompanied by epidote ± calcite.

Chalcedonic quartz is rare but sometimes occurs in veins as fibrous growths perpendicular to the vein wall and as radiating sheaves of crystals in spherical structures of probable diagenetic origin (Sec. 4.4.2).

4.2.2 Hematite

Hematite is a ubiquitous component of all red cherts but is uncommon in green varieties. When present in relatively minor quantities, it forms a fine dust in the interstices of the quartz groundmass and with increasing concentration tends to aggregate into irregular clots (Plate 4.5) which often render large portions of the thin sections virtually opague. When present in large quantities, hematite may form discrete beds.

4.2.3 Aluminosilicate Minerals

The term "aluminosilicate minerals" is herein used for convenience when referring to the suite of minerals listed below which contain aluminum and silica as well as various other major element cations. These minerals are commonly observed in thin section as microcrystalline aggregates, the individual crystals of which are irresolvable in thin section but single detrital grains are often coarse enough to identify optically. The aluminosilicate minerals are more commonly detected, both optically and by X-ray diffraction, in the green rocks rather than their red counterparts, this being due partly to their relatively greater abundance in the former (cf. Sec. 5.2.2) but also to the obscuring effect of hematite which renders much of the red specimens opaque in thin section and is the cause of considerable interference in X-ray diffraction.

Sericite and Illite

Sericite and illite have both been identified by X-ray diffraction in some samples but they are too fine grained to be distinguished from each other in thin section. In the Roberts Arm and Fortune Harbour suites, they occur principally as microcrystalline aggregates distinguishable from chlorite by their high birefringence but in the Gull Pond suite are more often seen as individual flakes aligned parallel to the bedding. They are often associated with other detrital minerals in quartz and/or hematite-poor beds and are occasionally seen replacing feldspar grains and as cavity fillings (Sec. 4.5).

X-ray diffraction indicates that illite is more common than sericite in the Roberts Arm and Fortune Harbour suites while in the Gull Pond suite, sericite appears to be more prevalent.

Chlorite

Chlorite is seldom present in sufficient quantities to be identified by X-ray diffraction but is often present in thin section where it occurs almost exclusively as microcrystalline aggregates in the quartz groundmass. It commonly shows very low first order interference colours but in some specimens of interpillow material, gives anomalous Berlin-blue interference colours.

Epidote and Clinozoisite

Epidote and less commonly clinozoisite were identified in a large number of samples both optically and by X-ray diffraction. They occur both as vein fillings associated with quartz and calcite and as microcrystalline aggregates in the groundmass, usually associated with sericite/illite and/or chlorite. These minerals are especially common in the green samples and in many cases are probably responsible for their colour. Epidote is often present partially or completely replacing detrital feldspar grains.

Feldspar

Feldspar is commonly a minor detrital component in samples from the present study and where individual grains are visible they are often partially or completely altered to sericite, chlorite and/or epidote. Large detrital feldspar grains are occasionally seen concentrated in narrow tuffaceous beds within the chert associated with detrital quartz, pyroxene and lithic fragments. Sodic plagioclase was detected by X-ray diffraction in some samples in amounts greater than those seen in any thin section, suggesting that considerable plagioclase may be sporadically present in optically irresolvable microcrystalline aggregates.

Pumpellyite

Pumpellyite was identified in a few thin sections and in one X-ray diffractogram, all from the Roberts Arm suite, occurring as rare individual grains in late quartz veinlets and occasionally as micro-crystalline aggregates.

4.2.4 Calcite

Calcite is present in some samples as a coarse to fine-grained vein filling associated with epidote and quartz. It is occasionally seen as discrete grains in the chert groundmass and is especially common in interpillow material adjacent to the chert-pillow interface.

4.2.5 Opaque Minerals

Next to hematite, pyrite is the most common opaque mineral present in the chert and ferruginous sedimentary rocks but is rarely abundant. Small pyrite cubes are sometimes disseminated throughout the groundmass, and broken edges on some grains suggest that they, at least, are detrital. Vein-fillings of pyrite are sometimes present near the volcanic rock/chert interface where the chert is interstitial to pillows.

Magnetite is a rare detrital component in the Roberts Arm and Fortune Harbour suite but is somewhat more common in the Gull Pond suite, where it occasionally forms almost massive lenses in highly ferruginous chert proximal to the Southwest Shaft copper deposit (Sec. 3.4.4).

4.3 Mineralogic Distribution of the Principal Major Elements

Major element analyses of all samples referred to in this section are presented in Table 4.1. In all samples examined optically or by X-ray diffraction, the proportion of non-detrital free quartz is directly correlative with the concentration of SiO_2 and there is no doubt that in most siliceous samples, this mineral accounts for the majority of the SiO_2 present. In rare cases, samples very rich in aluminosilicate minerals may be relatively deficient in non-detrital free quartz and thus contribute a significant proportion of the SiO_2 present in the rock (e.g. RA67G).

Fe_2O_3 is present in most samples mainly as hematite, with a typically minor contribution being made by magnetite and Fe^{3+}-rich aluminosilicates such as epidote and pumpellyite. There are five samples in the Roberts Arm suite which appear in hand specimen to be virtually without hematite but contain in excess of 6% Fe_2O_3 (RA67G, RA120, RA123, RA143B, RA161G) and X-ray diffraction of two of these samples confirmed the paucity of hematite and indicated the presence of anomalously large amounts of epidote and/or pumpellyite. No other minerals identified on these diffractograms are capable of carrying sufficient amounts of Fe_2O_3 to account for its concentration in these samples and it thus appears that in some cases, significant amounts of Fe_2O_3 may be attributed to the presence of epidote and pumpellyite.

The variety of aluminosilicate minerals identified in thin section and by X-ray diffraction (Sec. 4.2.3) can easily account for the Al_2O_3 content of most samples. The concentrations of major elements other

TABLE 4.1

MAJOR ELEMENT COMPOSITION OF SELECTED SAMPLES

Weight %	RA46	RA52	RA67G	RA89	RA120	RA123	RA143B	RA161G	RA190B	GP75	FH4G	FH41A	FH64
Fe_2O_3	4.93	20.44	6.37	6.49	3.77	6.97	7.19	15.41	3.33	3.98	0.00	4.46	0.94
TiO_2	.36	0.00	0.00	0.00	.64	.22	0.00	.11	.20	.19	0.00	0.31	0.00
SiO_2	68.9	64.0	56.8	83.3	57.1	43.0	44.3	47.8	77.3	24.1	94.7	64.6	82.6
CaO	.56	1.53	19.7	3.91	15.63	23.6	20.43	14.28	.89	.34	.08	1.82	0.26
K_2O	3.3	.07	.03	0.00	.02	0.00	0.00	0.00	.34	2.51	.24	4.08	0.45
MgO	.97	2.33	.57	1.04	.41	.26	1.49	2.20	1.31	.79	.73	2.18	0.60
Al_2O_3	13.70	3.27	11.5	1.12	14.3	20.60	14.30	10.4	7.24	5.54	1.84	12.1	8.23
FeO	.63	3.02	.61	1.57	.65	.64	1.06	1.14	3.39	1.45	2.14	0.43	0.68
Na_2O	2.34	0.00	0.00	.01	0.00	.01	0.00	0.00	1.43	.20	0.00	0.11	2.61
MnO	.07	.07	.05	.04	.09	.04	.04	.11	.26	.11	.09	0.08	0.71

than Al_2O_3 associated with the aluminosilicate minerals (TiO_2, CaO, K_2O, MgO, FeO, Na_2O) are often very low, however, and the mineral phases containing them are commonly too fine grained to identify with certainty in thin section. However, by examining samples which are relatively enriched in one or two of these elements to the exclusion of the others, it is often possible to identify the major aluminosilicate mineral carrying the element in question and this identification can be used in conjunction with the chemical composition of various samples to infer the principal mineralogic distribution of this element throughout the sample suites. The following discussion reports the preliminary results of examination of selected samples which meet the above criterion and is expanded in Chapter 5.

a) CaO: The most widespread CaO-bearing mineral identified optically and by X-ray diffraction was epidote, although calcite veins are common in a few samples and clinozoisite and pumpellyite are occasional minor constituents. Extremely CaO-rich samples such as RA67G commonly contain very large amounts of epidote in thin section and give pronounced epidote peaks on the diffractograms. Plagioclase was seldom identified in the absence of anomalously high Na_2O concentrations, and calcic feldspar is thus not thought to contribute significant amounts of CaO to the whole rock composition.

b) K_2O: K_2O enriched samples from all areas (e.g. GP75, RA46, FH41A) commonly contain a relative abundance of illite and/or sericite in thin section and X-ray diffraction of K_2O-rich samples commonly results in peaks characteristic of these two minerals. Illite and sericite are therefore thought to be the principal K_2O-bearing mineral in most samples.

c) MgO and FeO: Because of the close positive correlation between these two elements throughout the sample suites (Sec. 5.3.1), they are thought to generally occur in the same mineral. Sample RA52, which contains dominantly MgO and FeO as its aluminosilicate-related component, contains a fine-grained detrital fraction identified as chlorite in thin section. Likewise, samples which give X-ray diffraction chlorite peaks are commonly those which contain MgO+FeO K_2O,CaO,Na_2O.

Occasional samples anomalously high in FeO were observed in hand specimen and/or thin section to carry disseminated pyrite.

d) Na_2O concentrations are commonly very low and the only mineral identified in thin section which carries major amounts of this element was detrital plagioclase. Sample FH64, which carries anomalously high Na_2O, was found to give pronounced X-ray diffraction albite peaks and it seems likely that this mineral is responsible for Na_2O concentrations in most samples.

4.4 Sedimentary Structures

4.4.1 Bedded Deposits

A number of bedded red chert and ferruginous sedimentary rocks, as well as some green varieties, are colour-laminated in hand specimen (Plate 4.1) and details of these laminae are clearly seen in thin section. Individual laminae vary in thickness from less than 0.1 mm to +1 cm and while some are remarkably continuous on outcrop scale, many others are lensoid and discontinuous (Plate 4.2). Laminae in the red samples commonly result mainly from variations in hematite content, with

PLATE 4.1 Colour-laminated ferruginous chert. Dark grey laminae are shaly members.

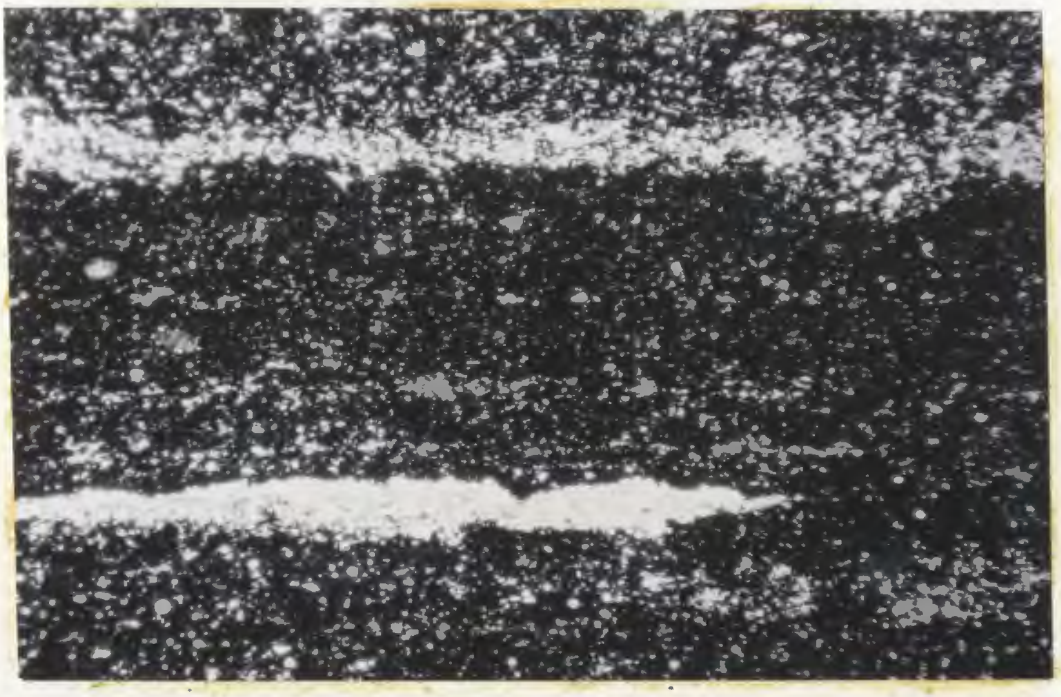

PLATE 4.2 Fine lamination in ferruginous chert. Matrix is dominantly hematite, quartz and silicic tuff fragments. Lense in lower half is dominantly silicic tuff fragments. Plane polarized light. x40.

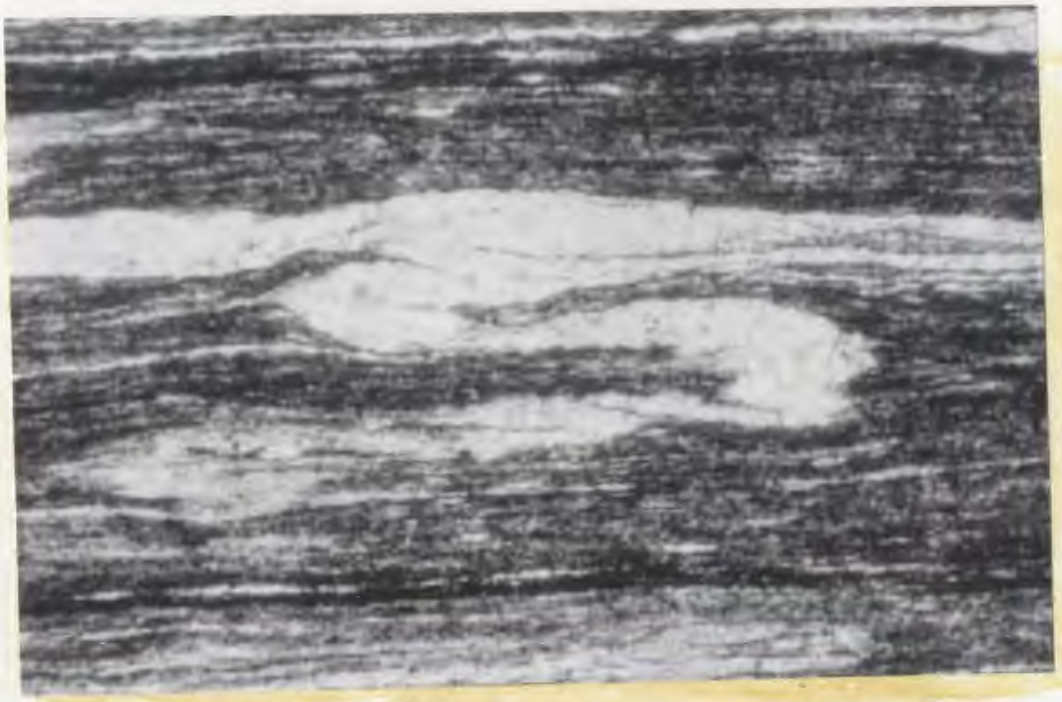

PLATE 4.3 Intra-laminae slump fold modified by later deformation. Folded bed is silicic tuff interbedded with finely laminated hematite-quartz chert. Plane polarized light. x125.

lighter-coloured bands being relatively depleted in this mineral but may also be caused by differential concentration of microcrystalline aluminosilicate minerals or coarse clastic and/or tuffaceous interbeds (Plate 4.2). Laminae contacts are often sharp but are more commonly rather diffuse and gradational.

Small scale sedimentary structures are rare in hand specimen but are more commonly viewed in thin section, especially where laminae contacts are sharp. The most common structures seen in thin section are intra-laminae slump folds (Plate 4.3) in which one or more laminae are deformed while beds above and below are not. Individual laminae are sometimes disconnected and streaked out at the broken ends, suggesting that some soft-sediment boudinage has taken place. In some cases, the disconnected bedding fragments are deformed and bunched up at one end (Plate 4.4) suggesting that the disconnected pieces have occasionally moved laterally while in a plastic state, causing deformation along the leading edge.

Transport of unconsolidated chert on a somewhat larger scale was noted in one sample where poorly sorted fragments of pale reddish chert up to 5 cm in length are present in a dark grey siliceous matrix. The fragments are seen in thin section to be dominantly formed of microcrystalline quartz with scattered hematite clots and abundant radiolarian remains (see Sec. 4.5) and are virtually free of aluminosilicate minerals. The quartz matrix is mainly finer-grained than in the fragments, contains no hematite and few radiolaria, but has scattered detrital feldspar laths and occasional clots of microcrystalline clay minerals.

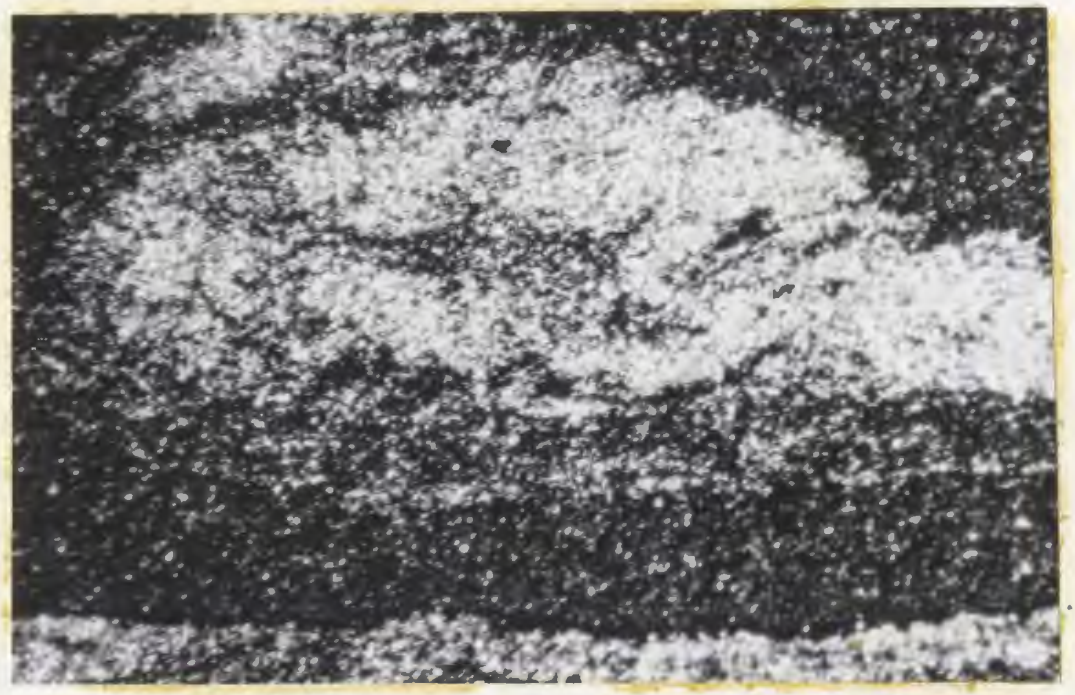

PLATE 4.4 Soft-sediment deformation on the leading edge of a tuffaceous bed in red chert which has undergone lateral transport. Suggested sense of movement is from left to right. Crossed nichols. x40.

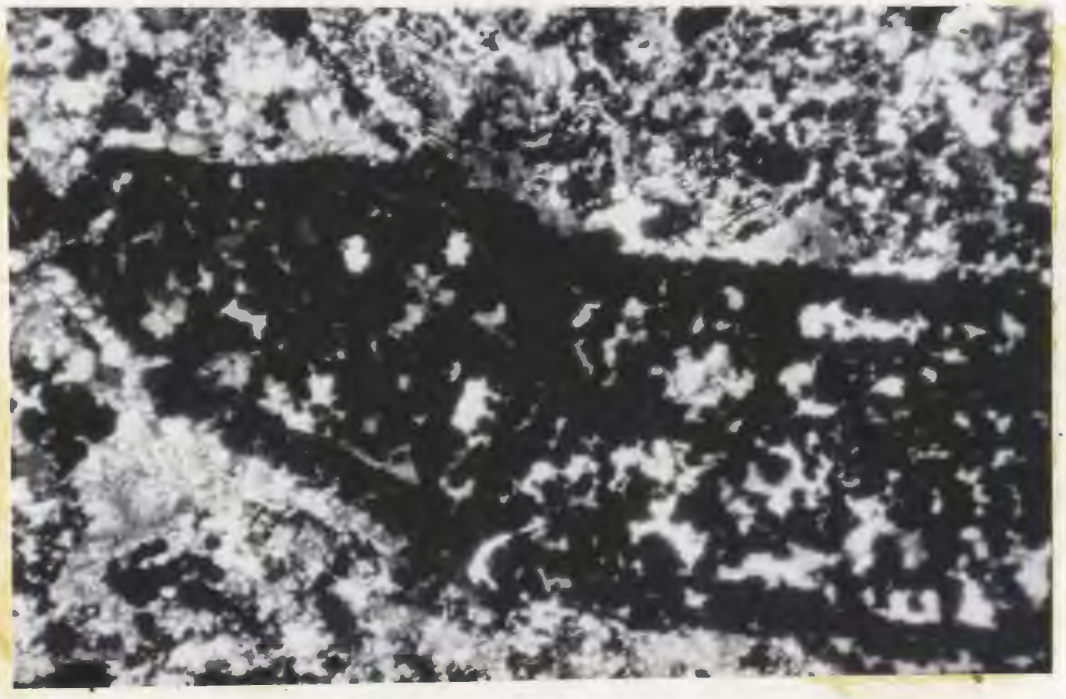

PLATE 4.5 Part of a hematite-rich fragment in a more quartzose matrix in interpillow chert. Crossed nichols. x50.

The fragment boundaries are definite but irregular and without sharp edges and the fragments are therefore interpreted to have been transported while in a plastic state. The uniformity of clast composition and the absence of exotic fragments indicates that transport was probably over a very short distance and involved only a minor amount of sediment.

Scour and fill structures were noted in some outcrops, generally in the more shaly members, and some tuffaceous interbeds show a crude size gradation but laminae in the bedded chert and ferruginous sediments seldom show evidence of current reworking.

Post-depositional readjustments, as reflected in the sedimentary structures, thus seem to have been limited to minor slumping, possibly in response to slight density contrasts and/or depositional slope instability.

4.4.2 Interpillow Deposits

Interpillow chert is seen in thin section to be composed dominantly of quartz, hematite and minor clots of aluminosilicate minerals. Quartz crystals are commonly much coarser than those in the bedded varieties and hematite is commonly present in sufficient quantities to render much of the thin section opaque. Aluminosilicate minerals, especially those rich in CaO, tend to increase in concentration towards the chert-pillow lava contact, and epidote with lesser amounts of pumpellyite and chlorite are common in the contact region. Calcite is ubiquitous in most contacts, often obscuring the contact itself, and calcite veins are common in both chert and pillow lava.

A breccia-like texture is often visible in hand specimen in which irregular bright red fragments of varying shape are chaotically

intermixed in a quartz-hematite matrix. This feature is seldom visible in thin sections due to their hematite-caused opacity but occasionally the fragments are preserved in a more quartzose matrix (Plate 4.5). The fragments are often elongate and somewhat curved, with sharp boundaries and angular corners.

These fragments are reminiscent of broken beds which may have been intruded in a semi-consolidated state by the pillow lava, resulting in disruption of the beds and their being squeezed into the pillow interstices. Alternatively, they could be laminae formed chemically by deposition of chert in the pillow interstices and subsequently disrupted by minor late readjustments of pillow geometry.

Macro-spheroids ranging up to 1.5 mm in diameter comprise up to 60% of the rock in some interpillow samples. They are seen in thin section (Plate 4.6) to consist dominantly of micrographic quartz near the center giving way outwards to radiating chalcedony. Concentric bands of hematite, commonly overgrown by the chalcedony, are present in the outer 1/2 to 1/3 of the structures. Where these structures are in contact, their mutual sides are flattened suggesting interference during growth. However, the structures are commonly separated by a fine film of hematite and/or clay, and crystals of one structure are never seen intergrown with those of an adjacent structure. The outer edges of these spheroids are commonly diffuse, marked by the outer growth limit of the various chalcedony crystals.

The origin of these structures is not presently known. Their mutually flattened edges, lack of nucleii and lack of concentric banding in the inner 1/2 to 2/3 indicate that they are not recrystallized ooids.

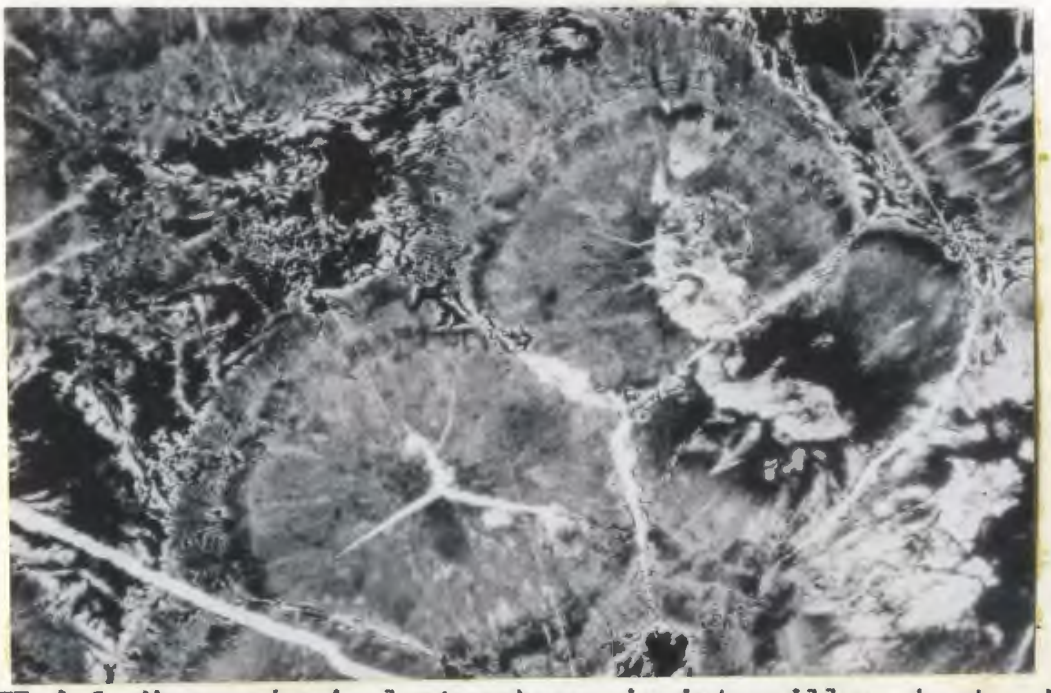

PLATE 4.6 Macrospherical structures in interpillow chert. Micrographic quartz in the center of the spheres gives way to radiating chalcedony in the outer 1/2 to 1/3 which overgrows concentric hematite bands. Note flattened edges at mutual contacts and lack of overgrowth of adjacent structures. Plane polarized light. x50.

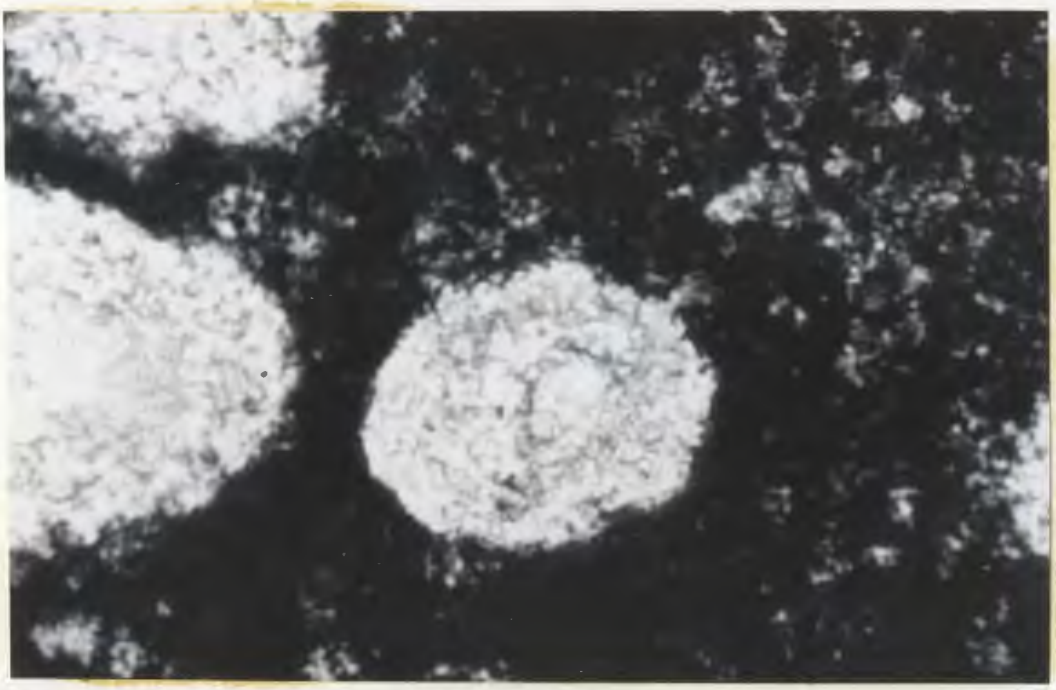

PLATE 4.7 Radiolarian remains in hematite-chert. Infilling material is dominantly quartz with lesser clay material (grey). Note faint suggestion of an outer wall in the central specimen. Crossed nichols. x500.

A possible origin is suggested by the work of Elliston (1963 a,b) and Nashar (1963) who suggested that colloidal material in a partially consolidated, water-rich sediment will flocculate into large aggregates in response to the application of shearing stress. These aggregates later crystallize in response to compaction, dehydration and possibly elevation of temperature (Elliston, 1963a, Plate 1). In the case of the present sediments, this stress could have been exerted either by the extrusion of pillows into a partially consolidated sediment or by post-depositional readjustment of the pillows causing disruption of partially consolidated material in their interstices.

There is no evidence of baking of the chert near the pillow lava contacts and field and petrographic evidence is not conclusive as to whether the chert in the pillow interstices pre- or post-dates pillow extrusion. Geochemical evidence pertaining to this problem is presented in Chapter 5.

4.5 Radiolarian (?) Remains

A majority of the samples examined in thin section contain widely varying concentrations of microspherical structures ranging in diameter up to 0.3 mm (Plate 4.7). They are commonly filled with micrographic quartz which is normally considerably coarser than that in the groundmass, suggesting it may have originated as cavity fillings. Less commonly, the spheres are partially or completely filled with microcrystalline clay minerals and/or hematite (Plate 4.7). In many

samples, the spheres are scattered at random throughout the specimen while in others they are concentrated in specific horizons, commonly those rich in hematite and/or detrital material. On the rare occasions when they are in mutual contact, the spheres are tangentially welded (Plate 4.8). Preservation seems to be enhanced in the hematite and shale-rich rocks and where the spheres are present in highly siliceous samples, they are often partially destroyed (Plate 4.9). The only suggestion of internal structure in these spheres is a faint, poorly preserved outer wall in some specimens (Plate 4.7).

Sampson (1923) described similar features from the cherts of Notre Dame Bay and interpreted them to be radiolaria as did Ruedemann and Wilson (1936) from cherts of similar age in New York. Similar forms interpreted to be radiolaria have been reported from many DSDP cores (e.g. Heath and Moberly, 1971; Berger and von Rad, 1972; von Rad and Rosch, 1974) where a complete gradation from opaline radiolarian ooze to indurated quartz chert can be observed and the progressive destruction of internal structures of the radiolaria can be recorded. Most recent workers agree that dissolution of opaline tests during diagenesis will result in the destruction of most internal structures and possibly complete obliteration of the test (Wise and Weaver, 1974).

In summary, the following considerations suggest that the microspheres observed in thin section and described above are poorly preserved radiolarian remains:

1) The internal micrographic quartz is relatively coarse-grained and this, coupled with the occurrence of internal clay and hematite, suggests infilling of an original cavity.

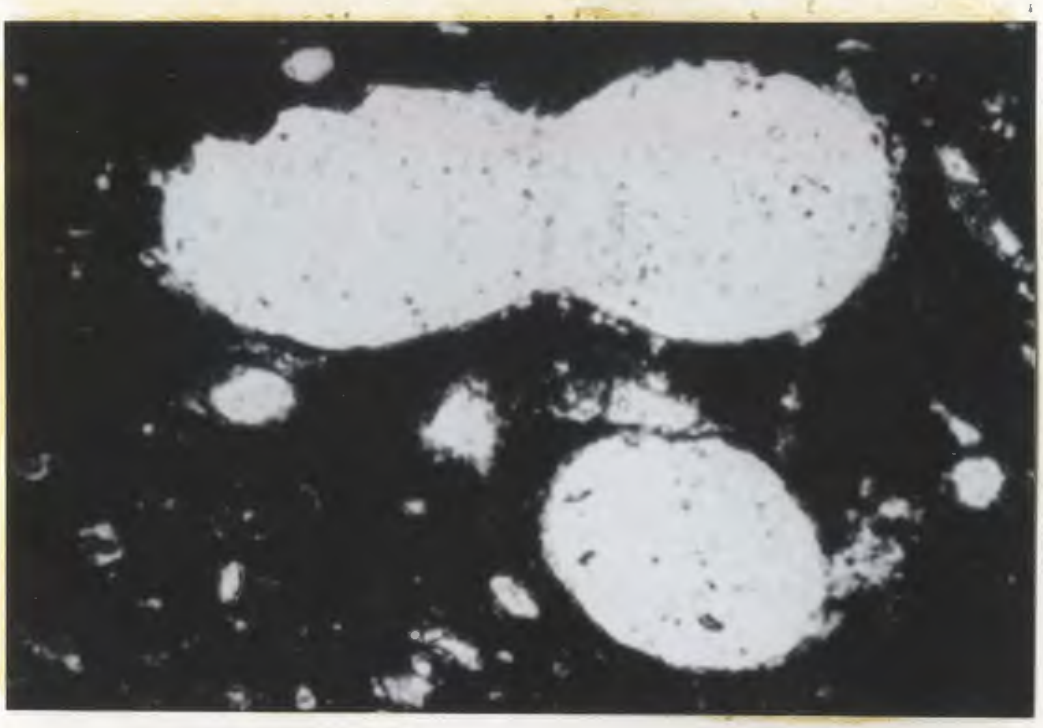

PLATE 4.8 Tangentially welded radiolarian remains. Plane polarized light. x500.

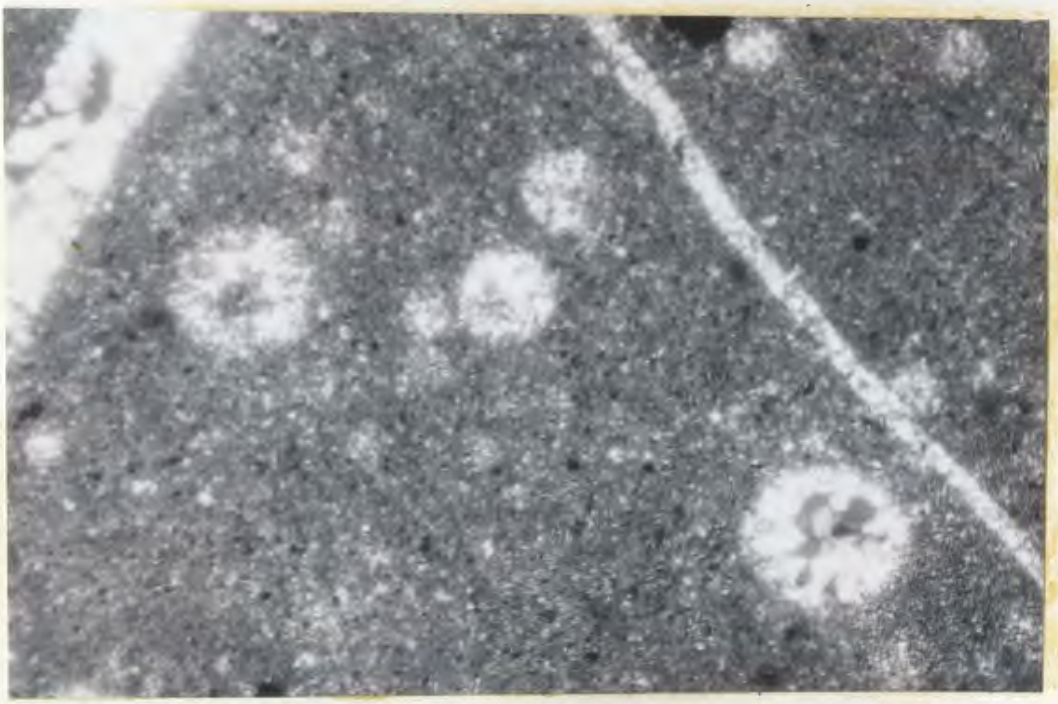

PLATE 4.9 Radiolarian remains in various stages of preservation in highly siliceous chert. Groundmass is dominantly micrographic quartz. Well-preserved radiolaria are present (e.g. lower-right) but many are partially destroyed and appear as ghosts. Crossed nichols. x40.

2) The general lack of concentric banding and/or nucleii indicates that these are not recrystallized ooids. Sharp outer boundaries and tangential welding rather than flattening at mutual contacts indicates that they are probably not diagenetic growth features or recrystallized silica globules.

3) The occasional presence of a poorly preserved outer wall indicates than an original outer wall may have been a universal characteristic, i.e. suggesting a biogenic origin.

4) The similarity in size, general appearance and occurrence of these spheres to radiolaria described in sediments of a similar age as well as those present in more recent rocks suggests that they are likewise radiolaria.

4.6 Summary

Quartz and hematite are the dominant minerals present in the chert and ferruginous sediments studied during the present project. Non-detrital, microcrystalline quartz comprises the groundmass of most samples and is diluted by varying concentrations of hematite which occurs as a fine dust surrounding quartz crystals, as irregular clots, and occasionally as discrete beds. A ubiquitous detrital component is present which ranges from occasional tuffaceous fragments to discrete tuff interbeds and microcrystalline aggregates in the siliceous groundmass. The dominant minerals in this fraction are illite, sericite, chlorite, and epidote with lesser albite and clinozoisite and, in the Roberts Arm suite, pumpellyite. Calcite, pyrite and magnetite are sporadically present.

Concentrations of the various major elements can usually be related to the presence of specific minerals identified optically or by X-ray diffraction.

Sedimentary structures in the bedded sedimentary rocks indicate that most were deposited in relatively quiet water and locally disrupted by soft sediment deformation probably due to density contrasts and/or depositional slope instability.

Petrographic evidence is inconclusive as to whether interpillow chert was originally deposited before or after extrusion of the host pillow lava.

Microspherical features present in a majority of bedded samples are interpreted to be poorly preserved radiolarian remains.

CHAPTER 5

GEOCHEMISTRY

5.1 Methods

A total of 247 samples comprising chert and ferruginous sedimentary rocks associated with volcanic rocks of the Roberts Arm and Cottrell's Cove Groups, of which 80 were from the Gull Pond area, 115 from the Roberts Arm area and 52 from the Fortune Harbour area, were analysed for 10 major and 10 trace elements. Major element compositions were determined with a Perkin-Elmer Model 303 atomic absorption spectrometer and trace element compositions with a Phillips Model 1220C X-ray fluorescence spectrometer. FeO content was found by titration according to the method of Wilson (1955), described by Maxwell (1968, p. 419). Gold was determined commercially by Bondar-Clegg and Company for 179 selected samples of which 61 were from the Gull Pond area, 76 from the Roberts Arm area and 42 from the Fortune Harbour area. Loss on ignition was determined for all samples.

All analyses were performed on unsieved whole rock powders and details of sample preparation techniques, analytical methods, and the precision and accuracy of the analyses can be found in Appendix B.

A variety of statistical techniques were applied to the data in order to interpret the compositions of and chemical trends both in the various geographic suites and in selected subgroups within these suites. The main emphasis in the Roberts Arm and Fortune Harbour areas was directed towards chemically distinguishing contrasting lithotypes and samples of differing modes of occurrence, as well as seeking stratigraphic variations

vertically throughout the volcanic sequence. The principal concern in the Gull Pond area was to find chemical variations along strike within the single stratigraphic unit associated with base metal mineralization and to define chemical variation between this unit and similar lithotypes apparently unrelated to mineralization.

5.2 Results

The average major and trace element compositions and the standard deviations from the mean concentrations for the three geographic suites are presented in Table 5.1 and histograms showing the distribution of the various element concentrations for the three areas can be found in Appendix D.

5.2.1 Comparative Compositions of the Geographic Suites

A comparison of major element concentrations as presented in Table 5.1 indicates the following:

1) The chemical composition of all suites is dominated by SiO_2 and to a lesser extent (in the Gull Pond and Roberts Arm suites) Fe_2O_3, which together comprise 84 to 91% of the mean rock composition. This reflects quartz and hematite respectively being the dominant mineral components in most samples.

2) There are significant differences in the sediment composition between the three suites. The Roberts Arm suite is relatively depleted in SiO_2 and enriched in Fe_2O_3, reflecting the greater proportion of ferruginous shale and mudrocks as opposed to true chert in this area. This feature is also reflected in a relative enrichment of FeO, MgO, CaO and Na_2O, elements present mainly in detrital chlorite, epidote and plagioclase in this suite. The Fortune Harbour suite, while showing a marked depletion in Fe_2O_3 is enriched by a factor of two in K_2O, presumably reflecting a relative preponderance of illite in the clay fraction. The Gull Pond suite is the most siliceous of the three and a relative paucity of detrital material in the samples is suggested by a slight but consistent relative depletion in Al_2O_3, CaO, MgO, K_2O, FeO and Na_2O.

TABLE 5.1

MEAN CHEMICAL COMPOSITION OF THE GEOGRAPHIC SUITES

	Roberts Arm		Fortune Harbour		Gull Pond	
Weight %	Mean	S.D.*	Mean	S.D.	Mean	S.D.
Fe_2O_3	9.89	13.12	3.42	3.11	7.18	6.31
TiO_2	.26	.14	.25	.11	.22	.56
SiO_2	75.09	16.94	81.87	11.31	84.54	9.19
CaO	3.36	4.69	1.37	1.41	.78	1.14
K_2O	.64	1.05	1.29	1.15	.65	.69
MgO	1.22	1.52	.96	.73	.68	.49
Al_2O_3	4.83	4.57	5.13	3.63	2.81	2.14
FeO	1.37	1.53	.87	.81	.80	.68
Na_2O	.61	1.18	.60	.84	.47	.68
MnO	.22	.56	.43	.53	.93	1.76
L.O.I.**	2.66	3.34	2.03	1.57	.61	.35
ppm						
Zr	45	46	53	43	31	11
Sr	138	341	61	63	51	23
Rb	25	32	48	41	28	18
Zn	36	21	45	21	30	16
Cu	15	25	14	50	10	14
Ba	235	377	458	653	444	547
Nb	12	14	9	7	12	14
Ni	38	31	31	10	30	13
Cr	30	104	16	6	16	13
Au***	20	16	67	38	72	50

* - standard deviation

** - loss on ignition

*** - Au in ppb

3) CaO, Na_2O, MgO, and FeO tend to increase in concentration from Gull Pond to Fortune Harbour to Roberts Arm respectively. This trend coincides with an increasing volume of mafic relative to silicic volcanic rocks in the volcanic sequence and indicates that these elements are present in the detrital fractions whose compositions reflect their sources.

4) None of the geographic suites is internally homogenous in composition and very high standard deviations for most elements in all suites reflects the considerable range of compositions present (see also histograms, Appendix D).

5) The distribution of element concentrations as depicted in the histograms (Appendix D) shows that in spite of the differences noted above, the element concentrations in each suite follow broadly similar distribution patterns. The main exception to this is the distribution of Al_2O_3, MgO and K_2O in the Fortune Harbour suite which, in contrast to the other two suites, shows neither heavy weighting in the low-concentration ranges nor scattered anomalously high values.

The relative major element composition of the three suites is best illustrated in a triangular plot of their three major components; quartz (SiO_2), hematite (Fe_2O_3) and the detrital fraction (Al_2O_3 + CaO + K_2O + MgO + FeO + Na_2O) as shown in Fig. 5.1. Most samples in all suites lie in one or both of two linear trends which converge at the quartz apex, one of which parallels the quartz-"detritus" join, representing various shaley to cherty sediments without significant hematite, and the other of which shows a linear decrease in quartz concentration with increasing hematite+"detritus" content. Both trends are present in the Roberts Arm

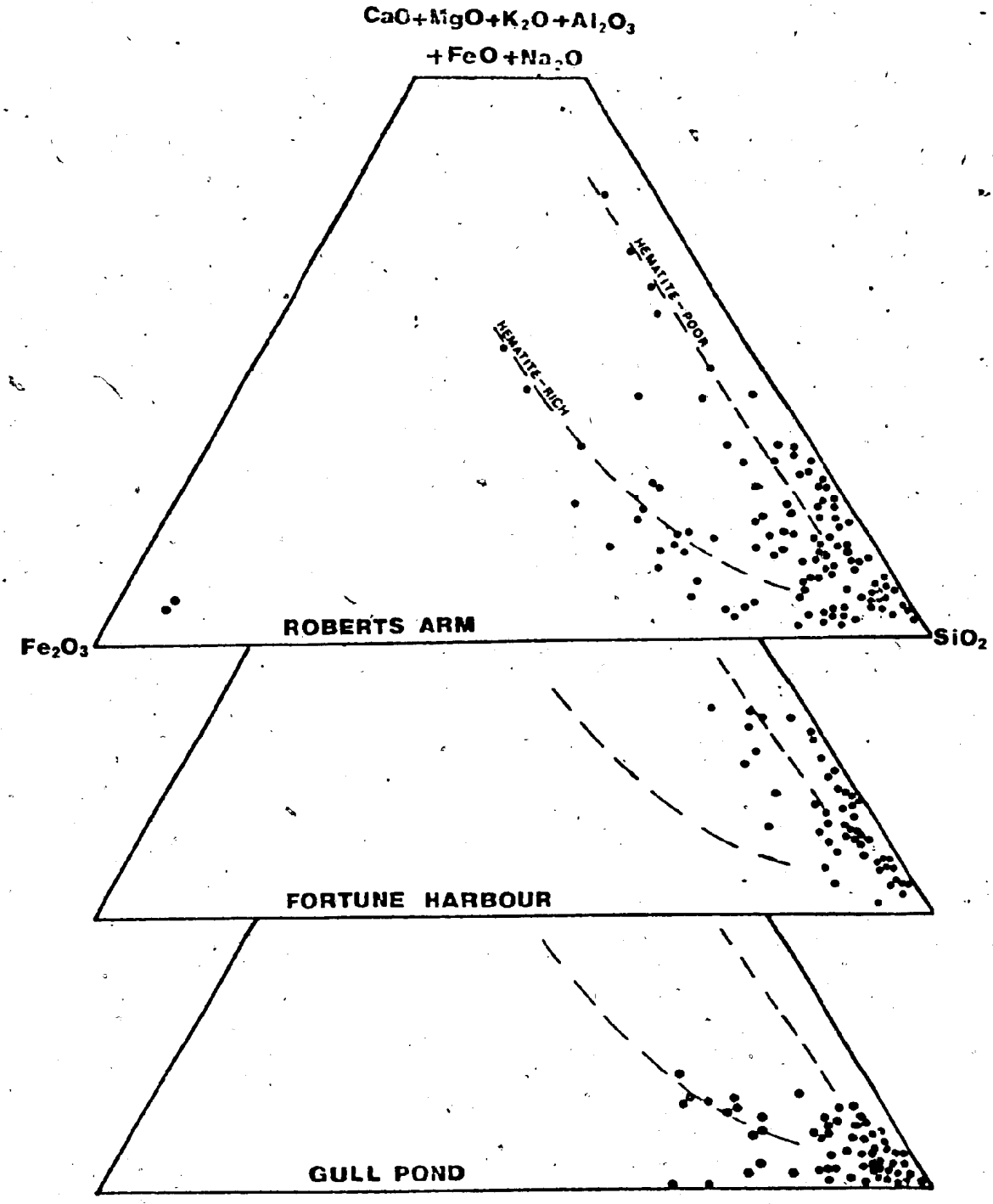

FIG. 5.1 Comparative compositions of the three geographic sample suites as a function of SiO_2/Fe_2O_3/"detritus" ratio.

suite while samples from the Fortune Harbour and Gull Pond suites plot almost exclusively in the low-hematite and high-hematite trends respectively. This diagram emphasises the siliceous nature of the majority of the samples and shows that the increase of hematite and detritus in the ferruginous sedimentary rocks is a sympathetic relationship. Each trend is internally continuous showing no breaks between the quartz-rich and detrital-rich end members indicating that all gradations of sedimentary type from relatively pure quartz chert to shale and ferruginous shale are present.

The trace element concentrations presented in Table 5.1 and their distribution as shown in the histograms (Appendix D) indicate the following:

1) Most trace elements are present in very small concentrations and, with the exception of Ba in all suites and Sr in the Roberts Arm suite, average less than 100 ppm.

2) Au is considerably depleted in the Roberts Arm suite relative to the other two and is somewhat enriched in the Gull Pond suite relative to the Fortune Harbour suite.

3) With the exception of Au, Ba and Rb, the Gull Pond suite carries consistently lower trace element concentrations than the Roberts Arm and Fortune Harbour suites.

4) The relatively high Sr mean concentration in the Roberts Arm suite results from a few anomalous samples and the Sr histogram for this suite in Appendix D indicates that excluding these few samples, Sr distribution is in fact similar in all suites.

5.2.2 Comparative Composition of Lithologic Subgroups

Three pairs of lithologic subgroups are compared, viz: 1) red versus green samples from the Roberts Arm + Fortune Harbour suites, 2) bedded sedimentary rocks versus interpillow sediments from the Roberts Arm Group and 3) samples from the Gullbridge ferruginous chert horizon versus those units from the Gull Pond suite apparently unrelated to mineralization. The mean concentrations and standard deviation from the mean concentrations of all subgroups are presented in Tables 5.2, 5.3 and 5.4 together with the statistical significance of the compositional variations according to the Mann-Whitney U Test (see Appendix B).

Red versus Green Sedimentary Rocks from the Roberts Arm and Fortune Harbour Suites

Samples from the Gull Pond suite were not included in these subgroups due to their lack of green varieties. The green subgroup also includes a few samples in shades of grey, white and buff.

The mean element concentrations for these subgroups as shown in Table 5.2 indicate the following:

1) Fe_2O_3 and SiO_2 are significantly enriched in the red subgroup, reflecting its relative enrichment in quartz and hematite.

2) Al_2O_3, FeO, and Na_2O, as well as MgO and K_2O to a lesser extent, are significantly higher in the green subgroup, indicating that all major detrital minerals are relatively enriched in the green rocks.

3) Zr and Sr are significantly enriched in the green subgroup while Au is the only trace element to be enriched in the red rocks.

TABLE 5.2

MEAN COMPOSITION - RED AND GREEN SUBGROUPS

	Red Subgroup		Green Subgroup		P**** %
Weight Percent	Mean	S.D.*	Mean	S.D.*	
Fe_2O_3	8.69	10.67	2.84	3.76	99.999
TiO_2	.24	.11	.27	.14	99.9
SiO_2	79.49	13.76	74.43	14.31	99.999
CaO	2.04	2.59	5.35	7.39	
K_2O	.68	.85	1.64	1.80	
MgO	1.01	1.16	4.22	.82	
Al_2O_3	3.67	3.33	9.82	4.35	99.999
FeO	1.12	1.38	1.22	.61	99.79
Na_2O	.47	1.10	1.50	1.40	98.75
MnO	.33	.62	.13	.62	
L.O.I.**	2.28	1.58	2.74	1.74	
ppm					
Zr	36	29	88	57	99.999
Sr	70	142	318	624	99.99
Pb	26	25	52	56	
Zn	36	19	47	29	
Cu	11	17	27	74	
Ba	264	509	441	517	96.47
Nb	7	3	10	5	98.78
Ni	36	27	32	27	
Cr	16	6	16	7	
Au***	25	32	13	33	99.89

* - Standard deviation

** - Loss on Ignition

*** - Au in ppb

**** - Probability that element concentrations form separate populations - for elements where p >95%.

Bedded versus Interpillow Sediments from the Roberts Arm Group

Samples for this subgrouping were taken only from the Roberts Arm suite as interpillow material is rare in the Fortune Harbour suite and non-existent in the Gull Pond suite. In addition, only red samples are included in these subgroups due to the relative paucity of green interpillow sediments.

The element concentrations for these subgroups as shown in Table 5.3 indicate that:

1) The mean concentration of Fe_2O_3 is slightly higher in the interpillow subgroup while Al_2O_3, K_2O, MgO, FeO and Na_2O are significantly enriched in the bedded rocks. In view of the two subgroups' similar SiO_2 (and hence quartz) contents, this probably indicates that a somewhat higher detrital component present in the bedded rocks is having the effect of relatively diluting their hematite content.

2) CaO is considerably enriched in the interpillow subgroup as is MnO in the bedded rocks and the ratio Fe_2O_3/MnO is extremely high in the interpillow subgroup reflecting its relative depletion in MnO.

3) Zr, Rb, and Zn are significantly enriched in the bedded subgroup, probably reflecting their close association with the detrital fraction in these rocks.

Mineralization-Related Sediments versus Those Apparently Unrelated to Mineralization in the Gull Pond Suite

The first Gull Pond subgroup consists of samples taken from the horizon spatially related to the Gullbridge and Southwest Shaft deposits (hereafter called the "mineralization" subgroup) while the second comprises samples from various other stratigraphic levels

TABLE 5.3

MEAN COMPOSITION - BEDDED AND INTERPILLOW SUBGROUPS

	Bedded Subgroup		Interpillow Subgroup		P**** %
Weight Percent	Mean	S.D.*	Mean	S.D.*	
Fe_2O_3	10.02	14.77	11.83	8.50	
TiO_2	.24	.10	.22	*****	99.999
SiO_2	77.21	15.92	77.26	13.48	
CaO	1.53	1.50	3.54	3.92	99.87
K_2O	.68	.89	.15	.13	96.77
MgO	1.34	1.15	.72	.94	99.72
Al_2O_3	4.65	3.61	2.15	2.92	99.999
FeO	1.56	1.83	.76	.54	98.92
Na_2O	.82	1.63	.08	.13	99.7
MnO	.45	.88	.05	.04	99.999
L.O.I.**	1.79	.94	2.62	1.99	99.999
ppm					
Zr	43	33	25	28	
Sr	65	59	95	265	
Rb	27	24	10	6	99.67
Zn	42	22	23	7	99.999
Cu	15	28	11	11	
Ba	218	358	104	188	
Nb	8	3	7	3	
Ni	35	16	45	48	
Cr	17	7	15	6	97.79
Au***	7	13	14	18	

* - Standard deviation

** - Loss on Ignition

*** - Au in ppb

**** - Probability that element concentrations form separate populations - for elements where p > 95%.

***** - One analysis

apparently unrelated to mineralization (hereafter called the "mixed" subgroup) in the Gull Pond area.

The major and trace element average concentrations of the subgroups presented in Table 5.4 indicate that:

1) The mineralization subgroup is considerably enriched in Fe_2O_3 and depleted in SiO_2 relative to the mixed subgroup, reflecting relative proportions of free quartz and hematite in the two groups; $Fe_2O_3 + SiO_2$ is roughly equal in both groups, suggesting that a relatively uncomplicated covariation between these two minerals dominates the chemistry of both Gull Pond subgroups.

2) The mean concentration of MnO is considerably higher in the mineralization subgroup but this is principally due to three highly manganiferous samples (GP 14, MnO = 9.6%; GP153A, MnO = 9.0%; GP153B, MnO = 8.6%) in this horizon (note the high standard deviation). Excluding these three samples, the mean concentration of MnO in the mineralization subgroup is 0.43% (S.D. = .41), somewhat lower than that of the mixed subgroup and probably a more realistic figure for purposes of intergroup comparisons.

3) The mixed subgroup has slightly but significantly higher concentrations of TiO_2, K_2O, Al_2O_3 and Na_2O reflecting its more prominent detrital component.

4) Barium is the only trace element significantly enriched in the mineralization subgroup and this by a considerable amount. Most other trace elements (except gold) are slightly but consistently depleted in these rocks relative to the mixed subgroup.

TABLE 5.4

MEAN COMPOSITION - GULL POND MINERALIZATION AND MIXED SUBGROUPS

	Mineralization Subgroup		Mixed Subgroup		P**** %
Weight Percent	Mean	S.D.*	Mean	S.D.*	
Fe_2O_3	9.48	6.40	3.55	3.41	99.999
TiO_2	.13	.06	.31	.80	
SiO_2	83.03	10.71	88.1	3.96	99.999
CaO	.78	1.27	.48	.27	96.43
K_2O	.41	.52	.77	.58	99.999
MgO	.62	.49	.61	.27	
Al_2O_3	2.14	1.70	3.12	1.89	99.77
FeO	.91	.71	.59	.43	95.75
Na_2O	.40	.62	.50	.74	99.72
MnO	1.99	2.49	.65	.62	
L.O.I.**	.51	.30	.55	.33	98.54
ppm					
Zr	28	9	34	10	99.71
Sr	47	24	52	19	95.92
Rb	19	7	38	19	99.999
Zn	25	15	31	11	99.47
Cu	9	8	13	19	99.64
Ba	604	728	279	145	99.22
Nb	10	2	16	21	99.88
Ni	31	16	28	9	
Cr	16	7	17	4	99.69
Au***	71	68	53	28	

* - Standard deviation

** - Loss on Ignition

*** - Au in ppb

**** - Probability that element concentrations form separate populations - for elements where p >95%.

5.3 Statistical Examination of Chemical Data

The chemical data for ferruginous chert and associated sedimentary rocks in the Upper Ordovician-Silurian volcanic sequence were subjected to a variety of statistical tests in order to determine the relationships between various elements and to identify any chemical trends present in the data. The descriptions of these tests can be found in Appendix B and the results of each test are discussed separately below.

5.3.1 Pearson Correlation Coefficients

In an initial attempt to identify chemical relationships within the data, Pearson Correlation Matrices were calculated for the three geographic suites. The complete matrices and the significance of the correlations therein are presented in Appendix C.

Douglas (1976, in prep.) suggested as a result of his study of Cambrian sedimentary rocks in Eastern Newfoundland that the correlation coefficients calculated for the elements in his samples were influenced by two factors:

1) A mineralogical association factor where elements which are present in a specific mineral are positively correlated to a degree determined by the amount of this mineral present in the rock.

2) A mineral grouping factor in which there is a positive correlation of elements within a mutually gradational group of minerals and a negative correlation between these and the concentration of elements in an opposing group. In the present study, this takes the form of a dilution factor in which the dilution of one or more preponderant minerals (in this case quartz

and to a lesser extent hematite) by various other minerals (e.g. detritus) will result in all elements associated with the latter showing a strong negative correlation with the former.

Major Element Correlations

The major elements in each suite which are significantly correlated are summarized in Fig. 5.2. Analysis of the results presented in Appendix C and Fig. 5.2 suggests the following relationships:

1) A strong negative correlation of most elements with SiO_2 is present in all suites, reflecting the dilution of quartz, the dominant component, by all other minerals.

2) Fe_2O_3 shows no significant consistent correlation with other minerals, with the exception of a negative correlation with SiO_2 in the Roberts Arm and Gull Pond suites. The lack of positive correlations suggests that the concentration of hematite is not related to the presence of other mineral phases, while the lack of negative correlations indicates that the concentration of hematite relative to quartz is commonly too low to show a dilution trend with other minerals. The dilution factor represented by the negative correlation of Fe_2O_3 and SiO_2 in the Roberts Arm and Gull Pond suites is not present in the Fortune Harbour suite due to this suites' uniformly low Fe_2O_3 concentrations (Sec. 5.2.1).

3) The general positive correlation of CaO, K_2O, MgO, FeO, and Na_2O with Al_2O_3 indicates that these elements are mainly present in aluminosilicate minerals. The very strong positive correlation of Al_2O_3 with K_2O and MgO in all suites as well as the mutual correlation of K_2O and MgO in the Gull Pond and Fortune Harbour suites suggests that chlorite and illite ± sericite are generally the major aluminosilicate components. This relationship is

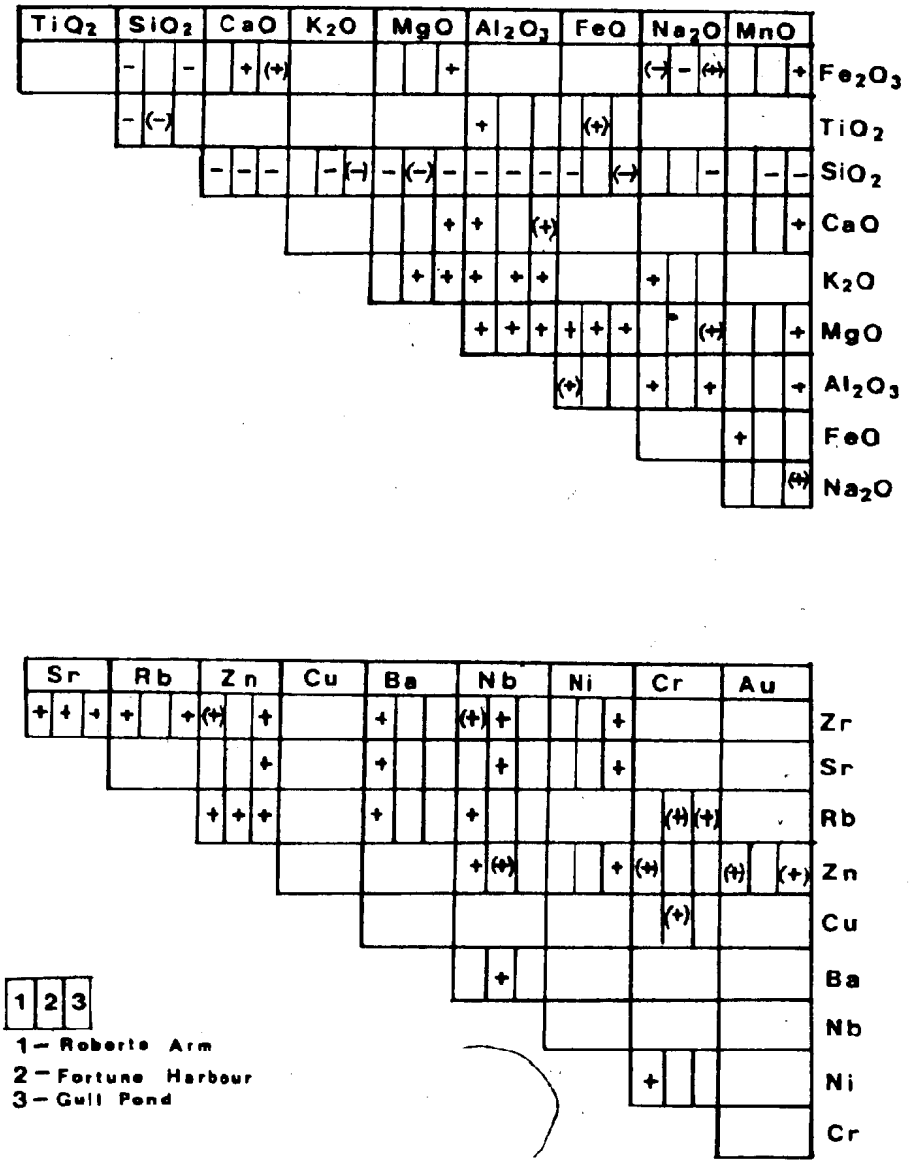

FIG. 5.2 Principal element correlations in the geographic suites; + signifies positive correlation at significance better than 0.001; - signifies negative correlation at significance better than 0.001; parentheses indicate correlations at significance between 0.005 and 0.001.

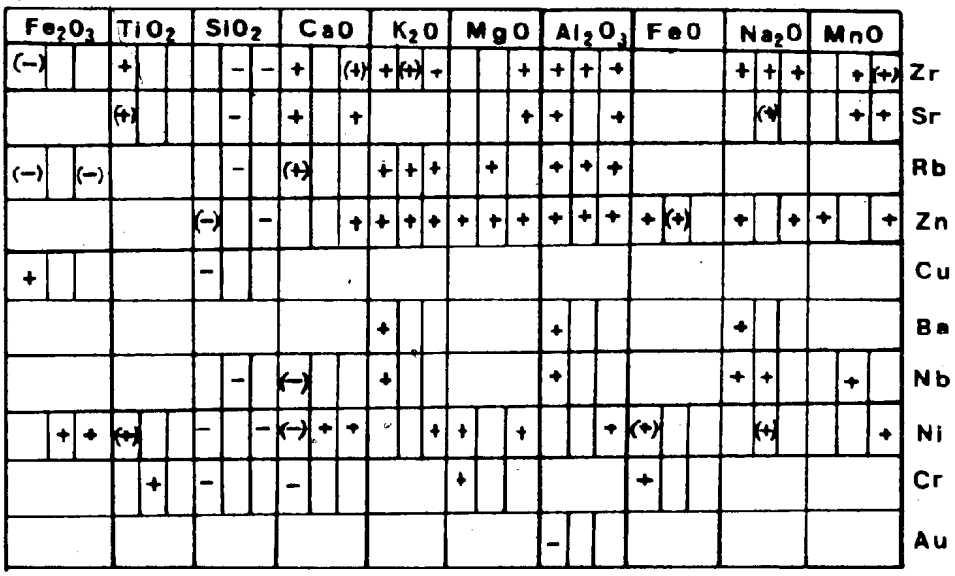
Fe_2O_3
TiO_2
SiO_2
CaO
K_2O
MgO
Al_2O_3
FeO
Na_2O
MnO
Zr
Sr
Rb
Zn
Cu
Ba
Nb
Ni
Cr
Au

Fig. 5.2 (cont'd)

overshadowed in the Roberts Arm suite by the strong positive correlation of CaO and Na_2O with Al_2O_3 suggesting that other major aluminosilicate components, probably epidote and detrital plagioclase, are prominent in this suite.

4) The strong positive MgO-FeO correlation reflects their mutual presence in chlorite. Because MgO exhibits a much stronger negative correlation with SiO_2 and positive correlation with Al_2O_3 than does FeO, it is likely that the chlorite is magnesium rich, but in the absence of mineral analyses, no quantitative estimates are possible.

5) MnO shows no significant correlations in the Roberts Arm and Fortune Harbour suites but is positively correlated with CaO, MgO, Al_2O_3, Fe_2O_3 and Na_2O in the Gull Pond suite. There are a number of alternative explanations for these correlations:

a) The lack of correlation between MnO and the other major elements in the Roberts Arm and Fortune Harbour suites probably indicates that MnO was supplied chemically in these areas and thus is not related in supply to the detrital minerals. Alternatively, the small amounts of MnO present in the Roberts Arm suite may be present in the various detrital minerals while being either too low in concentration or too scattered in mineralogic distribution to produce a positive correlation.

b) The positive correlation of MnO with other major elements in the Gull Pond suite suggests that MnO concentrations in this area may be due to the incorporation of larger amounts of this element into a major detrital mineral such as chlorite, thus producing the correlations via a mineralogic association factor. Alternatively, the MnO may be present as a discrete detrital phase linked to the other major elements

by a mineral grouping factor. A third possibility is that MnO is present in a discrete mineral phase which was chemically precipitated in environment where increased availability and/or environments suitable for the precipitation of MnO coincided with the introduction of a large detrital component. The highly siliceous nature of the Gull Pond suite relative to the other two suites would enhance any correlations produced by the above mechanisms because all other components are present in small (i.e. more nearly equal) amounts. Thus the collective dilution of quartz by the other components (i.e. chemical and detrital) will result in a relatively strong positive correlation of the elements via a mineral grouping factor.

Correlation of Major and Trace Elements

The significant correlations between major and trace elements are summarised in Fig. 5.2 and suggest the following relationships:

1) Rb, Zn, Sr and Zr are positively correlated with Al_2O_3 in all suites (except Sr in the Fortune Harbour suite) indicating that these trace elements are commonly present in the aluminosilicate minerals. Rb exhibits a strong correlation with K_2O, suggesting that it is principally bound in illite and sericite, while a similar correlation between Zr and Na_2O (and to a lesser extent CaO) probably reflects the related detrital contribution of plagioclase and zircon via a mineral grouping factor. Zn is consistently correlated with MgO, K_2O, and Al_2O_3 suggesting this element's preference for the clay fraction.

2) Sr correlates well with CaO and Al_2O_3 in the Roberts Arm and Fortune Harbour suites and with MnO in the Gull Pond and Fortune Harbour suites. MnO is considerably enriched in the Fortune Harbour and Gull Pond suites relative to the Roberts Arm suite (Table 5.1) and the above latter correlation suggests that, at least in the Fortune Harbour and Gull Pond suites, MnO was originally deposited as manganese carbonate.

3) Ba is positively correlated with K_2O, Al_2O_3 and Na_2O only in the Roberts Arm suite, coinciding with a considerable depletion of Ba in this suite relative to the other two. This suggests that most of the Ba in the Roberts Arm suite is either incorporated in aluminosilicate minerals or contributed as a discrete detrital phase along with these minerals. In the Gull Pond and Fortune Harbour suites, increased amounts of a discrete Ba-bearing mineral phase may have been chemically precipitated and concentrations of this element are thus unrelated to detrital supply. The minor Ba associated with the detrital fraction may also be present in these latter two suites but the excess amounts of the chemical phase would mask this relationship.

4) Ni in the Gull Pond suite is positively correlated with Fe_2O_3, CaO, K_2O, MgO, Al_2O_3 and MnO and negatively with SiO_2.

Trace Element Correlations

Consistent correlations are not as prevalent among trace elements as among the majors, probably due to a scattering of these elements among several mineral phases and/or to the generally low amounts of these elements in the rocks. Significant correlations summarized in Fig. 5.2 suggest the following:

1) The only consistent trace element correlations between all groups are the positive correlation of Zr with Sr and of Rb with Zn. In addition, Zn and Rb are positively correlated in the Roberts Arm and Gull Pond suites. This reflects the previously noted preference of Zn, Rb and Sr for the aluminosilicate minerals via a mineralogical association factor and the related detrital contribution of zircon via a mineral grouping factor.

2) Barium is positively correlated with Zr, Sr and Rb in the Roberts Arm suite probably reflecting its presence either in the aluminosilicate minerals in this suite or as detrital barite correlated with other detrital components via a mineral grouping factor.

5.3.2 Scattergrams

All major element analyses were plotted against SiO_2 in order to visually examine the chemical trends discussed in section 5.2.1. Selected scattergrams which illustrate the principal trends are presented in Figs. 5.3 to 5.10. The dominant feature in all scattergrams is a cluster of points near the horizontal axis in the high-silica range which contains those samples composed dominantly of free quartz. The trends generally terminate in this cluster and contain samples in which significant dilution of quartz by other minerals has taken place.

The scattergrams for Al_2O_3 versus SiO_2 in Fig. 5.3 show that both an upper relatively steep trend and a lower, more shallow trend are developed in the Gull Pond suite. The former is made up of samples containing greater than 8% Fe_2O_3 while the latter comprises mainly samples with less than 4% Fe_2O_3. Although these two trends are not as well defined in the Roberts Arm or Fortune Harbour suites, the relatively high Fe_2O_3

FIG. 5.3 Scattergrams of Al_2O_3 versus SiO_2 for the geographic suites. Dots represent samples having intermediate Fe_2O_3 concentrations.

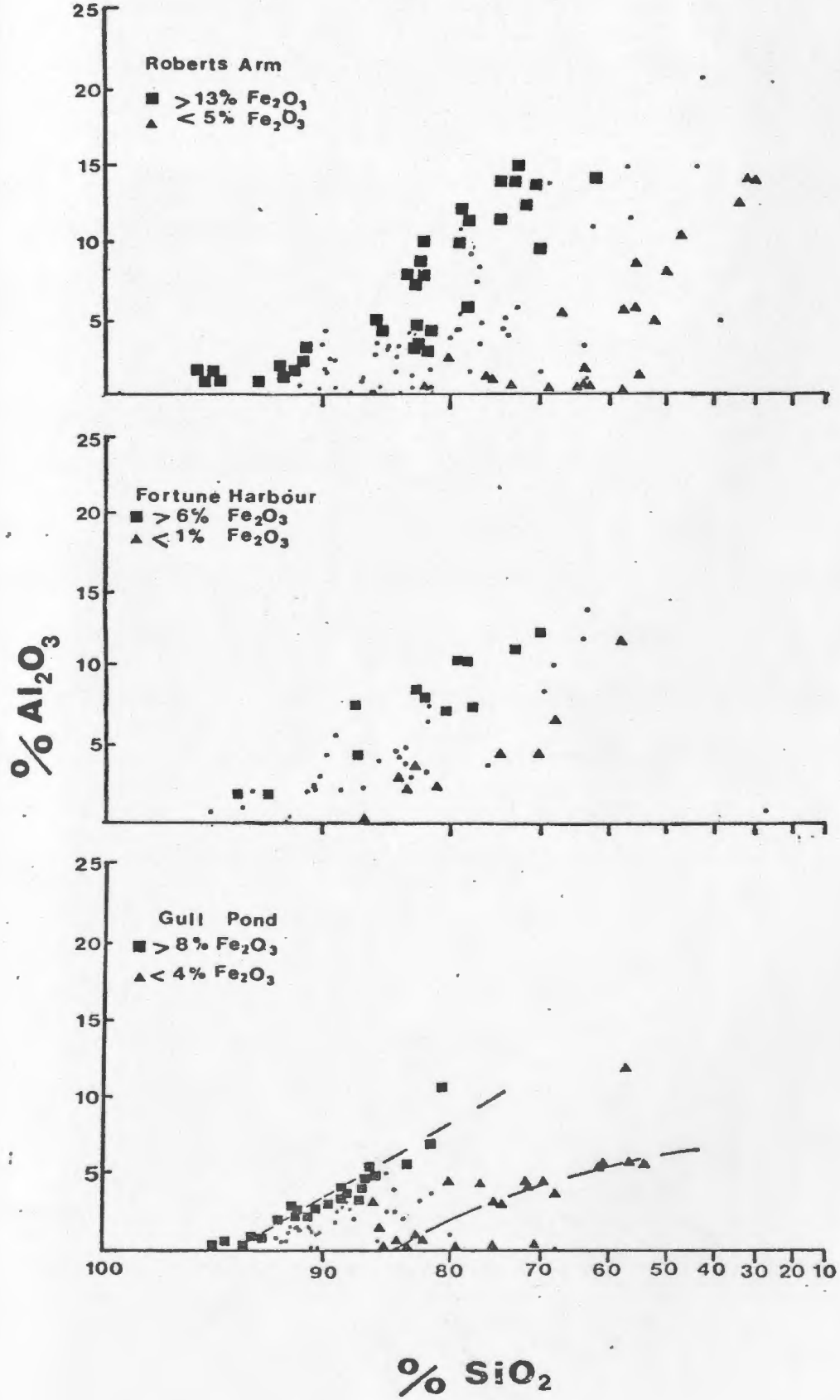

samples tend to plot along the lower boundary of the groups and the relatively low Fe_2O_3 samples along their upper boundary in both cases. This feature is further discussed with respect to the Gull Pond suite on page 116.

Most of the K_2O, CaO, Na_2O, MgO and FeO versus SiO_2 scattergrams show two separate sample groupings (e.g. Fig. 5.4). The first of these forms a negative linear trend originating in the high-silica cluster which reflects the dilution of quartz by increasing amounts of the aluminosilicate mineral(s) containing the element in question. The second group generally plots in a diffuse trend subparallel to the SiO_2 axis showing a wide variation in SiO_2 with little corresponding change in the concentration of the other element. In this group, dilution of quartz is being accomplished by minerals which do not contain the element in question (i.e. hematite and/or other aluminosilicate minerals). These two trends are particularly well developed on the K_2O/SiO_2 diagram for the Roberts Arm Group (Fig. 5.4), where a number of samples containing a quartz-free fraction dominated by K_2O lie along a line connecting the high-silica cluster with the theoretical composition of illite, suggesting that the chemistry of these samples is dominated by a dilution of quartz by this mineral. This linear trend is also present in the Fortune Harbour and, to a lesser extent, the Gull Pond suites.

The presence of substantial quantities of CaO-bearing aluminosilicate minerals in the Roberts Arm and Gull Pond suites is illustrated by the CaO versus SiO_2 scattergrams in Fig. 5.5. A number of samples plot along a

FIG. 5.4 Scattergrams showing K_2O versus SiO_2 for the geographic suites.

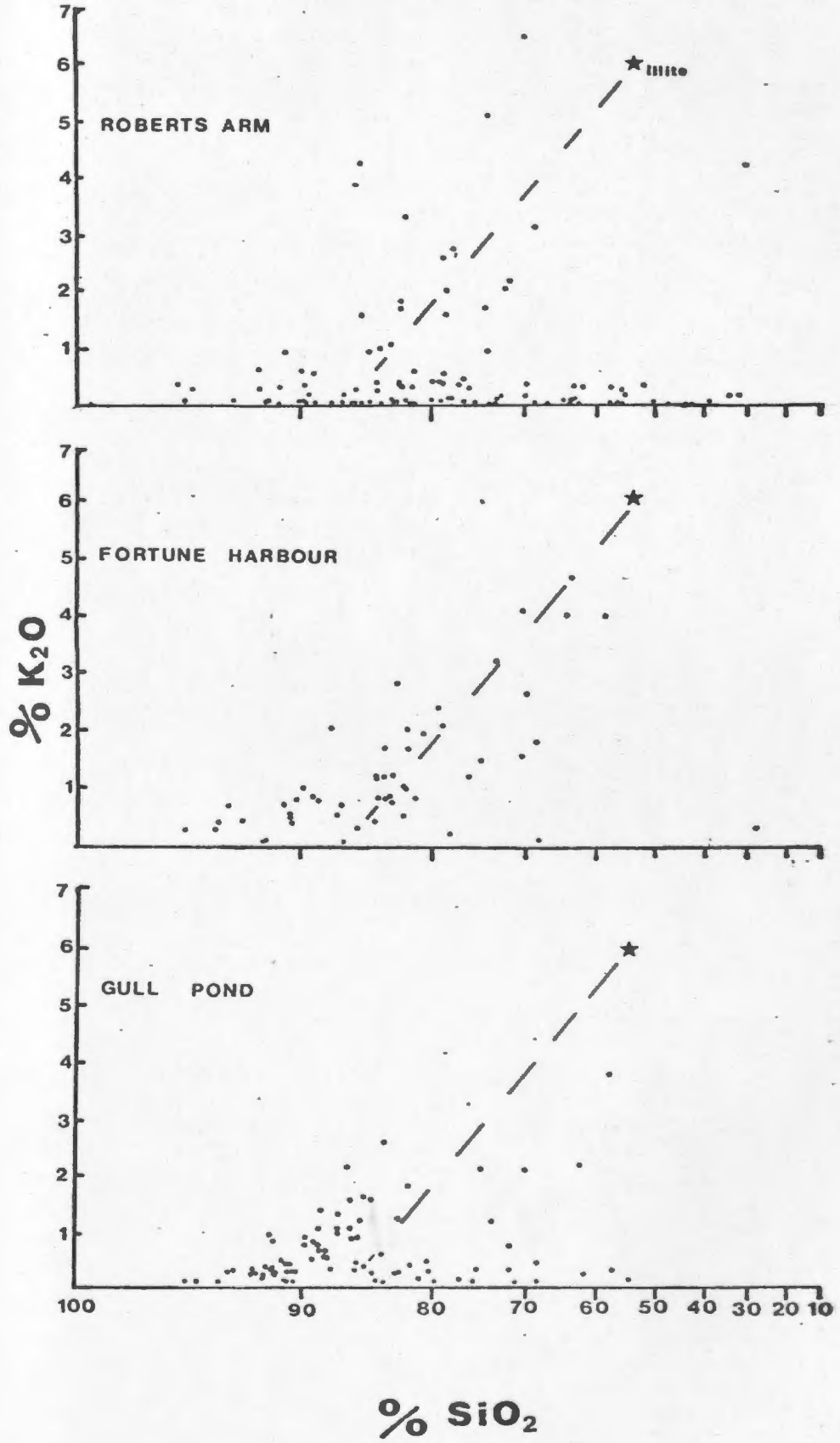

FIG. 5.5 Scattergrams showing CaO versus SiO_2 for the geographic suites.

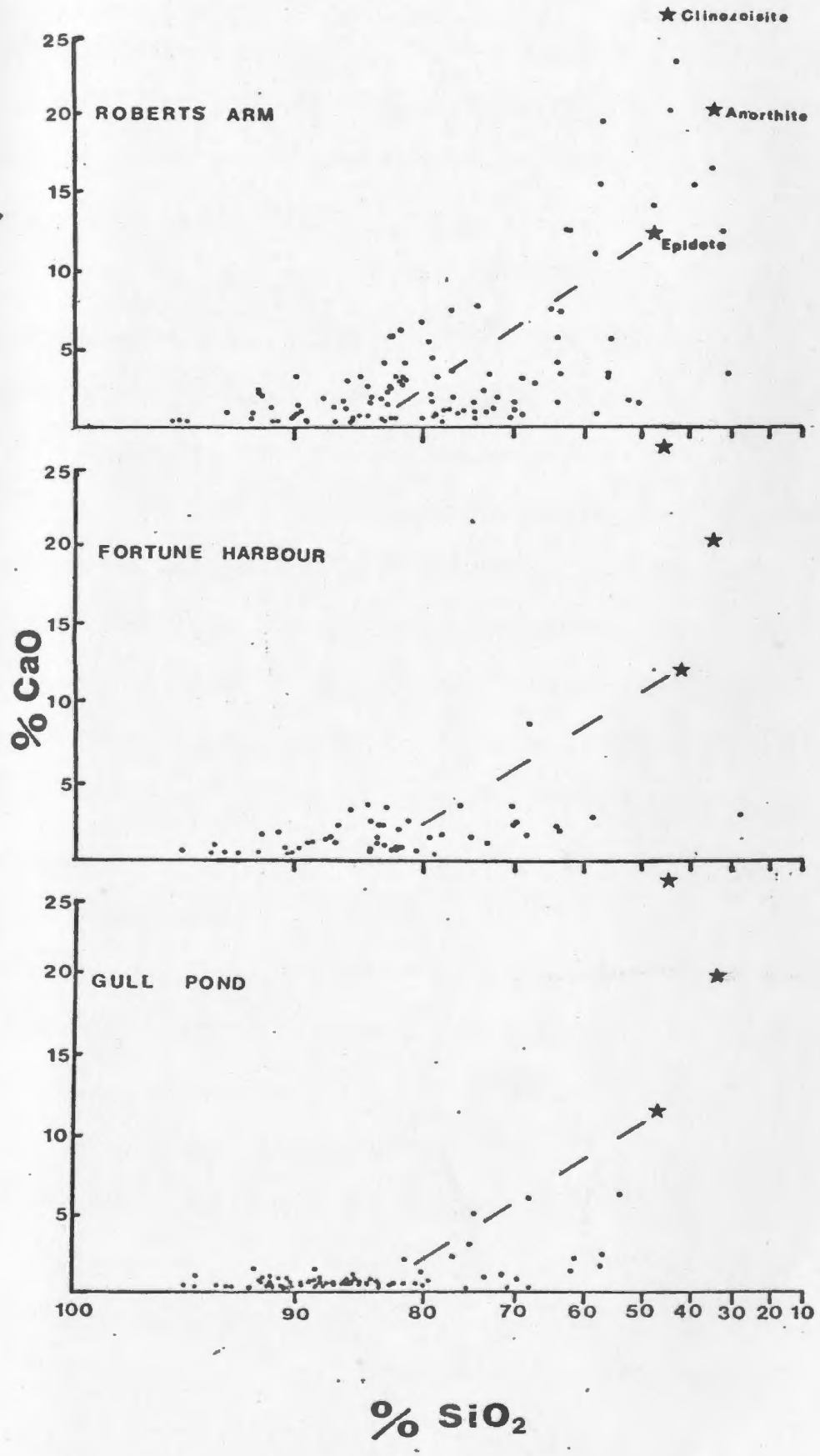

rather diffuse negative linear trend which links the theoretical compositions of epidote, clinozoisite and anorthite with the high-silica cluster. Optical mineralogy and X-ray diffraction studies (Chapter 4) indicate that the former two are the dominant CaO-bearing aluminosilicate minerals in all suites.

The presence of plagioclase as a principal component of the detrital fraction in the Roberts Arm suite is illustrated by Fig. 5.6 showing SiO_2 plotted against Na_2O where a number of samples lie along the line connecting the high-silica cluster with albite.

The relative homogeneity of the red and green subgroups with respect to most elements is reflected in their scattergram plots which commonly display linear trends caused by samples from both subgroups. However the majority of samples in the green subgroup tend to plot in the upper (i.e. high-concentration) part of the Al_2O_3, CaO, K_2O, MgO, and Na_2O versus SiO_2 diagrams (e.g. Fig. 5.7) reflecting their uniformly high aluminosilicate component and the paucity of low-aluminosilicate samples in this subgroup.

Fe_2O_3 in the green subgroup forms a relatively ill-defined trend below that formed by the red subgroup (Fig. 5.7) reflecting the fact that high-Fe_2O_3 contents in this subgroup are generally accompanied by considerable amounts of other elements besides SiO_2. The plot of CaO versus Fe_2O_3 for the green subgroup (Fig. 5.8) shows a rather vague linear relationship between these elements supporting the contention made in Section 4.3.2. that Fe_2O_3 in hematite-poor rocks occurs principally in

FIG. 5.6 Scattergrams showing Na_2O versus SiO_2 for the geographic suites

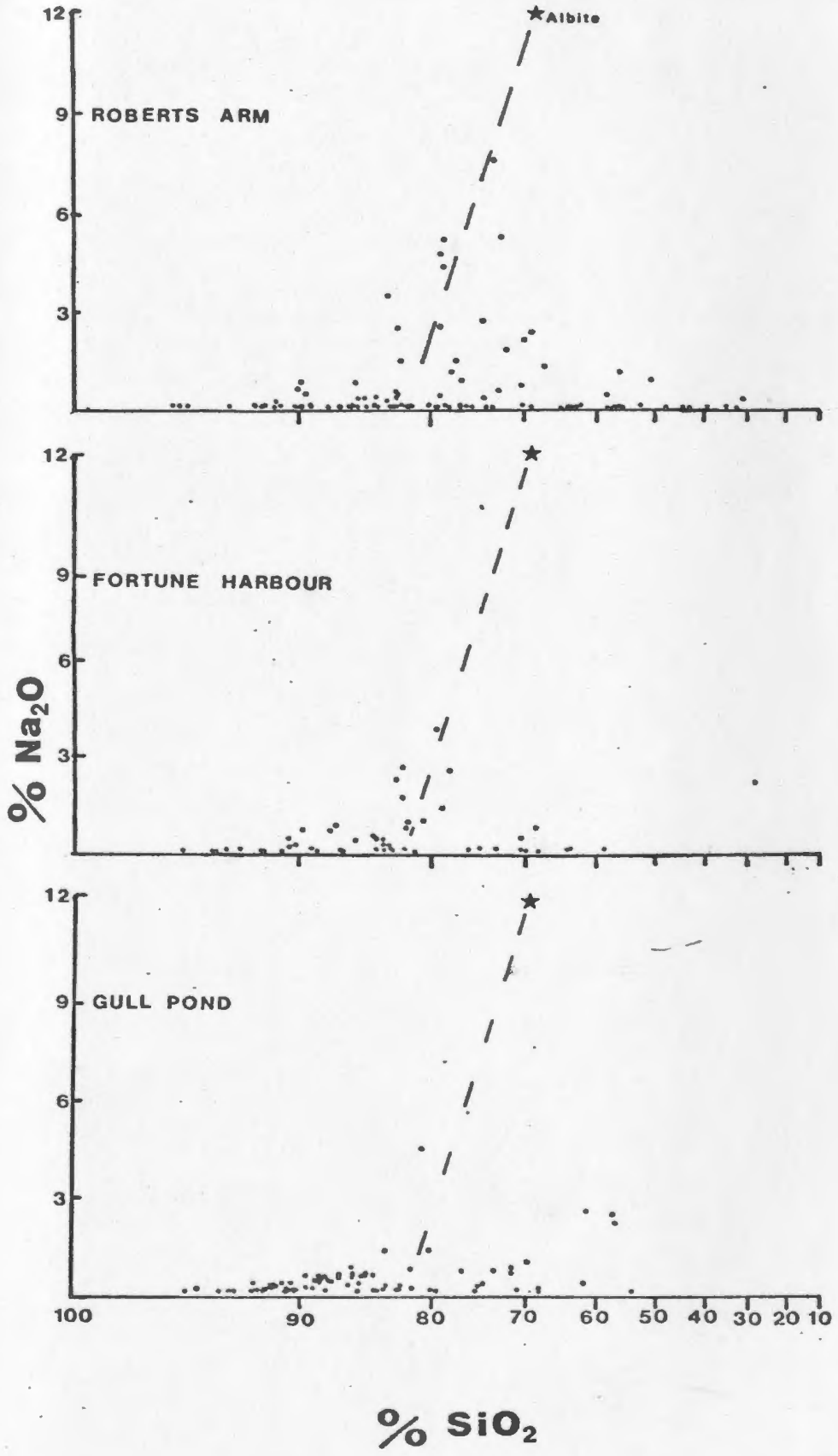

FIG. 5.7 Selected scattergrams comparing the composition of the red and green subgroups.

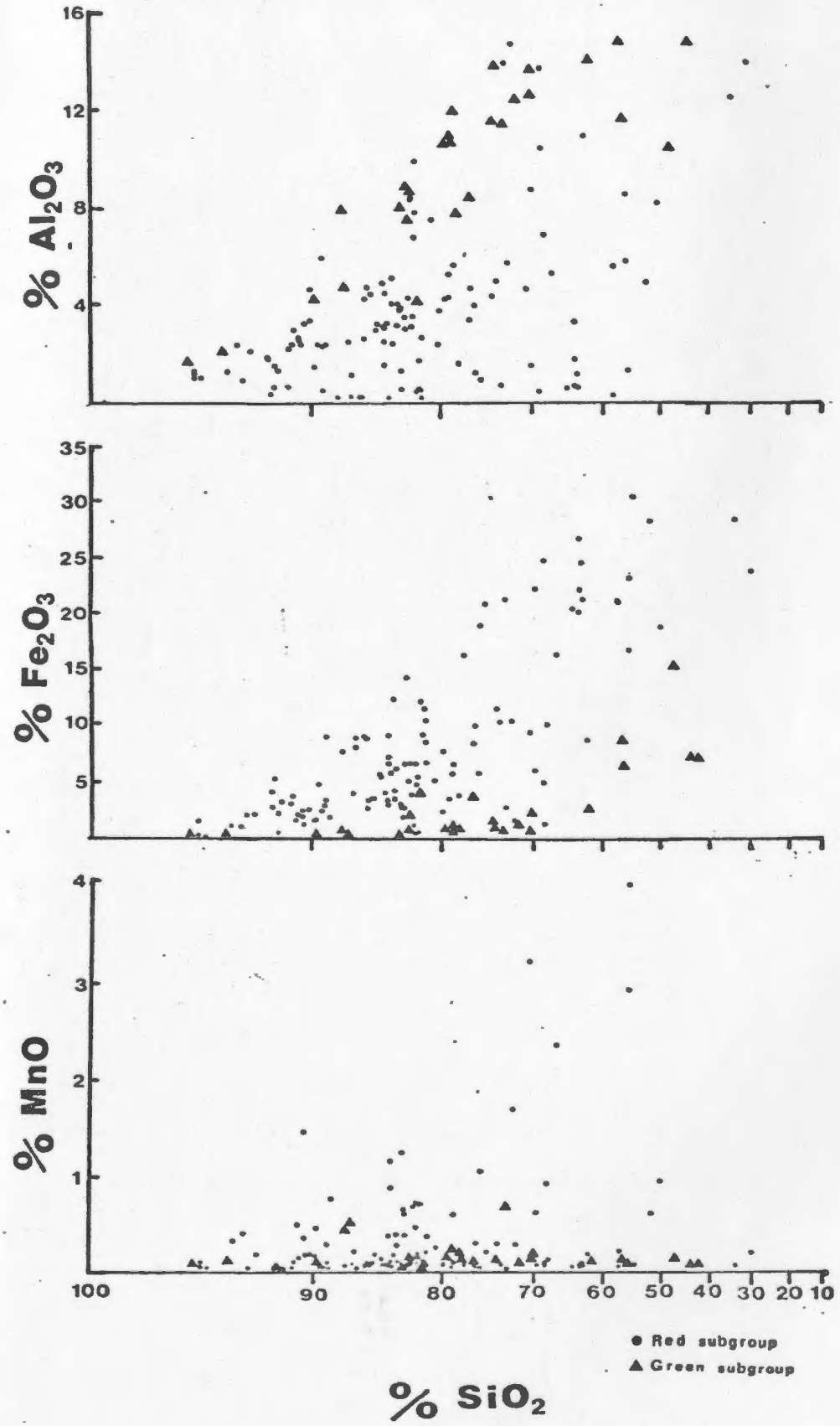

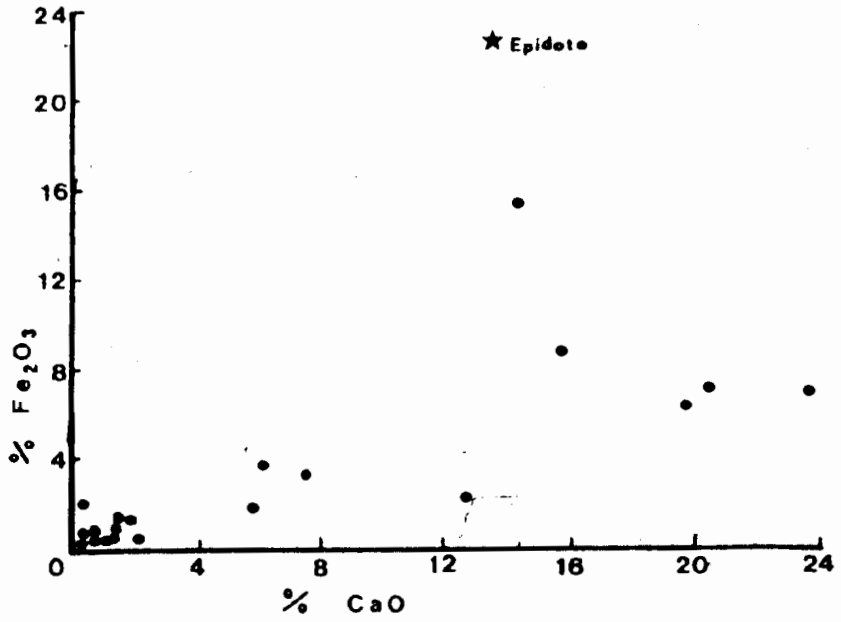

FIG. 5.8 Scattergram showing Fe_2O_3 versus CaO in the green subgroup.

CaO + Fe_2O_3-bearing aluminosilicate minerals (e.g. epidote, pumpellyite). The low trend of Fe_2O_3 versus SiO_2 in the green subgroup is thus probably a result of the presence of substantial quantities of other elements (mainly Al_2O_3, CaO) in the Fe_2O_3-bearing minerals of this subgroup as opposed to the absence of these elements in hematite, the principal Fe_2O_3-bearing mineral in the red subgroup.

The green subgroup also shows a tendency to cluster on the MnO versus SiO_2 diagram (Fig. 5.7) and shows a considerably smaller spread of MnO values than does its red counterpart.

The relative homogeneity of the bedded and interpillow subgroups with respect to Fe_2O_3 and SiO_2 is illustrated by Fig. 5.9 but other chemical trends in these subgroups tend to emphasize the relatively higher aluminosilicate component in the former subgroup. This is well illustrated in the K_2O and Na_2O versus SiO_2 diagrams (Fig. 5.9) where linear trends reflecting the dilution of quartz by illite/sericite and plagioclase respectively are composed entirely of samples from the bedded subgroup. This feature is not as evident in the MgO and FeO diagrams (Fig. 5.9) suggesting that the excess aluminosilicate component in the bedded subgroup results from higher concentrations of illite/sericite and plagioclase rather than chlorite.

The outstanding difference between these groups is illustrated on the TiO_2 versus SiO_2 diagram (Fig. 5.9) in which only one sample in the interpillow subgroup contains detectable TiO_2.

MnO shows a very restricted range of values in the interpillow subgroup as opposed to the bedded subgroup where it ranges up to 4% (Fig. 5.9).

FIG. 5.9 Selected scattergrams comparing the composition of the bedded and interpillow subgroups.

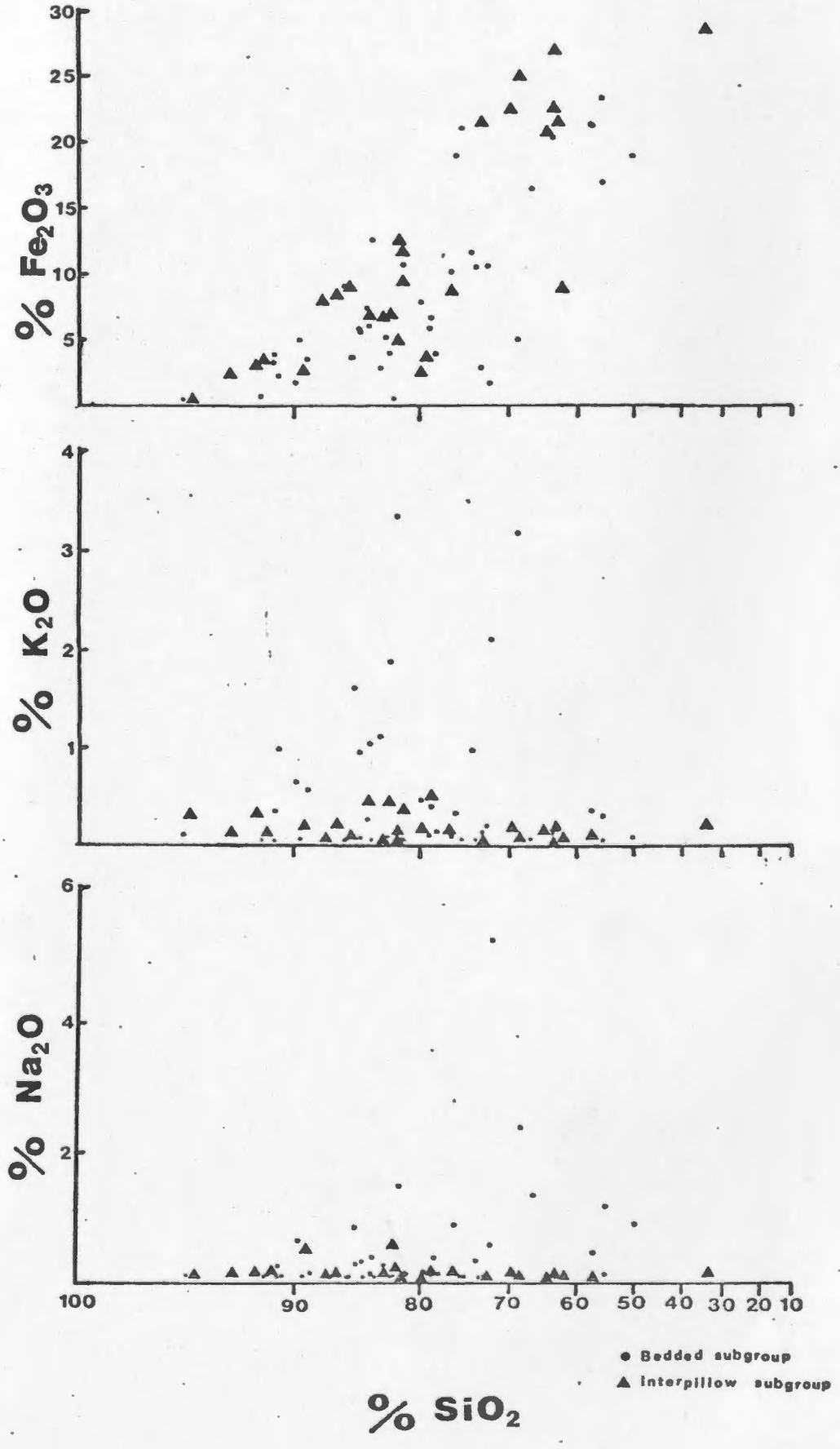

FIG. 5.9 (Continued)

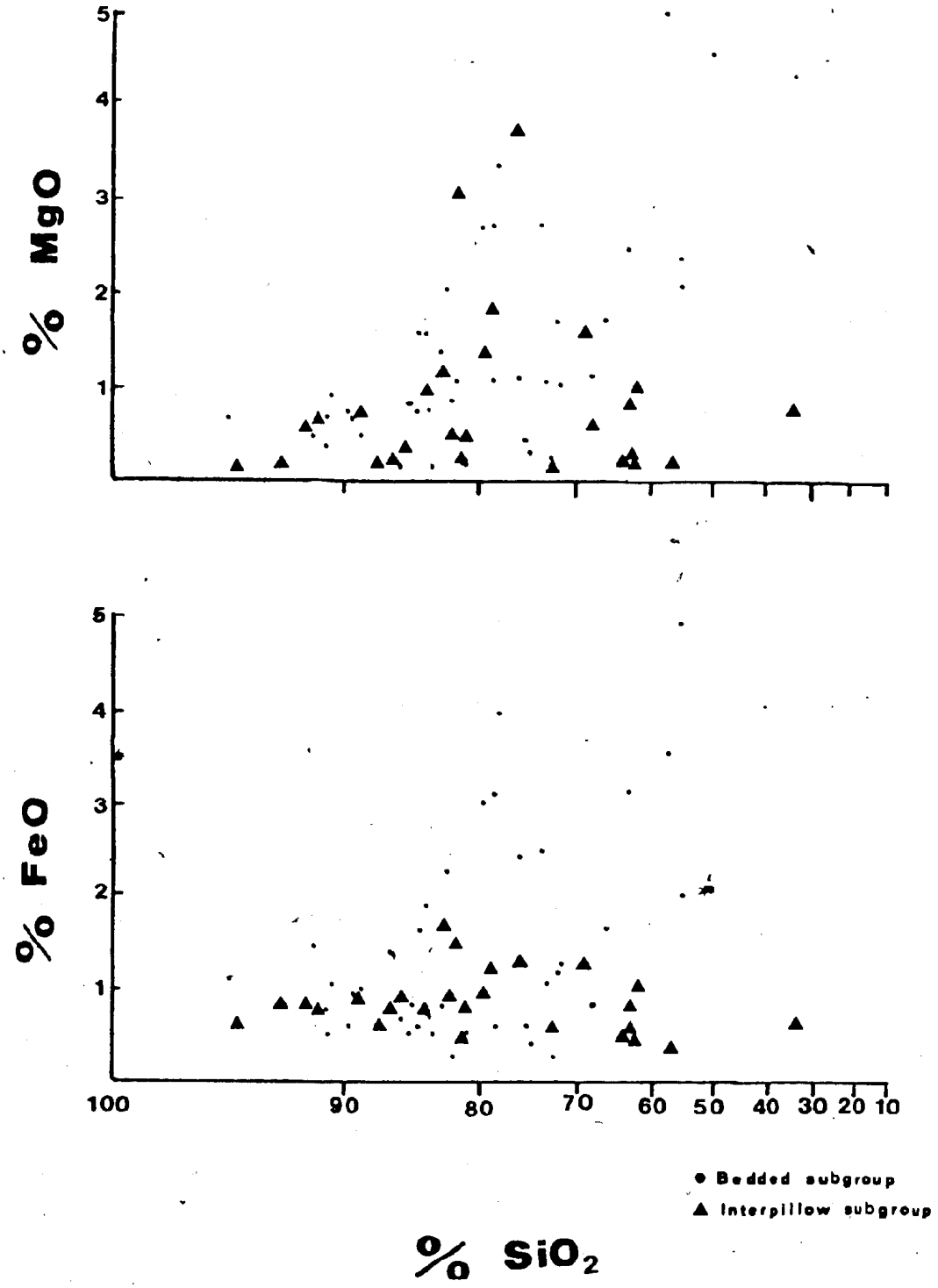

FIG. 5.9 (Continued)

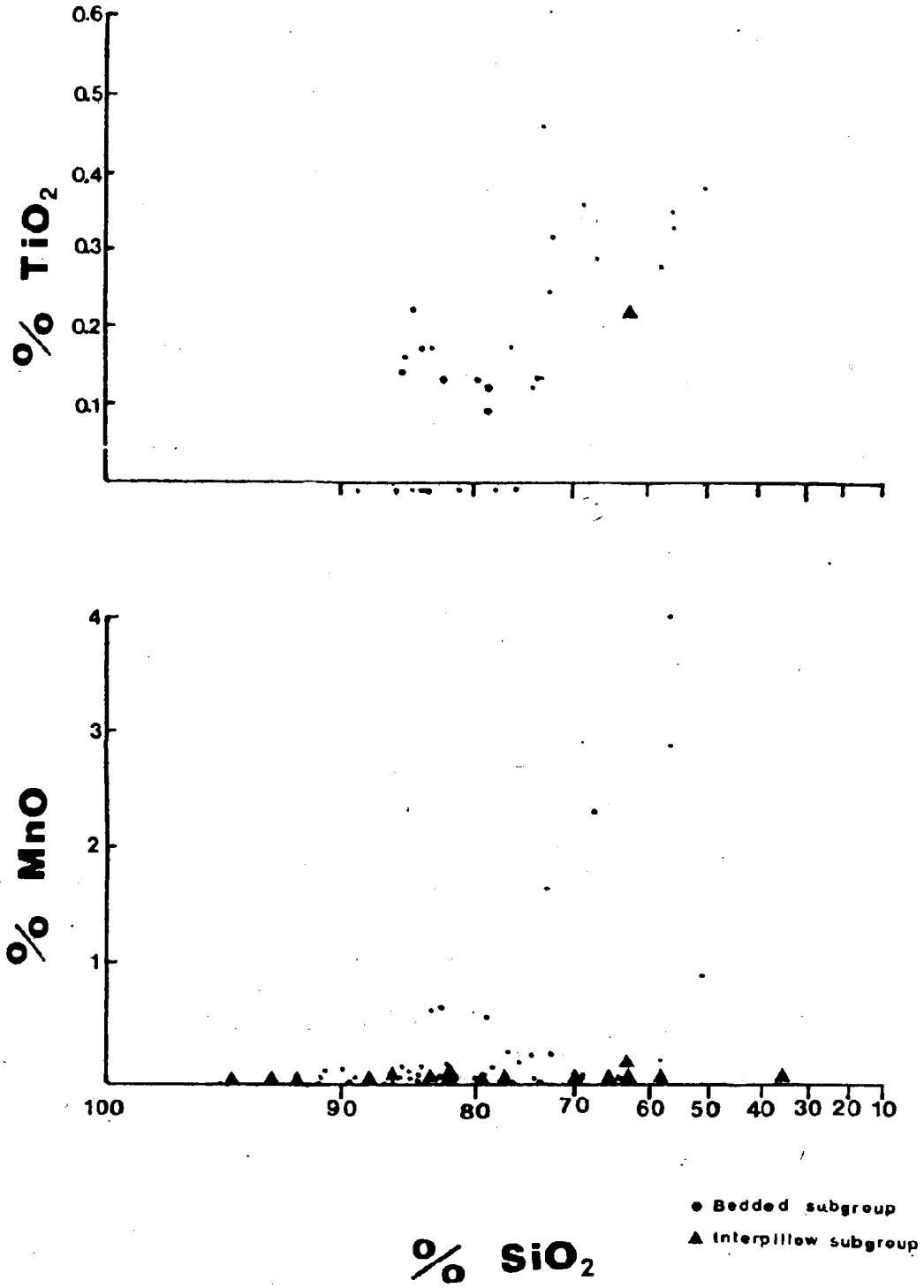

Scattergrams for the Gull Pond mineralization and mixed subgroups (Fig. 5.10) show that in general, elements in the latter subgroup tend to either cluster in restricted areas (e.g. CaO) or to form good linear trends (e.g. K_2O) while in the former subgroup, element concentrations are more widely scattered.

The reason for this is illustrated by the Fe_2O_3 versus SiO_2 diagram (Fig. 5.10) where the mineralization subgroup forms a relatively linear trend over a wide range of Fe_2O_3 values while the mixed samples cluster in a small area at the low-Fe_2O_3 end of the diagram. The strong linearity of the trends of most other elements versus SiO_2 in the mixed group is probably a direct result of this subgroup's limited Fe_2O_3 range and its chemistry is thus dominated by a simple dilution of quartz by aluminosilicate minerals. In the mineralization subgroup, however, the presence of a third major variable, Fe_2O_3, complicates the pattern and produces the observed scatter.

This effect is clearly illustrated by the Al_2O_3 versus SiO_2 diagram where the mixed subgroup lies in a fairly linear trend which parallels the trend developed by the Fortune Harbour suite and is separate and distinct from the somewhat more shallow linear trend formed by the mineralization subgroup (Fig. 5.10). It would appear that the former trend reflects a straightforward dilution of quartz by aluminosilicate minerals while in the latter trend, the addition of considerable extra hematite along with increasing amounts of aluminosilicate minerals causes a significantly greater dilution of quartz. The distinct separation of

FIG. 5.10 Selected scattergrams comparing the composition of the mineralization and mixed subgroups.

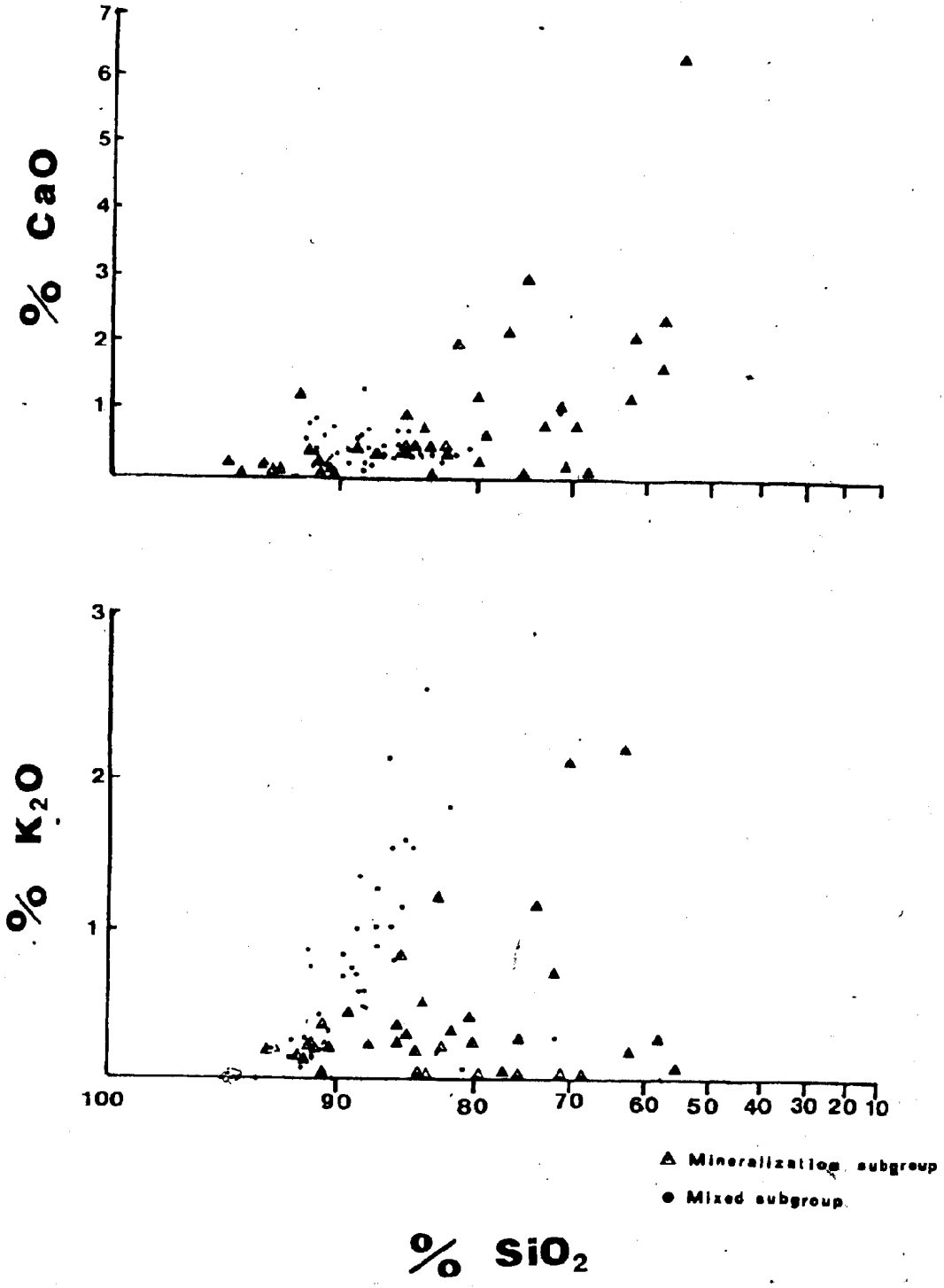

FIG. 5.10 (Continued)

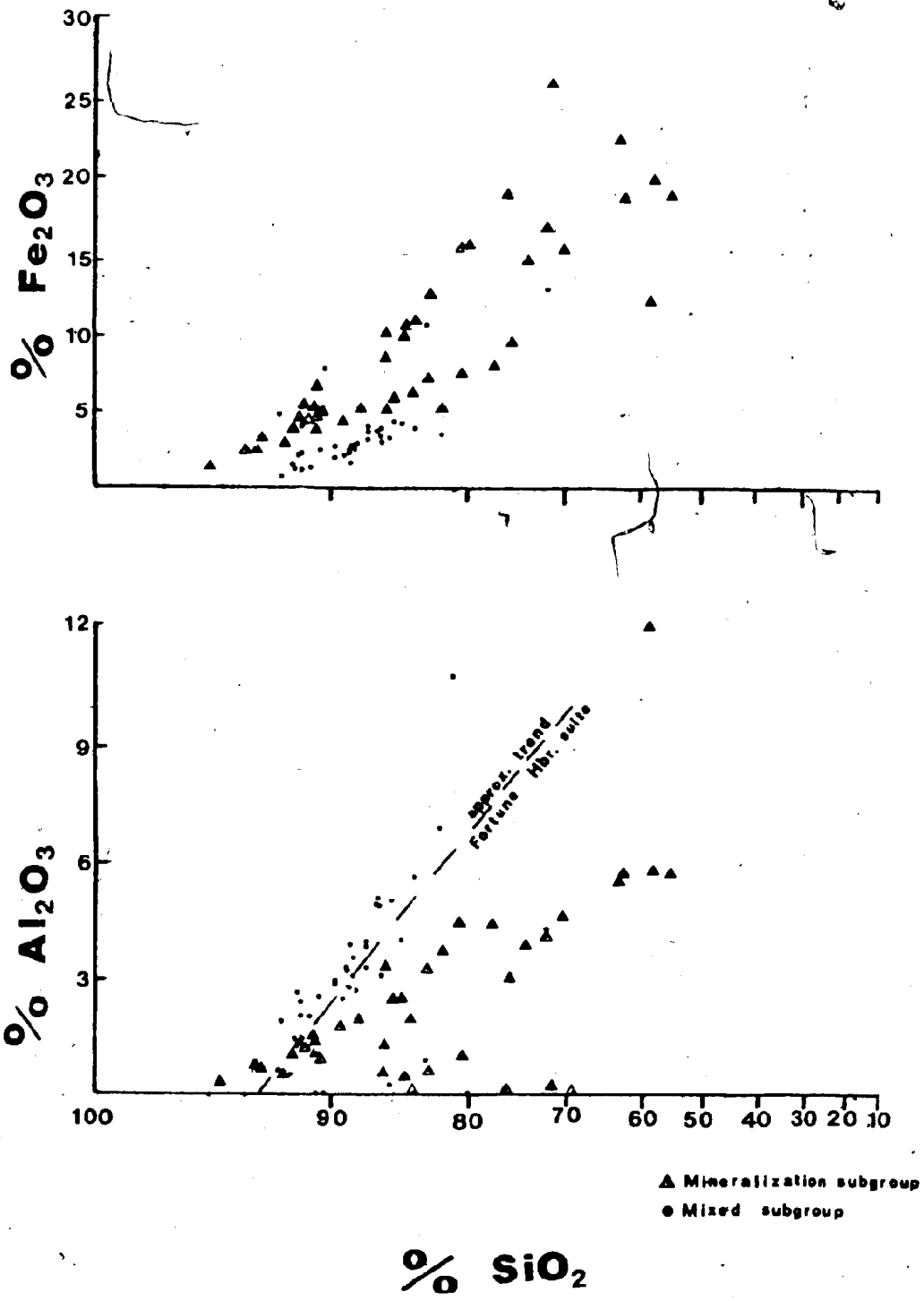

these trends suggests that the excess hematite in the mineralization subgroup was contributed in distinctly higher amounts than were available during the formation of rocks comprising both the mixed subgroup and the Fortune Harbour suite.

5.3.3 Stratigraphic Variability in the Roberts Arm and Fortune Harbour Suites

Samples from the Roberts Arm and Fortune Harbour suites were subdivided according to their stratigraphic level within the volcanic sequence and analysed statistically to see if a consistent, stratigraphically-controlled chemical variation is present. The Mann-Whitney U Test was applied to the element concentrations of samples from the upper and lower halves of the volcanic section in the two respective areas. In the Roberts Arm area, samples were taken from an almost complete coastal section through the sequence from Sop's Arm to Woodford's Arm (Fig. B.1) and in the Fortune Harbour area from a coastal section along the northwest arm of Fortune Harbour and from highway road cuts.

The mean concentration of elements in the upper and lower halves of the two sections, their standard deviations and the probability level at which they are different are presented in Table 5.5. It can be seen that although differences between elements are significant at a high level of probability within the Roberts Arm and Fortune Harbour sections respectively, there are no consistent differences from one area to the other.

Further analysis of the stratigraphically higher and lower groups by discriminant function analysis likewise did not show any consistent differences in the samples corresponding to their stratigraphic position in the volcanic succession.

TABLE 5.5

COMPOSITION AND PROBABILITY OF DIFFERENCE OF STRATIGRAPHIC SUBGROUPS, ROBERTS ARM AND FORTUNE HARBOUR SUITES

	ROBERTS ARM				FORTUNE HARBOUR			
	Upper		Lower		Upper		Lower	
Weight percent	Mean	P**	Mean	P	Mean	P	Mean	P
Fe_2O_3	9.01		10.57		3.05		2.99	
TiO_2	.01		.04		.05		.07	
SiO_2	81.53		78.20		86.7		85.2	
CaO	2.94		2.95		1.13		.82	
K_2O	.18		.36		.88		.97	
MgO	.59		.59		.76		.87	
Al_2O_3	2.58		2.08		3.65		4.85	
FeO	.73		.78		.82		.60	
Na_2O	.07		1.97		.30		.89	
L.O.I.**	1.64		2.94	98.99%	2.16		1.92	
MnO	.03		.12	95.61%	.32		.44	
ppm								
Zr	33		30		39		45	
Sr	105		70		65		48	
Rb	16		19		41		34	
Zn	25		27		41		44	
Cu	11		14		21		9	
Ba	108		271	95.89%	608		245	97.32%
Nb	6		8		5		8	
Ni	50		32		29		28	
Cr	16		18		15		15	

* - Loss on Ignition

** - Probability that samples from the two groups form separate populations with respect to each variable - for p > 95%.

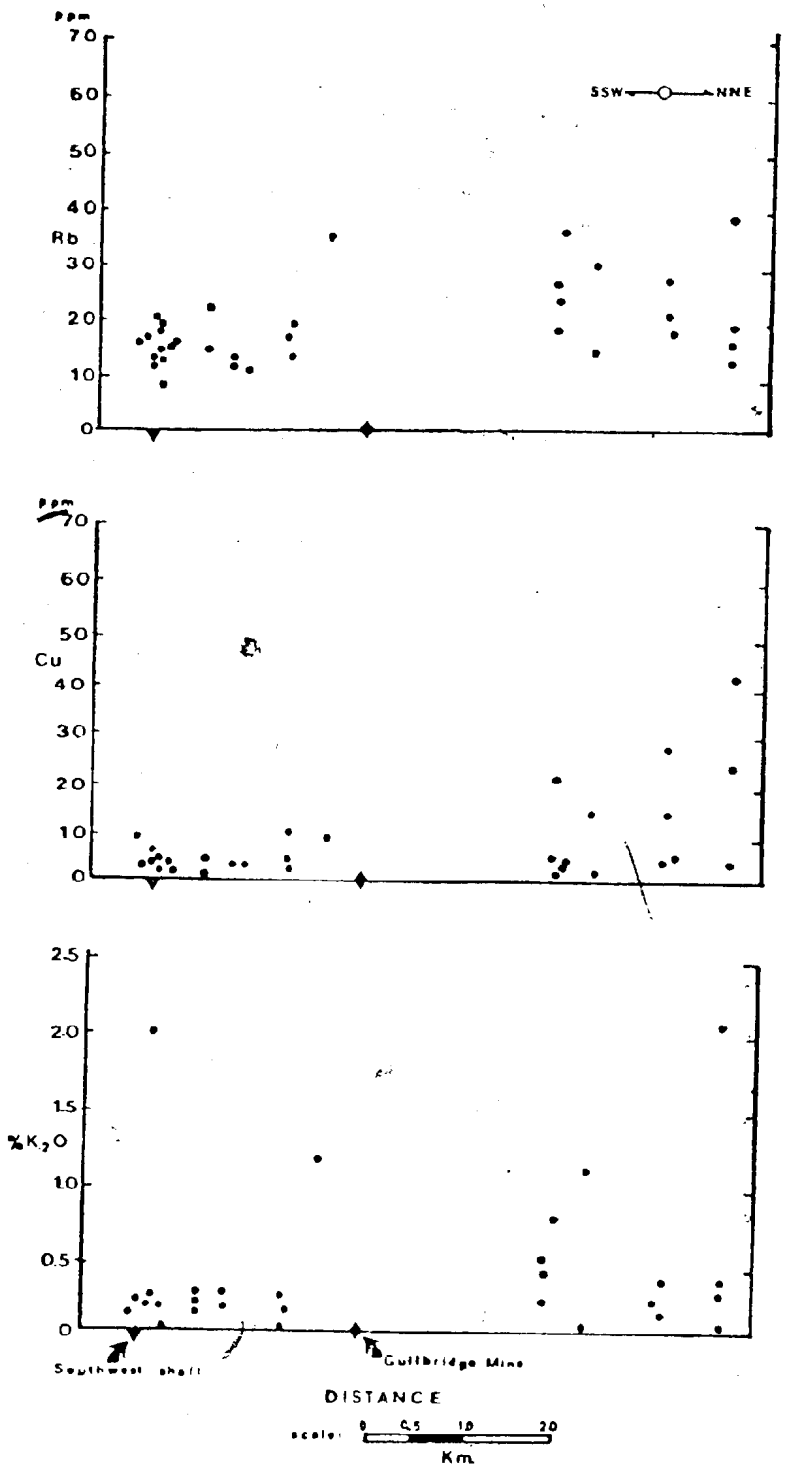

FIG. 5.11 Longitudinal section through the Gullbridge and Southwest shaft deposits showing lateral variation of selected elements.

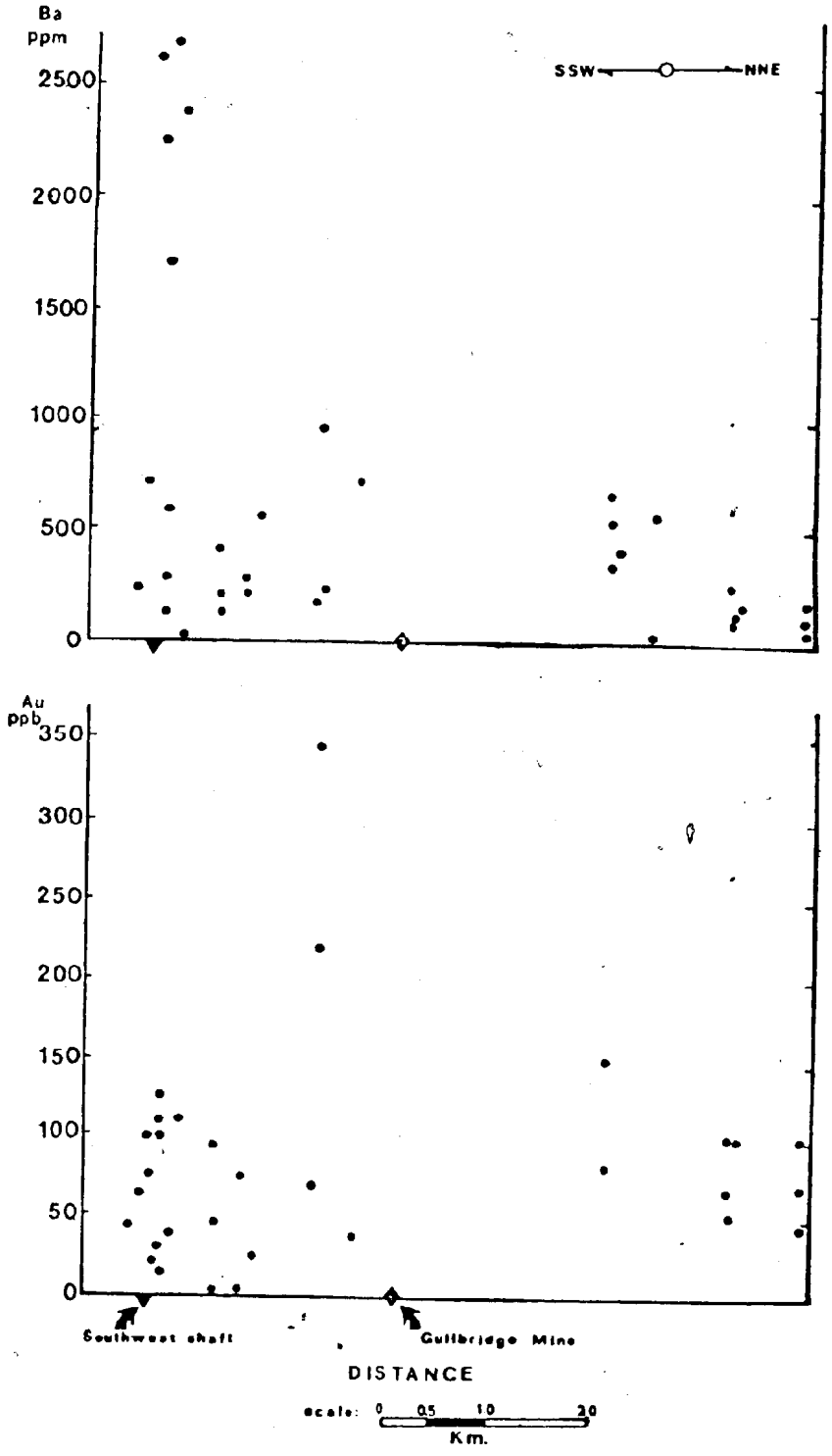

FIG. 5.11 (Continued)

5.4 Lateral Variability Within The Gullbridge Ferruginous Chert

Concentrations of all elements in the Gullbridge ferruginous chert were plotted on a longitudinal section of this horizon in order to show any variations along strike. Most elements were found to be very evenly distributed within this horizon and few obvious trends are developed. The only suggestion of a trend among the major elements is the slight tendency of K_2O to increase from south to north, possibly reflecting a slight relative enrichment in illite (Fig. 5.11). This trend is mirrored in the trace elements by Rb (see Sec. 5.3.1) and by Cu which shows a clear enrichment in many samples of the northern region (Fig. 5.11).

The concentration of Ba in this subgroup does not show any gradual trend but all Ba concentrations greater than 1500 ppm occur near the south end of the exposed horizon in the area of the Southwest shaft. Similarly, anomalously high Au values are restricted to the area immediately south of the Gullbridge orebody (Fig. 5.11).

5.5 Comparison with the Chemistry of Cherty and Ferruginous Sediments From Other Areas

The average composition of 253 chert and ferruginous sedimentary rock associated with the Upper Ordovician-Silurian volcanic succession in Notre Dame Bay (hereafter referred to as the Notre Dame Bay suite) is presented in Table 5.6 together with analyses of various modern and ancient deposits analagous in chemistry. It can be seen from this table that while many of the world-wide sediment types possess some chemical similarities with the Notre Dame Bay suite, none are strictly comparable in all elements.

Table 5-6: Comparison of present samples with chert and ferruginous sediments from other areas.

	*	1	2	3	4	5	6	7	8	9	10	11	12	13
Fe_2O_3	7.61	3.40	7.04	6.73	7.26	19.29	3.38	4.53	3.53	5.53	1.00	1.43	.83	4.03
TiO_2	.24	0.59	.75	.68	.25	.21	.17	.28	.27		Tr.	.20	.91	.65
SiO_2	79.68	67.36	55.08	65.05	85.39	44.11	84.64	80.87	87.66	91.1	86.56	79.92	80.65	53.38
CaO	2.08	1.74	.72	2.06	.82	1.96	.63	1.35	.38	.32	2.13	.11	1.42	3.12
MgO	.83	2.29	2.92	3.08	1.12	3.85	.84	1.71	.61	.71	.76	1.4	1.73	2.45
K_2O	.99	2.15	2.65	3.14		.97	1.17	1.13	.93	.10	1.80	3.38	2.35	3.25
Al_2O_3	4.32	11.33	16.28	15.1	4.57	4.40	5.28	6.55	4.47	.78	1.90	7.44	6.39	15.47
FeO	1.08	1.42	.64								.35	.68	.83	2.46
Na_2O	.61	1.64	1.18	1.32		1.00		.62	1.32	.03	.41	.55	.28	1.31
MnO	.71	.19	.58	1.29	.26	4.79	.52	.51	.22	.12	.06	.06	.12	Tr.
Zr	.43	170	132		59		49							
Sl	95	230	371											
Zn	37				100	321	36	195				96	203	
Cu	14	370	350		130	979	139	106				33	21	
Ba	352	1050	1416			1500	342	64						
Ni	34	330	295		43	1004	52	31				23	27	
Cr	22	97	63		34		37	38				33	29	

* - Avg. concentration, 247 samples, present study.

1 - Avg. siliceous ooze (El Wakeel and Riley, 1961)
2 - Avg., 11 recent marine red clays (El Wakeel and Riley, 1961)
3 - Radiolarian ooze (Cressman, 1962)
4 - Avg., 18 radiolarites (Audley-charles, 1965)
5 - East Pacific metalliferous sediments, Avg. 8 samples (Sayles and Bischoff, 1973)
6 - Red chert from Ligurian ophiolite (Bonatti et al., 1976)
7 - Cyprus radiolite, Avg. 3 samples (Robertson and Hudson, 1973)
8 - Avg. 5 samples, red and green chert (Cressman, 1962)
9 - Archean chert in Algoma-type iron formation. Avg. 3 samples (after Beukes, 1973)
10 - Avg. 15 cherts (after Pettijohn, 1957)
11 - M1 mudstone, Matsumine Mine, Japan. Avg. 3 samples (after Tono 1974)
12 - M2 mudstone, Matsumine Mine, Japan. Avg. 4 samples (after Tono, 1974)
13 - Avg. shale (after Clarke, 1924)

All modern sediments have considerably lower concentrations of SiO_2 and higher concentrationsof Al_2O_3, MgO, K_2O, Na_2O and FeO, with the exception of the East Pacific metalliferous sediments which have similar Al_2O_3, Na_2O and K_2O concentrations but considerably higher MgO. The only modern sediments comparable in Fe_2O_3 concentration to the Notre Dame Bay suite are marine red clays, while siliceous and radiolarian oozes are considerably depleted and the East Pacific metalliferous sediments are considerably enriched in this element, relative to the Notre Dame Bay suite.

The major element composition of the various ancient and modern siliceous and ferruginous sediments listed in Table 5.6 are compared to the Notre Dame Bay suite in Fig. 5.12. Most sediment types plot either near the SiO_2 apex or within the low-iron trend defined by the Fortune Harbour and part of the Roberts Arm Groups (Sec. 5.1.1). The only sediments to plot in the high-iron trend are metalliferous sediments from the East Pacific Ocean floor.

The trace element compositions shown in Table 5.6 indicate that modern pelagic deposits are considerably enriched in most trace elements relative to ancient lithified deposits. Trace element concentrations in red radiolarian chert reported by Bonatti, et al. (1976) exhibit the closest correlation with the Notre Dame Bay suite of all reported sediment types. Zn is depleted in the Notre Dame Bay suite relative to most deposits, and copper is depleted relative to all except the Kuroko M1 and M2 mudstones.

In comparison with Clarke's (1924) average shale, the Notre Dame Bay suite is considerably enriched in SiO_2, Fe_2O_3 and MnO, while

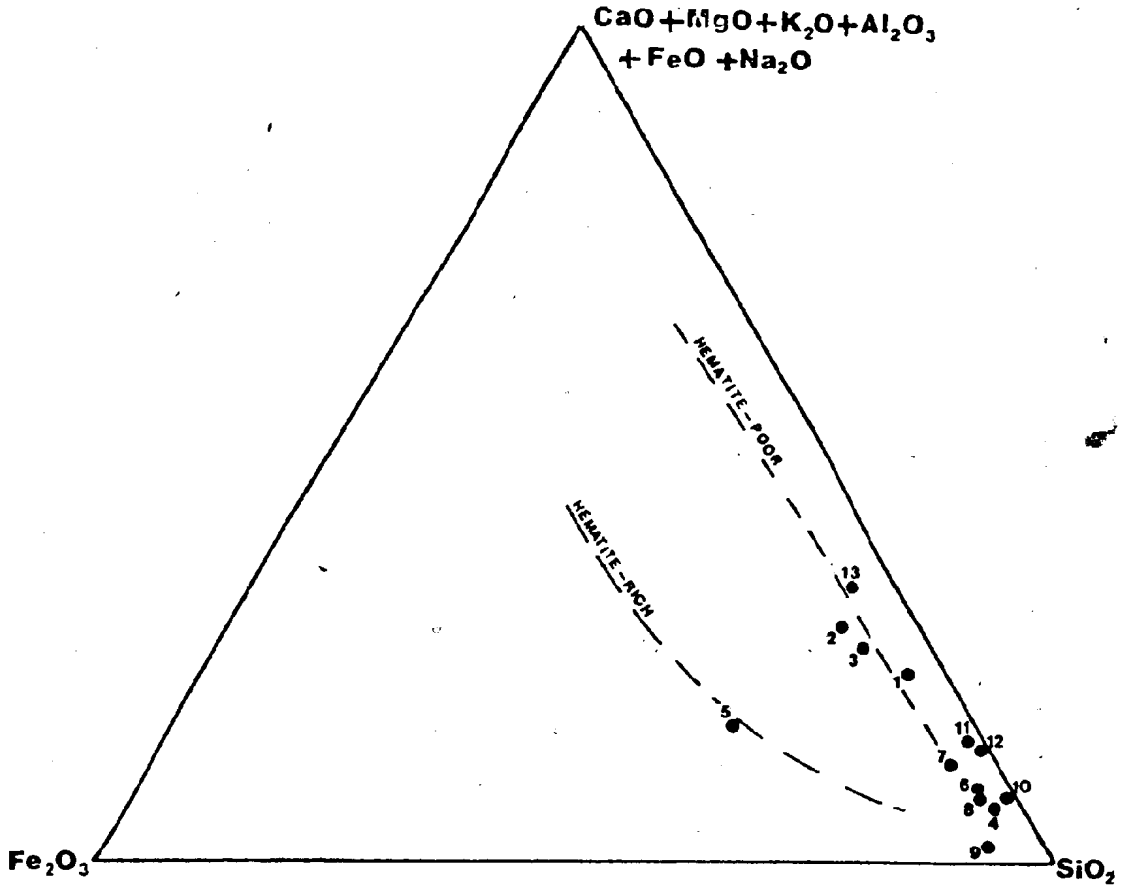

FIG. 5.12 Composition of various sedimentary rocks from other areas (see Table 5.6) compared with those of the present study (see also Fig. 5.1). Key to numbers is same as Table 5.6.

being relatively depleted in all other major elements. However, relative to other ancient cherty sedimentary rocks, the Notre Dame Bay suite is considerably enriched in Fe_2O_3 and slightly enriched in CaO and MnO while having similar to slightly lower concentrations of all other major elements.

In spite of the overall depletion of the aluminosilicate-related elements in the Notre Dame Bay suite relative to Clarke's (1924) average shale, the sediment fraction containing these elements is chemically very similar to lutites from other areas. This is illustrated by Fig. 5.13 adapted from MacKenzie & Garrels (1971) which compares world-wide lutite compositions with those of igneous rocks on the basis of Na_2O/Al_2O_3 and K_2O/Al_2O_3 ratios. The plotted position of the average Notre Dame Bay samples lies close to the general variation trend for fine-grained sedimentary rocks, indicating that this fraction is composed of "normal" shaly sediment. The slight enrichment of Na_2O in the Notre Dame Bay suite relative to most other ancient deposits probably reflects a volcanogenic origin for at least part of the detrital fraction. MacKenzie and Garrels (1971) note that alteration of volcanic detritus consisting chiefly of plagioclase (Na, Ca, Al, Si) and pyroxene (Ca, Mg, Fe, Si) to an albite (Na, Al, Si), chlorite (Mg, Fe, Al, Si), epidote (Ca, Al, Si) assemblage results in a relative depletion of Ca, Mg, and Fe and enrichment of Na and H_2O in the end product. The Na_2O content of the Notre Dame Bay suite, while being slightly enriched relative to ancient deposits, is considerably depleted relative to modern Pacific pelagic deposits which are formed dominantly of basaltic detritus and plot high in the Na_2O-rich part of the diagram (Fig. 5.13). This may suggest either that a portion of this

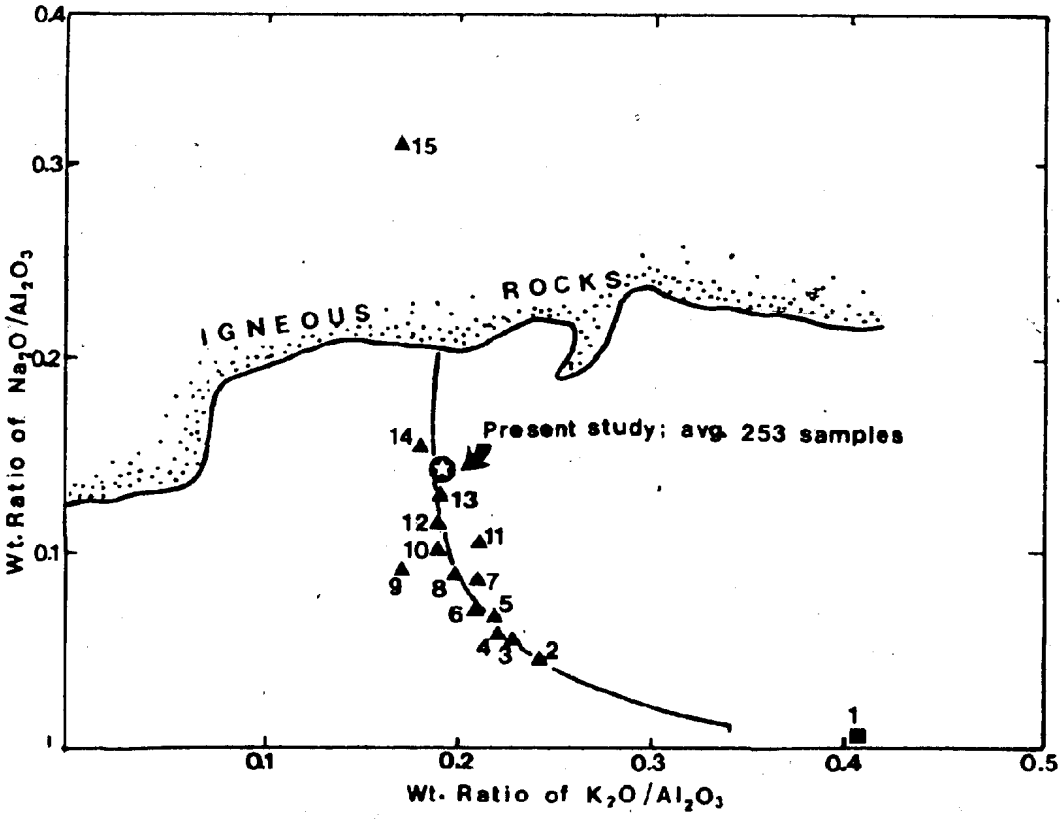

FIG. 5.13 Composition of lutites from other areas compared with those of igneous rocks in terms of their Na_2O and K_2O contents; 1 - illite composition; 2 - avg. Paleozoic shale, Russ. Plat.; 3 - avg. Russ. Plat. shale; 4 - 33 PC slates; 5 - avg. Paleozoic shale (Clarke, 1924); 6 - 36 Paleozoic slates; 7 - avg. shale (Clarke, 1924); 8 - 79 slates and phyllites; 9 - avg. pelagic sed.; 10 - 41 mica schists; 11 - 85 low-grade pelites; 12 - 70 high-grade pelites; 13 - avg. Mes.-Cen. shale; 14 - 61 slates; 15 - avg. Pacifi pelagic sed. (after Mackenzie and Garrels, 1971).

material in the Notre Dame Bay suite was derived from normal weathering and erosion processes or that a significant portion of the detrital component was composed of siliceous volcanic material carrying little plagioclase and no pyroxene which would tend to dilute the Na_2O-enrichment in these rocks relative to the Pacific pelagic deposits.

The relation of this feature to the relative enrichment in SiO_2 of the Notre Dame Bay suite is clearly shown in Fig. 5.14 adapted from MacKenzie and Garrells, (1971). Most samples from the Fortune Harbour and Gull Pond suites plot in a linear trend bounded at the low-silica end by the composition of the average Paleozoic shale and showing a progressive increase in SiO_2 content with relatively little change in the composition of the detrital fraction. The trends lie outside the field of modern siliceous sediments in an area of higher SiO_2/Al_2O_3 and lower $(Na_2O+CaO)/K_2O$ values. Assuming that samples from the Gull Pond and Fortune Harbour suites were chemically analagous to modern siliceous sediments at the time of deposition, it would appear that diagenesis and lithification has caused a shift in composition in the direction indicated by the arrows. This is consistent with the compositional changes during chert development postulated by Berger and von Rad (1972) and von Rad and Rosch (1974) in which progressive chertification leads to a relative increase in the concentration of microcrystalline quartz and a corresponding decrease in the relative concentration of the various aluminosilicate minerals (see Fig. 2.1). The relative decrease of $(Na_2O+CaO)/K_2O$ ratio may have been enhanced by post-depositional processes in which alteration of a detrital component carrying plagioclase + pyroxene ± olivine to clay + albite + epidote would result in a loss of CaO (as well as Mg and Fe) while K_2O and

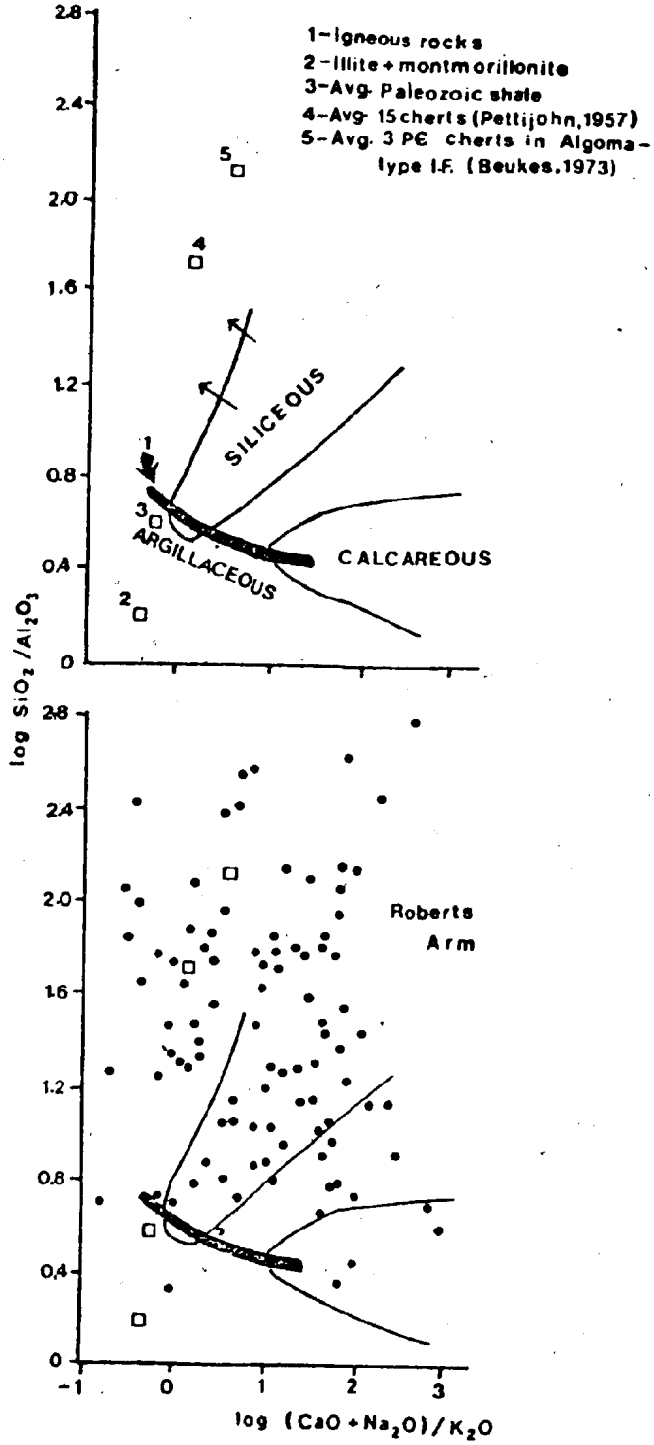

FIG. 5.14 Chemical compositions of modern sediments compared with those of the present study on the basis of log (SiO_2/Al_2O_3) and log ($Na_2O+CaO)/K_2O$ (after Mackenzie and Garrels, 1971).

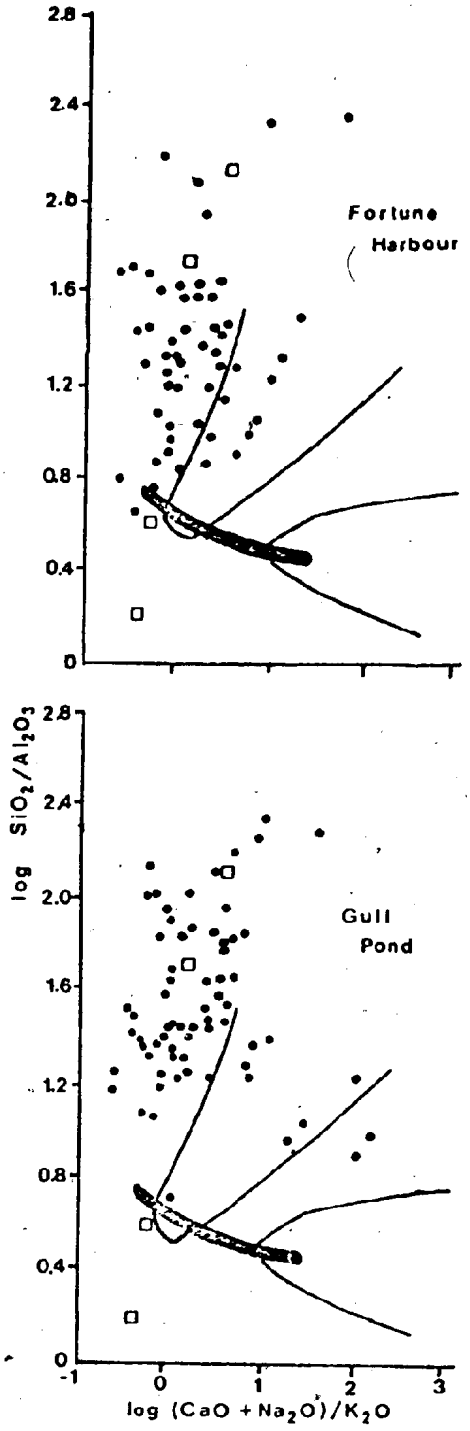

FIG. 5.14 (Continued)

Na_2O are conserved or gain slightly (MacKenzie and Garrels, 1971). The relative paucity of Na_2O with respect to CaO resulted in its gain being masked by the quantitatively larger loss of CaO, with the net result being a decrease in $(Na_2O+CaO)/K_2O$.

The trend of the Gull Pond and Fortune Harbour samples on this diagram includes both the average composition of 15 cherty sediments reported by Pettijohn (1959) and 3 Archean ferruginous cherts reported by Beukes (1973) suggesting that features illustrated by this diagram have general applicability.

Samples from the Roberts Arm suite show considerably more scatter on this diagram and approximately one half of the samples are enriched in $(Na_2O+CaO)/K_2O$ relative to the Gull Pond and Fortune Harbour samples. This probably reflects the relatively higher CaO concentrations in the Roberts Arm suite (Table 5.1) and suggests that these sediments were originally more calcareous than their counterparts in other areas.

5.6 Summary of Results

The principal chemical trends in the chert and ferruginous sedimentary rocks associated with the Upper Ordovician-Silurian volcanic rocks of Central Newfoundland are strongly influenced by the mineralogy of these rocks. Three major components are commonly present in the rocks which are represented by specific major elements and are normally associated with specific trace elements. Concentrations of SiO_2 and Fe_2O_3 reflect the presence of quartz and hematite respectively while Al_2O_3, CaO, K_2O, MgO, FeO and Na_2O represent a detrital aluminosilicate fraction composed

principally of illite, sericite, chlorite, epidote and albite. MnO appears to be commonly present in a discrete mineral phase and was probably orignally deposited in the Gull Pond and Fortune Harbour suites as a manganese carbonate. In some cases, MnO may be present as a trace component of the aluminosilicate minerals.

Trace elements, with the exception of Au and sometimes Ba, are commonly associated with the aluminosilicate fraction and can often be related to specific minerals.

The principal chemical trend in these rocks is a negative correlation of most components with SiO_2, which reflects the dilution of quartz by all other minerals. Relationships between elements associated with the aluminosilicate component are strongly influenced by the mineralogy of this component and can usually be related to the presence of specific minerals.

The Gull Pond and Fortune Harbour suites are internally homogeneous but show distinct differences between themselves and with the relatively inhomogeneous Roberts Arm suite. Fe_2O_3 is relatively depleted in the Fortune Harbour suite as are SiO_2, MnO, Ba, and Au in the Roberts Arm suite and most of the aluminosilicate-related elements in the Gull Pond suite.

Green sedimentary rocks in the present study are chemically distinguished from their red counterparts by a relative depletion in Fe_2O_3 and a relative enrichment in elements related to the aluminosilicate component. Bedded sedimentary rocks in the Roberts Arm suite are enriched in the aluminosilicate-related elements and slightly depleted in Fe_2O_3 relative to lithologically similar rocks present in pillow interstices in the volcanic rocks.

There is no consistent variation in the chemistry of these sedimentary rocks according to their stratigraphic position, indicating that neither the progressive chemical development of the related volcanism nor the changing bulk chemistry of the associated volcanic rocks substantially influences their chemical composition.

A continuous ferruginous chert horizon in the Gull Pond area which is spatially related to two volcanogenic base metal sulphide deposits shows distinct chemical differences from other similar lithologies in this area, being enriched in Fe_2O_3, MnO and Ba and slightly enriched in Au. This horizon displays no lateral chemical trends except for a slight enrichment of K_2O, Rb and Cu from south to north. Maximum concentrations of Ba and Au occur proximal to the Southwest shaft and Gullbridge deposits respectively.

The sedimentary rocks of the present study exhibit chemical similarities with modern and ancient chert and ferruginous sediments from other areas but are strictly comparable to none. They are enriched in SiO_2 and Fe_2O_3 and depleted in most other major elements relative to recent marine sediments, and enriched in Fe_2O_3 relative to similar ancient deposits. The aluminosilicate fraction is similar in bulk composition to lutites from other areas and the dilution of free quartz by this fraction produces compositions similar to those of chert and ferruginous sediments in ancient marine volcanic environments.

CHAPTER 6

GENESIS OF CHERT AND FERRUGINOUS SEDIMENTS IN CENTRAL NEWFOUNDLAND

6.1 Introduction

The geochemical, petrologic and field evidence presented in previous chapters leads to a number of conclusions concerning the genesis of the chert and ferruginous sedimentary rocks associated with the Upper Ordovician-Silurian volcanic sequence of Central Newfoundland. This chapter summarizes these conclusions, suggesting sources of the various components in these rocks and presenting an interpretation of the environmental conditions prevailing during their deposition and diagenesis.

6.2 Source of the Sedimentary Components

6.2.1 SiO_2

The evidence that most, if not all, of the non-detrital quartz in modern and ancient chert and siliceous sediments from various areas is of biogenic origin (cf. Sec. 2.2) can be successfully applied to siliceous lithologies studied during the present project. The sporadic presence of radiolarian remains in various stages of decomposition in the bedded deposits may indicate that radiolarian tests were common constituents of the original sediment and that their dissolution supplied large amounts of silica to interstitial waters during diagenesis (Wise and Weaver, 1974). Additional silica may have been supplied in the subsurface through the breakdown of volcanic debris, but its quantitative importance cannot be assessed. The precipitation of cristobalite and its

inversion to quartz in the manner suggested by Heath and Moberly (1971) is considered to be the most likely mechanism for the formation of non-detrital quartz in the siliceous lithologies of the present study.

6.2.2 Fe_2O_3

Corliss (1971) suggested that in areas of active volcanism, sea water circulating in recently extruded basalt would become heated and enriched in a number of components, one of them being iron. He noted that these metal-enriched solutions could be expected to precipitate a ferric hydroxide floc upon their discharge into the marine environment which would either settle in topographic lows near the discharge point or be widely dispersed, depending on the presence of bottom currents. Spooner and Fyfe (1973), noting that metamorphic paragenesis of ophiolitic rocks in East Liguria indicated temperatures of up to 400^{o}C as shallow as 300 m below the original rock-water interface, presented a model of sub-sea floor metamorphism and mass transfer involving the circulation of sea water in the heated rocks. They suggested that hematite in ferruginous chert overlying the volcanic assemblage was formed from iron which was leached from the underlying basalts by heated sea water and subsequently precipitated as hydrous ferric oxides upon the discharge of these waters into the marine environment. Recent experimental investigations of the leaching of basalt at elevated temperatures (Bischoff and Dickson, 1975; Hajash, 1975) confirmed that substantial enrichment of iron as well as other elements in the aqueous solution could be accomplished by this mechanism.

The distribution of Fe_2O_3 in the Roberts Arm, Fortune Harbour and Gull Pond suites indicates that similar processes of iron enrichment

were operative during deposition of these sedimentary rocks. The highest Fe_2O_3 concentrations are present in the Roberts Arm suite where the ferruginous sedimentary rocks are commonly hosted by mafic rather than siliceous volcanic rocks and where the mafic volcanic sequence is by far the thickest of the three areas. It is inferred that this relatively large mafic volcanic mass contributed correspondingly large amounts of iron to subsurface hydrothermal water and this is reflected in the composition of the resulting chemically precipitated sedimentary rocks.

Similarly, the relatively iron-rich Gullbridge ferruginous chert occurs immediately above a thick basal basaltic sequence which is inferred to be the source of iron for this unit.

The ferruginous sedimentary rocks of the Gull Pond mixed subgroup and the Fortune Harbour suite are commonly hosted by silicic pyroclastic rocks and their relative paucity of Fe_2O_3 may reflect in part the relatively iron-poor volcanic sequence which hosts them and which formed their subsurface during deposition.

6.2.3 TiO_2, CaO, K_2O, MgO, FeO, Na_2O, Al_2O_3

These elements occur in aluminosilicate minerals which are dominantly of detrital origin. The composition of the detrital fraction suggests that this material is chemically comparable to "normal" shaly sediment but with a distinct Na-enrichment, suggesting that it is dominantly composed of volcanic debris rather than the products of weathering and erosion. Possible sources for this material include water-borne tuff and previously deposited bottom sediment redistributed by bottom currents.

6.2.4 MnO

Manganese may be introduced in substantial quantities into the submarine environment by the same mechanisms responsible for the introduction of iron (e.g. Corliss, 1971; Fyfe and Spooner, 1973; Bischoff and Dickson, 1975; Hajash, 1975) and the positive correlation of MnO and Fe_2O_3 in the Gull Pond suite suggests that, at least in this area, such mechanisms were operative. The two elements may become strongly fractionated, depending on Eh conditions either in the subsurface or in the marine environment (Krauskopf, 1957; Bonatti et al., 1976) and this may account for their lack of correlation in the Roberts Arm and Fortune Harbour suites (see also Sec: 6.3).

6.2.5 Trace Elements

Generally low trace element concentrations and the correlations they display (Sec. 5.3.1) indicate that most were supplied to these sedimentary rocks dominantly by the detrital fraction.

Ba is relatively enriched in the Fortune Harbour and Gull Pond suites relative to the Roberts Arm suite, coinciding with the relative abundance of Ba-rich silicic volcanic host rocks in the former suites. Chemical evidence suggests that Ba enrichment in the former two suites is not related to detrital supply implying a leaching of Ba in the subsurface, followed by its precipitation as a discrete mineral phase in the submarine sedimentary environment.

Gold is likewise enriched in the Gull Pond and Fortune Harbour suites and the lack of chemical correlations displayed by this element suggests that it too was supplied by hydrothermal solutions.

6.3 Depositional Environment of the Bedded Deposits

Bedded sedimentary rocks of the Roberts Arm, Fortune Harbour and Gull Pond suites range in composition from relatively pure chert to siliceous and/or ferruginous shale and tuff. They occur as small, discontinuous, conformable lenses within the Upper Ordovician-Silurian sequence suggesting that they were originally deposited in topographic depressions in the volcanic sequence. They are commonly intercalated with tuff and, less commonly, with chloritic sediments and graded turbidite deposits, and while occurring dominantly within silicic pyroclastic sequences in the Gull Pond and Fortune Harbour suites, they are commonly hosted by mafic pillow lava in the Roberts Arm Group.

The chert and ferruginous sedimentary rocks are commonly laminated on a scale ranging from 1 mm to several centimeters, mainly due to the differential concentration of hematite and, less commonly, tuffaceous and/or clastic material. The more shaly members sometimes display evidence of current reworking but these effects are rarely seen in highly siliceous and/or ferruginous members. Internal structures in the latter reflect only slight readjustments probably due to initial slope instability and/or density contrasts between layers.

The depth of water during deposition can be inferred from other geological evidence. Kanmera (1974) suggested that the presence of silicic pyroclastic rocks interbedded with chert in the Paleozoic-Mesozoic volcanic sequence of Japan indicated a water depth during deposition of less than 500 m. Similar lithologies associated with the chert and ferruginous sediments in Central Newfoundland suggest that a similar

interpretation is applicable in this area. Strong (1973) suggested that pillow size and vesicularity in the Roberts Arm Volcanics indicated that relatively shallow water depths prevailed during their extrusion, reinforcing the above interpretation.

Relatively rapid deposition of the bedded sedimentary rocks is inferred from the following considerations:

1) Rapid clastic sedimentation and pyroclastic deposition in an active island arc environment would tend to dilute slowly accumulating chemical sediments (e.g. Kanmera, 1974; Dickenson, 1974; Garrison, 1974).

2) Low heavy metal contents in analagous sediments are interpreted by Bonatti et al. (1972) to be characteristic of rapidly deposited hydrothermal deposits because slow precipitation of iron and manganese hydroxides would result in extensive scavenging of heavy metals from the sea water. Figure 6.1 illustrates that on the basis of heavy metal versus iron and manganese content, these rocks fall within the rapidly deposited, hydrothermal field of Bonatti et al. (1972).

3) Rapid accumulation of large amounts of ferruginous sediment has been observed in modern, hydrothermally-supplied basins (e.g. Zelenov, 1964; Butuzova, 1966; Bonatti et al., 1973).

Geochemical conditions prevailing in the depositional basins during sedimentation are reflected in the oxidation state of iron and in the Mn/Fe ratio (Krauskopf, 1957). Hematite (Fe_2O_3) is the preponderant iron mineral in the chemical sedimentary rocks of Central Newfoundland. The following considerations suggest that ferric compounds were the original precipitates and that little or no reduction of this iron was accomplished during diagenesis:

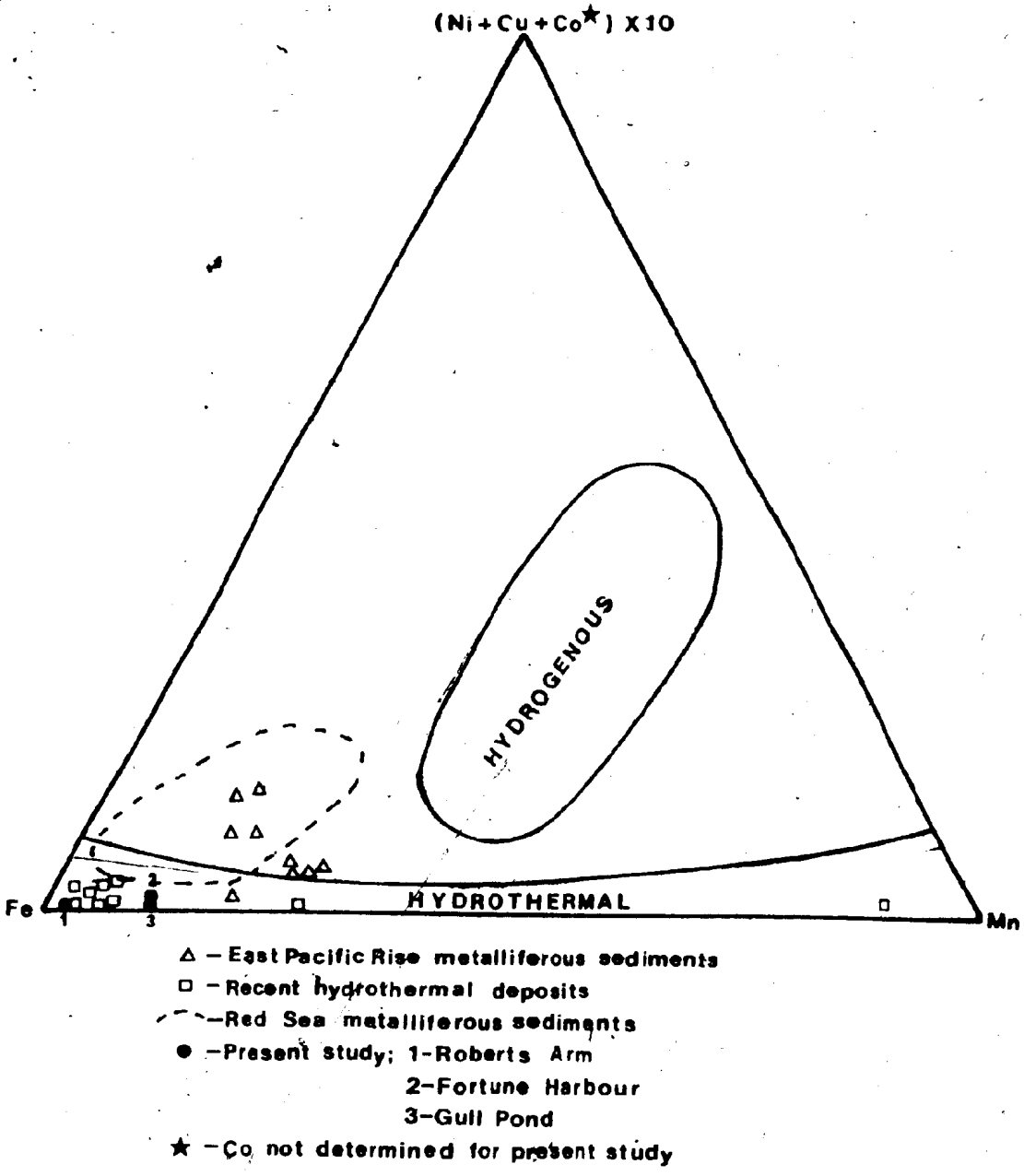

FIG. 6.1 Classification of hydrothermal and hydrogenous ferromanganese deposits according to Fe/Mn/(Ni+Cu+Co) ratio (after Bonatti et al., 1972). Note that although Co was not determined during the present study, it would have to be enriched by more than a factor of 10 to cause these samples to plot outside the hydrothermal field, a circumstance that data of other workers (e.g. Audley-Charles, 1965; Sayles and Bischoff, 1973; Bonatti et al., 1976) suggest is highly unlikely.

1) Curtis and Spears (1968) showed that the only iron compounds in equilibrium with sea water in the marine environment are hematite and other ferric compounds, although ferrous iron compounds may attain equilibrium with pore waters of the underlying sedimentary mass (Fig. 6.2). Thus, iron will precipitate in the marine water column only in ferric compounds.

2) There is no textural or other evidence to suggest that hematite in the present study areas formed by the oxidation or replacement of ferrous compounds.

3) James and Howland (1955) suggested that original Fe^{3+}/Fe^{2+} ratios are retained in sedimentary rocks even to high grades of metamorphism. Thus the oxidation state of iron in the present rocks has probably not been affected by either the dominantly greenschist or lower regional metamorphic grade or by the somewhat more severe thermal metamorphism in the Gull Pond area.

4) In most modern submarine iron-precipitating localities, ferric hydroxides form the observed iron-rich sediments (e.g. Zelenov, 1964; Ferguson and Lambert, 1972; Bonatti et al., 1973).

5) The experimental evidence of Bischoff and Dickson (1975) and Hajash (1975) indicates that sea water will become increasingly acidic through reaction with basalt at elevated temperatures. Upon discharge of these waters into the marine environment, mixing with sea water will result in an increase in their pH up to a maximum of about 8.

It can be seen from Fig. 6.3 that in the presence of amorphous silica, hematite is the stable iron mineral at pH less than 8 down to a minimum Eh of approximately -0.2.

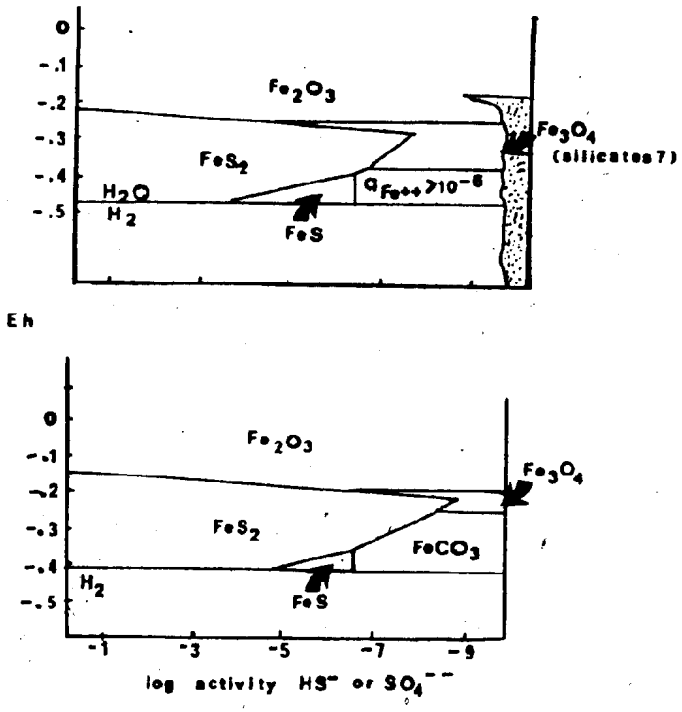

FIG. 6.2 Stability of iron minerals as a function of Eh and activity HS^-; UPPER: pH=8, $a_{HCO_3^-}=10^{-3.5}$, solid stability at $Fe^{2+} < 10^{-6}$, i.e. comparable with marine depositional waters; LOWER: pH=7, $a_{HCO_3^-} = 10^{-2.5}$, solid stability at $Fe^{2+} < 10^{-3}$, i.e. comparable to conditions in bottom sediments with restricted pore water circulation (after Curtis and Spears, 1968).

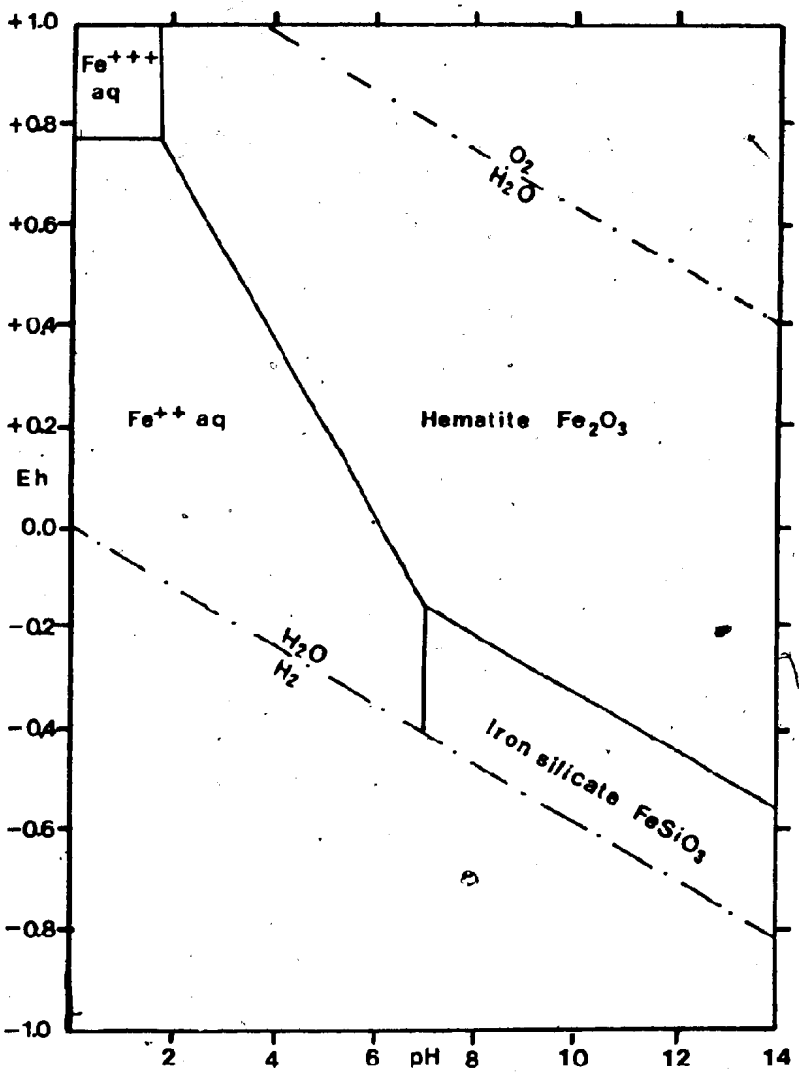

FIG. 6.3 Eh-pH diagram showing stability fields of iron oxides and iron metasilicate at 25°C, 1 atmosphere and in the presence of water and solid silica glass (after Garrels and Christ, 1965).

The above factors suggest that most of the hematite-bearing sedimentary rocks studied during the present project were formed under oxidizing to mildly reducing conditions and that these conditions normally prevailed until such time as the iron compounds were fixed in the sediment.

This interpretation can be extended to the green (i.e. hematite-poor) cherts of the Roberts Arm and Fortune Harbour areas even though their Fe^{3+}/Fe^{2+} ratios are considerably lower than in their red counterparts. Table 5.2 shows that the Fe^{3+} concentrations are similar in both lithotypes and geochemical evidence presented in Sec. 5.3.1 suggests that Fe^{2+} is dominantly present in chlorite and was contributed to the original sediment in the detrital fraction. The low Fe^{3+}/Fe^{2+} ratio in the green rocks thus results from a paucity of Fe^{3+} supply rather than the reduction of hematite to ferrous silicates during diagenesis and does not demand that different Eh conditions be postulated for the two lithotypes.

Locally more reducing conditions during deposition of the Gull Pond mineralization subgroup are indicated by minor amounts of magnetite in small pods near the top of this horizon.

Oxidizing conditions in the depositional basins are also suggested by the presence of significant amounts of manganese which geochemical evidence suggests was originally deposited as manganese carbonate (Sec. 5.3.1). A comparison of figures 6.4 and 6.5 shows that rhodochrosite ($MnCO_3$) is stable over a wide range of Eh and pH values in the presence of abundant CO_2 and that for Eh >0 and pH > 6, its stability

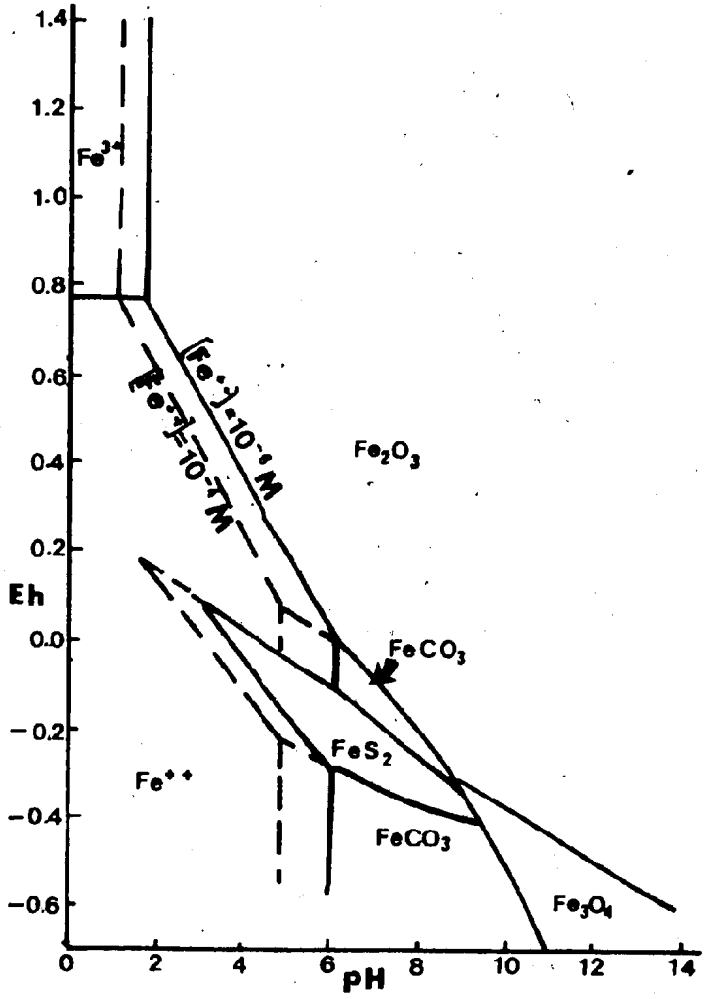

FIG. 6.4 Eh-pH diagram showing stability fields of common iron minerals for $[Fe^{2+}] = 10^{-6}M$ and $[Fe^{2+}] = 10^{-4}M$. Total activity dissolved carbonate is 1M and of dissolved sulfur is $10^{-6}M$ (after Garrels and Christ, 1965).

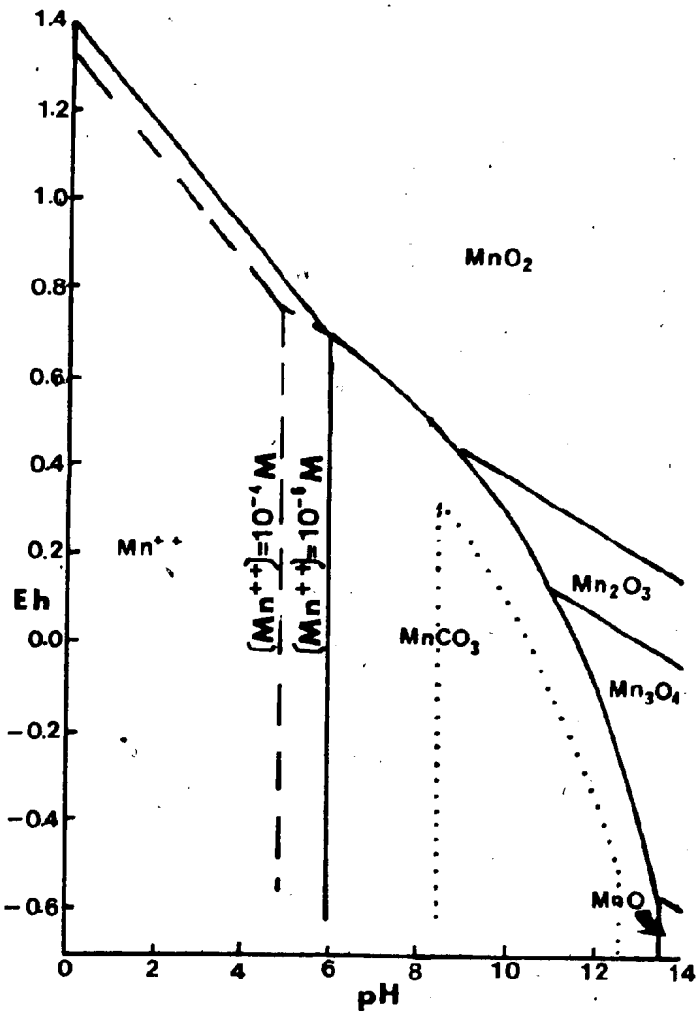

FIG. 6.5 Eh-pH diagram showing stability fields of common manganese minerals for $[Mn^{2+}] = 10^{-6}M$ and $[Mn^{2+}] = 10^{-4}M$. Assumed concentrations as in Fig. 6.4. Dotted line outlines $MnCO_3$ stability field for when total carbonate equals 0.001M. (after Garrels and CHrist, 1965 and Krauskopf, 1967).

field overlaps that of Fe_2O_3. Fig. 6.5 also indicates that for decreasing CO_2 activity, the stability field of rhodochrosite becomes smaller and at very low CO_2 concentrations (dotted line), manganese minerals will not precipitate in the normal range of marine environments except in the presence of very high manganese concentrations (Krauskopf, 1967).

The MnO/Fe_2O_3 ratios for the Gull Pond mixed subgroup and the Fortune Harbour suite are considerably higher than those in the Gull Pond mineralization subgroup (excluding three highly manganiferous samples, see Sec. 5.2.2) and the bedded deposits of the Roberts Arm suite (Table 6.1). The separation of iron from manganese may be accomplished at almost any stage in the chemical development of hydrothermal fluids due to the mobility of manganese relative to iron in solution, especially under conditions which are not strongly oxidizing (Krauskopf, 1957). Although Krauskopf (1957) suggested that iron and manganese are commonly leached from basalt in approximately their original proportions, recent experimental evidence (Tables 6.2 and 6.3) suggests that at moderately elevated temperatures (i.e. up to 400°C), sea water reacting with basalt will acquire a substantially higher Mn/Fe ratio than was present in the source rocks (Bischoff and Dickson, 1975; Hajash, 1975). At temperatures as high as 500°C, a considerably lower Mn/Fe ratio may result (Table 6.2). During ascent of the metal-charged solutions, partition of iron and manganese may occur in the subsurface resulting from the deposition of pyrite under reducing conditions in which manganese is highly mobile (e.g. Bonatti et al., 1976). Upon their discharge on the sea bottom, the mobility of manganese relative to iron may carry it beyond the initial

TABLE 6.1

MEAN MnO/Fe_2O_3 RATIOS FOR CENTRAL NEWFOUNDLAND CHERT AND FERRUGINOUS SEDIMENTS

	Fe_2O_3 %	MnO %	MnO/Fe_2O_3
Gull Pond Mineralization Subgroup	9.48	.45*	.05
Gull Pond Mixed Subgroup	3.55	.65	.18
Roberts Arm Bedded Subgroup	10.02	.45	.04
Roberts Arm Interpillow Subgroup	11.83	.05	.004
Fortune Harbour Suite	3.42	.43	.13

* - excludes three highly manganiferous samples in this subgroup

TABLE 6.2

CHANGES IN Mn/Fe RATIO IN SEA WATER WITH TIME THROUGH REACTION WITH BASALT AT ELEVATED TEMPERATURES

Initial Comp. of basalt: Fe_2O_3 = 3.68%, MnO = .17%, $MnO_3Fe_2O_3$ = .67

	Time	Fe (ppm)	Mn (ppm)	Mn/Fe
Changes in initial sea water with time at 200 C and 500 bars	24 hr.	15	10	.67
	212 hr.	35	25	.71
	552 hr.	28	35	1.21
	785 hr.	33	32	.97
	2928 hr.	16	17	1.06
	4752 hr.	5	5	1.00

Data from Bischoff and Dickson (1975)

TABLE 6.3

CHANGES IN Mn/Fe RATIO IN SEA WATER THROUGH REACTION WITH BASALT AT INCREASING TEMPERATURES

Initial Comp. of Basalt: Fe_2O_3 = 7.15%, MnO = 12%, $MnO_3Fe_2O_3$ = .02

Changes in	Sample #	Pressure (bars)	Time (days)	Fe (ppm)	Mn (ppm)	Mn/Fe
Initial sea water	20	500	6.3	.4	.26	.65
with incr. temp.	18	500	5.8	.4	.27	.68
	19	700	4.8	3.6	4.1	1.14
	21	800	3.3	1057	90	.09

Data from Hajash (1975)

iron-precipitating localities perhaps resulting in a facies gradation in the precipitate of increasing Mn/Fe values away from the discharge vent (e.g. Krauskopf, 1957; Butuzova, 1966). Finally, reducing conditions in the interstitial waters of the sediment during diagenesis may result in remobilization of previously deposited manganese and its subsequent migration out of the system.

It is evident that there are too many unknown variables to explain with certainty the variation in the MnO/Fe_2O_3 ratio in the present study areas. It is suggested however that the association of the Roberts Arm bedded deposits and the Gull Pond mineralization subgroup with dominantly basaltic sequences and especially the presence of a pervasive sulfide-rich zone underlying the latter suggests that hydrothermal fluids in these areas would probably have been more manganese-rich than those feeding the Fortune Harbour suite and the Gull Pond mixed subgroup. The variation in this ratio thus probably results from differing environmental conditions either during deposition or early diagenesis by one or both of the following mechanisms:

1) Relatively lower Eh conditions may have prevailed at the depositional sites of the Roberts Arm suite and the mineralization subgroup, resulting in manganese being removed from the system. This is supported by the previously noted local occurrence of magnetite pods in the latter deposit.

2) Higher CO_2 activity in the depositional basins of the Gull Pond mixed subgroup and the Fortune Harbour suite with an attendant increase in the $MnCO_3$ stability field (Fig. 6.5) could have led to the deposition

of rhodochrosite under Eh conditions similar to those prevailing at the depositional sites of their manganese-poor counterparts.

6.4 Deposition of Interpillow Ferruginous Chert

Petrographic evidence presented in Section 4.4.2 is inconclusive as to whether the interpillow ferruginous cherts pre- or post-date extrusion of the lavas - i.e. whether pre-existing sediments were squeezed into the pillow interstices during lava extrusion or whether the sediment later filled pre-existing interpillow voids. However, the paucity of TiO_2, Na_2O and most trace elements in these rocks strongly suggests that they were deposited in the subsurface removed from the more or less continuous detrital sedimentation occurring on the sea floor. In addition, the extremely high Fe_2O_3/MnO ratio in these rocks (Table 6.1) argues for a depositional environment substantially different from their bedded counterparts. It is inferred that the interpillow ferruginous chert post-dates the hosting pillow lavas and was deposited dominantly by heated, metal-rich solutions circulating in the subsurface. Deposition was probably caused by mixing of the hydrothermal solutions with sea water already present in the interpillow voids. The resultant cooling of these solutions accompanied by increases in both pH and Eh probably led to the precipitation of ferric hydroxides and possibly quartz (cristobalite?).

Some circulation of relatively unaltered sea water is implied by the fact that conditions in the voids never became reducing enough to reduce Fe^{3+} to Fe^{2+} but its circulation was apparently not great enough to create an environment sufficiently oxidizing to allow extensive precipitation of manganese.

6.5 Conclusions

The following conclusions concerning the genesis of the Upper Ordovician-Silurian chert and ferruginous sediments in Central Newfoundland are inferred from the present study:

1) The bedded deposits were formed fairly rapidly in local sea-floor topographic depressions during periods of relative volcanic quiescence. Relatively quiet bottom conditions prevailed in the depositional basins but regional instability is indicated by periodic turbidity deposits.

2) Interpillow ferruginous chert was precipitated in the pillow interstices by circulating iron and silica-rich solutions probably in response to mixing with relatively unaltered sea water. Post-depositional brecciation was probably accomplished by later minor readjustments of pillow geometry.

3) The bedded sedimentary rocks are formed from elements contributed by biogenic, hydrothermal and detrital sources as follows:

i) SiO_2 was contributed principally through the dissolution of opaline (radiolarian) tests and non-detrital quartz was probably formed in the manner suggested by Heath and Moberly (1971). An additional contribution of silica through the breakdown of volcanic debris is inferred but its quantitive importance cannot be assessed.

ii) Fe_2O_3, MnO, Ba and Au were introduced to the depositional environment principally by metal-rich hydrothermal fluids. Mixing of these waters with sea water resulted in precipitation of ferric hydroxides which accumulated in nearby topographic depressions. Manganese may have also precipitated as

hydroxides but was present in the sediment dominantly in carbonate minerals. The mineralogic disposition of Ba and Au is not known but it is inferred that these elements formed discrete mineral phases close to their discharge vents.

iii) TiO_2, CaO, Na_2O, FeO, Mgo, K_2O, Al_2O_3 and most trace elements were contributed dominantly by detrital material, probably mainly of tuffaceous origin.

4) The predominance of hematite as the iron-bearing phase suggests the prevalence of oxidizing to mildly reducing conditions during deposition and diagenesis of these sediments. Green, hematite-deficient chert does not necessarily reflect reducing conditions but may have formed during periods of suspended fumarolic activity when little hydrothermally-supplied iron was available.

5) Differing Fe_2O_3/MnO ratios suggest that slightly different environmental conditions existed in different areas. The Roberts Arm bedded deposits and the Gull Pond mineralization subgroup appear to have been deposited in a somewhat more reducing and/or CO_2-deficient environment than those in the Fortune Harbour suite and the Gull Pond mixed subgroup.

CHAPTER 7

ECONOMIC SIGNIFICANCE

7.1 Introduction

Hutchinson (1973) noted that massive sulfide deposits in marine volcanic rocks from a variety of geologic times and various tectonic settings display a number of unifying characteristics, one of which is the common presence of overlying thin, siliceous, iron- and manganese-rich sedimentary rocks. This feature is evidenced in the case of the Gullbridge and Southwest shaft volcanogenic copper deposits (Upadhyay, 1970; Upadhyay and Smitheringale, 1972; Swinden, 1975) by the Gullbridge ferruginous chert horizon, a remarkably continuous unit which overlies and extends beyond the two deposits along a strike length of over 10 km (Swinden, 1975).

A principal objective of the present study was to attempt to relate the chemical composition of the Gullbridge ferruginous chert to the underlying mineral deposits and thus perhaps develop a useful tool for mineral exploration in similar geological situations. Accordingly, the chemical data was analyzed in a search both for a chemical signature which would uniquely distinguish this unit from similar lithologies within the volcanic sequence and for lateral variations within the horizon which would indicate proximity to the underlying mineralization.

This chapter briefly summarizes the occurrence of siliceous and ferruginous sedimentary rocks associated with massive sulfide deposits in various geologic settings, with emphasis on attempts to use these rocks in mineral exploration and presents conclusions reached during the present study concerning the similar application of the geochemistry of the Gullbridge ferruginous chert horizon.

7.2 Siliceous and Ferruginous Sedimentary Rocks Associated with Volcanogenic Massive Sulfide Deposits

"Exhalative" iron formation related in time and space to volcanogenic massive sulfide deposits has been extensively documented in the Archean greenstone belts of the Canadian Shield (Ridler, 1970; Hutchinson et al., 1971; Goodwin and Ridler, 1970; Ridler, 1971; Hutchinson, 1973) and the similarities between these deposits and those of the present study have been previously noted (Sec. 2.4). Hutchinson et al.(1971) proposed that this spatial relation was also a genetic one and that discharge of hydrothermal fluids from fumarolic vents at basin centers resulted in successive facies of chemical sediments ranging in general from proximal massive sulfide deposits and sulfide facies iron formation to progressively more distal exhalative carbonate and oxide facies iron formation (see Fig. 2.6). Ridler (1971) suggested that recognition of the exhalative facies throughout the greenstone belts would provide a powerful regional exploration tool in the search for massive sulfide deposits in that the aereal extent of the sulfide facies delineates a paleoenvironment favourable for massive sulfide deposition.

Phanerozoic massive sulfide deposits are typically associated with epiclastic sedimentary rocks rather than chemically precipitated chert and iron formation (Hutchinson, 1972) but good examples of the latter have been documented in the Bathurst, New Brunswick mining camp (McAllister, 1960; Davies, 1972; Whitehead, 1973). The massive sulfide deposits in this area are Lower to Middle Ordovician in age and occur in pods or lenses occupying topographic depressions which are often

connected and overlain by thin layers of various facies of iron formation (Davies, 1972; Whitehead, 1973). Whitehead (1973) noted that the Mn/Fe ratio in the iron formation tends to increase away from the sulfide deposits at the Heath Steele mine and suggested that this indicates a progressive change from reducing conditions in the basin center (the site of sulfide deposition) to more oxidizing conditions at the basin margins.

"Kuroko-type" massive sulfide deposits of Miocene age in Japan are associated with felsic domal centers in an island arc environment and are sometimes directly overlain by a thin bed of ferruginous chert (tetsusekiei bed) followed by one or more siliceous mudstone horizons interbedded with the hanging wall tuff (Horikoshi, 1969; Lambert, 1973 (Fig. 7.1). Lambert (1973) noted that anomalously high concentrations of Zn, Cu and Pb are occasionally present in the mudstone and attributed this feature to the local discharge of post-ore, metal-rich solutions in the depositional basins. Tono (1974) showed that Ba, Zn, Cu and Pb were locally enriched in the mudstone overlying the Matsumine deposit but while attributing this feature to the effects of mineralization, did not speculate as to whether the cause was contemporaneous hydrothermal activity or post-depositional migration of the metallic ions.

Massive sulfide deposits in the Troodos ophiolite complex in Cyprus are commonly overlain by a ferruginous, manganiferous, metalliferous horizon (umber) which is in turn overlain by red jasper, siltstone and radiolarian chert apparently lithologically similar to the Gullbridge ferruginous chert. As at Gullbridge, these units are often separated from the ore horizon by post-ore volcanic rocks. Constantinou and Govett (1972)

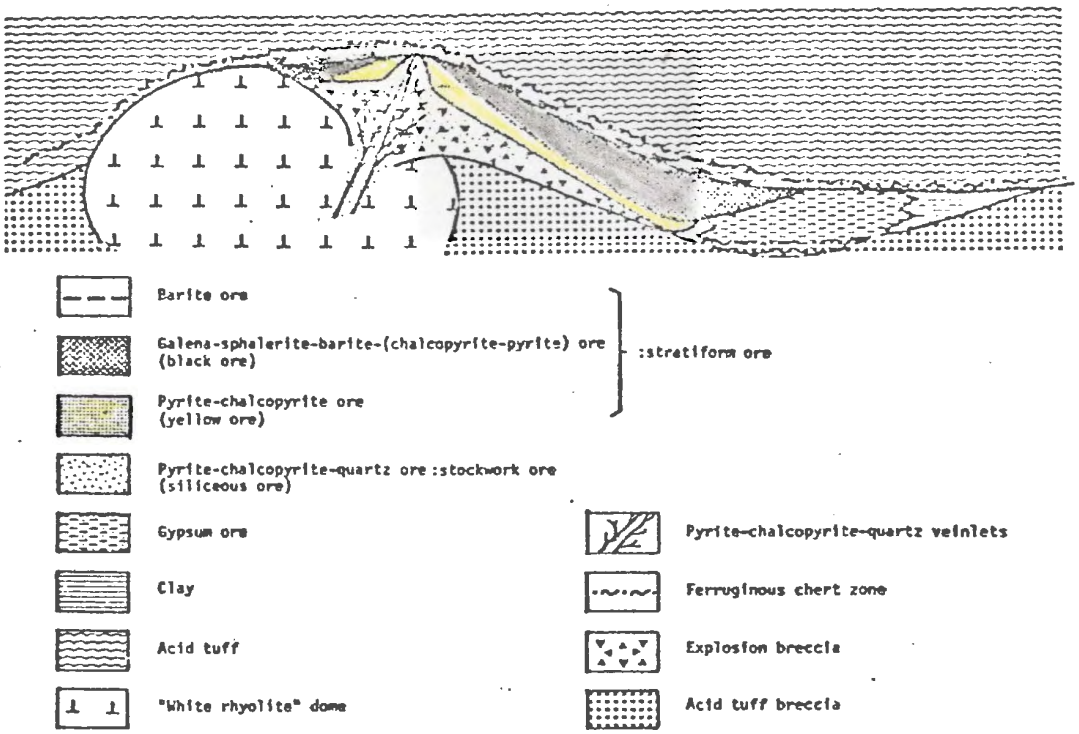

Schematic cross section of a typical Kuroko deposit.

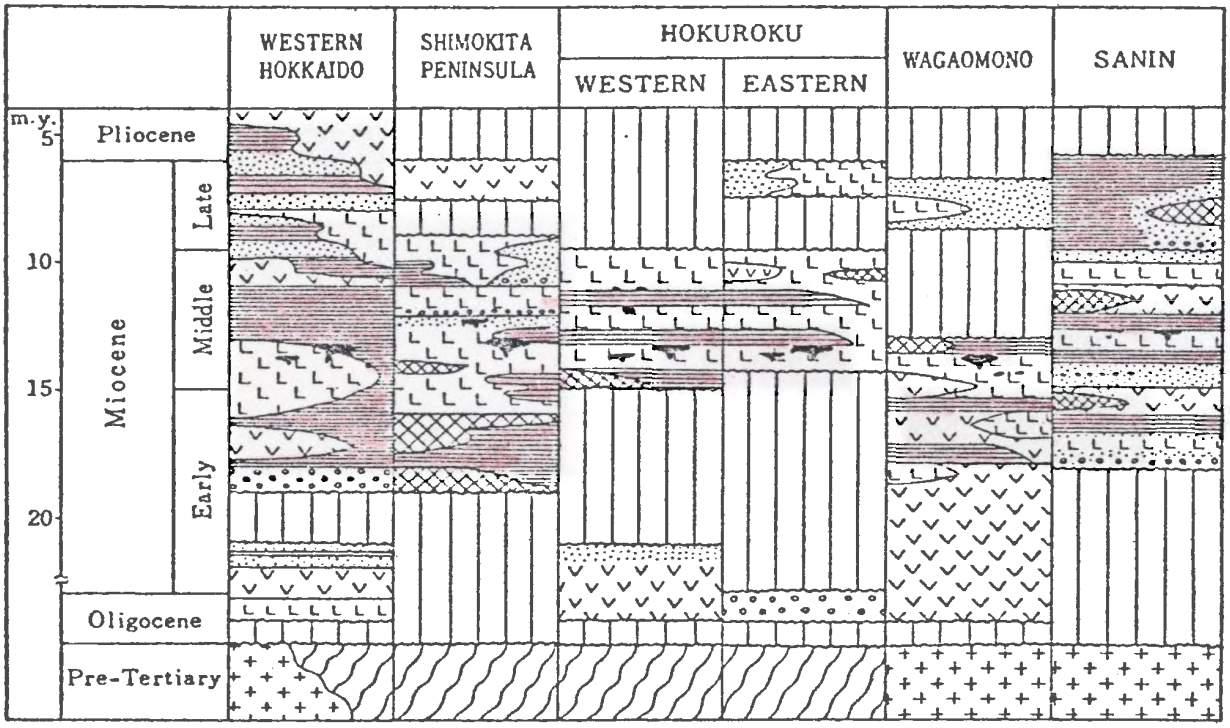

Schematic stratigraphic columns of major Kuroko districts.

Fig. 7.1. Spatial relation of ferruginous chert (tetsusekei bed) and mudstones to Kuroko deposits (from Sato, 1974).

showed that there is a sharp increase in Cu and Zn concentrations in the umber close to the mineral deposits as compared with umber away from the mineralization.

Robertson and Hudson (1974) noted that the radiolarites and related rocks commonly directly overlie the umber and proposed a genetic link between them, suggesting that the hydrothermal solutions which fed the umber also contributed, by virtue of their high silica contents, to the preservation of the radiolarite.

7.3 Application of the Present Study to Mineral Exploration

The spatial association of ferruginous chert with volcanogenic copper deposits at the Gullbridge mine raises the possibility that conditions which resulted in ore deposition may also be reflected in the chemical composition of the ferruginous chert. The search for geochemical anomalies in the ferruginous chert can be approached from two angles: 1) A regional approach in which a chemical signature is sought which uniquely distinguishes this unit from other similar lithologies unrelated to mineralization; this approach has been used with some success in volcanic rocks to distinguish those which host sulfide deposits from those which are barren (e.g. Davenport and Nichol, 1972; Govett and Pantazis, 1971; Thurlow, 1974); 2) A detailed approach in which lateral chemical variations are sought within the ferruginous chert which reflect the location of the underlying mineralization; this may be caused either by the concentration of particularly insoluble components near the fumarolic vents during deposition or by later dispersion of elements out of the mineralized zone into the overlying

rocks. The latter mechanism has been credited with forming trace element haloes in rocks overlying sulfide deposits from a variety of areas (e.g. Whitehead and Govett, 1974; Goodfellow, 1974; Gale, 1969).

The first of the above approaches is predicated on the assumption that the hydrothermal fluids which contributed in part to the formation of the ferruginous chert are related to those which took part in the mineralizing episode, either by being post-mineralization exhalations of the residual mineralizing fluids or by having passed through the sulfide-rich fumarolic vents at a later time, thus acquiring a distinctive chemical signature. It follows that meaningful chemical differences between the Gullbridge ferruginous chert and those horizons unrelated to mineralization should be sought in those elements which are inferred to have been contributed by hydrothermal processes, viz. Fe_2O_3, MnO, Ba and Au.

Table 7-1 presents a comparison of the mean concentrations of Fe_2O_3, MnO, Ba and Au in the Gullbridge ferruginous chert with those from the Fortune Harbour and Roberts Arm suites and the Gull Pond mixed subgroup. All of these elements are seen to be moderately to highly enriched in the former horizon relative to the others with the exception of Fe_2O_3 which has comparable concentrations in the Roberts Arm suite. Figure 7-2 shows that with respect to the covariation of Ba and Au with Fe_2O_3+MnO, the vast majority of the samples unrelated to mineralization fall in the area under a smooth curve, reflecting the fact that while some samples may be enriched in one or the other of these elements, few carry anomalous amounts of more than one. However, almost half of the Gullbridge ferruginous

TABLE 7.1

MEAN CONCENTRATIONS OF Fe_2O_3, MnO, Ba AND Au FOR SELECTED GROUPS

	Fe_2O_3 %	MnO %	Ba (ppm)	Au (ppb)
Gullbridge ferruginous chert	9.48	1.99	604	71
Gull Pond mixed subgroup	3.55	.65	239	53
Roberts Arm suite	9.89	.22	235	20
Fortune Harbour suite	3.42	.43	458	67

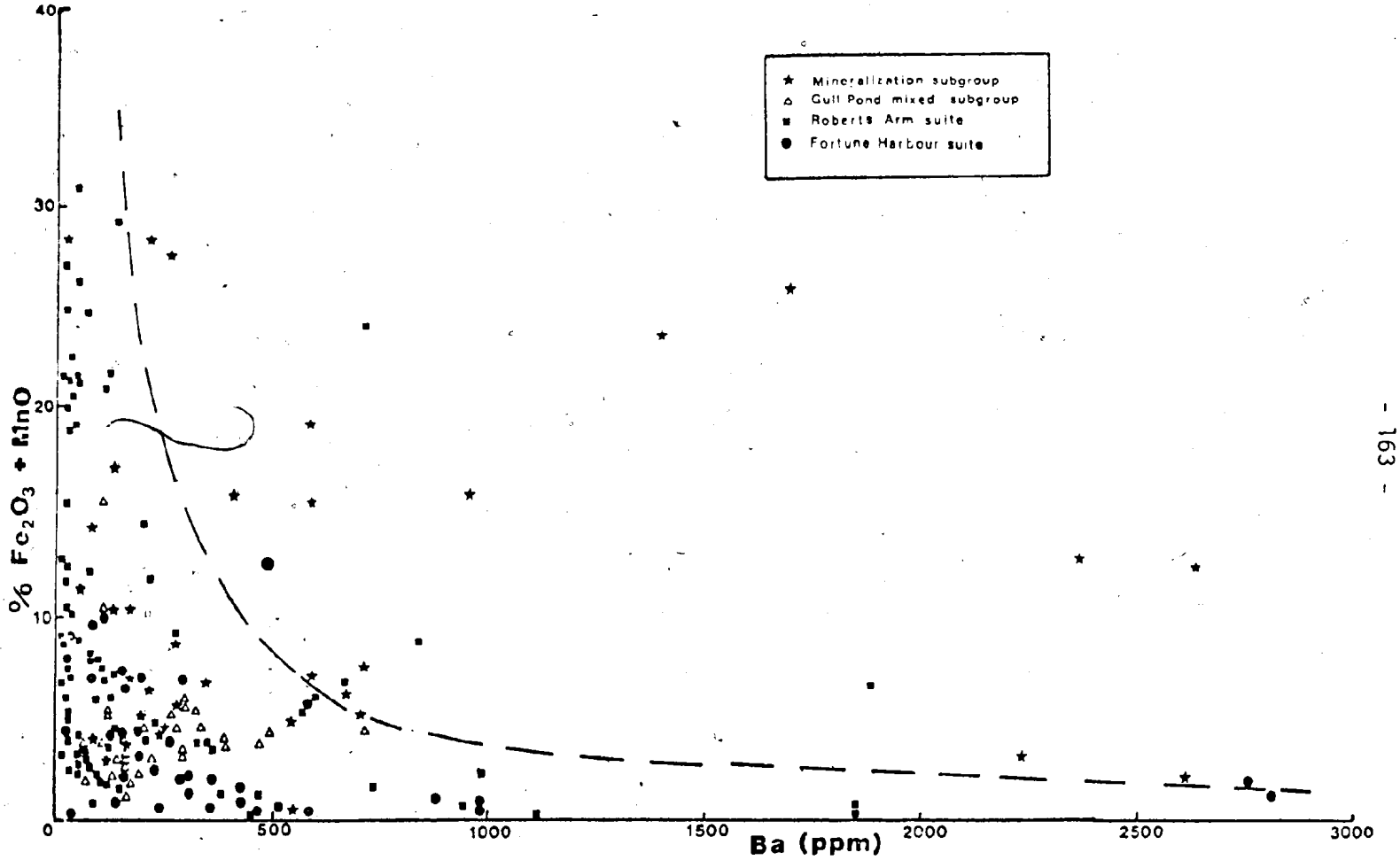

FIG. 7.2 Empirical chemical distinction between Gullbridge ferruginous chert and similar lithologies unrelated to mineralization according to concentrations of Fe_2O_3, MnO, Ba and Au.

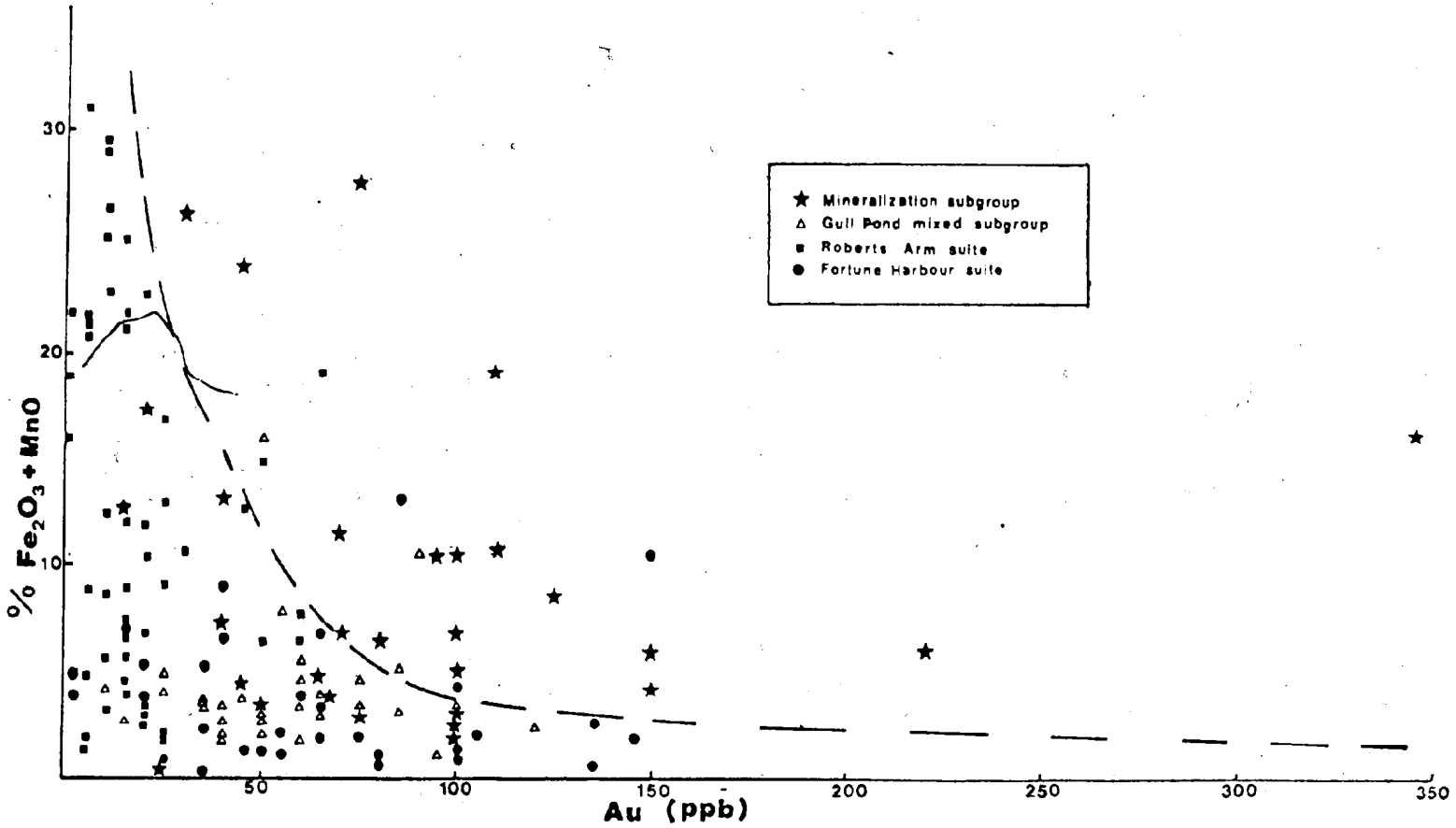

FIG. 7.2 (Continued)

TABLE 7.2

NUMBER OF SAMPLES PLOTTING OUTSIDE THE SMOOTH CURVES IN FIG. 7.2

Fig. 7.2 (Ba)

	No. of Samples	No. of Samples Outside Curve	% of Samples Outside Curve
1. Gullbridge ferruginous chert	39	16	41
2. Gull Pond mixed subgroup	35	0	-
3. Roberts Arm bedded subgroup	115	4	3.5
4. Fortune Harbour suite	53	2	3.8
Total (2-4)	203	6	3.0

Fig. 7.2 (Au)

1. Gullbridge ferruginous chert	32	17	53.1
2. Gull Pond mixed subgroup	33	3	9.1
3. Roberts Arm bedded subgroup	76	2	2.6
4. Fortune Harbour suite	47	3	6.4
Total (2-4)	188	8	4.3

chert samples are enriched in more than one of the hydrothermally contributed elements and plot to the right of the curve(s) (Table 7-2). This suggests that although it may not be possible to identify any given sample as being related or unrelated to the mineralization, the Gullbridge ferruginous chert samples as a group contain chemical features, probably related to the underlying mineralization, which distinguish them from other groups.

Statistical reproduction of the above empirical approach was attempted by calculating discriminant functions, using Fe_2O_3, MnO, Ba and Au as variables, for the mineralization subgroup and the Gull Pond mixed subgroup, Roberts Arm suite and Fortune Harbour suite respectively. The discriminant indexes, mean group values and individual sample values (see Appendix B for description) are plotted in Fig. 7.3 and indicate that the empirical separation of the groups can be reproduced statistically. The mineralization subgroup is separate as a group from the others in all cases although the separation is somewhat less well defined for the Fortune Harbour suite than for the other two. As in the empirical approach, more samples from the mineralization subgroup than from the alternate groups are misclassified (i.e. fall on the wrong side of the discriminant index) and thus any given sample related to mineralization is more likely to be mistaken as being unrelated to mineralization than vice versa although the groups as a whole appear to be quite distinct. Fe_2O_3 and Ba respectively contribute significantly to the variation between groups in two cases while gold is a significant factor in all three cases. Mno does not significantly enhance the separation in any case and for the mixed

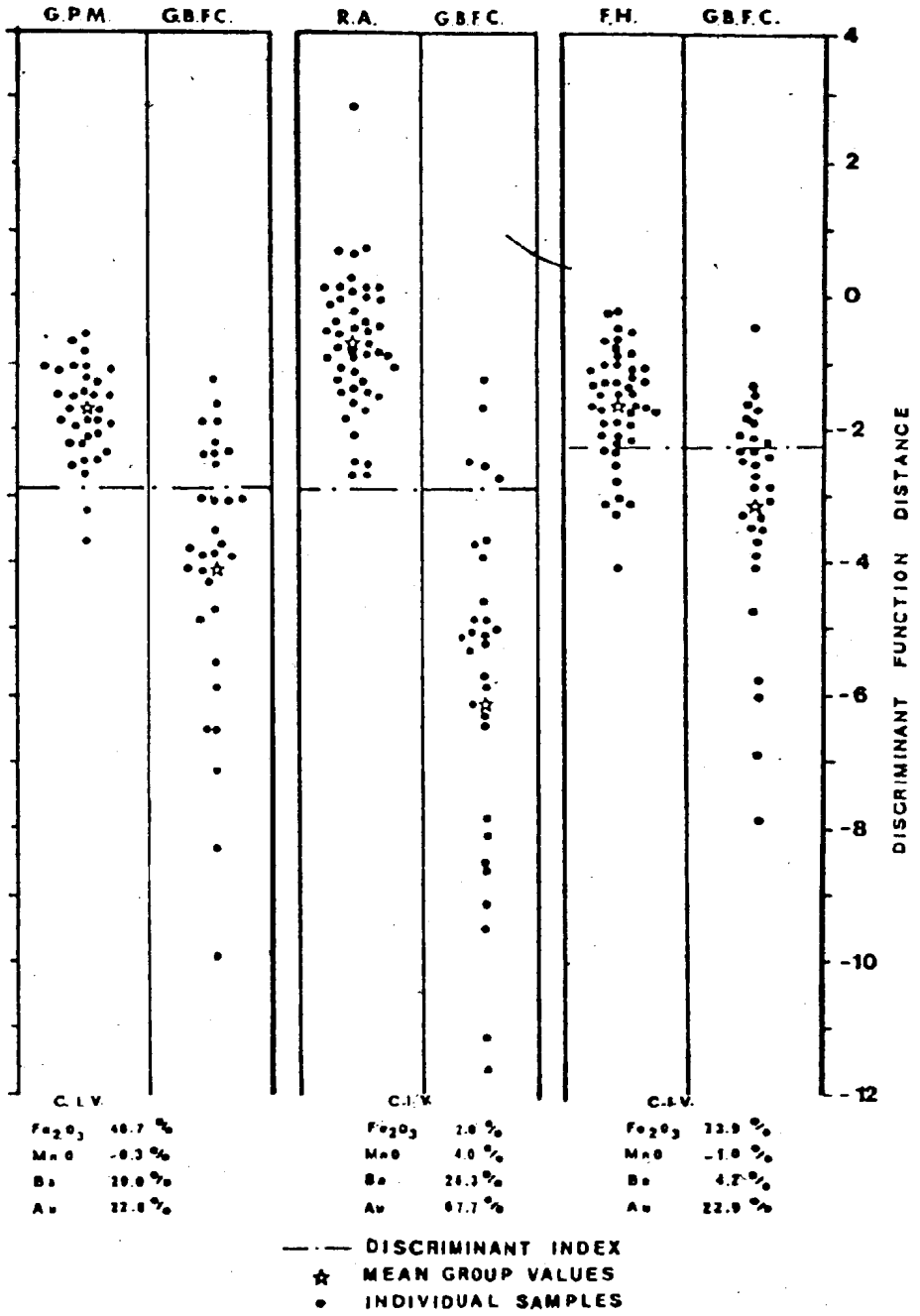

FIG. 7.3 Summary of discriminant function analysis of the Gullbridge ferruginous chert and other similar lithologies unrelated to mineralization. G.P.M.-Gull Pond mixed subgroup; G.B.F.C. - Gullbridge ferruginous chert; R.A. - Roberts Arm bedded subgroup; F.H. - Fortune Harbour suite; C.I.V. - contribution of the individual variables to the respective discriminant functions.

subgroup and the Fortune Harbour suite, actually detracts slightly from the separation (i.e. provides a negative contribution to the variance, Fig. 7.3).

The general applicability of this feature to regional mineral exploration cannot be assessed in the absence of further supporting data from similar sedimentary rocks associated with sulfide mineralization in other areas. It appears, however, that fluids which are responsible for sulfide deposition may impart a distinctive chemical signature to associated chemically precipitated sedimentary rocks and this could prove to be a useful regional exploration tool. This chemical signature need not necessarily be defined by any or all of the elements mentioned above but in order to be meaningfully applied, should be defined by elements whose presence in the sediments is related either to the mineralizing process or to the prior presence of spatially associated sulfide deposits.

As noted in section 5.4, there are no chemical trends developed along strike in the Gullbridge ferruginous chert which indicate the location of the underlying mineral deposits. However locally high concentrations of Ba occur in 4 samples very near the Southwest shaft deposit and two samples with highly anomalous gold values are present approximately 200 meters south of the Gullbridge mine. In view of the fact that Ba has previously proven a useful indicator of mineralization in other areas (Tono, 1974; Thurlow, 1974), it is tempting to attribute the Ba enrichment in these samples to the discharge through the Southwest shaft fumarolic vent of hydrothermal fluids related to mineralization. These samples are tightly clustered near the deposit and all are closer

to the associated sulfide zone than is the nearest exposure of ferruginous chert to the Gullbridge ore zone so the possibility of a similar Ba-enrichment in the latter area cannot be assessed. Even if this effect is related to mineralization, its usefulness in exploration is severely limited by the narrow strike length of the anomaly and its sporadic occurrence.

The Au "anomaly" occurs at least 200 meters from the Gullbridge ore deposit and considering that it only comprises two samples and is not present at all at the Southwest shaft, is not presently thought to be either an indicator of proximal fumarolic activity or a useful exploration guide.

7.4 Conclusions

1) Samples from the Gullbridge ferruginous chert horizon can be distinguished chemically from other lithologically similar groups on the basis of the covariation of Fe_2O_3 + MnO with Ba and Au. These elements are inferred to have been introduced hydrothermally to the sediments during deposition and this distinction may thus be genetically related to the presence of the Gullbridge and Southwest shaft volcanogenic copper deposits, stratigraphically below and spatially related to the Gullbridge ferruginous chert.

2) Further data are needed to test the general applicability of the above feature. The ability to chemically distinguish chemical sedimentary rocks which are respectively related and unrelated to mineralization has the potential of being a useful regional exploration tool.

3) Lateral chemical variations within the Gullbridge ferruginous chert horizon do not appear to provide useful information on the location of the underlying mineral deposits. A possible exception to this is the high concentration of Ba in a few samples directly overlying the Southwest shaft deposit, a feature which may be genetically related to mineralization. However the limited strike length and sporadic nature of this feature probably severely limit its use as an exploration tool.

CHAPTER 8

SUMMARY

The following is a brief summary of the findings of this study:

1) Chert, ferruginous sediments and associated sedimentary rocks are a ubiquitous although volumetrically minor constituent of the Upper Ordovician-Silurian volcanic sequence of central Newfoundland. A complete range from relatively pure chert to siliceous and ferruginous shale is present.

2) Bedded chemical sediments are intimately associated with a variety of volcanic lithologies ranging from pillow lava and pillow breccia to silicic flows and pyroclastic rocks. They typically occur in small, discontinuous, lenses and pods conformable with the volcanic stratigraphy.

3) Interpillow chert is abundant in the middle to upper part of the volcanic sequence in the Roberts Arm area, less common in the Fortune Harbour area and apparently absent in the Gull Pond area. It often exhibits an internal brecciated texture and does not commonly form coherent beds.

4) The principal minerals present in these sediments are quartz, hematite, epidote (± clinozoisite), illite, sericite, chlorite and sodic plagioclase. Minor amounts of calcite, pyrite, magnetite, pumpellyite and chalcopyrite are present locally.

5) Chemical trends in the chert and ferruginous sediments are strongly influenced by the mineralogy of the rocks and can usually

be related to the presence of specific minerals or groups of minerals. The mineralogic distribution of elements inferred from chemical and mineralogic data are summarized below:

a) SiO_2 is dominantly present in non-detrital quartz although typically minor amounts are contributed by the various aluminosilicate minerals.

b) Fe_2O_3 commonly reflects the presence of hematite, although significant amounts may rarely be contributed by epidote and/or pumpellyite.

c) Al_2O_3 is dominantly contributed by the various aluminosilicate minerals. CaO is commonly present in epidote and/or clinozoisite but in some cases reflects the presence of calcite. MgO and FeO are dominantly present in chlorite although ferrous iron is occasionally contributed in significant amounts by magnetite and/or pyrite. K_2O and Na_2O are present in illite/sericite and plagioclase respectively.

6) Probable sources of the components are as follows:

a) SiO_2 was probably supplied to the bedded deposits primarily through the breakdown of siliceous organisms although an indeterminate amount may have been contributed through the breakdown of volcanic detritus. Non-detrital quartz is inferred to have formed by maturation in the manner suggested by Heath and Moberly (1971). Substantial amounts of silica in the interpillow chert may have precipitated inorganically.

b) Fe_2O_3, MnO, Ba and Au were probably introduced to the depositional environment primarily by submarine hydrothermal exhalations.

c) TiO_2, CaO, Na_2O, FeO, MgO, K_2O and Al_2O_3 and all trace elements except Ba and Au were probably contributed mainly be detrital material.

7) There are no consistent variations in the chemistry of these sediments according to their stratigraphic position and it is inferred that neither the chemical development of the associated volcanism nor the changing bulk chemistry of the associated volcanic rocks substantially influences the composition of the associated chemical sediments.

Oxidizing to mildly reducing conditions prevailed throughout the deposition and early diagenesis of these chemical sediments. Slightly more reducing and/or CO_2 deficient conditions may have prevailed during the formation of the Roberts Arm suite and the Gullbridge ferruginous chert than during formation of the Fortune Harbour suite and the Gull Pond mixed subgroup.

8) The Gullbridge ferruginous chert is stratigraphically above and spatially related to two volcanogenic copper deposits and can be chemically distinguished from similar lithologies apparently unrelated to mineralization on the basis of Fe_2O_3, MnO, Ba, and Au concentrations. This latter feature may be genetically related to the underlying mineralization as these elements are interpreted to have been contributed by hydrothermal processes possibly related to the mineralization episode, and may constitute a useful regional exploration tool. Further data are needed to test its general applicability.

9) Lateral variations within the Gullbridge ferruginous chert do not appear to serve as a reliable, consistent guide to the underlying mineralization. Although high Ba values in chert proximal to the Southwest shaft deposit may reflect the presence of this deposit, these high values appear to be too restricted in strike length and sporadic in occurrence to be of use in exploration.

In summary, the present study has focused on a wide range of chemical sedimentary rocks associated with early Paleozoic volcanism in an island arc environment. The data and conclusions presented in the various chapters and summarized above provide an insight into the physico-chemical conditions prevailing on the sea floor and the ensuing sedimentary processes that occurred during this stage of volcanism in Central Newfoundland. They also suggest that the processes which contributed to the formation of these sediments may, in some cases, have been processes which also result in the formation of base metal sulfide deposits. Some areas for further work are indicated by the results of this study. For example, many previous workers have suggested that preservation of chemical sediments should be rare in an active arc environment (e.g. Dickenson, 1974; Garrison, 1974) but the present study suggests that, in some cases, this process may be relatively widespread. Whether this is due, in the present case, to a relative lack of contemporaneous clastic sedimentation or to special physico-chemical conditions is not clear. Further detailed studies in similar volcanic regimes could indicate whether preservation of chemical sediments is, in fact, more widespread than previously reported and help

clarify the relationship between clastic and chemical sedimentation in this type of environment.

It is noteworthy that most of the chemical sedimentation in this volcanic sequence apparently occurred in the oxide facies in contrast to other similar areas where the silicate, carbonate and sulfide facies are more extensively developed (e.g. Goodwin, 1962; McAllister, 1960; Davies, 1972). This may imply that reducing conditions (i.e. favourable for sulfide deposition) were not extensively developed in Notre Dame Bay during this phase of volcanism. Further detailed mapping with close attention to and a careful search for chemical sediments of various facies might further elucidate this question.

The use of oxide facies chemical sediments as a regional guide to sulfide deposits appears to show some promise but the general applicability of the results of the present study are still indeterminate. Further data from similar volcanic sequences could provide a test of the usefulness of this method. The Lower-Middle Ordovician volcanic sequence in Central Newfoundland, which contains both sulfide deposits and considerable chemical sediments, is suggested as a possible area for this work.

REFERENCES

Abbey, S., 1968. Analysis of rocks and minerals by atomic absorption spectrometry; Pt. 2: Determination of total iron, magnesium, calcium, sodium and potassium. Geol. Surv. Can., Pap. 68-20, 21 p.

Alexandrov, E.A., 1973. The Precambrian banded iron-formations of the Soviet Union. Econ. Geol., v. 68, pp. 1035-1062.

Audley-Charles, M.G., 1965. Some aspects of the chemistry of Cretaceous siliceous sedimentary rocks from Eastern Timor. Geochim. et Cosmochim. Acta, v. 29, pp. 1175-1192.

Bayley, R.H. and James, H.L., 1973. Precambrian iron-formations of the United States. Econ. Geol., v. 68, pp. 934-959.

Berger, W.H. and von Rad, U., 1972. Cretaceous and Cenozoic sediments from the Atlantic Ocean, Leg 14, Deep Sea Drilling Project. In: Initial Reports of the Deep Sea Drilling Project, v. XIV (D.E. Hayes, A.C. Pim et al., Eds.), pp. 787-954, U.S. Government Printing Office, Washington.

Beukes, N.J., 1973. Precambrian iron-formations of Southern Africa. Econ. Geol., v. 68, pp. 960-1004.

Bignell, R.D., Tooms, J.S. and Cronan, D.S., 1976. Red Sea metalliferous brine precipitates. In: Metallogeny and Plate Tectonics (D.F. Strong, Ed.), Geol. Assoc. Can., Sp. Pap. 14.

Bird, J.M. and Dewey, J.F., 1970. Lithosphere plate-continental margin tectonics and the evolution of the Appalachian Orogen. Bull. Geol. Soc. Amer., v. 81, pp. 1031-1060.

Bischoff, J.L., 1969. Red Sea geothermal brine deposits: their mineralogy, chemistry and genesis. In: Hot Brines and Heavy Metal Deposits in the Red Sea (E.T. Degens and D.A. Ross, Eds.), pp. 368-401. Springer-Verlag, New York Inc.

_____ and Dickson, F.W., 1975. Seawater-basalt interaction at 200°C and 500 bars: implications for origin of sea-floor heavy-metal deposits and regulation of sea water chemistry. Earth Planet. Sci. Letts., v. 25, pp. 385-397.

Bonatti, E., Honnorez, J., Joensuu, O., and Rydell, H., 1973. Submarine iron deposits from the Mediterranean Sea. In: The Mediterranean Sea, A Natural Sedimentation Laboratory (D.J. Stanley, Ed.), pp. 701-710. Dowden, Hutchinson and Ross, Stroudsburg, Pennsylvania.

Bonatti, E. and Joensuu, O., 1966. Deep sea iron deposits from the South Pacific. Science, v. 154, p. 643.

_____, Kraemer, T., and Rydell, H., 1972. Classification and genesis of submarine iron-manganese deposits. In: Ferromanganese Deposits on the Ocean Floor: Internat. Decade on Ocean Exploration, pp. 149-161.

_____, Zerbi, M., Kay, R., and Rydell, H., 1976. Metalliferous deposits from the Apennine Ophiolites: Mesozoic equivalents of modern deposits from modern spreading centers. Bull. Geol. Soc. Amer., v. 87, pp. 83-94.

Borchert, H., 1960. Genesis of marine sedimentary iron ore. Inst. Min. Metall. Trans., v. 69, pp. 261-279.

Bostrom, K., 1970. Submarine volcanism as a source for iron. Earth Planet. Sci. Letts., v. 9, pp. 348-354.

_____, Joensuu, S., Valdis, S., and Riera, M., 1972. Geochemical history of the S. Atlantic Ocean sediments since Late Cretaceous. Mar. Geol., v. 12, pp. 85-123.

_____, and Peterson, M.N.A., 1966. Precipitates from hydrothermal exhalations on the East Pacific Rise. Econ. Geol., v. 61, pp. 1258-1265.

_____, and Peterson, M.N.A., 1969. The origin of aluminum-poor ferromanganoan sediments in areas of high heat flow on the East Pacific Rise. Mar. Geol., v. 7, pp. 427-447.

_____, Peterson, M.N.A., Joensuu, S., and Fisher, D.E., 1969. Aluminum-poor ferromanganoan sediments on active oceanic ridges. J. Geophys. Res., v. 74, pp. 3261-3270.

Bostock, H.H., 1975. Volcanic rocks of the Appalachian Province: Roberts Arm Group, Newfoundland (2E). Geol. Surv. Can., Pap. 75-1, Part A, pp. 1-3.

_____, 1976. Volcanic rocks of the Appalachian Province: Roberts Arm Group, Newfoundland (2E and 12H). Geol. Surv. Can., Pap. 76-1A, pp. 173-176.

Bramlette, M.N., 1946. The Monterey Formation of California and the origin of its siliceous rocks. Prof. Pap. U.S. Geol. Surv. 212, pp. 1-55.

Butuzova, G. Yu., 1966. Iron ore sediments of the fumarole field of Santorin volcano, their composition and origin. Dokl. Akad. Nauk., v. 368, pp. 215-217.

Calvert, S.E., 1974. Deposition and diagenesis of silica in marine environments. In: Pelagic Sediments: On Land and Under the Sea (K.J. Hsü and H.C. Jenkyns, Eds.), Spec. Pub. Int. Assoc. Sediment., No. 1, pp. 273-299.

Church, W.R., and Stevens, R.K., 1971. Early Paleozoic ophiolite complexes of Newfoundland Appalachians as mantle-oceanic crust sequences. J. Geophys. Res., v. 76, pp. 1460-1466.

Clarke, F.W., 1924. The data of geochemistry. Bull. U.S. Geol. Surv. 770.

Constantinou, G. and Govett, G.J.S., 1972. Genesis of sulphide deposits, ochre and umber of Cyprus. Inst. Min. Metall. Trans., v. 81, pp. B34-B46.

Corliss, J.B., 1971. The origin of metal-bearing submarine hydrothermal solutions. J. Geophys. Res., v. 76, pp. 8128-8138.

_____, Graf, J.L., Skinner, B.J., and Hutchinson, R.W., 1972. Rare earth data for iron and manganese sediments associated with the sulphide deposits of the Troodos Massif, Cyprus. Prog. Abstr. Geol. Soc. Amer., v. 4, no. 7, pp. 426-477.

Craig, H., 1969. Geochemistry and origin of the Red Sea Brines. In: Hot Brines and Recent Heavy Metal Deposits in the Red Sea (E.T. Degens and D.A. Ross, Eds.), pp. 208-244. Springer-Verlag, New York, Inc.

Cressman, E.R., 1962. Data of Geochemistry, sixth edition, Chapter T, non-detrital siliceous sediments. U.S. Geol. Surv. Prof. Pap. 440-T, 23 p.

Cronan, D.S., 1972. The Mid-Atlantic Ridge near 45°N. XVII; Al, As, Hg, and Mn in ferruginous sediments from the median valley. Can. J. Earth Sci., v. 9, pp. 319-323.

Curtis, C.D. and Spears, D.A., 1968. The formation of sedimentary iron minerals. Econ. Geol., v. 63, pp. 257-270.

Davenport, P.H. and Nichol, I., 1973. Bedrock geochemistry as a guide to areas of base-metal potential in volcano-sedimentary belts of the Canadian Shield. In: Geochemical Exploration, 1972 (M.J. Jones, Ed.), pp. 45-47. Inst. Min. Metall.

Davies, J.L., 1972. The geology and geochemistry of the Austin Brook Formation, Gloucester County, New Brunswick, with special emphasis on the Austin Brook iron formation. Unpubl. Ph.D. Thesis, Carleton University, Ottawa, 254 p.

Davies, T.A. and Supko, P.R., 1973. Oceanic sediments and their diagenesis: some examples from deep-sea drilling. J. Sedim. Petrol., v. 43, pp. 381-390.

Davis, E.F., 1918. The radiolarian cherts of the Franciscan group. Univ. Calif. Publs. Bull. Dept. Geol., v. 11, pp. 235-432.

Dean, P.L., 1973. The geology of the northern half of the Fortune Harbour Peninsula. Unpub. Geol. Surv. Can., Open file report, 31 p.

_____, and Strong, D.F., 1975. The volcanic stratigraphy, geochemistry and metallogeny of the Central Newfoundland Appalachians. Paper presented at the 28th ann. mtg., Geol. Assoc. Can., Waterloo, Ontario.

_____, 1976. Geological compilation maps of Notre Dame Bay. Open file release, Nfld. Dept. Mines and Energy and Geol. Surv. Can., 10 maps, with marginal notes.

Dewey, J.F. and Bird, J.M., 1971. Origin and emplacement of the ophiolite suite: Appalachian ophiolites of Newfoundland. J. Geophys. Res., v. 76, pp. 3179-3207.

Dickenson, W.R., 1974. Sedimentation within and beside ancient and modern magmatic arcs. In: Modern and Ancient Geosynclinal Sedimentation. (R.H. Dott, Jr. and R.H Shaver, Eds.), Soc. Econ. Paleon. Mineral. Sp. Pub. No. 19, pp. 230-239.

Dietz, R.S., 1963. Collapsing continental rises: an actualistic concept of geosynclines and mountain building. J. Geol., v. 71, pp. 314-333.

Dorr, J.V.N. Jr., 1974. Iron-formation in South America. Econ. Geol., v. 68, pp. 1005-2022.

Douglas, G.V., Williams, D. and Rove, O.N., 1940. Copper deposits of Newfoundland. Nfld. Geol. Surv., Bull. 20, 176 p.

Douglas, J., 1976. Geochemical studies of Cambrian manganese deposits in eastern Newfoundland. Unpub. Ph.D. Thesis, Memorial University of Newfoundland, St. John's (in prep.).

Dymond, J., Corliss, J.B., Heath, G.R., Field, C.W., Dasch, E.J., and Veeh, H.H., 1973. Origin of metalliferous sediments from the Pacific Ocean. Bull. Geol. Soc. Amer., v. 84, pp. 3355-3372.

El Wakeel, S.K. and Riley, J.P., 1961. Chemical and mineralogical studies of deep-sea sediments. Geochim. et Cosmochim. Acta, v. 25, 110-146.

Elderfield, H., Gass, I.G., Hammond, A., and Bear, L.M., 1972. The origin of ferromanganese sediments associated with the Troodos Massif of Cyprus. Sedimentology, v. 19, pp. 1-19.

Elliston, J.N., 1963. Sediments of the Warramunga Geosyncline. In: Syntaphral Tectonics, Univ. Tasmania, Hobart, pp. L1-L45.

_____, 1963a. Gravitational movement in the Warramunga Geosyncline. In: Syntaphral Tectonics, Univ. Tasmania, Hobart, pp. C1-C17.

Ernst, W.G. and Calvert, S.E., 1969. An experimental study of the recrystallization of porcellanite and its bearing on the origin of some bedded cherts. Am. J. Sci., v. 267-A, pp. 114-133.

Espenshade, G.H., 1937. Geology and mineral deposits of the Pilleys Island area. Nfld. Dept. Nat. Res., Geol. Sec., Bull. 6, 56 p.

Ferguson, J. and Lambert, I.B., 1972. Volcanic exhalations and metal enrichments at Matupi Harbour, New Britain, P.N.G. Econ. Geol. v. 67, pp. 25-37.

_____, Lambert, I.B., and Jones, H.E., 1974. Iron sulphide formation in an exhalative-sedimentary environment, Talasea, New Britain, P.N.G. Mineral. Deposita (Berl.), v. 9, pp. 33-47.

Gale, G.H., 1969. The primary dispersion of Cu, Zn, Ni, Co, Mn and Na adjacent to sulphide deposits, Springdale Peninsula, Newfoundland. Unpub. M.Sc. Thesis, Memorial University of Nfld., St. John's, Nfld., 143 p.

Garrels, R.M. and Christ, C.C., 1965. Solutions, Minerals and Equilibria. Harper and Row, New York. 450 p.

Garrison, R.E., 1974. Radiolarian cherts, pelagic limestones and igneous rocks in eugeosynclinal assemblages. In: Pelagic Sediments: On Land and Under the Sea (K.J. Hsü and H.C. Jenkyns, Eds.), Spec. Pub. Int. Assoc. Sediment., No. 1, pp. 367-399.

Gibson, T.G. and Towe, K.M., 1971. Eocene volcanism and the origin of Horizon A. Science, v. 172, pp. 152-154.

Gill, J.E., 1927. Origin of the Gunflint iron-bearing formation. Econ. Geol., v. 27, pp. 687-728.

Goodfellow, W.D., 1975. Major and minor element haloes in volcanic rocks at Brunswick No. 12 sulphide deposit, N.B., Canada. In: Geochemical Exploration, 1974 (I.C. Elliot and W.K. Fletcher, Eds.), pp. 279-295. Elsevier, Amsterdam.

Goodwin, A.M., 1956. Facies relations in the Gunflint iron formation. Econ. Geol., v. 51, pp. 565-595.

_____, 1962. Structure, stratigraphy and origin of iron formations, Michipicoten area, Algamo District, Ontario. Bull. Geol. Soc. Amer., v. 73, pp. 561-586.

_____, 1973. Archean iron formations and tectonic basins of the Canadian Shield. Econ. Geol., v. 68, pp. 915-933.

_____, 1973a. Plate tectonics and the evolution of the Archean crust. In: Symposium on Continental drift and plate tectonics - implications for the earth sciences: Newcastle, NATO Adv. St. Inst.

_____ and Ridler, R.H., 1970. The Abitibi orogenic belt. Geol. Surv. Can., Pap. 70-40, p. 1-24.

Govett, G.J.S. and Pantazis, Th. M., 1971. Distribution of Cu, Zn, Ni, and Co in the Troodos pillow series, Cyprus. Inst. Min. Metall. Trans., v. 80, pp. B27-B46.

Gross, G.A., 1965. Geology of iron deposits in Canada, vol. 1, general geology and evaluation of iron deposits. Geol. Surv. Can., Econ. Rept. 22, 181 p.

Gruneau, H.R., 1965. Radiolarian cherts and associated rocks in space and time. Eclog. Geol. Helv., v. 58, pp. 157-208.

Gruner, J.W., 1922. Organic matter and the origin of the Biwabik iron-bearing formation of the Mesabi range. Econ. Geol., v. 17, pp. 407-460.

Gullbridge Mines Ltd. Staff. Unpub. reports, maps and sections, Gullbridge, Nfld.

Hajash, A., 1975. Hydrothermal processes along mid-ocean ridges: an experimental investigation. Contr. Mineral. Petrol., v. 53, pp. 205-226.

Hayes, J.J., 1951. Preliminary map: Marks Lake, Newfoundland. Geol. Surv. Can., Pap. 51-20.

Heath, G.R. and Moberly, R. Jr., 1971. Cherts from the Western Pacific, Leg 7, Deep Sea Drilling Project. In: Initial Reports of the Deep Sea Drilling Project, Vol. VII (E.L. Winterer, Ed.), pp. 991-1007. U.S. Government Printing Office, Washington.

Helwig, J.A., 1967. Stratigraphy and structural history of the New Bay area, North Central Newfoundland. Unpub. Ph.D. Thesis, Columbia University, New York, 211 p.

Heyl, G.R., 1936. Geology and mineral deposits of the Bay of Exploits area, Newfoundland. Nfld. Dept. Nat. Res., Geol. Sec., Bull. 3, 42 p.

Horikoshi, E., 1969. Volcanic activity related to the formation of the Kuroko-type deposits in the Kosaka district, Japan. Mineral. Deposita (Berl.), v. 4, pp. 321-345.

Horne, G.S. and Helwig, J.A., 1969. Ordovician stratigraphy of Notre Dame Bay, Newfoundland. In: North Atlantic Geology and Continental Drift (M. Kay, Ed.), Amer. Assoc. Petrol. Geol., Mem. 12, pp. 388-407.

Hutchinson, R.W., 1973. Volcanogenic sulphide deposits and their metallogenic significance. Econ. Geol., v. 68, pp. 1223-1244.

_____, Ridler, R.H., and Suffel, G.G., 1971. Metallogenic relationships in the Abitibi Belt, Canada: a model for Archean metallogeny. Can. Min. Metall. Bull., v. 64, pp. 48-57.

Iwao, S., 1970. Clay and silica deposits of volcanic affinity in Japan. In: Volcanism and ore genesis (T. Tatsumi, Ed.), pp. 267-284, University of Tokyo Press, Tokyo.

James, H.L., 1954. Sedimentary facies of iron formation. Econ. Geol., v. 40, pp. 235-291.

_____, 1966. Data of geochemistry, sixth edition, chapter W, Chemistry of the iron-rich sedimentary rocks. U.S. Geol. Surv. Prof. Pap. 440-W, 61 p.

_____ and Howland, A.C., 1955. Mineral facies in iron- and silica-rich rocks. Bull. Geol. Soc. Amer., v. 66, Abstr., p. 1580.

_____ and Sims, P.K. (Eds.), 1973. Precambrian iron-formations of the world. Econ. Geol., v. 68, 1220 p.

Kalliokoski, J., 1951. Preliminary map, Gull Pond, Newfoundland. Geol. Surv., Pap. 51-1, 9 p.

_____, 1955. Gull Pond, Newfoundland. Geol. Surv. Can., Pap. 54-4.

Kanmera, K., 1974. Paleozoic and Mesozoic geosynclinal volcanism and associated chert sedimentation. In: Modern and ancient geosynclinal sedimentation (R.H. Dott and R.H. Shaver, Eds.), Spec. Pubs. Soc. Econ. Paleon. Mineral., No. 19, pp. 162-173.

Kean, B.F., 1973. Stratigraphy, petrology and geochemistry of volcanic rocks of Long Island, Newfoundland. Unpub. M.Sc. Thesis, Memorial University of Nfld., St. John's, Nfld., 155 p.

_____ and Strong, D.F., 1975. Geochemical evolution of an island arc of the Central Newfoundland Appalachians. Am. J. Sci., v. 275, pp. 97-118.

Krauskopf, K.B., 1956. Distribution and precipitation of silica at low temperatures. Geochim. et Cosmochim. Acta., v. 10, pp. 1-27.

_____, 1957. Separation of iron and manganese in sedimentary processes. Geochim. et Cosmochim. Acta., v. 12, pp. 61-84.

_____, 1967. Introduction to geochemistry. McGraw-Hill, New York, 488 p.

Krumbein, W.C. and Garrels, R.M., 1952. Origin and classification of chemical sediments in terms of pH and Eh oxidation-reduction potentials. J. Geol., v. 60, pp. 1-33.

LaBarge, G.L., 1973. Possible biological origin of Precambrian iron-formation. Econ. Geol., v. 68, pp. 1098-1109.

Lambert, I.B., 1973. The features and genesis of the Kuroko-type Cu-Zn-Pb-Ag-Au deposits of Japan, with comments on some other ore deposits of volcano-sedimentary sequences. Invest. Rept. 98, Min. Res. Lab. Div. of Mineral., C.S.I.R.O., Canberra, 53 p.

Lancelot, Y., 1973. Chert and silica diagenesis in sediments from the Central Pacific. In: Initial Reports of the Deep Sea Drilling Project, Vol. XVII (E.L. Winterer, J.I. Ewing et al., Eds.), pp. 377-506. U.S. Government Printing Office, Washington.

MacKenzie, F.T. and Garrels, R.M., 1971. Evolution of sedimentary rocks. Norton, New York, 397 p.

MacLean, H.J., 1947. Geology and mineral deposits of the Little Bay area. Nfld. Geol. Surv. Bull. 22.

Maxwell, J.A., 1968. Rock and mineral analysis. Interscience Publishers, 584 p.

McAllister, A.L., 1960. Massive sulphide deposits in New Brunswick. Can. Min. Metall. Bull., v. 53, pp. 88-98.

Miller, A.L., Densmore, C.D., Degens, E.T., Hathaway, J.C., Manheim, F.T., McFarlin, P.F., Pocklington, R. and Jokela, A., 1966. Hot brines and recent iron deposits in deeps of the Red Sea. Geochim. et Cosmochim. Acta., v. 30, pp. 341-359.

Murray, A.H. and Howley, J.P., 1881. Geological survey of Newfoundland. E. Stanford, London, 536 p.

_____, 1918. Reports of the Geological Survey of Newfoundland from 1881-1909.

Neale, E.R.W. and Nash, W.G., 1963. Sandy Lake (east half), Newfoundland. Geol. Surv. Can., Pap. 63-28.

Noranda Mines Staff, 1971. Unpubl. geol. maps, Southwestern Notre Dame Bay. Gander, Nfld.

Offedahl, C., 1958. A theory of exhalative-sedimentary ores. Geol. Foren. Stolkholm Forh., v. 8, no. 1, pp. 1-19.

Pettijohn, F.J., 1956. Sedimentary rocks (second edition). Harper and Row, New York, 718 p.

Puchelt, H., 1973. Recent iron sediment formation at the Kameni Islands, Santorini (Greece). In: Ores in sediments (G.C. Amstutz and A.J. Bernard, Eds.), pp. 227-246, Springer-Verlag, Heidelberg.

Pushkina, Z.V., 1967. Iron, manganese, silicon, phosphorous, boron and aluminum in sea water in the area of Santorin Volcano. Lith. and Min. Res., v. 2, pp. 218-225.

Ramsey, A.T.S., 1973. A history of organic siliceous sediments in oceans. In: Organisms and continents through geologic time (N.F. Hughes, Ed.), Spec. Pap. Palaeont., v. 12, pp. 199-234.

Ridler, R.H., 1970. Relationship of mineralization to volcanic stratigraphy in the Kirkland Lake-Larder Lakes area. Trans. Geol. Assoc. Can., v. 21, pp. 33-42.

Ridler, R.H., 1971. Relationship of mineralization to stratigraphy in the Archean Rankin Inlet-Ennadai belt. Can. Min. J., v. 92, pp. 3-7.

Robertson, A.H.F. and Hudson, J.D., 1973. Cyprus umbers: chemical precipitates on a Tethyan ocean ridge. Earth Planet. Sci. Letts., v. 18, pp. 93-101.

_____, 1974. Pelagic sediments in the Cretaceous and Tertiary history of the Troodos Massif, Cyprus. In: Pelagic sediments: on land and under the sea (K.J. Hsü and H.C. Jenkyns, Eds.), Spec. Pubs. Int. Assoc. Sediment., no. 1, pp. 273-299.

Ruedemann, R. and Wilson, T.Y., 1936. Eastern New York Ordovician cherts. Bull. Geol. Soc. Amer., v. 47, pp. 1535-1586.

Sampson, E., 1923. The ferruginous chert formations of Notre Dame Bay, Newfoundland. J. Geol., v. 31, pp. 571-598.

Sato, T., 1974. Distribution and geological setting of the Kuroko deposits. In: Geology of Kuroko deposits (Ishihara, S., Ed.), Min. Geol. Sp. Issue, no. 6, Soc. Min. Geol. Japan, pp. 1-10.

Sayles, F.I. and Bischoff, J.L., 1973. Ferromanganoan sediments in the equatorial East Pacific. Earth Planet. Sci. Letts., v. 18, pp. 330-336.

Siever, R., 1962. Silica solubility, 0^{0}-200^{0} C., and the diagenesis of siliceous sediments. J. Geol., v. 70, pp. 127-150.

Smitheringale, W.G., 1972. Low potash Lushs Bight tholeiites, ancient oceanic crust in Newfoundland? Can. J. Earth Sci., v. 9, pp. 574-588.

Spooner, E.T.C. and Fyfe, W.S., 1973. Sub-sea floor metamorphism, heat and mass transfer. Contrib. Mineral. Petrol., v. 42, pp. 287-304.

Strakhov, N., 1959. Schema de la diagenese des depots marins. Eclog. Geol. Helv., v. 51, pp. 761-767.

Stevens, R.K., 1970. Cambro-Ordovician flysch sedimentation and tectonics in west Newfoundland and their possible bearing on a Proto-Atlantic Ocean. Geol. Assoc. Can., Spec. Pap. No. 7, pp. 165-177.

Strong, D.F., 1972. Sheeted diabases on Central Newfoundland: new evidence for Ordovician sea-floor spreading. Nature, v. 235, pp. 102-104.

Strong, D.F., 1973. Lushs Bight and Roberts Arm Groups of Central Newfoundland: possible juxtaposed oceanic and island-arc volcanic suites. Bull. Geol. Soc. Amer., v. 84, pp. 3917-3928.

_____, 1975. Volcanic regimes in the Newfoundland Appalachians. Paper presented at the 28th ann. mtg., Geol. Assoc. Can., Waterloo, Ont.

_____ and Payne, J.G., 1973. Early Paleozoic volcanism and metamorphism of the Moreton's Harbour area, Newfoundland. Can. J. Earth Sci., v. 19, pp. 1363-1379.

Sutton, J. and Bridgewater, D., 1974. The Precambrian. Sci. Progr., v. 61, pp. 401-420.

Swinden, H.S., 1975. Report of geologic mapping of the Gullbridge Mines Ltd. property, Great Gull Pond, Newfoundland. Unpub. rept. for Atlantic Coast Copper Corp. Ltd., Saint John, N.B.

Thurlow, J.G., 1974. Lithogeochemical studies in the vicinity of the Buchans massive sulphide deposits, Central Newfoundland. Unpub. M.Sc. thesis, Memorial University of Newfoundland, St. John's, Newfoundland, 171 p.

Thurston, D.R., 1972. Studies on bedded cherts. Contrib. Mineral. Petrol., v. 36, pp. 324-334.

Tono, N., 1974. Minor elements distribution around Kuroko deposits in northern Akita, Japan. In: Geology of Kuroko Deposits, Min. Geol. Spec. Issue, No. 6, pp. 399-420.

Trendall, A.F., 1973. Precambrian iron-formations of Australia. Econ. Geol., v. 68, pp. 1023-1034.

Upadhyay, H.D., 1970. Geology of the Gullbridge copper deposit, Central Newfoundland. Unpub. M.Sc. thesis, Memorial University of Newfoundland, St. John's, Nfld.

_____ and Smitheringale, W.G., 1972. Geology of the Gullbridge copper deposit: volcanogenic sulphides in cordierite-anthophyllite rocks. Can. J. Earth Sci., v. 9, pp. 1061-1073.

van Hise, C.R. and Lieth, C.K., 1911. The geology of the Lake Superior region. U.S. Geol. Surv., Mon. 52, 641 p.

von der Borch, C. and Rex, R., 1970. Amorphous iron oxide precipitates in sediments cored during Leg V, D.S.D.P. In: Initial Reports of the Deep Sea Drilling Project, V. V (D. McManus et al., Eds.) pp. 541-544, U.S. Government Printing Office, Washington.

_____, Nesteroff, W.D. and Galehouse, J.S., 1971. Iron rich sediments cored during Leg 8 of the Deep Sea Drilling Project. In: Initial Reports of the Deep Sea Drilling Project, V. VIII (J. Tracey et al., Eds.), pp. 829-836, U.S. Government Printing Office, Washington.

von Rad, U. and Rosch, H., 1974. Petrography and diagenesis of deep sea cherts from the central Atlantic. In: Pelagic sediments: on land and under the sea (K.J. Hsü and H.C. Jenkyns, Eds.), Spec. pubs. Int. Assoc. Sediment., no. 1, pp. 327-347.

Wanless, R.K., Stevens, R.D., Lachance, G.R. and Rimsaite, R.Y.J., 1965. Age determinations and geological studies, Part 1, Isotopic ages report 5. Geol. Surv. Can., Pap. 64-17, Pt. 1, 126 p.

Whitehead, R.E., 1973. Environment of stratiform sulphide deposition, variation in Mn:Fe ratio in host rocks at Heath Steele Mine, New Brunswick, Canada. Mineral. Deposita (Berl.), v. 8, pp. 148-160.

_____ and Govett, G.J.S., 1974. Exploration rock geochemistry - detection of trace halos at Heath Steele Mines (N.B., Canada) by discriminant analysis. J. Geochim Explor., v. 3, pp. 371-386.

Wilson, A.D., 1955. A new method for the determination of ferrous iron in rocks and minerals. Bull. Geol. Surv. Gr. Brit., v. 9, pp. 56-58.

Williams, H., 1962. Botwood (west half) map area, Newfoundland (2E W½). Geol. Surv. Can., Pap. 62-9, 16 p.

_____, 1964. Botwood, Newfoundland. Geol. Surv. Can., Map 60-1963.

_____, 1964a. The Appalachians in northwestern Newfoundland - a two-sided symmetrical system. Amer. J. Sci., v. 262, pp. 1137-1158.

Wise, S.W. Jr., Buie, B.F. and Weaver, F.M., 1972. Chemically precipitated cristobalite and the origin of chert. Eclog. Geol. Helv., v. 65, pp. 157-163.

Wise, S.W. Jr. and Weaver, F.M., 1974. Chertification of oceanic sediments. In: Pelagic sediments: on land and under the sea (K.J. Hsü and H.C. Jenkyns, Eds.), Spec. Pubs. Int. Assoc. Sediment., No. 1, pp. 301-326.

Zelenov, K.K., 1964. Iron and manganese exhalations of the submarine Banu Wahu volcano (Indonesia). Dokl. Akad. Sci. U.S.S.R., Earth Sci. Sec., v. 155, pp. 94-96.

APPENDIX A

INDIVIDUAL SAMPLE ANALYSES

ROBERTS ARM SUITE

SAMPLE	RA2	RA3	RA5	RA6	RA8	RA11A	RA11B	RA12	RA13	RA14	RA15
SIO2	56.00	74.50	83.50	50.50	76.80	56.00	67.10	72.80	52.40	89.70	72.00
TIO2	0.35	0.16	0.0	0.38	0.18	0.33	0.29	0.25	0.17	0.0	0.40
AL2O3	8.47	13.80	7.85	8.10	4.55	5.75	5.16	5.85	4.80	4.00	12.40
FE2O3	10.47	0.74	0.0	19.06	10.02	23.53	16.48	10.46	28.69	0.0	1.28
FEO	4.83	0.04	2.46	10.32	2.30	1.86	1.50	1.03	5.54	2.04	1.68
MNO	4.00	0.07	0.02	0.42	0.27	2.90	2.33	1.67	0.60	0.05	0.07
MGO	2.46	0.04	0.85	4.50	0.97	1.96	1.59	1.57	4.46	1.71	2.77
CAO	3.04	0.89	0.20	1.42	1.80	3.39	2.60	3.30	1.49	0.55	1.40
NA2O	0.05	2.67	3.42	0.84	0.82	1.12	1.30	0.51	0.09	0.79	1.79
K2O	0.25	5.12	0.08	0.04	0.04	0.0	0.03	0.17	0.38	0.32	2.22
LOI	2.65	1.36	1.01	4.56	1.15	1.59	1.47	1.72	3.21	1.78	2.88
TOTAL	98.67	100.64	99.29	100.64	98.90	98.43	99.85	99.13	101.83	100.94	98.79
ZR	56	85	65	50	43	40	46	43	41	40	112
SR	102	144	57	75	123	65	62	141	44	46	143
RB	19	148	16	13	13	15	11	18	7	18	90
ZN	80	48	48	65	26	63	58	52	56	39	82
CU	0	4	8	17	3	0	2	2	34	4	5
BA	111	1850	33	23	32	50	30	76	143	96	380
SN	9	15	12	13	9	10	10	9	6	5	14
NI	65	17	10	70	44	57	52	60	43	24	18
CR	13	8	13	32	27	32	24	28	16	11	12
AU	15			0	20	10		10	10	20	

SAMPLE	RA16	RA17	RA18	RA19	RA20	RA22	RA22A	RA23	RA25	RA34	RA38
SIO2	74.50	78.30	70.20	85.30	78.90	84.60	78.50	57.90	78.60	89.10	81.60
TIO2	0.13	0.66	0.28	0.0	0.30	0.0	0.0	0.26	0.20	0.0	0.0
AL2O3	4.20	13.30	13.60	2.80	10.70	2.32	5.51	5.48	11.20	2.10	0.0
FE2O3	11.55	2.41	2.10	5.58	0.58	7.26	3.69	21.48	0.56	3.24	10.58
FEO	2.36	0.10	1.61	0.44	1.12	1.79	3.89	3.44	1.62	0.87	0.37
MNO	0.26	0.01	0.16	0.11	0.21	0.08	0.16	0.21	0.23	0.06	0.04
MGO	2.64	0.09	1.81	0.81	1.99	1.47	3.30	4.95	0.79	0.35	0.01
CAO	0.33	0.75	0.38	0.50	0.38	0.50	3.06	0.64	0.62	0.13	3.95
NA2O	0.28	7.54	0.71	0.24	4.69	0.07	0.05	0.39	4.29	0.06	0.02
K2O	0.94	0.09	5.60	0.92	0.53	0.22	0.09	0.33	2.04	0.54	0.0
LOI	1.98	0.57	2.63	0.70	1.56	1.36	3.08	3.14	0.99	0.73	3.22
TOTAL	99.17	99.42	100.06	97.20	100.96	99.67	101.33	98.24	101.14	97.18	99.79
ZR	36	111	115	31	81	24	31	43	85	28	16
SR	46	92	98	56	72	27	44	51	135	41	31
RB	31	10	203	49	18	10	7	21	39	28	12
ZN	56	13	74	29	51	30	47	50	38	29	13
CU	10	7	5	5	22	13	3	3	5	5	7
BA	218	48	984	93	Ma	107	50	125	680	363	9
SN	8	13	10	11	14	6	4	5	10	8	9
NI	44	11	23	28	18	23	38	48	20	13	41
CR	13	10	9	14	12	13	12	13	15	12	12
AU	15	-		10		15		15		10	10

ROBERTS ARM SUITE

SAMPLE	RA34	RA41	RA44	RA46	RA49	RA52	RA53	RA54	RA55A	RA55B	RA55C
SIO2	89.90	4.30	83.60	88.90	7.57	64.00	55.30	86.50	64.00	63.30	58.00
TIO2	0.0	0.0	0.18	0.36	0.0	0.0	0.0	0.0	0.0	0.0	0.0
AL2O3	3.21	0.45	3.92	13.70	1.58	3.27	1.18	0.0	0.58	0.46	0.10
FE2O3	1.41	3.02	2.49	4.98	87.04	20.44	30.89	8.99	22.49	21.57	21.20
FEO	0.48	0.88	0.70	0.68	1.41	3.02	0.51	0.52	0.41	0.30	0.16
MNO	0.16	0.02	0.64	0.07	0.03	0.07	0.04	0.02	0.03	0.04	0.01
MGO	0.63	0.24	1.27	0.97	1.53	2.38	0.55	0.0	0.09	0.05	0.0
CAO	0.41	1.03	1.70	0.56	0.37	1.53	5.56	1.39	5.68	7.33	11.09
NA2O	0.59	0.0	0.22	2.34	0.0	0.0	0.04	0.0	0.0	0.0	0.0
K2O	0.01	0.0	0.08	3.18	0.0	0.07	0.19	0.0	0.10	0.12	0.01
LOI	0.84	1.01	3.47	3.00	1.38	3.16	4.55	1.38	4.92	6.26	9.79
TOTAL	98.26	97.73	99.27	98.74	100.91	97.94	98.81	98.80	98.30	99.38	99.90
ZR	28	21	34	94	8	25	17	21	16	17	20
SR	37	35	42	80	15	32	61	30	33	38	59
RB	26	13	43	102	1	14	15	12	6	6	3
ZN	30	13	52	77	20	52	22	10	21	21	20
CU	1	7	4	9	145	1	0	30	0	0	0
PB	147	10	144	569	77	23	45	21	33	46	52
NI	4	11	10	12	0	11	9	8	3	2	4
CO	16	16	24	33	80	46	37	21	19	20	19
CR	13	12	14	26	17	18	14	12	15	18	15
AU	0	0	20			0	5	0	20	5	5

SAMPLE	RA55D	RA56	RA59	RA63	RA67B	RA67G	RA70	RA78	RA79	RA82	RA84
SIO2	64.90	86.30	82.90	79.00	92.00	56.80	32.50	86.00	6.90	91.20	62.80
TIO2	0.0	0.0	0.0	0.13	0.0	0.0	0.81	0.15	0.0	0.0	0.27
AL2O3	0.46	0.0	2.89	5.16	1.31	11.50	14.00	4.60	1.18	2.08	10.90
FE2O3	20.81	8.30	6.60	6.45	0.31	6.37	0.53	3.50	89.48	3.60	8.85
FEO	0.35	0.77	0.75	0.43	1.36	0.61	5.81	0.37	1.14	0.36	0.89
MNO	0.03	0.08	0.08	0.58	0.0	0.05	0.14	0.08	0.03	0.09	0.18
MGO	0.06	0.22	0.36	0.96	0.34	0.57	6.90	0.72	0.99	0.55	0.86
CAO	7.45	0.90	2.47	4.29	1.93	19.70	12.60	0.0	0.49	0.19	12.65
NA2O	0.0	0.01	0.50	0.33	0.0	0.0	0.02	0.79	0.0	0.21	0.01
K2O	0.09	0.0	0.41	0.36	0.0	0.03	0.19	4.31	0.01	0.32	0.0
LOI	6.33	0.83	1.75	1.71	1.78	6.39	26.71	1.10	1.26	0.80	1.62
TOTAL	100.28	97.91	98.66	99.40	99.03	102.02	99.71	101.67	101.48	99.40	98.98
ZR	18	21	38	41	47	228	60	38	0	26	168
SR	92	60	188	82	286	2261	218	37	19	22	1483
RB	7	14	19	24	8	0	15	47	0	16	7
ZN	21	22	17	36	17	20	65	40	24	28	20
CU	0	4	9	8	145	7	41	4	48	1	7
PB	36	837	113	139	1851	1685	56	349	80	208	17
NI	5	7	9	11	3	0	4	12	0	8	8
CO	19	24	34	46	36	32	124	19	73	21	44
CR	16	11	15	19	38	21	727	19	16	13	21
AU	5	15	15	0				40	0	0	

ROBERTS ARM SUITE

SAMPLE	RA89	RA92	RA98	RA100	RA102	RA103	RA109	RA110	RA112	RA113	RA116
SIO2	83.30	87.20	74.70	89.90	90.90	82.80	81.50	63.60	31.00	76.30	81.70
TIO2	0.0	0.0	0.48	0.0	0.0	0.14	0.0	0.0	0.0	0.0	0.0
AL2O3	1.12	0.70	11.40	1.40	2.87	4.20	0.32	1.07	14.00	1.05	0.35
FE2O3	8.49	10.19	1.22	22.56	1.93	3.83	8.61	24.92	24.10	19.01	11.54
FEO	1.57	0.75	1.99	1.11	0.94	0.11	1.17	1.10	6.25	0.48	0.31
MNO	0.04	0.0	0.09	0.05	0.14	0.07	0.18	0.06	0.19	0.01	0.10
MGO	1.04	0.09	1.97	1.49	0.41	0.72	1.17	1.39	7.95	0.28	0.05
CAO	3.91	1.01	1.44	1.52	0.07	2.36	2.84	3.33	3.43	0.41	3.03
NA2O	0.01	0.0	2.67	0.08	0.02	0.04	0.01	0.02	0.31	0.02	0.02
K2O	0.0	0.04	1.73	0.14	0.95	1.85	0.58	0.31	4.30	0.28	0.0
LOI	2.86	0.74	2.27	2.23	1.31	3.23	4.52	5.41	7.05	1.27	2.49
TOTAL	100.36	100.73	99.91	100.46	99.94	99.95	100.90	101.71	98.58	99.29	99.59
ZR	17	19	132	15	29	39	18	17	26	16	13
SR	37	52	185	45	21	62	37	35	91	31	17
RB	14	7	38	15	37	64	15	16	122	9	2
ZN	17	21	87	27	28	34	17	20	71	21	20
CU	9	3	15	2	2	17	8	8	11	6	37
BA	5	664	470	33	96	229	14	70	712	39	18
NB	8	5	14	7	5	9	9	8	0	4	6
NI	26	34	35	37	27	33	24	40	47	19	19
CR	11	17	24	11	17	17	9	10	24	12	9
AU	50	25	5	10	25	0	5	15	0	65	20

SAMPLE	RA117	RA117R	RA117G	RA118	RA119	RA120	RA121	RA123	RA125	RA127	RA128
SIO2	92.00	95.70	96.30	89.90	74.60	57.10	64.00	43.00	78.00	87.10	85.90
TIO2	0.0	0.0	0.0	0.0	0.0	0.84	0.0	0.22	0.0	0.0	0.0
AL2O3	0.23	0.88	1.40	0.25	0.62	14.80	1.69	20.60	1.40	0.92	0.38
FE2O3	12.31	0.0	0.0	9.07	21.55	8.77	27.08	6.97	16.39	8.05	10.74
FEO	0.29	0.51	0.71	0.49	0.41	0.65	0.65	0.64	1.45	0.63	0.47
MNO	0.09	0.01	0.05	0.02	0.02	0.09	0.06	0.04	0.05	0.0	0.05
MGO	0.03	0.01	0.18	0.0	0.02	0.41	0.69	0.76	0.32	0.05	0.04
CAO	2.71	0.06	0.06	0.05	2.21	15.63	3.97	23.60	0.08	0.04	0.25
NA2O	0.01	0.01	0.05	0.0	0.0	0.0	0.02	0.01	0.02	0.02	0.01
K2O	0.0	0.26	0.37	0.01	0.0	0.07	0.0	0.0	0.12	0.18	0.02
LOI	2.01	0.45	0.62	0.70	0.56	2.28	2.59	4.84	1.29	0.68	0.81
TOTAL	99.68	97.87	99.76	99.69	98.99	100.39	100.75	100.18	99.12	97.67	98.67
ZR	15	21	20	13	13	260	14	133	13	16	124
SR	29	25	21	15	17	2331	42	1231	22	20	577
RB	14	16	19	4	3	0	13	0	6	6	24
ZN	12	22	31	23	22	24	23	18	46	22	14
CU	45	7	4	25	0	8	2	36	3	3	4
BA	19	122	125	5	12	48	21	0	55	83	120
NB	8	11	7	9	5	4	6	1	5	6	12
NI	26	17	19	25	23	43	31	19	19	18	21
CR	12	19	13	12	11	37	12	24	21	10	14
AU	45			25	0		0		25	0	20

VERY FAINT COPY

ROBERTS ARM SUITE

SAMPLE	RA131	RA134	RA135	RA137	RA138	RA139	RA140	RA141	RA143A	RA143B	RA145
SIO2	77.00	82.80	82.60	91.80	77.00	34.90	39.00	80.00	81.90	44.30	79.30
TIO2	0.38	0.0	0.0	0.0	0.0	0.0	0.21	0.0	0.0	0.0	0.0
AL2O3	8.26	7.30	7.60	1.18	3.28	12.54	4.41	7.23	3.97	14.80	4.13
FE2O3	3.49	1.77	1.98	3.10	8.54	28.65	3.02	7.20	3.71	7.19	3.44
FEO	0.40	0.76	0.91	0.67	1.18	0.44	4.49	0.81	0.76	1.06	1.10
MNO	0.07	0.06	0.05	0.01	0.05	0.04	0.35	0.07	0.01	0.04	0.03
MGO	0.17	0.0	0.04	0.55	3.68	8.57	8.81	1.27	0.68	1.49	1.73
CAO	7.40	5.63	5.70	1.77	3.50	16.87	15.55	6.56	6.03	20.43	5.31
NA2O	0.03	0.32	0.41	0.04	0.08	0.04	0.03	0.08	0.0	0.0	0.03
K2O	0.47	0.33	0.30	0.05	0.06	0.18	0.06	0.10	0.0	0.0	0.43
LOI	1.50	1.18	1.02	1.58	3.01	4.08	22.42	3.10	2.07	6.54	4.03
TOTAL	98.63	100.13	100.01	100.75	100.39	98.31	98.95	96.42	99.13	95.85	99.53
ZN	124	112	93	22	36	11	29	22	19	21	21
SR	577	545	449	68	118	22	87	53	33	50	40
RB	44	7	19	4	12	4	13	16	5	2	23
ZR	14	19	14	21	33	24	76	21	32	38	33
CU	4	4	10	5	20	6	15	10	6	9	4
BA	120	114	178	47	14	0	42	52	28	25	61
NB	12	5	8	4	6	0	7	11	5	4	3
NI	41	19	21	80	202	32	89	69	101	139	96
CR	14	14	12	14	19	16	896	23	15	23	28
AU		25		20	10	10		0			

SAMPLE	RA146	RA147	RA149	RA150	RA151	RA152	RA153	RA154	RA155	RA156	RA158
SIO2	93.70	92.40	90.10	92.40	84.50	96.00	75.80	84.30	96.00	68.90	83.00
TIO2	0.0	0.0	0.0	0.0	0.18	0.0	0.0	0.0	0.0	0.0	0.0
AL2O3	0.70	3.69	0.25	1.59	3.13	1.05	0.74	0.0	1.09	0.25	3.37
FE2O3	1.65	2.69	4.72	4.08	5.83	0.11	21.14	12.50	0.11	25.06	4.94
FEO	0.69	0.70	0.68	0.58	0.58	0.99	0.24	0.36	0.99	0.65	2.16
MNO	0.01	0.01	0.03	0.03	0.04	0.02	0.20	0.17	0.02	0.08	0.06
MGO	0.05	0.46	0.10	0.30	0.64	0.56	0.14	0.0	0.56	0.42	1.95
CAO	0.65	0.65	0.23	0.26	1.39	0.10	0.90	1.65	0.10	3.04	1.97
NA2O	0.04	0.05	0.01	0.08	0.34	0.04	0.0	0.0	0.04	0.0	0.02
K2O	0.05	0.27	0.04	0.62	1.01	0.05	0.0	0.0	0.05	0.02	0.05
LOI	0.92	1.04	0.64	0.84	2.40	1.10	0.65	0.66	1.10	1.39	2.22
TOTAL	98.86	99.96	98.40	100.76	100.04	100.02	99.81	99.64	100.02	99.79	99.74
ZN	18	22	15	34	39	39	14	16	22	16	29
SR	30	50	17	40	52	52	23	22	26	18	40
RB	4	18	3	34	46	64	14	15	5	1	16
ZR	22	25	22	19	25	30	36	16	21	27	55
CU	10	11	10	6	90	0	1	1	4	8	6
BA	104	71	25	138	601	350	26	8	61	21	26
NB	7	4	7	7	8	4	11	8	4	0	9
NI	32	34	18	21	42	29	48	29	24	121	30
CR	11	14	10	12	28	26	11	11	13	15	14
AU	5	15	20	15	15	0	5	25	10	10	5

ROBERTS ARM SUITE

SAMPLE	RA158A	RA159	RA160	RA161A	RA161C	RA163	RA164	RA165A	RA165B	RA165C	RA166
SIO2	79.10	85.20	62.20	74.20	47.80	89.60	80.00	83.00	92.00	89.80	82.40
TIO2	0.10	0.23	0.27	0.14	0.11	0.0	0.14	0.11	0.0	0.0	0.0
AL2O3	4.40	3.05	14.00	4.90	10.40	1.76	3.86	3.89	1.03	1.61	2.96
FE2O3	5.65	5.45	2.32	10.43	15.41	4.69	7.77	2.16	0.25	0.52	4.67
FEO	3.21	1.50	1.05	0.91	1.14	0.80	2.91	1.18	0.73	0.56	1.37
MNO	0.08	0.05	0.08	0.06	0.11	0.02	0.07	0.0	0.0	0.0	0.07
MGO	2.05	1.47	1.37	0.42	2.20	0.53	2.63	0.65	0.32	0.20	3.00
CAO	1.95	3.09	12.80	7.84	14.78	1.13	0.27	1.24	2.26	3.10	3.03
NA2O	0.03	0.0	0.10	0.0	0.0	0.03	0.12	0.0	0.0	0.0	0.12
K2O	0.07	0.03	0.43	0.0	0.0	0.03	0.43	0.04	0.04	0.06	0.08
LOI	2.75	2.00	4.81	2.56	5.11	1.74	2.19	2.71	1.86	1.90	2.41
TOTAL	99.56	102.07	99.68	101.74	96.56	99.33	100.19	94.98	98.49	97.75	100.11
ZN	33	25	71	31	29	24	32	24	22	18	70
SR	31	31	48	31	45	35	34	33	31	25	40
RB	2	3	6	2	2	13	20	6	7	5	14
ZR	71	49	40	42	70	21	46	27	24	22	30
CU	6	7	107	1	21	17	9	0	0	4	7
BA	145	21	32	15	17	28	81	266	250	18	24
NB	7	0	24	5	4	7	6	10	6	3	7
NI	32	31	37	38	48	22	32	23	22	18	47
CR	17	13	13	16	18	15	16	32	27	11	15
AU		0		30		0	0	5	0		15

SAMPLE	RA169	RA170	RA171	RA172	RA173	RA174	RA176A	RA177	RA178	RA179	RA180
SIO2	86.20	89.40	88.00	84.70	81.80	83.30	77.90	85.80	72.50	82.70	82.30
TIO2	0.0	0.0	0.0	0.0	0.0	0.0	0.23	0.17	0.32	0.17	0.0
AL2O3	7.43	7.17	0.0	1.40	1.61	0.35	9.08	4.32	14.70	8.49	9.80
FE2O3	2.50	2.27	7.73	6.58	9.25	14.66	1.70	3.40	1.38	0.31	0.15
FEO	0.72	0.79	0.46	0.62	0.65	0.56	1.55	0.68	1.15	0.97	1.37
MNO	0.03	0.02	0.05	0.03	0.05	0.02	0.28	0.17	0.28	0.10	0.16
MGO	0.41	0.57	0.05	0.84	0.31	0.04	1.10	0.70	0.91	0.62	0.97
CAO	2.12	0.72	1.65	2.47	2.55	0.10	0.89	0.31	1.04	0.26	0.37
NA2O	0.05	0.43	0.01	0.05	0.06	0.01	1.12	0.24	5.21	2.42	1.42
K2O	0.27	0.15	0.02	0.60	0.30	0.04	2.79	1.58	2.09	1.69	3.35
LOI	3.48	1.23	1.50	3.01	2.51	0.62	2.13	1.07	1.79	1.24	1.75
TOTAL	98.41	97.70	99.47	100.08	99.09	99.48	98.77	98.44	101.37	98.92	101.66
ZN	25	28	15	24	34	23	137	36	194	69	68
SR	40	72	34	58	48	30	132	45	259	93	73
RB	12	18	16	21	17	15	105	68	62	46	81
ZR	6	21	19	15	24	18	80	36	95	49	100
CU	10	8	10	29	20	1	13	7	13	6	11
BA	76	97	95	664	274	204	567	326	733	657	1113
NB	3	11	9	10	7	12	7	10	10	12	15
NI	27	15	50	35	28	76	27	25	23	20	18
CR	31	18	12	15	36	11	10	18	8	9	11
AU	40	0	60	40		50		20			

HOWERTS ARM SUITE

SAMPLE	RA183	RA184	RA190A	RA190B	RA190C
SIO2	78.60	79.00	74.10	77.30	69.90
TIO2	0.40	0.20	0.25	0.20	0.28
AL2O3	11.90	9.80	8.68	7.24	9.46
FE2O3	0.68	0.02	0.11	3.38	2.19
FEO	0.86	0.81	3.00	1.89	6.48
MNO	0.17	0.05	0.18	0.26	0.43
MGO	0.51	0.59	1.27	1.81	2.89
CAO	0.81	1.64	1.68	0.89	0.89
NA2O	5.13	2.44	1.15	1.43	2.11
K2O	1.60	2.67	0.89	0.34	0.37
LOI	1.13	1.00	1.79	2.06	3.74
TOTAL	101.59	97.99	100.10	98.80	98.59
ZN	144	101	56	53	71
SR	359	179	121	103	78
RB	50	58	21	8	10
ZR	49	26	30	32	56
CU	7	7	67	93	22
BA	945	1610	340	182	136
NB	9	11	3	8	9
NI	19	30	40	46	49
CR	8	10	19	16	18
AU			40		

FORTUNE HARBOUR SUITE

SAMPLE	FH1	FH2	FH4B	FH4G	FH5	FH6	FH7A	FH8	FH9	FH10A	FH10B
SIO2	79.00	90.50	98.00	94.70	87.70	80.80	88.00	88.90	73.50	83.50	68.70
TIO2	0.13	0.0	0.0	0.0	0.0	0.28	0.0	0.0	0.14	0.0	0.55
AL2O3	10.60	2.70	0.78	1.84	4.60	7.40	7.80	2.20	11.40	3.88	10.40
FE2O3	0.41	1.20	1.58	0.0	0.06	5.17	0.42	1.68	0.15	1.70	1.05
FEO	1.66	1.50	0.66	2.14	2.79	0.37	1.92	0.41	1.19	1.76	4.51
MNO	0.09	0.14	0.07	0.09	0.48	0.25	0.40	0.75	0.66	0.36	0.91
MGO	2.96	0.67	0.12	0.73	1.36	0.65	1.56	0.47	1.96	1.57	2.21
CAO	0.0	0.08	0.33	0.08	1.26	0.19	1.10	0.83	0.71	0.56	1.38
NA2O	1.33	0.15	0.03	0.0	0.85	1.01	0.63	0.02	0.13	0.14	0.79
K2O	2.07	0.36	0.21	0.24	0.51	1.96	2.07	0.73	3.25	0.70	1.86
LOI	3.16	1.15	0.76	1.38	2.78	2.08	4.06	2.25	4.95	2.85	6.98
TOTAL	101.62	97.93	100.14	101.20	101.86	100.14	107.96	98.24	98.24	96.87	99.28
ZR	76	24	25	21	40	56	66	24	92	31	85
SR	36	21	28	23	58	65	56	35	51	31	98
RB	87	18	17	16	31	78	94	37	115	33	55
ZN	36	84	20	14	103	36	87	29	106	59	46
CU	2	4	16	376	11	4	15	3	11	2	5
BA	463	309	426	402	287	582	519	174	981	398	360
NB	8	6	4	7	11	5	11	3	21	5	8
NI	24	23	21	22	25	34	37	30	27	30	32
CR	12	14	26	28	17	12	14	14	9	15	29
AU	135	45				35	25	35	55	55	

FORTUNE HARBOUR SUITE

SAMPLE	FH12	FH13	FH14	FH15	FH16	FH17	FH18	FH19	FH20	FH21	FH22
SIO2	84.10	84.10	83.60	82.40	70.60	92.00	68.40	78.30	81.50	90.60	90.20
TIO2	0.0	0.0	0.0	0.0	0.0	0.0	0.0	0.23	0.0	0.0	0.11
AL2O3	3.90	5.00	3.08	3.40	4.60	0.40	6.80	7.60	2.50	2.50	3.10
FE2O3	4.70	3.37	2.49	6.68	9.51	2.01	10.24	0.82	6.66	1.77	2.49
FEO	0.66	0.56	0.37	1.04	0.0	0.68	1.10	1.67	0.41	0.41	0.44
MNO	0.36	0.25	1.23	0.13	1.20	0.01	0.13	0.09	0.37	0.33	0.16
MGO	0.01	0.07	0.71	1.24	1.07	0.12	0.96	2.53	0.47	0.64	0.46
CAO	0.08	1.16	1.94	1.62	3.23	1.27	8.57	1.31	2.26	0.42	0.10
NA2O	0.38	0.21	0.18	0.07	0.04	0.0	0.03	2.51	0.0	0.20	0.27
K2O	1.15	1.69	0.81	0.96	1.55	0.02	0.04	0.17	0.79	0.49	0.76
LOI	2.61	2.65	3.47	2.63	5.46	1.49	3.41	2.80	2.89	1.84	1.32
TOTAL	98.45	99.06	98.60	100.17	99.26	98.00	99.68	98.03	97.85	99.20	99.41
ZN	32	37	30	78	42	21	28	60	30	29	28
SR	47	31	45	53	58	46	38	80	27	32	25
RB	54	66	43	47	60	4	5	8	24	24	31
ZR	36	39	45	37	48	19	32	34	33	41	34
CL	6	5	4	6	25	2	6	7	2	8	13
BA	281	786	196	83	499	198	119	144	150	143	145
NB	7	8	3	2	9	8	5	14	5	5	9
NI	30	30	38	33	48	19	85	25	31	26	25
CR	16	16	11	14	16	10	18	16	11	19	20
AU	80	45	40	65	85	75	150	100	15	105	135

SAMPLE	FH23	FH25	FH26	FH29	FH32	FH33	FH34	FH35	FH37	FH38	FH39
SIO2	93.30	74.50	87.30	87.10	84.70	83.00	79.50	70.40	82.20	84.90	86.20
TIO2	0.0	0.0	0.0	0.0	0.0	0.0	0.28	0.20	0.26	0.26	0.14
AL2O3	1.90	3.90	2.10	0.03	3.00	8.69	10.60	12.60	6.67	4.76	4.10
FE2O3	1.90	5.80	3.82	9.01	9.28	0.38	0.45	0.49	5.34	3.91	3.18
FEO	0.42	0.16	0.53	0.46	0.19	0.36	0.73	0.77	0.46	0.57	0.56
MNO	0.15	1.04	0.19	0.01	0.36	0.03	0.12	0.09	0.17	0.04	0.06
MGO	0.46	1.58	1.21	0.05	0.51	0.22	0.29	0.67	0.74	0.48	0.39
CAO	0.0	3.25	0.77	1.93	0.34	0.27	1.20	2.03	0.42	3.28	2.90
NA2O	0.08	0.04	0.04	0.0	0.11	2.23	3.77	0.43	0.77	0.48	0.34
K2O	0.37	1.18	0.64	0.0	1.19	2.85	2.46	4.15	2.01	0.36	0.24
LOI	1.08	4.62	2.06	0.85	1.18	0.80	0.67	4.00	1.79	0.92	0.73
TOTAL	99.66	98.09	98.86	99.44	100.86	98.83	100.01	95.83	100.78	99.96	98.84
ZN	23	39	26	17	30	78	111	86	68	61	66
SR	26	41	25	15	33	60	115	80	80	259	301
RB	17	31	19	3	62	73	37	149	113	17	14
ZR	29	54	35	20	34	30	34	50	47	31	31
CU	6	30	14	6	4	0	3	4	4	7	5
BA	319	189	149	27	84	983	593	383	324	25	64
NB	3	8	4	7	4	11	10	8	9	5	9
NI	26	41	27	25	33	22	20	20	33	28	29
CR	18	13	14	13	11	26	9	8	24	15	16
AU	0	0	65	40	0		0	0	0	25	65

FORTUNE HARBOUR SUITE

SAMPLE	FH40	FH41A	FH41B	FH41C	FH43	FH44	FH45	FH48	FH53	FH54	FH55
SIO2	83.40	64.60	59.00	64.00	75.20	92.20	70.00	84.00	91.00	94.00	94.50
TIO2	0.0	0.31	0.36	0.30	0.19	0.0	0.40	0.0	0.0	0.0	0.0
AL2O3	3.70	12.10	12.00	14.00	4.48	0.11	8.68	2.24	2.17	2.17	1.07
FE2O3	2.65	4.46	10.60	6.46	12.04	5.32	6.11	6.37	1.43	0.87	1.06
FEO	0.70	0.43	0.50	0.36	0.80	0.59	2.85	0.41	0.24	0.0	0.16
MNO	0.59	0.08	0.13	0.12	0.43	0.04	0.61	0.08	0.48	0.37	0.30
MGO	0.40	2.18	2.54	2.18	1.51	0.0	1.51	0.45	0.47	0.15	0.14
CAO	3.10	1.87	2.41	1.52	1.17	0.10	2.22	1.87	1.36	0.10	0.70
NA2O	0.03	0.11	0.11	0.14	0.16	0.0	0.05	0.07	0.0	0.11	0.0
K2O	1.20	4.08	4.05	4.75	1.45	0.0	2.66	0.77	0.69	0.64	0.35
LOI	4.20	4.46	6.07	4.96	2.38	0.31	5.29	2.35	2.01	0.81	1.38
TOTAL	100.23	95.15	97.87	98.79	99.85	98.67	100.38	98.56	99.85	99.17	99.66
ZN	36	107	93	94	37	15	74	29	46	20	31
SR	71	49	55	51	24	16	40	29	84	20	69
MN	82	181	134	151	58	4	99	40	29	24	14
ZR	42	67	64	74	40	20	62	30	36	25	23
CU	10	0	0	0	10	5	15	11	8	5	8
BA	171	755	745	782	204	21	298	162	2751	882	2810
NB	9	14	12	15	0	3	15	4	0	1	0
NI	33	34	33	38	50	26	43	31	29	21	19
CR	18	31	23	28	15	13	26	15	14	10	9
AU	35	185	35	0	40	20	40	0	145	50	100

SAMPLE	FH56	FH57	FH58	FH60	FH61	FH62	FH63	FH64
SIO2	84.70	89.20	82.60	84.70	82.10	90.60	89.80	82.60
TIO2	0.0	0.0	0.14	0.21	0.0	0.21	0.0	0.0
AL2O3	2.94	5.80	8.31	4.33	7.70	2.38	4.50	8.23
FE2O3	2.98	2.71	0.71	3.33	0.36	2.44	1.40	0.94
FEO	0.0	0.64	0.88	0.41	1.97	0.07	1.03	0.68
MNO	0.87	0.24	0.48	1.14	0.68	1.44	0.43	0.71
MGO	0.34	0.65	1.72	0.86	1.97	0.60	0.74	0.60
CAO	2.26	0.76	0.45	0.15	0.53	0.45	0.39	0.26
NA2O	0.04	0.10	1.68	0.42	0.91	0.39	0.69	2.61
K2O	0.80	0.84	1.01	1.14	1.68	0.43	0.98	0.45
LOI	3.45	1.67	1.97	2.25	2.89	1.82	1.77	1.87
TOTAL	98.78	102.83	99.43	98.94	100.11	100.83	101.88	98.90
ZN	65	30	70	31	54	27	33	79
SR	124	31	72	25	60	38	36	116
MN	28	17	35	69	73	23	45	14
ZR	58	34	88	49	77	36	53	76
CU	4	5	15	9	5	15	4	11
BA	3291	195	242	276	427	134	298	119
NB	0	4	14	7	19	3	2	19
NI	49	27	31	38	24	30	28	23
CR	15	14	10	15	9	14	18	9
AU	65	75	80	100	80	20	65	35

GULL POND SUITE

SAMPLE	GP3	GP5	GP6	GP7	GP13A	GP13B	GP14	GP15	GP17	GP21	GP22
SIO2	92.50	94.00	90.90	93.70	72.00	58.00	54.50	73.90	86.10	84.30	88.00
TIO2	0.0	0.0	0.0	0.0	0.08	0.25	0.23	0.23	0.0	0.0	0.09
AL2O3	0.69	0.79	1.78	0.68	4.06	11.94	5.80	3.76	3.24	1.98	1.91
FE2O3	3.07	2.88	4.08	3.42	16.75	15.06	18.76	14.71	5.19	6.41	5.27
FEO	0.85	0.88	0.84	0.48	2.11	3.55	1.12	1.09	0.79	3.23	1.08
MNO	0.04	0.02	0.04	0.03	0.48	0.47	9.60	0.77	0.04	0.19	0.67
MGO	0.08	0.13	0.29	0.10	1.86	2.60	1.73	0.79	0.78	0.99	0.48
CAO	1.46	0.11	0.11	0.11	1.05	1.62	6.24	0.74	0.96	0.44	0.33
NA2O	0.04	0.0	0.11	0.0	0.62	2.40	0.01	0.70	0.24	0.05	0.35
K2O	0.14	0.20	0.35	0.20	0.68	3.73	0.04	1.17	0.78	0.49	0.22
LOI	1.08	0.42	0.58	0.39	1.19	1.42	0.11	0.66	0.87	0.84	0.50
TOTAL	99.55	99.01	98.78	99.11	100.48	98.04	97.96	98.47	98.99	98.77	98.90
ZR	41	14	23	20	30	76	37	34	38	27	31
SR	43	27	36	28	58	90	38	47	51	39	69
RB	18	21	28	21	24	66	15	30	36	24	19
ZN	35	12	17	14	65	86	58	43	29	27	22
CU	5	27	14	4	9	14	2	14	4	21	6
BA	162	121	247	90	213	772	22	586	407	350	671
NB	11	9	13	10	7	13	11	8	11	8	13
NI	21	17	19	18	43	58	66	46	20	27	25
CR	12	15	17	14	14	16	11	14	15	20	11
AU	100	100	67	50	80					80	150

SAMPLE	GP22A	GP23	GP25	GP27	GP30	GP31	GP33	GP34	GP35	GP36	GP40
SIO2	91.70	88.30	82.00	85.60	79.80	91.50	96.00	94.50	91.00	95.50	91.50
TIO2	0.07	0.10	0.13	0.0	0.0	0.09	0.0	0.0	0.0	0.0	0.0
AL2O3	1.27	1.76	3.85	2.40	0.0	1.31	0.0	0.0	1.50	0.33	1.26
FE2O3	4.64	4.60	5.40	6.15	15.70	5.64	1.73	2.78	5.50	0.38	4.52
FEO	1.28	0.84	1.30	1.02	3.17	0.54	1.03	0.99	1.34	0.68	1.08
MNO	0.06	0.15	1.98	0.64	0.16	0.49	0.10	0.25	0.32	0.08	0.11
MGO	0.12	0.86	1.97	0.52	0.25	0.20	0.0	0.0	0.22	0.0	0.58
CAO	0.42	0.44	2.02	0.46	0.63	0.22	0.26	0.19	0.16	0.05	0.03
NA2O	0.09	0.19	0.14	0.61	0.0	0.20	0.0	0.0	0.0	0.13	0.21
K2O	0.21	0.63	0.30	0.27	0.0	0.15	0.0	0.01	0.05	0.0	0.20
LOI	0.53	0.74	0.90	0.53	0.31	0.30	0.40	0.36	0.44	0.26	0.59
TOTAL	99.99	99.14	99.79	98.20	100.07	100.64	99.52	99.08	100.53	97.41	100.08
ZR	24	42	44	26	19	27	28	25	16	19	21
SR	41	51	106	48	31	38	63	50	27	30	28
RB	19	27	19	17	13	19	12	13	14	11	22
ZN	14	25	43	26	15	17	12	11	19	11	24
CU	7	9	5	10	3	4	6	4	5	4	4
BA	199	547	256	168	956	217	2611	2235	325	548	201
NB	11	10	13	14	9	12	6	8	10	7	11
NI	21	45	39	31	28	24	16	16	28	7	18
CR	17	15	13	16	12	20	19	14	17	15	14
AU		150		70	345	220	100	75		25	45

GULL POND SUITE

SAMPLE	GP42	GP43	GP44A	GP44R	GP50A	GP50R	GP51	GP52	GP53	GP54	GP55
SIO2	80.80	90.50	80.50	48.40	87.50	85.70	86.00	89.70	88.90	88.80	91.80
TIO2	0.0	0.0	0.17	0.06	0.06	0.15	3.52	0.07	0.09	0.07	0.0
AL2O3	1.04	0.88	4.36	0.0	3.77	4.95	0.70	2.91	3.23	3.12	2.56
FE2O3	4.89	5.15	7.58	32.40	3.67	4.40	3.27	2.01	2.42	2.64	2.20
FEO	0.46	0.59	0.88	0.11	0.33	0.07	0.35	0.61	0.28	0.16	0.31
MNO	0.06	0.06	2.42	0.14	0.35	0.74	0.92	0.43	0.81	0.87	0.79
MGO	0.42	0.15	0.96	0.0	0.70	1.03	0.85	0.56	0.81	0.68	0.49
CAO	0.14	0.03	1.90	0.05	0.30	0.30	0.69	0.39	0.63	0.68	0.19
NA2O	0.06	0.10	1.39	0.0	0.59	0.48	0.51	0.50	0.48	0.29	0.17
K2O	0.21	0.20	0.80	0.0	1.24	1.54	1.10	0.66	0.68	0.97	0.83
LOI	0.53	0.40	0.84	0.23	0.69	0.81	0.52	0.58	0.51	0.68	0.11
TOTAL	98.61	98.06	99.73	101.59	99.70	100.17	97.93	98.42	98.84	98.36	99.65
ZR	23	20	48	18	49	39	38	33	31	30	31
SR	34	26	91	25	65	62	59	51	81	33	38
RB	17	14	17	13	71	53	48	33	43	47	47
ZN	22	16	37	14	45	36	38	27	40	34	32
CU	4	5	23	0	7	8	4	5	5	5	4
BA	702	280	547	486	495	322	702	189	295	183	294
NB	6	7	12	6	12	10	14	128	8	10	11
NI	20	19	43	30	37	34	31	25	30	30	32
CR	13	13	15	13	18	24	18	11	18	18	22
AU	65	100			45		65	120	50	35	75

SAMPLE	GP58	GP59	GP64	GP65	GP65A	GP66	GP67	GP70	GP75	GP76	GP77
SIO2	87.60	88.80	88.40	90.60	92.00	88.50	85.10	86.90	84.10	86.60	88.70
TIO2	0.89	0.0	0.10	0.0	0.13	0.0	0.16	0.13	0.19	0.13	0.13
AL2O3	3.58	7.70	3.48	2.46	1.40	3.02	3.91	4.84	5.54	2.99	3.81
Fe2O3	4.45	1.70	2.63	2.66	1.39	2.98	4.30	3.71	3.98	3.93	2.81
FEO	0.22	1.06	0.33	0.83	0.48	0.66	0.08	0.68	1.45	0.33	0.71
MNO	0.02	1.07	1.07	0.13	0.76	1.35	1.41	0.10	0.11	1.38	0.45
MGO	0.12	0.79	0.91	0.56	0.17	0.45	0.45	0.75	0.79	0.62	0.49
CAO	0.46	1.33	0.47	0.77	0.83	0.70	0.33	0.26	0.34	0.33	0.19
NA2O	0.48	0.40	0.04	0.30	0.06	0.52	0.56	0.20	0.20	0.50	0.39
K2O	0.87	0.56	0.57	0.31	0.26	0.47	1.49	2.07	2.51	0.76	1.11
LOI	0.78	1.17	1.01	0.58	0.54	0.28	0.46	0.76	0.82	0.64	0.56
TOTAL	100.19	99.58	98.96	99.20	98.02	98.93	98.25	100.40	100.03	98.03	99.25
ZR	42	38	29	29	29	36	41	41	37	36	33
SR	58	91	52	61	87	85	46	49	45	60	41
RB	49	32	41	22	19	21	60	82	75	38	62
ZN	34	36	34	34	19	29	27	43	45	31	37
CU	8	12	72	4	7	4	24	3	6	7	6
BA	123	158	161	223	196	207	299	390	720	296	295
NB	14	12	50	13	11	10	6	8	10	9	10
NI	30	28	35	19	22	30	38	26	22	32	30
CR	20	13	15	12	12	18	17	19	17	15	18
AU	25	15	35	40	40	10	60	35		85	85

GULL POND SUITE

SAMPLE	GP79	GP80	GP82	GP85	GP86	GP87	GP89	GP92	GP93	GP95	GP96
SIO2	89.70	91.60	89.20	91.60	87.80	88.60	91.60	82.50	86.20	77.40	75.40
TIO2	0.0	0.0	0.0	0.0	0.13	0.0	0.0	0.20	0.06	0.09	0.12
AL2O3	2.80	2.33	2.64	1.97	3.22	4.80	1.40	5.40	1.74	4.32	2.96
FE2O3	4.89	1.42	2.30	2.49	3.14	3.02	4.21	22.33	10.10	7.80	9.59
FEO	0.78	0.58	0.72	0.15	0.18	0.95	0.63	0.96	0.43	0.09	0.10
MNO	0.09	0.75	1.27	1.04	1.61	0.56	0.07	1.47	0.24	3.47	4.45
MGO	0.59	0.91	0.46	0.26	0.52	0.71	0.09	1.37	0.09	1.37	0.44
CAO	0.19	0.38	0.60	0.90	0.33	0.70	0.41	1.17	0.41	2.18	2.98
NA2O	0.13	0.24	0.39	0.20	0.56	0.60	0.18	0.30	0.0	0.68	0.18
K2O	0.80	0.72	0.71	0.25	0.98	1.49	0.16	2.11	0.34	0.03	0.25
LOI	0.41	0.55	0.99	0.91	0.52	0.91	0.27	0.43	0.40	0.54	0.40
TOTAL	97.46	98.46	98.68	99.27	98.99	100.34	99.00	98.24	99.51	97.97	97.25
ZR	31	26	33	33	34	40	25	42	25	47	32
SR	85	37	47	102	46	63	45	48	58	139	113
NB	46	29	36	20	49	71	21	39	19	33	18
ZN	32	30	28	18	27	40	14	59	15	43	33
CU	10	13	3	24	95	17	6	0	4	41	23
BA	136	135	73	112	268	476	338	1394	171	55	82
NB	14	12	12	8	12	13	10	6	11	12	11
DI	41	25	25	25	42	35	18	68	37	45	48
CR	19	19	15	17	16	20	16	18	47	32	12
AU	50	50	60	60	60	100	25	45	100	70	0

SAMPLE	GP102	GP103	GP108	GP115	GP119	GP122	GP128	GP131	GP135	GP136	GP137
SIO2	91.10	88.30	82.10	81.00	92.70	88.30	84.80	82.90	80.30	85.00	76.00
TIO2	0.0	0.14	0.0	0.0	0.0	0.12	0.0	0.0	0.0	0.0	0.0
AL2O3	1.98	5.01	8.78	10.64	1.83	2.84	0.43	0.61	0.98	2.45	0.09
FE2O3	1.45	3.51	3.85	0.0	1.05	3.07	10.68	12.60	15.63	9.88	18.91
FEO	0.13	0.57	0.05	0.60	0.71	0.98	0.79	0.17	0.25	0.61	1.81
MNO	0.35	0.11	0.48	0.01	0.07	0.05	0.07	0.28	0.18	0.41	0.70
MGO	0.32	0.72	1.16	0.55	0.49	1.10	0.85	0.87	0.23	0.72	0.0
CAO	0.63	0.45	0.30	0.41	0.0	0.19	0.71	0.34	0.19	0.36	0.0
NA2O	0.38	0.60	0.68	4.38	0.26	0.39	0.01	0.22	0.04	0.01	0.0
K2O	0.42	0.96	1.75	0.45	0.26	0.46	0.02	0.19	0.23	0.16	0.0
LOI	1.16	1.11	1.15	0.70	0.28	1.68	1.03	0.26	0.39	0.67	0.44
TOTAL	97.02	100.14	98.10	98.74	97.65	98.98	98.59	98.24	98.47	100.27	97.45
CR	27	42	58	75	24	29	19	36	18	25	21
SR	37	45	56	51	29	39	29	54	27	26	25
NB	28	48	81	13	20	30	14	15	15	15	8
ZN	41	38	71	48	27	25	16	31	19	20	12
CU	5	5	4	19	7	37	3	4	2	7	0
BA	175	394	1286	42	167	164	12	2367	406	124	584
NB	13	14	12	19	15	11	11	6	10	11	10
NI	16	31	36	8	14	24	27	29	28	28	27
CR	41	20	27	16	22	16	12	11	12	14	10
AU	60	75	35	38	95	65	110	40	0	95	110

GULL POND SUITE

SAMPLE	GP136	GP139	GP140	GP142	GP145	GP146	GP148	GP149	GP150	GP153A	GP153B
SIO2	90.60	71.30	84.10	86.30	70.10	90.40	92.20	72.00	92.10	62.10	57.60
TIO2	0.0	0.0	0.0	0.0	0.0	0.0	0.0	0.13	0.0	0.20	0.13
AL2O3	0.0	0.24	0.0	0.55	4.53	0.0	0.51	4.20	1.00	5.60	5.71
FE2O3	6.78	25.96	10.88	8.56	15.43	7.82	1.66	12.75	4.05	18.64	19.80
FEO	0.26	0.17	0.0	0.49	1.19	0.37	1.46	1.82	0.64	0.29	0.0
MNO	0.09	0.19	1.52	0.09	1.57	0.02	0.19	2.84	0.03	0.00	0.60
MGO	0.0	0.0	0.0	0.0	1.78	0.0	0.34	1.39	0.23	0.87	1.18
CAO	0.0	0.15	0.0	0.38	0.77	0.38	0.60	0.97	0.38	2.09	2.34
NA2O	0.0	0.17	1.31	0.0	0.97	0.0	0.0	0.80	0.06	2.52	2.10
K2O	0.0	0.0	0.0	0.23	2.03	0.0	0.08	0.26	0.12	0.17	0.25
LOI	0.0	0.30	0.42	0.24	1.36	0.40	1.17	0.81	0.43	0.19	0.07
TOTAL	97.95	98.43	98.23	96.82	99.84	99.39	98.21	97.97	99.04	101.82	97.78
ZR	17	24	33	18	35	17	22	41	17	39	41
SR	29	45	59	29	39	25	39	53	35	60	69
NB	14	13	14	19	20	8	17	14	16	12	13
ZN	12	15	15	13	57	12	15	57	15	52	66
CU	3	0	5	3	0	3	6	4	9	4	0
BA	565	1494	2435	278	130	10	73	112	242	261	214
NB	8	8	8	7	11	11	13	10	8	13	10
NI	26	30	26	23	59	20	14	59	20	65	67
CR	12	10	15	13	18	12	13	19	20	11	17
AU	100	30	15	125	20	55	40	50	45	75	

SAMPLE	GP155	GP159	GP161
SIO2	83.20	92.80	83.80
TIO2	0.0	0.0	0.0
AL2O3	0.82	0.55	3.21
FE2O3	10.47	4.44	7.20
FEO	1.30	0.39	1.47
MNO	0.02	0.04	0.08
MGO	0.19	0.0	1.15
CAO	0.19	0.0	0.41
NA2O	0.04	0.0	0.11
K2O	0.15	0.13	1.17
LOI	0.36	0.33	0.96
TOTAL	96.74	99.08	98.86
ZR	23	24	41
SR	33	29	74
NB	18	16	35
ZN	14	14	37
CU	5	1	9
BA	114	121	712
NB	11	11	9
NI	28	19	34
CR	20	12	24
AU	90	75	40

APPENDIX B

Sample Collection and Preparation

Hand specimens weighing 1 - 1½ pounds were collected in the field using a four lb. sledge hammer. In the Roberts Arm and Fortune Harbour areas, sampling was carried out along traverses of the best exposed stratigraphic sections through the volcanic sequence, i.e. in road cuts and along coastal sections, and representative samples were collected wherever chert and ferruginous sediments were exposed. In the Gull Pond area, the emphasis was on sampling laterally continuous horizons along strike and these horizons were commonly walked out and sampled at regular intervals, depending on exposure.

At all stations, an attempt was made to obtain a sample representative of the outcrop. Where diverse physical characteristics of the sediments at a single station made this impractical, multiple samples were taken representative of all types present. Where individual deposits were more than 2 meters thick, systematic sampling across the section was carried out, the sample interval depending on the thickness and exposure.

247 samples were chosen for analysis. A number of samples were rejected because they were extensively veined by quartz, calcite, epidote, etc. or showed other evidence of extensive alteration (e.g. shearing with secondary minerals developed along shear planes). Those samples to be analyzed were washed and broken into chips, the largest dimension of which was less than 0.75 cm. Chips containing an outside

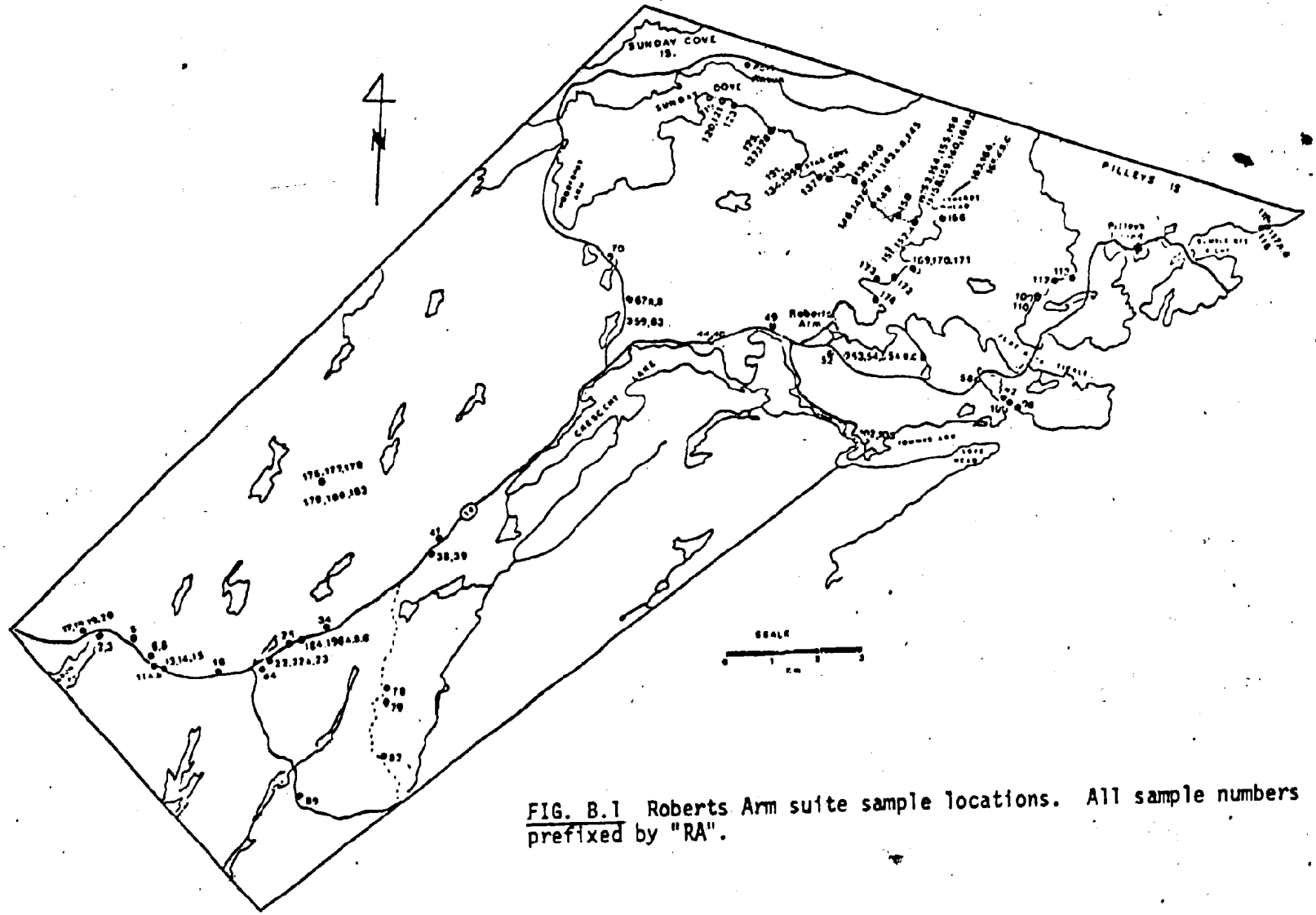

FIG. B.1 Roberts Arm suite sample locations. All sample numbers prefixed by "RA".

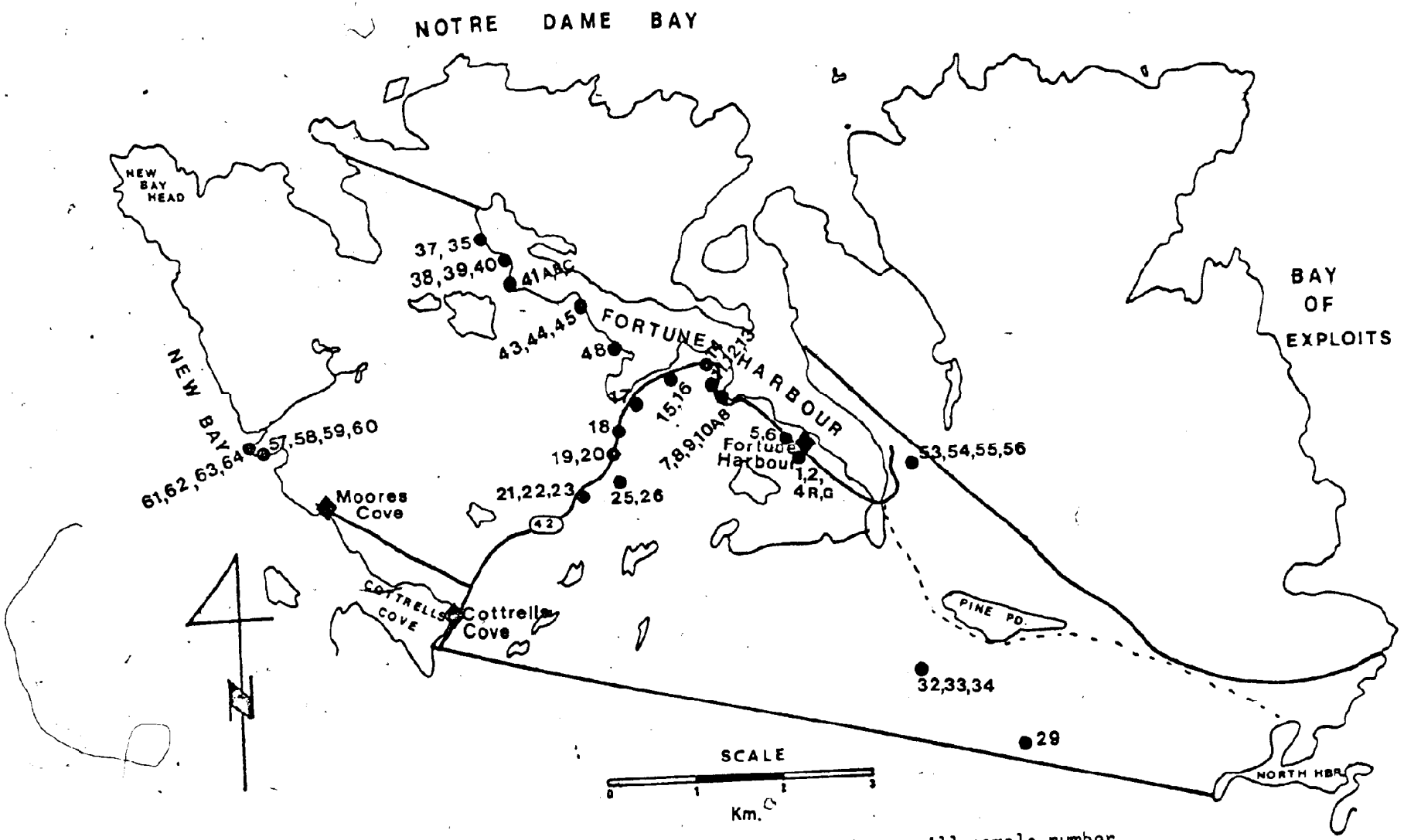

FIG. B.2 Fortune Harbour suite sample locations. All sample number prefixed by "FH".

FIG. B.3 Gull Pond suite sample locations.

All sample numbers
prefixed by "GP".

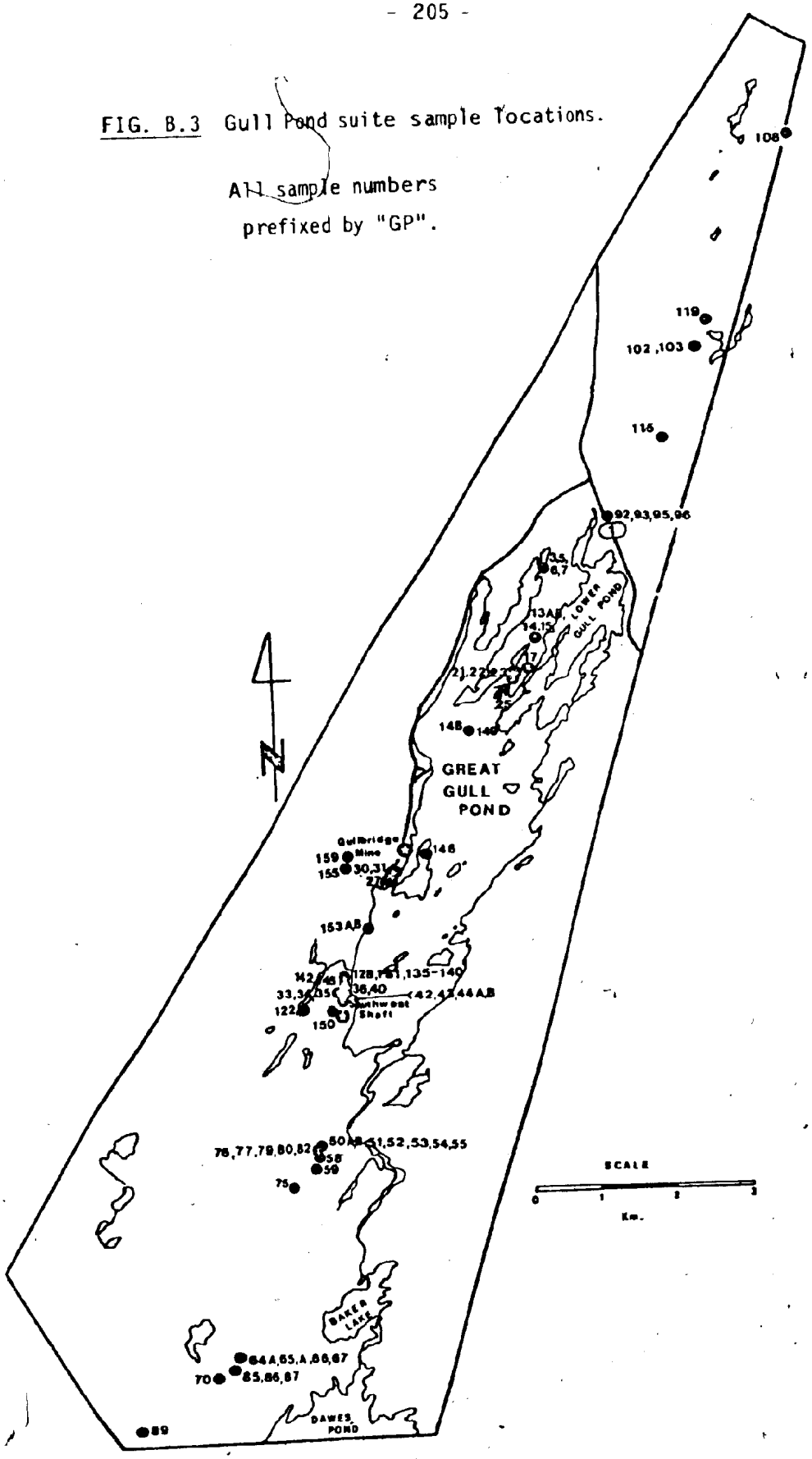

surface of the original specimen and those containing visible veinlets were discarded and the remainder stored in a clean plastic bag prior to crushing. A representative sampling of these chips was crushed in a siebtechnik tungsten-carbide swing mill for 2-3 minutes producing a rock powder of -200 mesh as determined by random sieving. The rock powder was put in 4 oz. bottles and heated overnight at 110° C.

Analytical Procedures

Major Elements

Major elements were determined on a Perkin-Elmer 303 atomic absorption spectrophotometer equipped with recorder readout. Rock powders were mixed to ensure homogeneity and exactly 0.2000 grams placed in a digestion bottle. 5 ml. HF was added and the samples were heated over a water bath. After subsequent cooling, 50 ml. of saturated boric acid solution was added and the solution again heated over a water bath until complete digestion was effected. The samples were then made up to 200 ml. with distilled water.

Standards were prepared in a manner similar to that described by Abbey (1968).

Ferrous iron was determined by titration according to the method of Wilson (1955) as described in Maxwell (1968). 5 ml. of ammonium vanadate solution was added to approximately 1.2 grams of sample and the resulting solution was mixed in an automatic shaker overnight. 10 ml. of sulphuric-phosphatic mixed acid was then added to the sample and the resulting solution mixed with 200 ml. of saturated

boric acid solution. 10 ml. of ferrous ammonium sulfate solution and 1 ml. of barium diphenylamine sulphonate indicater were added and the sample titrated with standard potassium dichromate solution to a grey end point.

Loss on ignition was determined by weighing a known amount of sample into a porcelain crucible and heating at 1050°C for two hours followed by cooling in a dessicator and subsequent reweighing to determine the weight percent loss of volatiles.

Analytical accuracy and precision of major element analyses are presented in Tables B.1 and B.2.

Trace Elements

Nine trace elements were determined by X-ray fluorescence using a Phillips 1220-C spectrometer. Sample discs were prepared by mixing 1.5 g of rock powder with 2 - 3 drops of N-30-88 mowiol binding agent and pressing the resultant powder into a disc with boric acid backing at 15 T/in^2.

Precision and accuracy of trace element analyses are shown in Tables B.3 and B.4.

Statistical Procedures

Major and trace element analyses were punched on computer cards and the individual samples grouped into their respective geographic suites and lithologic subgroupings. Mean and standard deviation were calculated for all elements and all data subgroupings.

A standard statistical program was employed to plot variation diagrams and histograms for all major subgroupings and to calculate Pearson Correlation Coefficients for all elements in the geographic suites.

The Mann-Whitney U-test (Siegal, 1956) determines the probability that two sets of data are drawn from the same population. It was employed in the present program in a manner similar to that previously used by Davenport and Nichol (1972) and Thurlow (1974) to test the statistical significance of mean element concentrations differences between pairs of subgroups. This test is non-parametric and was used because of the small numbers of samples in some subgroups and because of the generally non-Gaussian distribution of element concentrations within the subgroups.

Discriminant analysis was employed to test the chemical differences between various pairs of subgroupings by deriving a function which would classify these subgroups by considering simultaneously a number of variables. A computer program was used which computed the discriminant index between the pairs of sample subgroups, the mean discriminant score for the respective subgroups, individual scores for each sample and the relative contribution made by each variable in deriving the function.

TABLE B.1

PRECISION OF MAJOR ELEMENT ANALYSES
(from replicate analyses)

	Number of Determinations	Mean	Standard Deviation
Fe_2O_3	7	6.38	.16
TiO_2	7	.13	.01
SiO_2	7	79.7	1.16
CaO	7	4.17	.07
K_2O	7	.35	.01
MgO	7	.97	.02
Al_2O_3	7	5.10	.11
FeO	7	.40	.01
Na_2O	7	.33	.02
MnO	7	.53	.02
L.O.I.	7	1.68	.03

TABLE B.2

ACCURACY OF MAJOR ELEMENT ANALYSES

Wt. %	A*	Mean	Standard Deviation	Number of Determinations
SiO_2	54.36	55.38	0.37	4
TiO_2	2.24	2.35	0.18	4
Al_2O_3	13.56	13.50	0.27	5
Fe_2O_3	13.40	13.00	0.28	5
CaO	6.94	6.63	0.07	4
MgO	3.46	3.57	0.06	5
Na_2O	3.26	3.23	0.05	5
K_2O	1.67	1.73	0.05	4
MnO	0.19	0.18	0.01	5

* Proposed values after Abbey (1968).

TABLE B.3

PRECISION OF TRACE ELEMENT ANALYSES

Sample		XC-1	XC-2	XC-3	XC-4	G-2 (st-2)
No. of Pellets		46	18	16	15	1 (10 runs)
Element:						
Zr	Mean (ppm)	129	90	195	109	326
	St. Dev.	22	8	23	11	7
Sr	Mean (ppm)	98	85	51	102	494
	St. Dev.	8	5	14	9	4
Rb	Mean (ppm)	51	123	146	132	171
	St. Dev.	7	8	10	12	2
Zn	Mean (ppm)	27	88	24	29	98
	St. Dev.	1	2	1	1	1
Cu	Mean (ppm)	15	14	14	11	18
	St. Dev.	2	3	3.	2	2
Ba	Mean (ppm)	1042	1194	966	973	1797
	St. Dev.	80	67	57	64	38
Nb	Mean (ppm)	15	15	19	21	15
	St. Dev.	2	4	3	3	3
Ni	Mean (ppm)	12	69	23	25	21
	St. Dev.	3	1	2	2	1
Cr	Mean (ppm)	12	53	N/A	N/A	7
	St. Dev.	4	4			1

TABLE B.4

ACCURACY OF TRACE ELEMENT ANALYSES

FROM CALIBRATION CURVES DATA

Element	Standard Deviation (s.d.)	Range	Mean	Number of Standards: No. of Pellets	Number of Standards: Stds.
Zr	20	s.d. to 700	200	18	12
Sr	18	s.d. - 1400	250	24	18
Rb	8	s.d. - 400	130	21	15
Zn	10	s.d. - 350	100	24	16
Cu	3	s.d. - 110	35	27	16
Ba	46	s.d. - 1900	700	20	14
Nb	4	s.d. - 300	32	19	13
Ni	21	s.d. - 2400	410	24	16
Cr 400 ppm	7	s.d. - 400	50	18	12
Cr 400 ppm	140	400 - 4000	2800	5	4

N.B.

Standard deviation could be considered an estimate of standard error of y given x.

Number of pellets represents the number of individual points used on the calibration curve which may include a duplicate of some standards especially U.S.G.S. standards, while the "standards" column represents the number of different standards used from various agencies.

APPENDIX C

CORRELATION MATRICES

(bracketed numbers indicate significance of correlation)

ROBERTS ARM SUITE

	Fe_2O_3	TiO_2	SiO_2	CaO	K_2O	MgO	Al_2O_3	FeO	Na_2O	MnO	Zr	Sr	Rb	Zn	Cu	Ba	Nb	Ni	Cr
TiO_2	-0.073 (0.319)																		
SiO_2	-0.703 (0.001)	-0.452 (0.031)																	
CaO	0.018 (0.426)	0.204 (0.095)	-0.524 (0.001)																
K_2O	-0.197 (0.032)	-0.131 (0.213)	-0.057 (0.293)	-0.199 (0.027)															
MgO	0.064 (0.257)	0.228 (0.048)	-0.494 (0.001)	0.163 (0.045)	0.100 (0.171)														
Al_2O_3	-0.218 (0.012)	0.524 (0.001)	-0.406 (0.001)	0.453 (0.001)	0.535 (0.001)	0.287 (0.001)													
FeO	0.065 (0.248)	0.232 (0.065)	-0.382 (0.001)	-0.022 (0.409)	0.010 (0.460)	0.386 (0.001)	0.263 (0.003)												
Na_2O	-0.290 (0.054)	0.276 (0.044)	-0.041 (0.350)	-0.217 (0.021)	0.289 (0.006)	-0.056 (0.297)	0.567 (0.001)	0.007 (0.476)											
MnO	0.096 (0.152)	0.081 (0.333)	-0.183 (0.028)	-0.031 (0.375)	-0.038 (0.362)	0.189 (0.027)	0.107 (0.140)	0.310 (0.001)	0.810 (0.662)										
Zr	-0.275 (0.002)	0.529 (0.001)	-0.169 (0.036)	0.298 (0.001)	0.310 (0.001)	-0.029 (0.417)	0.309 (0.001)	0.024 (0.460)	0.514 (0.001)	0.026 (0.395)									
Sr	-0.090 (0.174)	0.384 (0.005)	-0.107 (0.017)	0.559 (0.001)	-0.040 (0.350)	-0.086 (0.283)	0.433 (0.001)	-0.089 (0.234)	0.060 (0.367)	-0.024 (0.400)	0.780 (0.001)								
Rb	-0.232 (0.068)	0.023 (0.443)	-0.017 (0.431)	-0.240 (0.006)	0.024 (0.001)	0.123 (0.104)	0.493 (0.001)	0.036 (0.361)	0.242 (0.012)	-0.010 (0.458)	0.456 (0.001)	0.080 (0.266)							
Zn	-0.113 (0.113)	0.160 (0.149)	-0.269 (0.002)	-0.049 (0.304)	0.493 (0.001)	0.579 (0.001)	0.511 (0.001)	0.523 (0.001)	0.321 (0.001)	0.360 (0.001)	0.267 (0.002)	-0.105 (0.132)	0.474 (0.001)						
Cu	0.327 (0.001)	-0.009 (0.479)	-0.311 (0.001)	0.052 (0.267)	-0.075 (0.258)	0.069 (0.248)	0.020 (0.422)	0.128 (0.099)	-0.027 (0.404)	-0.056 (0.291)	-0.030 (0.383)	-0.019 (0.426)	-0.123 (0.112)	-0.084 (0.196)					
Ba	-0.216 (0.012)	-0.096 (0.271)	0.041 (0.334)	-0.030 (0.376)	0.653 (0.001)	-0.064 (0.255)	0.393 (0.001)	-0.040 (0.336)	0.383 (0.001)	-0.066 (0.260)	0.433 (0.001)	0.279 (0.001)	0.830 (0.001)	0.196 (0.019)	0.166 (0.049)				
Nb	-0.204 (0.049)	-0.007 (0.462)	0.050 (0.392)	-0.238 (0.007)	0.362 (0.001)	-0.009 (0.464)	0.297 (0.001)	0.020 (0.428)	0.394 (0.001)	0.119 (0.114)	0.244 (0.006)	-0.108 (0.152)	0.446 (0.001)	0.290 (0.001)	0.044 (0.334)	0.206 (0.017)			
Ni	0.192 (0.022)	0.388 (0.005)	-0.353 (0.001)	0.246 (0.004)	-0.173 (0.046)	0.419 (0.001)	0.047 (0.313)	0.245 (0.004)	-0.192 (0.036)	0.129 (0.091)	-0.115 (0.111)	-0.023 (0.465)	-0.159 (0.048)	0.113 (0.114)	0.134 (0.089)	-0.166 (0.040)	-0.103 (0.144)		
Cr	-0.081 (0.159)	0.328 (0.011)	-0.318 (0.001)	0.328 (0.001)	-0.080 (0.220)	0.611 (0.001)	0.120 (0.106)	0.335 (0.001)	-0.085 (0.212)	0.024 (0.481)	-0.086 (0.476)	0.016 (0.423)	-0.050 (0.303)	0.236 (0.006)	0.075 (0.226)	-0.061 (0.262)	-0.102 (0.144)	0.292 (0.001)	
Au	0.022 (0.816)	-0.208 (0.177)	0.214 (0.022)	-0.168 (0.074)	-0.103 (0.321)	-0.172 (0.073)	-0.331 (0.001	-0.127 (0.148)	-0.256 (0.016)	-0.060 (0.676)	-0.254 (0.006)	-0.140 (0.136)	-0.150 (0.117)	-0.276 (0.003)	-0.055 (0.582)	-0.145 (0.225)	-0.134 (0.268)	-0.003 (0.727)	-0.097 (0.335)

FORTUNE HARBOUR SUITE

	Fe_2O_3	TiO_2	SiO_2	CaO	K_2O	MgO
TiO_2	0.228 (0.173)					
SiO_2	-0.257 (0.083)	-0.592 (0.004)				
CaO	0.444 (0.031)	0.287 (0.124)	-0.654 (0.001)			
K_2O	0.163 (0.128)	0.329 (0.586)	-0.464 (0.001)	-0.020 (0.447)		
MgO	0.067 (0.320)	0.287 (0.117)	-0.602 (0.002)	0.085 (0.279)	0.496 (0.001)	
Al_2O_3	-0.054 (0.351)	0.391 (0.049)	-0.681 (0.001)	0.112 (0.217)	0.844 (0.001)	0.670 (0.001)
FeO	-0.227 (0.440)	0.040 (0.002)	-0.229 (0.057)	0.025 (0.635)	0.037 (0.404)	0.478 (0.001)
Na_2O	-0.433 (0.001)	-0.031 (0.447)	-0.203 (0.268)	-0.178 (0.135)	0.004 (0.489)	0.003 (0.492)
MnO	-0.058 (0.246)	0.144 (0.278)	-0.665 (0.001)	0.145 (0.156)	-0.134 (0.174)	-0.128 (0.182)
Zr	-0.189 (0.090)	0.193 (0.048)	-0.834 (0.001)	-0.158 (0.133)	0.235 (0.006)	0.208 (0.009)
Sr	-0.187 (0.092)	-0.045 (0.426)	-0.442 (0.001)	0.295 (0.018)	-0.126 (0.189)	-0.165 (0.153)
Nb	0.137 (0.169)	0.213 (0.139)	-0.403 (0.001)	-0.011 (0.481)	0.951 (0.001)	0.531 (0.001)
Zn	-0.218 (0.060)	0.148 (0.275)	-0.290 (0.017)	-0.056 (0.342)	0.430 (0.001)	0.573 (0.001)
Cu	0.122 (0.254)	-0.189 (0.253)	0.113 (0.219)	-0.110 (0.331)	-0.147 (0.163)	-0.024 (0.436)
Ba	-0.186 (0.076)	0.216 (0.193)	0.351 (0.361)	-0.039 (0.394)	0.099 (0.247)	-0.108 (0.225)
Rb	-0.163 (0.102)	-0.023 (0.445)	-0.767 (0.001)	0.107 (0.238)	0.183 (0.109)	0.163 (0.134)
Ni	0.648 (0.001)	0.276 (0.127)	-0.304 (0.013)	0.097 (0.001)	0.065 (0.324)	0.228 (0.052)
Cr	0.191 (0.055)	0.451 (0.001)	-0.109 (0.238)	0.035 (0.402)	0.303 (0.015)	0.246 (0.049)
Au	-0.026 (0.857)	-0.335 (0.023)	0.062 (0.662)	0.184 (0.196)	-0.112 (0.435)	0.216 (0.124)

	FeO	Na_2O_3	FeO	Na_2O	Zr	Sr	Nb	Zn	Cu	Ba	Rb	Ni	Cr
FeO	0.284 (0.024)												
Na_2O_3	0.306 (0.019)	0.109 (0.247)											
FeO	-0.168 (0.115)	0.091 (0.266)	0.273 (0.033)										
Na_2O	0.412 (0.001)	0.231 (0.055)	-0.147 (0.164)	0.788 (0.011)									
Zr	0.048 (0.365)	0.022 (0.440)	0.379 (0.006)	0.588 (0.001)	0.680 (0.011)								
Sr	0.727 (0.001)	0.062 (0.337)	-0.162 (0.142)	-0.161 (0.125)	0.268 (0.026)	-0.145 (0.150)							
Nb	0.573 (0.001)	0.382 (0.003)	0.048 (0.376)	-0.033 (0.407)	0.267 (0.027)	0.009 (0.473)	0.477 (0.001)						
Zn	-0.136 (0.176)	0.219 (0.074)	-0.033 (0.418)	0.022 (0.441)	-0.059 (0.344)	-0.070 (0.317)	-0.120 (0.206)	-0.186 (0.206)					
Cu	0.012 (0.466)	-0.117 (0.213)	0.067 (0.358)	0.075 (0.299)	0.202 (0.076)	0.121 (0.196)	0.078 (0.292)	0.057 (0.344)	-0.015 (0.469)				
Ba	0.951 (0.001)	0.233 (0.060)	4.450 (0.001)	0.806 (0.011)	0.907 (0.001)	0.641 (0.001)	0.137 (0.174)	0.333 (0.010)	0.027 (0.430)	0.430 (0.011)			
Rb	0.157 (0.130)	0.067 (0.348)	-0.347 (0.009)	-0.093 (0.256)	-0.121 (0.196)	-0.148 (0.168)	0.128 (0.181)	0.097 (0.244)	-0.093 (0.263)	-0.144 (0.154)	-0.144 (0.217)		
Ni	0.250 (0.036)	0.294 (0.020)	-0.247 (0.044)	-0.173 (0.108)	-0.007 (0.481)	-0.138 (0.162)	0.340 (0.006)	0.017 (0.468)	0.306 (0.003)	-0.040 (0.390)	-0.048 (0.371)	0.183 (0.095)	
Cr	0.036 (0.797)	-0.094 (0.583)	-0.127 (0.399)	-0.151 (0.262)	-0.134 (0.337)	-0.116 (0.409)	-0.031 (0.826)	-0.011 (0.938)	-0.185 (0.208)	0.247 (0.078)	-0.074 (0.418)	0.248 (0.074)	-0.050 (0.722)
Au													

BULL POND SUITE

	Fe_2O_3	TiO_2	SiO_2	CaO	K_2O	MgO	Al_2O_3	FeO	Na_2O	MnO	Zr	Sr	Rb	Zn	Cu	Ba	Ni	Cr
TiO_2	-0.982 (0.282)																	
SiO_2	-0.830 (0.001)	0.835 (0.419)																
CaO	0.326 (0.002)	-0.006 (0.420)	-0.597 (0.001)															
K_2O	0.377 (0.256)	0.097 (0.288)	-0.327 (0.002)	0.026 (0.417)														
MgO	0.422 (0.001)	0.079 (0.433)	-0.695 (0.001)	0.376 (0.001)	0.522 (0.001)													
Al_2O_3	0.224 (0.026)	-0.249 (0.072)	-0.578 (0.001)	0.274 (0.009)	0.505 (0.001)	0.634 (0.001)												
FeO	0.205 (0.033)	-0.057 (0.371)	-0.302 (0.003)	0.065 (0.286)	0.263 (0.012)	0.382 (0.001)	0.225 (0.025)											
Na_2O	0.329 (0.003)	0.061 (0.463)	-0.423 (0.001)	0.081 (0.309)	0.154 (0.107)	0.315 (0.004)	0.743 (0.001)	0.743 (0.001)										
MnO	0.372 (0.001)	-0.020 (0.453)	-0.645 (0.001)	0.645 (0.001)	-0.104 (0.187)	0.360 (0.001)	0.346 (0.001)	-0.086 (0.217)	0.321 (0.003)									
Zr	0.056 (0.427)	0.067 (0.347)	-0.433 (0.001)	0.264 (0.069)	0.540 (0.001)	0.654 (0.001)	0.877 (0.001)	0.080 (0.238)	0.690 (0.001)	0.270 (0.006)								
Sr	-0.010 (0.359)	-0.003 (0.479)	-0.243 (0.013)	0.341 (0.001)	0.073 (0.267)	0.388 (0.001)	0.389 (0.001)	-0.065 (0.282)	0.252 (0.017)	0.377 (0.001)	0.567 (0.001)							
Rb	-0.322 (0.003)	0.184 (0.233)	0.026 (0.408)	-0.158 (0.080)	0.778 (0.001)	0.252 (0.015)	0.469 (0.001)	-0.058 (0.302)	-0.003 (0.490)	-0.143 (0.096)	0.492 (0.001)	0.101 (0.179						
Zn	0.243 (0.013)	0.054 (0.376)	-0.663 (0.001)	0.391 (0.001)	0.609 (0.001)	0.841 (0.001)	0.855 (0.001)	0.220 (0.024)	0.515 (0.001)	0.471 (0.001)	0.786 (0.001)	0.425 (0.001	0.487 (0.001)					
Cu	-0.141 (0.111)	-0.093 (0.304)	-0.009 (0.467)	-0.019 (0.435)	0.038 (0.376)	0.068 (0.235)	0.146 (0.111)	-0.110 (0.172)	0.085 (0.249)	0.094 (0.208)	0.126 (0.136)	0.208 (0.034	0.136 (0.118)	0.877 (0.255)				
Ba	0.175 (0.055)	-0.001 (0.497)	-0.030 (0.391)	-0.119 (0.146)	0.204 (0.039)	0.114 (0.167)	0.005 (0.483)	0.078 (0.244)	0.005 (0.483)	-0.139 (0.102)	0.567 (0.001)	0.038 (0.366)	-0.038 (0.364)	-0.080 (0.233)	-0.133 (0.123)			
Rb	-0.151 (0.036)	-0.028 (0.436)	0.072 (0.257)	-0.032 (0.256)	-0.013 (0.455)	-0.001 (0.496)	0.070 (0.271)	-0.045 (0.344)	0.047 (0.350)	-0.009 (0.468)	0.074 (0.251)	0.029 (0.396)	0.075 (0.248)	0.038 (0.366)	0.129 (0.132)	-0.161 (0.084)		
Ni	0.555 (0.001)	-0.047 (0.391)	-0.822 (0.001)	-0.822 (0.001)	0.349 (0.001)	0.672 (0.001)	0.515 (0.001)	0.115 (0.162)	0.256 (0.016)	0.700 (0.001)	0.484 (0.001)	0.399 (0.001)	0.144 (0.094)	0.723 (0.001)	0.173 (0.065)	-0.047 (0.431)	-0.030 (0.382)	
Cr	-0.222 (0.021)	0.050 (0.459)	-0.125 (0.127)	-0.138 (0.110)	0.136 (0.122)	0.004 (0.486)	0.129 (0.130)	0.136 (0.112)	0.019 (0.439)	-0.081 (0.230)	-0.104 (0.037)	0.173 (0.057)	0.256 (0.007)	0.129 (0.120)	0.042 (0.358)	-0.091 (0.204)	-0.096 (0.219)	0.061 (0.289)
Au	-0.074 (0.506)	0.017 (0.920)	0.235 (0.031)	-0.256 (0.022)	-0.265 (0.021)	-0.273 (0.018)	-0.309 (0.006)	0.176 (0.111)	-0.125 (0.299)	-0.285 (0.060)	-0.256 (0.018)	-0.222 (0.041)	-0.127 (0.267)	-0.308 (0.004)	-0.071 (0.534)	0.020 (0.855)	0.098 (0.366)	-0.174 (0.110)	0.031 (0.779)

APPENDIX D

ELEMENT HISTOGRAMS

(star followed by a number indicates the number of samples
which fall beyond the range of the histogram)

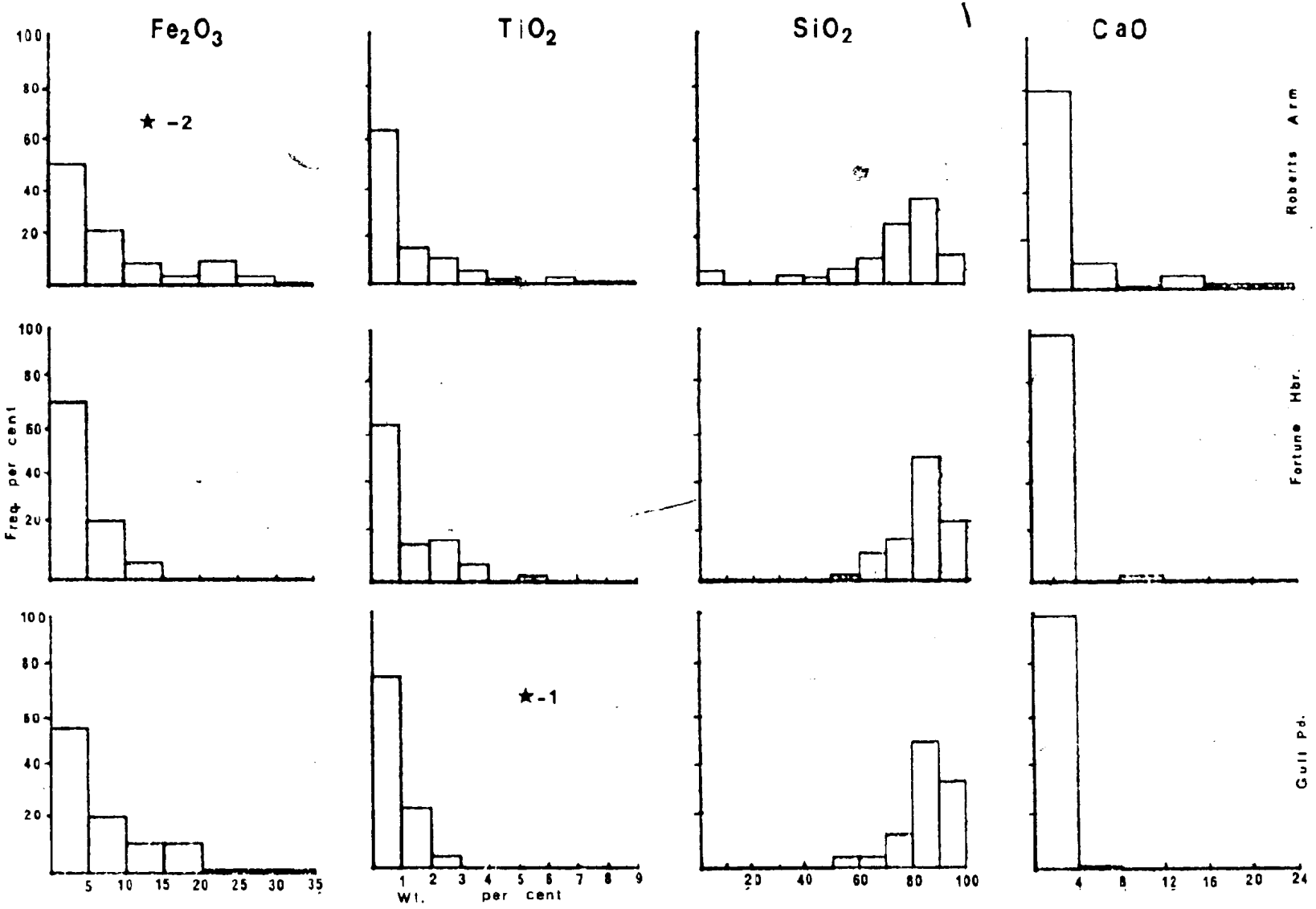
Fe_2O_3
TiO_2
SiO_2
CaO
★ -2
★ -1
Roberts Arm
Fortune Hbr.
Gull Pd.
Freq. per cent
Wt. per cent
100
80
60
40
20
5 10 15 20 25 30 35
1 2 3 4 5 6 7 8 9
20 40 60 80 100
4 8 12 16 20 24

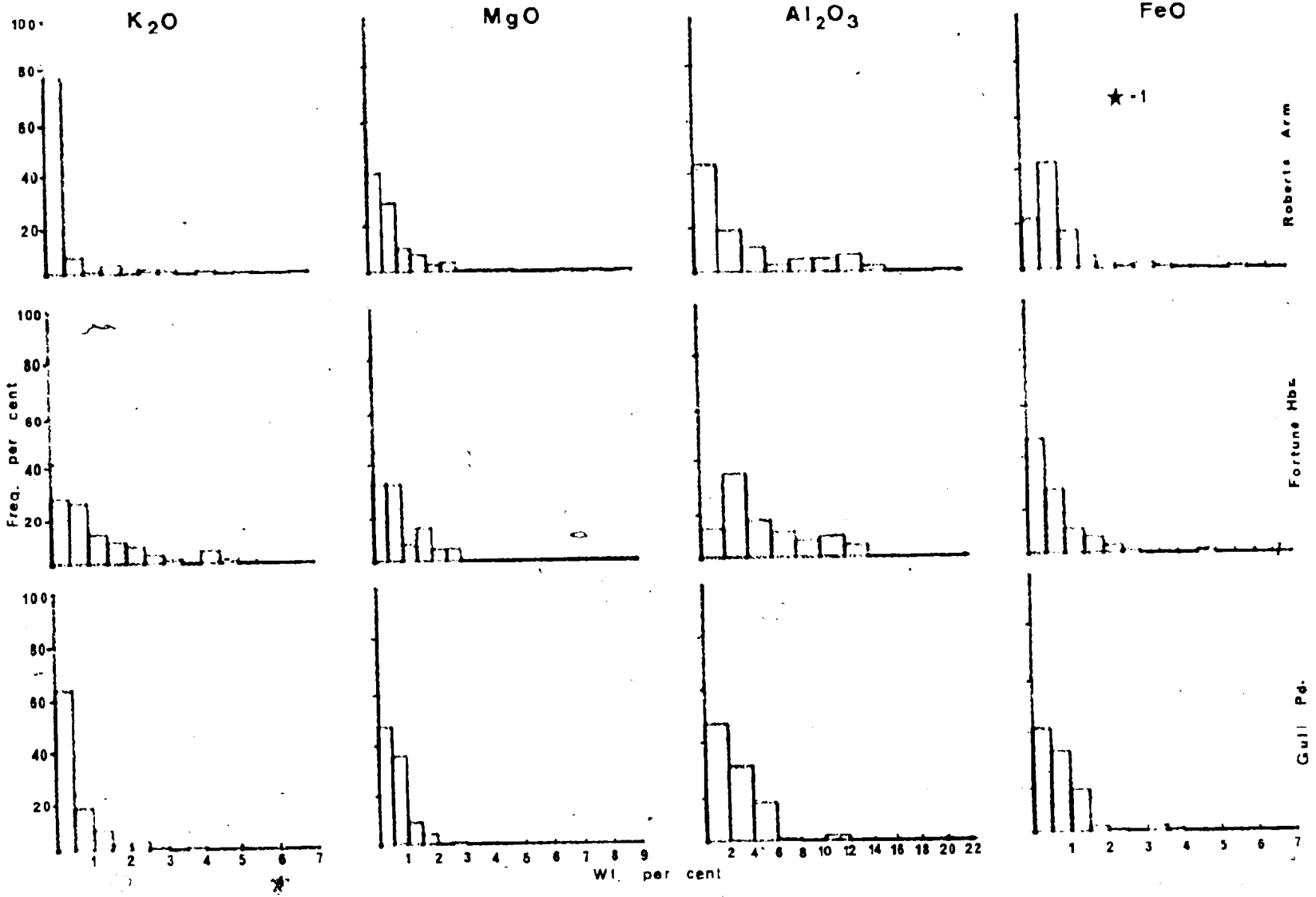
K_2O
MgO
Al_2O_3
FeO
★-1
Roberts Arm
Fortune Hbr.
Gull Pd.
Freq. per cent
Wt. per cent

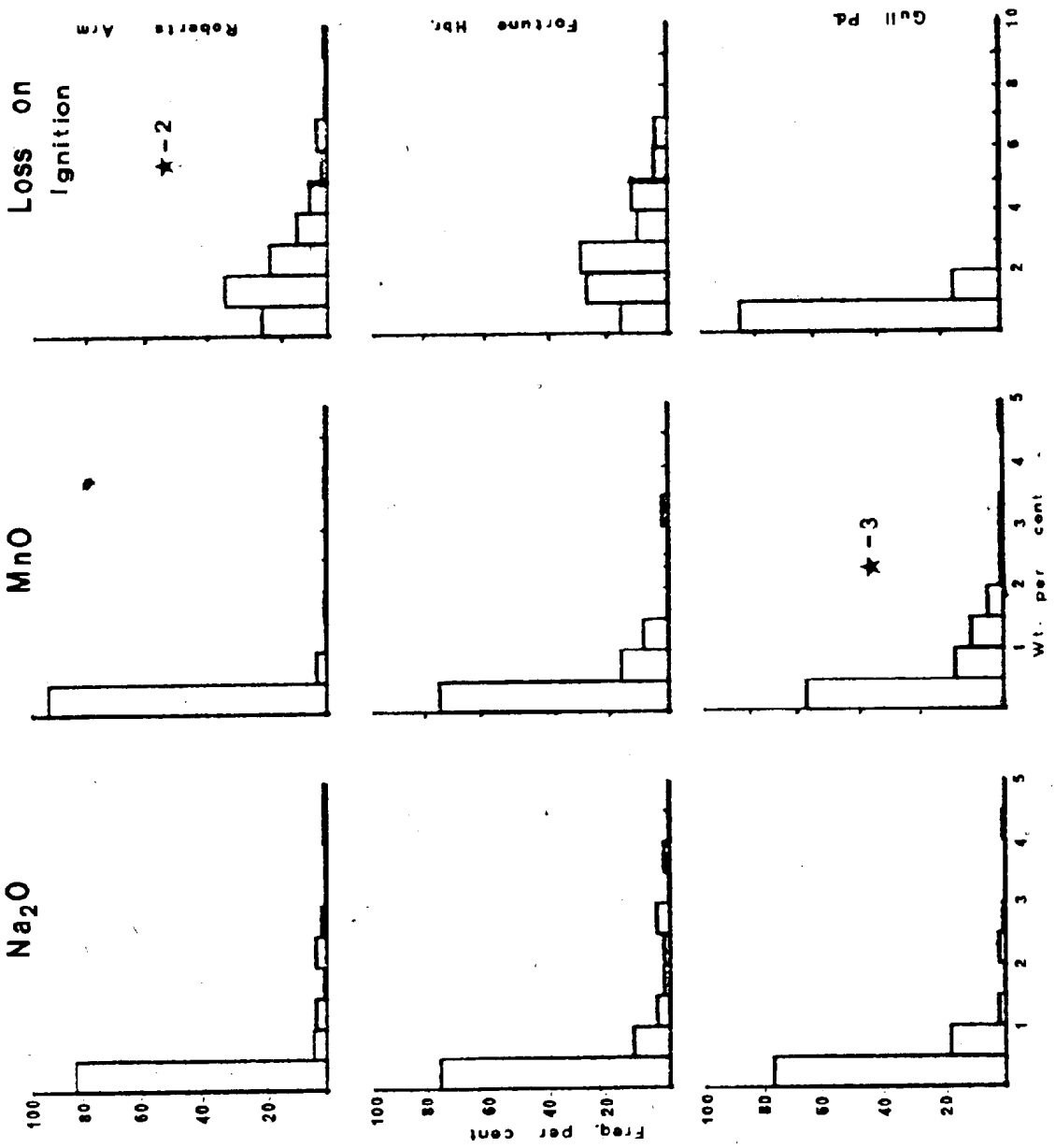
Loss on Ignition
MnO
Na_2O
Roberts Arm
Fortune Hbr.
Gull Pd
★-2
★-3
Freq. per cent
Wt. per cent

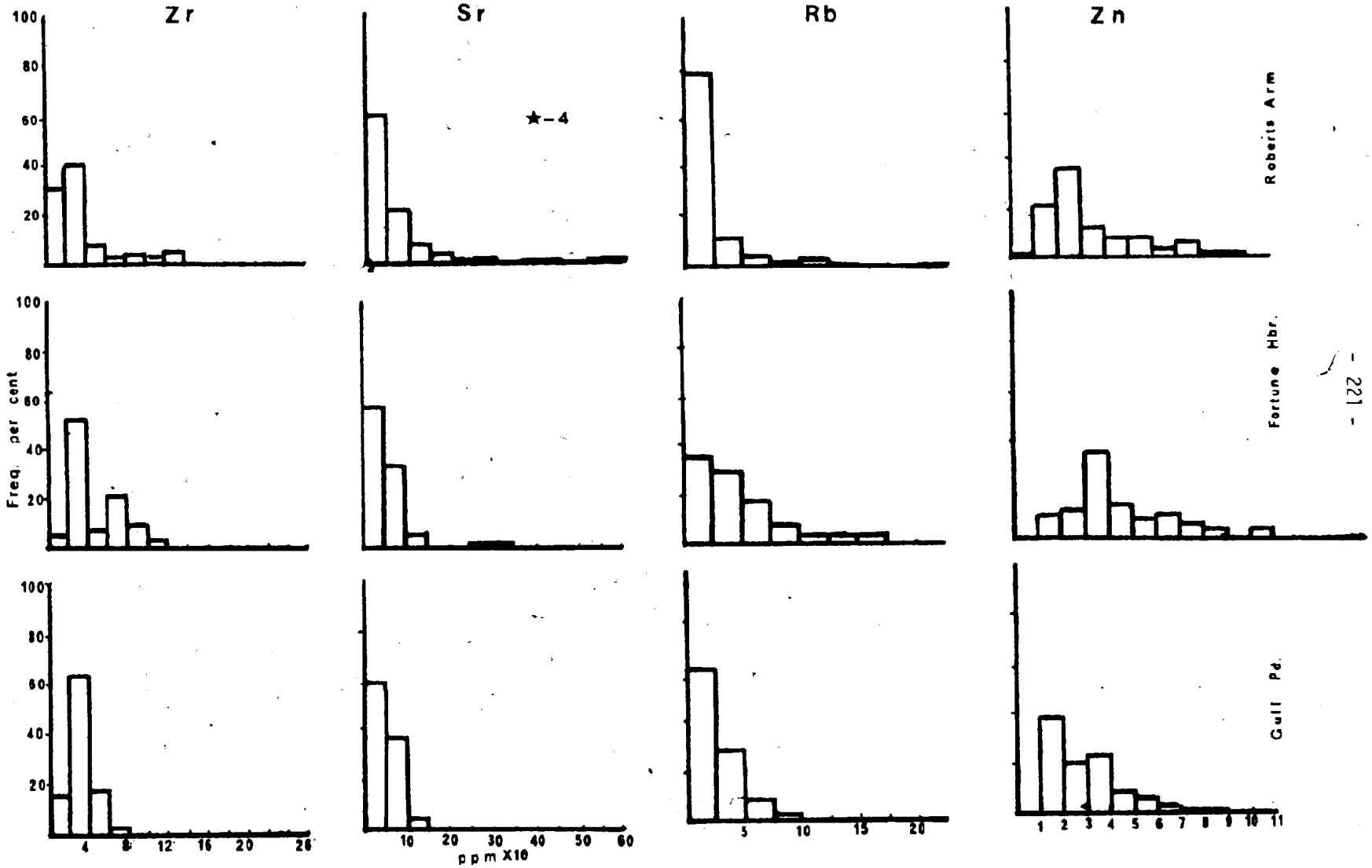
Zr
Sr
Rb
Zn
★-4
Roberts Arm
Fortune Hbr.
Gull Pd.
Freq. per cent
ppm X10

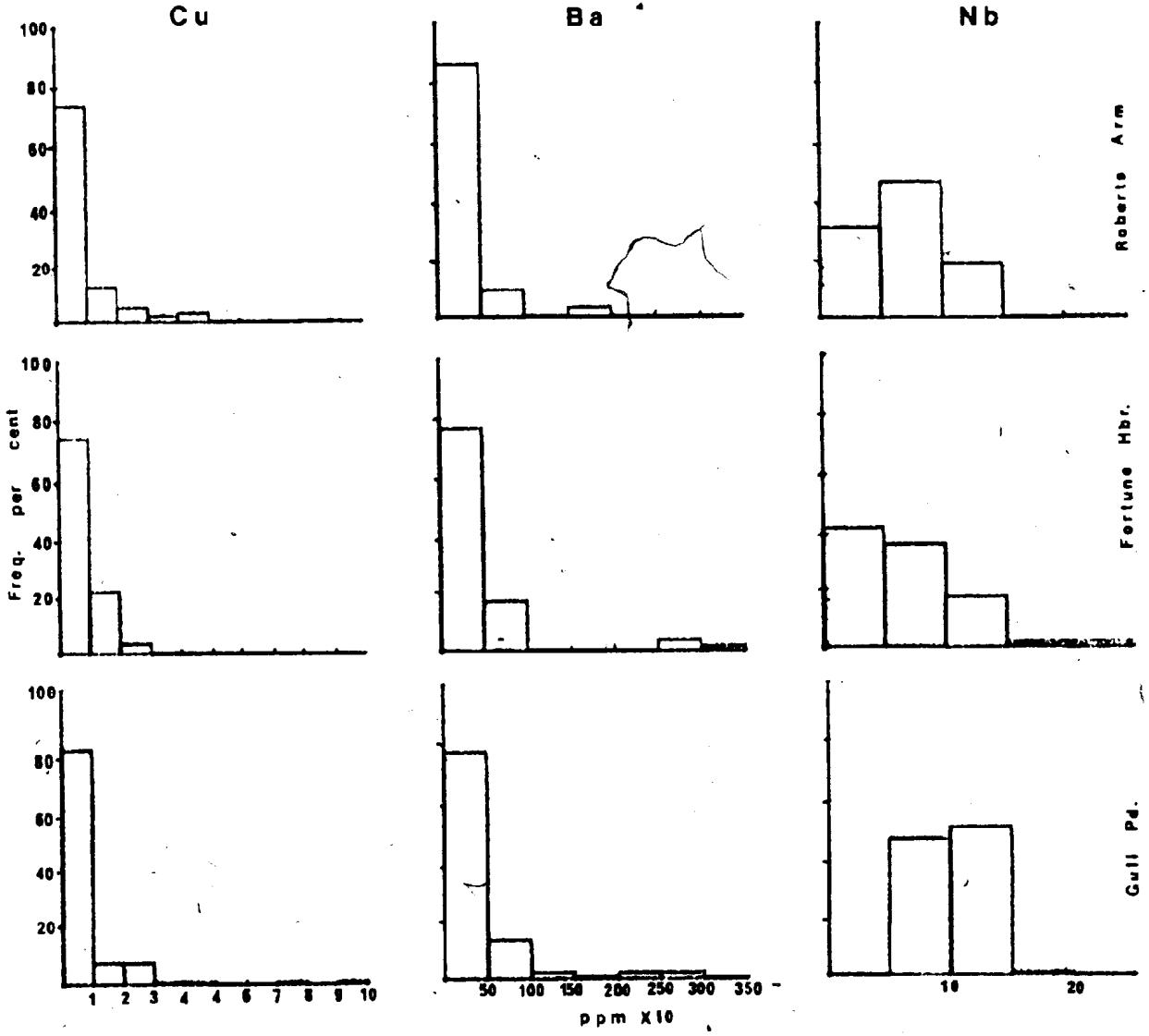
Cu
Ba
Nb
Freq. per cent
100
80
60
40
20
1 2 3 4 4 6 7 8 9 10
50 100 150 200 250 300 350
ppm X10
10 20
Roberts Arm
Fortune Hbr.
Gull Pd.

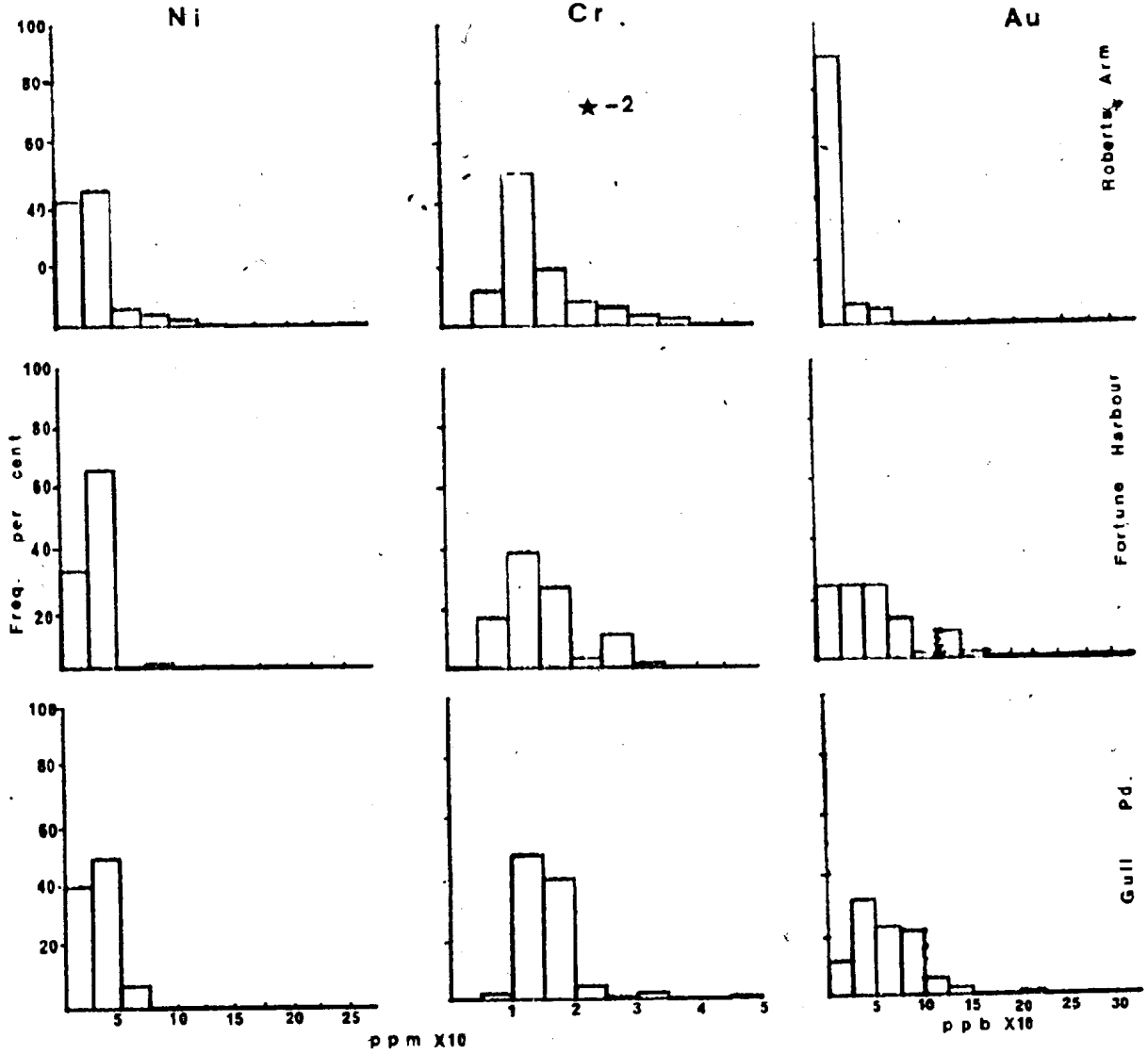
Ni
Cr.
Au
★-2
Roberts Arm
Fortune Harbour
Gull Pd.
Freq. per cent
100
80
60
40
20
0
5
10
15
20
25
1
2
3
4
5
30
ppm X10
ppb X10

APPENDIX E

SAMPLE DESCRIPTIONS

Abbreviations used:

SF - Silicic Flows
SPX - Silicic pyroclastics
MPL - Mafic pillow lavas and massive flows
MPX - Mafic pyroclastics

Bd - Bedded subgroup
I.P. - Interpillow subgroup
Min. - Mineralization subgroup
Mx - Mixed subgroup

Sample No.	Subgroup(s)	Colour	Host Rocks				Physical Features			Remarks
			SF	SPX	MPL	MPX	Lam.	Mass.	Bx.	
RA2	Red, Bd.	Red		✓			✓			
RA3	Gr.	Green		✓			✓			slump folds
RA5	Gr.,	Green			✓			✓		
RA6	Red, Bd.	Red			✓		✓			
RA9	Red, Bd.	Red			✓					
RA11-A	Red, Bd.	Red			✓		✓			
RA11-B	Red, Bd.	Red			✓		✓			
RA12	Red, Bd.	Red			✓		✓			
RA13	Red.	Red			✓		✓			
RA14		Green			✓		✓			
RA15		Green			✓			✓		
RA16	Red, Bd.	Red			✓			✓		
RA17	Red, Bd.	Red			✓			✓		
RA18	Green	Green			✓			✓		
RA19	Red, Bd.	Red			✓			✓		
RA20	Green	Green			✓		✓			
RA22	Red, Bd.	Red		✓				✓		
RA22A		Red, grey		✓	○			✓		Shaly Seal from RA22
RA23	Red, Bd.	Red		✓			✓			
RA25	Red, Bd.	Red	✓						✓	
RA34	Red, Bd.	Red	✓						✓	
RA38	Red, Bd.	Red			✓				✓	
RA39	Red, Bd.	Red			✓			✓		
RA41	Red, Bd.	Red			✓			✓		
RA44	Red, Bd.	Red			✓			✓		

Sample No.	Subgroup(s)	Colour	Host Rocks				Physical Features			Remarks
			SF	SPX	MPL	MPX	Lam.	Mass.	Bx.	
RA46	Red, Bd.	Red			✓			✓		
RA49		Red			✓					mass. hematite
RA52	Red, I.P.	Red			✓				✓	
RA53	Red.	Red			✓			✓	✓	
RA54	Red, I.P	Red			✓			✓	✓	
RA55A	Red, I.P.	Red			✓				✓	T
RA55B	Red, I.P.	Red			✓				✓	4 units - various shades
RA55C	Red, I.P.	Red			✓				✓	of red
RA55D	Red, I.P.	Red			✓				✓	I
RA58	Red, I.P	Red			✓				✓	
RA59	Red, I.P.	Red			✓			✓		
RA63	Red, Bd.	Red			✓					
RA67G	Green	Green			✓				✓	
RA67R	Red, Bd.	Red			✓			✓		
RA70		Buff			✓			✓		
RA78	Red, Bd.	Red		✓				✓		
RA79	Red, Bd.	Red		✓			✓			
RA82	Red, Bd.	Red		✓						
RA84	Red, I.P.	Red		✓						
RA89	Red, I.P.	Red		✓				✓		visible py.
RA92	Red, I.P.	Red			✓				✓	
RA98	Green	Green			✓			✓		
RA100	Red, I.P.	Red			✓				✓	
RA102	Red, Bd.	Red			✓		✓			
RA103	Red, Bd.	Red			✓		✓			

Sample No.	Subgroup(s)	Colour	Host Rocks				Physical Features			
			SF	SPX	MPL	MPX	Lam.	Mass.	Bx.	Remarks
RA109	Red	Red				✓			✓	
RA110		Red				✓				
RA112		Red			✓					
RA113	Red, Bd.	Red			✓				✓	
RA116	Red, I.P.	Red			✓				✓	
RA117	Red, I.P.	Red			✓				✓	
RA118	Red, I.P.	Red			✓				✓	
RA117G	Green	Green			✓			✓		
RA118	Red	Red			✓			✓		
RA119	Red, I.P.	Red			✓				✓	
RA120	Green	Green			✓			✓		
RA121	Red, I.P.	Red			✓				✓	
RA123	Green	Green			✓			✓		
RA125	Red	Red	✓					✓		
RA127	Red, I.P.	Red			✓				✓	
RA128A			✓							
RA128B			✓							
RA134	Green	White	✓					✓		
RA135	Green	Green			✓		✓			
RA137	Red, I.P.	Red			✓			✓		
RA138	Red, I.P.	Red			✓			✓		
RA139	Red, I.P.	Red			✓				✓	
RA140					✓					
RA141	Red, I.P.	Red			✓			✓		
RA143A	Green	Green			✓			✓		

Sample No.	Subgroup(s)	Colour	Host Rocks				Physical Features			Remarks
			SF	SPX	MPL	MPX	Lam.	Mass.	Bx.	
RA143B	Green	Green			✓			✓		
RA145	Red, I.P.	Red			✓			✓		
RA146	Red, I.P.	Red			✓			✓		
RA147	Red, I.P.	Red			✓			✓		
RA149	Red, I.P.	Red			✓					macrospherical Texture
RA150	Red	Red			✓			✓		
RA151	Red, Bd.	Red			✓		✓			
RA152	Red, Bd.	Red			✓			✓		
RA152A	Red, Bd.	Red			✓				✓	
RA153	Red, Bd	Red			✓				✓	
RA154	Red; Bd	Red			✓			✓		
RA155		Red				✓			✓	
RA156	Red, I.P.	Red			✓				✓	
RA158	Red, Bd.	Red			✓			✓		
RA158A	Red, Bd.	Red			✓			✓		
RA159	Red, Bd.	Red			✓			✓		
RA160	Green	Green			✓			✓		
RA161	Red, Bd.	Red			✓			✓		
RA164	Green	Green			✓			✓		
RA163	Red, Bd.	Red			✓		✓			
RA164	Red, Bd.	Red			✓			✓		
RA165A		Green			✓		✓			
RA165B		Red			✓		✓			
RA165C		Green			✓		✓			
RA166	Red, I.P.	Red						✓		

Sample No.	Subgroup(s)	Colour	Host Rocks				Physical Features			
			SF	SPX	MPL	MPX	Lam.	Mass.	Bx.	Remarks
RA169	Red	Red			✓			✓		
RA170	Red, I.P.	Red			✓			✓		
RA171	Red, I.P.	Red			✓			✓		
RA172	Red, I.P.	Red			✓				✓	
RA173	Red, I.P.	Red			✓				✓	
RA174	Red, I.P.	Red			✓					macrosphaeroid Texture
RA176	Green	Green	✓					✓		
RA177A	Green	Green		✓			✓			
RA178	Red, Bd.	Red		✓			✓			
RA179	Green	Green		✓				✓		
RA180		Green		✓				✓		
RA183	Green	Green		✓				✓		
RA184		Green		✓				✓		
RA190A		Red	✓				✓			
RA190B		Green	✓				✓			
RA190C		Green	✓	-			✓			
FH2	Red	Red		✓			✓			
FH4G	Green	Green		✓						
FH4R	Red	Red		✓						
FH5	Green	Green		✓				✓		
FH6	Red	Red		✓			✓			
FH7A	Green	Green-grey				✓		✓		
FH8	Red	Red				✓		✓		

Sample No.	Subgroup(s)	Colour	Host Rocks				Physical Features			
			SF	SPX	MPL	MPX	Lam.	Mass.	Bx.	Remarks
FH9	Green	Grey				✓		✓		
FH10A	Red	Red				✓	✓			
FH10B	Green	Grey-green				✓	✓			
FH12	Red	Red		✓				✓		
FH13	Red	Red		✓				✓		
FH14	Red	Red		✓				✓		
FH15	Red	Red				✓		✓		
FH16	Red	Red				✓		✓		
FH17	Red	Red			✓			✓		inter-pillow
FH18	Red	Red			✓			✓		
FH19	Green	Green			✓			✓		
FH20	Red	Red		✓				✓		
FH21	Red	Red			✓			✓		
FH22	Red	Red			✓			✓		
FH23	Red	Red			✓			✓		
FH25	Red	Red			✓		✓			
FH26	Red	Red			✓		✓			
FH29	Green	Green			✓			✓		inter-pillow
FH32	Red	Red		✓				✓		
FH33	Green			✓				✓		
FH34	Green	Green		✓				✓		
FH35	Green		✓							
FH37	Red	Red				✓		✓		
FH38	Red	Red				✓		✓		
FH39	Red	Red				✓	✓			

Sample No.	Subgroup(s)	Colour	Host Rocks				Physical Features			Remarks
			SF	SPX	MPL	MPX	Lam.	Mass.	Bx.	
FH40	Red	Red		✓				✓		
FH4A		Red		✓			✓			
FH4B				✓			✓			
FH4C				✓			✓			
FH43	Red	Red			✓		✓			
FH44	Red	Red			✓				✓	
FH45	Red	Red			✓		✓			
FH48	Red	Red		✓					✓	
FH53	Red	Red		✓					✓	
FH54	Red	Red		✓					✓	
FH55	Red	Red		✓					✓	
FH56	Red	Red		✓					✓	
FH57	Red	Red			✓			✓		
FH58	Green	Grey			✓			✓		
FH60	Red	Red			✓		✓			
FH61	Red	Red			✓		✓			
FH62	Red	Red			✓		✓			
FH63	Red	Red			✓		✓			
FH64	Green	dk. grey			✓			✓		
GP3	Min.	Red		✓			✓			
GP5	Min.	Red		✓			✓			
GP6	Min.	Red		✓			✓			

Sample No.	Subgroup(s)	Colour	Host Rocks				Physical Features			
			SF	SPX	MPL	MPX	Lam.	Mass.	Bx.	Remarks
GP7	Min.	Red		✓			✓			
GP13A	Min	Red		✓			✓			
GP13B	Min	Grey		✓			✓			shaly mbr.
GP14	Min.			✓						
GP15	Min.			✓						
GP17	Min.	Purple		✓			✓			composite - 2 narrow beds
GP21	Min.	Grey-purp.		✓				✓		
GP22	Min.	red-purp.		✓						
GP22A	Min	red-purp.		✓						
GP23	Min.	Red		✓			✓			
GP25	Min.	Red		✓			✓			
GP27	Min.	Red		✓			✓			
GP30	Min.	Red		✓			✓			
GP31	Min.	Red		✓			✓			
GP33	Min.	Red		✓					✓	
GP34	Min.	Red		✓			✓			
GP35	Min	Gray-red		✓			✓		✓	
GP36	Min.	Red		✓			✓			
GP40	Min.	Red		✓			✓			
GP42	Min.	Red-purp.			✓			✓		
GP43A	Min.	Red		✓				✓		
GP43B	Min.	Red		✓				✓		
GP50A	Mx.	Red-brown		✓			✓			
GP50B	Mx.	Red-brown		✓			✓			
GP51	Mx.	Red		✓			✓			

Sample No.	Subgroup(s)	Colour	Host Rocks				Physical Features			
			SF	SPX	MPL	MPX	Lam.	Mass.	Bx.	Remarks
GP52	Mx.	Red		✓			✓			
GP53	Mx.	Red		✓			✓			
GP54	Mx.	Red		✓			✓		✓	
GP55	Mx.	Red		✓			✓			
GP58	Mx.	Red		✓			✓			
GP59	Mx.	Red		✓			✓		✓	
GP64	Mx.	Red		✓			✓			
GP65	Mx.	Red		✓			✓			
GP65A	Mx.	Red		✓			✓			
GP66	Mx.	Red		✓			✓			
GP67	Mx.	Red		✓			✓			
GP70	Mx.	Grey		✓				✓		
GP71	Mx.	Purple		✓				✓		
GP76	Mx.	Red		✓			✓			
GP77	Mx.	Red		✓			✓			
GP79	Mx.	Pale Red		✓			✓			
GP80	Mx.	Red		✓			✓			
GP82	Mx.	Red		✓			✓			
GP85	Mx.	Red		✓			✓			
GP86	Mx.	Red		✓			✓			
GP87	Mx.	Purple		✓			✓			
GP89	Mx.	Purple		✓				✓		
GP92	Min.	Purple		✓			✓			
GP93	Min.	Red		✓			✓			
GP95	Min.	Red		✓			✓			

Sample No.	Subgroup(s)	Colour	Host Rocks				Physical Features			Remarks
			SF	SPX	MPL	MPX	Lam.	Mass.	Bx.	
GP96	Min.	Red		✓				✓		
GP102	Mx	Red	✓				✓			
GP103	Mx.	Grey-Red	✓				✓			
GP108	Mx.	Red		✓			✓			
GP115	Mx	Grey-Red		✓			✓			grey-shaly interbeds
GP119	Mx.	Red-Grey		✓			✓			grey-shaly interbeds
GP122	Mx	Red		✓			✓			
GP128	Min.	Red		✓			✓		✓	
GP131	Min	Red		✓			✓			
GP131'	Min.	Red		✓					✓	
GP136	Min.	Red		✓			✓			
GP137	Min.	Red Black		✓					✓	magnetite rich
GP138	Min.	Red		✓			✓			
GP139	Min.	red		✓			✓			
GP142	Min.	Red		✓			✓		✓	
GP145	Min.	Purple		✓			✓			
GP146	Mx.	Red			✓				✓	
GP148	Min.	Black		✓			✓			
GP149	Min.	Black		✓			✓			
GP150	Min.	Purple		✓			✓			
GP153A	Min.	Red		✓			✓			
GP153B	Min.	Red		✓			✓			
GP155	Mx.	Purple		✓			✓			
GP159	Mx.	Red		✓			✓			
GP161	Min.	Pale red		✓			✓			